



# Marine Sound Monitoring Report

## Newfoundland & Labrador Orphan Basin Exploration Drilling Program

<b>Document Number</b>	CN002-EV-REP-600-00010		
<b>Revision Code</b>	B03	<b>Revision Description</b>	For Review
<b>Retention Code</b>	EXP010	<b>Issue Date</b>	20/Feb/2024
<b>Review Cycle Code</b>	3	<b>Next Revision Date</b>	20/Feb/2027
<b>Security Classification</b>	<b>General</b>		
<b>Location (Region/Field)</b>	Newfoundland - Orphan Basin	<b>Well ID</b>	Ephesus F-94
<b>Legacy ID</b>	NA	<b>Rig Name</b>	STENA ICEMAX

<b>Signature Block</b>	<b>Name</b>	<b>Role</b>	<b>Signature / Date</b>
<b>Owner</b>	Dunphy, Robert	Environment Advisor	
<b>Stakeholder</b>	Drinkwater, John	Discipline Lead HSE&C	
<b>Stakeholder</b>	Kiely, Mark	Engineering Manager	
<b>Approver</b>	Sherritt, Allen	Senior Wells Manager	

## Revision History

Revision Date	Revision Code	Approver	Revision Description
20/Feb/2024	B03	Allen Sherritt	Address further regulatory comments
04/Jan/2024	B02	Allen Sherritt	To address regulatory comments
26/Sep/2023	B01		First draft
Click here to enter a date.			

## Operating Management System (OMS) – Sub Elements and Group Essentials

Sub Element	Sub Element Title	Group Essentials
3.6	Environment	
7.1	Regulatory	

## Reviewers

Name	Role	Type of Review	Date Reviewed
David Hedgeland		Technical	September 2023

# Marine Sound Monitoring Report

## 2023 Field Measurements of the *STENA ICEMAX*

JASCO Applied Sciences (Canada) Ltd

25 April 2024

### Submitted to:

Justin So  
WSP E&I Canada Limited  
Contract ME2282601

### Authors:

Pablo Borys  
Carmen B. Lawrence  
S. Bruce Martin  
Katie A. Kowarski

P001721-001  
Document 03199  
Version 3.1



## Suggested citation:

Borys, P., C.B. Lawrence, S.B. Martin, and K.A. Kowarski. 2024. Marine Sound Monitoring Report: 2023 Field Measurements of the *STENA ICEMAX*. Document 03199, Version 3.1. Technical report by JASCO Applied Sciences for WSP E&I Canada Limited.

## Report approved by:

<i>Version</i>	<i>Role</i>	<i>Name</i>	<i>Date</i>
1.0	Project Manager	Emily Maxner	15 Sep 2023
	Senior Scientific Reviewer	Bruce Martin	15 Sep 2023
2.0	Project Manager	Emily Maxner	25 Sep 2023
	Senior Scientific Reviewer	Bruce Martin	25 Sep 2023
3.0	Project Manager	Emily Maxner	03 Jan 2024
	Senior Scientific Reviewer	Bruce Martin	03 Jan 2024
3.1	Project Manager	Emily Maxner	20 Feb 2024
	Senior Scientific Reviewer	Bruce Martin	17 Feb 2024

# Contents

Executive Summary	1
1. Introduction	3
1.1. Project Overview	4
1.2. Background	9
1.2.1. Ambient Ocean Soundscape	9
1.2.2. Anthropogenic Contributors to the Soundscape	10
1.2.3. Soniferous Marine Life and Acoustic Monitoring	12
1.2.4. Changes to Sound as it Travels in the Ocean	15
2. Methods	18
2.1. Data Acquisition	18
2.1.1. Deployment Locations	18
2.1.2. Non-Acoustic Data	19
2.2. Automated Data Analysis	22
2.2.1. Soundscape and Time Series Analysis	22
2.2.2. Vessel Noise Detection	23
2.2.3. Marine Mammal Detection Overview	25
2.3. Detection Range Modelling	30
2.4. Sound Source Characterization	32
3. Results	35
3.1. Ambient Sound	35
3.1.1. Low-Frequency Results	35
3.1.2. High-Frequency Results	38
3.2. Sound Exposure Levels	40
3.3. Marine Mammals	42
3.3.1. Mysticetes	43
3.3.2. Odontocetes	45
3.4. Absolute Minimum Number of Animals Present	53
3.5. Detection Range Modeling	55
3.6. Support Vessels Source Levels	58
3.6.1. ALANTIC MERLIN	60
3.6.2. SIEM SYMPHONY	63
4. Discussion	67
4.1. Hearing Threshold Shifts	67
4.2. Ambient Sound and Vessel Source Levels	68
4.2.1. Correlations of Ambient Sound with Wind and Wave Activity.	68

---

4.2.2. Ambient Sound and Exceedances of 120 dB re 1 $\mu$ Pa	69
4.2.3. Support Vessel (SV) Source Levels	70
4.3. Marine Mammals	73
4.3.1. Mysticetes	73
4.3.2. Odontocetes	74
4.4. Implications of the Failure of the Recorder at 1 km	77
5. Conclusion	78
6. Glossary of Acoustics Terms	79
7. Acronymns	88
8. Literature Cited	91
Appendix A. Underwater Acoustic Recorders	A-1
Appendix B. Marine Mammal Detection Methodology	B-1
Appendix C. Detection Range Modelling Methods and Input Data	C-1
Appendix D. Vessel Source Level Results	D-1

## Figures

Figure 1. STENA ICEMAX.	5
Figure 2. Overview of the project area in the West Orphan Basin.	6
Figure 3. Support vessels for the STENA ICEMAX	7
Figure 4. Tracks of the support vessels during the time of this study. ALTO1 was within 2 km of the well site.	8
Figure 5. Wenz curves	9
Figure 6. Vessel traffic east of Newfoundland in 2023 around the general location of the study area	11
Figure 7. Fishing effort east of Newfoundland	12
Figure 8. A depiction of the geometric spreading of sound as it propagates away from an acoustic source.	16
Figure 9. Example of seasonal sound speed profiles	17
Figure 10. Study areas showing the recording locations ALTO 1 and ALTO 2 as red and blue stars, respectively, and the STENA ICEMAX as a black dot.	19
Figure 11. Wind speed and significant wave height data at ALTO1 station from 7 May to 1 July.	20
Figure 12. Sound speed profiles (SSPs) near the recording sites for 15 Apr, 15 May, 15 June, and 15 July 2023 as extracted from GLOPS archive.	21
Figure 13. Example of broadband and 40–315 Hz band sound pressure level (SPL), as well as the number of tonals detected per minute as a vessel approached a recorder, stopped, and then departed.	24
Figure 14. Example of a summary directional data presentation.	28
Figure 15. Data from Figure 14 where only the FW 20 Hz call detections have been selected and the BTI plot changed to a density plot.	29
Figure 16. Example of a polar plot to show the distribution of directions of arrival for (left) all species and for a single species (fin whale 130 Hz pulses).	29
Figure 17. Exercise 1 diagram.	32
Figure 18. Exercise 2 diagram.	33
Figure 19. Exercise 3 diagram.	34
Figure 20. ALTO 2 Low-frequency results. (Top) In band sound pressure level for the duration of the deployment. (Bottom) Long term spectrogram of received sound for the duration of the deployment.	36
Figure 21. ALTO 2 Low Frequency. Distribution of received sound levels as a function of frequency.	37
Figure 22. ALTO 2 high-frequency. (Top) In band sound pressure level for the duration of the deployment. (Bottom) Long term spectrogram of received sound for the duration of the deployment.	38
Figure 23. Spectrogram and pressure levels calculated from the recordings at ALTO2 around 18:00 on 17 June due to the presence of sperm whales.	39
Figure 24. ALTO 2 High Frequency. Distribution of received sound levels as a function of frequency.	40
Figure 25. Daily auditory frequency weighted sound exposure levels at the ALTO2 station	41
Figure 26. Fin whale: Waveform (top) and spectrogram (bottom) of 20 Hz pulses and 130 Hz notes recorded on 9 June 2023	43
Figure 27. Fin whale occurrence	43

Figure 28. Sei whale: Waveform (top) and spectrogram (bottom) of sei whale downsweeps recorded on 27 May 2023	44
Figure 29. Sei whale occurrence	44
Figure 30. Dolphins: Waveform (top) and spectrogram (bottom) of dolphin (unknown species) whistles and clicks on 1 June 2023	45
Figure 31. Pilot/killer whales: Waveform (top) and spectrogram (bottom) of whistles from either a pilot whale or killer whale on 7 July 2023	46
Figure 32. Dolphin whistle occurrence	46
Figure 33. Killer/Pilot whales: daily and hourly occurrence of killer/pilot whale whistles recorded from 10 Apr to 7 July 2023.	47
Figure 34. Delphinid click: Waveform (top) and spectrogram (bottom) of a delphinid click recorded on 1 June 2023	47
Figure 35. Dolphin click occurrence	48
Figure 36. NBHF click train: Waveform (top) and spectrogram (bottom) of NBHF clicks recorded on 27 June 2023	48
Figure 37. NBHF click: Waveform (top) and spectrogram (bottom) of a NBHF click recorded on 27 June 2023	49
Figure 38. NBHF click occurrence	49
Figure 39. Sperm whale click train: Waveform (top) and spectrogram (bottom) of sperm whale clicks recorded on 13 Apr 2023	50
Figure 40. Sperm whale occurrence	50
Figure 41. Northern bottlenose whale click train: Waveform (top) and spectrogram (bottom) of northern bottlenose whale clicks recorded on 16 Apr 2023	51
Figure 42. Northern bottlenose whale click: Waveform (top) and spectrogram (bottom) of a northern bottlenose whale click recorded on 9 May 2023	51
Figure 43. Northern bottlenose whale occurrence	52
Figure 44. AMN analysis of the Sei whale detections.	53
Figure 45. Example of sei whale calls arriving from at least two directions (green and red/orange) within the same 2-min, indicating that at least two whales were present on 2 July near ALTO 2.	54
Figure 46. Polar plot of the directions of arrival to the sei whale detections.	54
Figure 47. Recorded sound pressure levels around the time when the support vessels performed the exercises.	58
Figure 48. Sound pressure levels recorded around the approximate times of the exercises for support vessel SIEM Symphony.	59
Figure 49. ATLANTIC MERLIN track referenced by ALTO 2 position as a black triangle around the time of the exercises.	60
Figure 50. ATLANTIC MERLIN. (Top) Received levels during exercise 1 grouped by thruster level. (Bottom) Calculated source level using Equations 4 and 5 during exercise 1 grouped by thruster level.	61
Figure 51. ATLANTIC MERLIN. (Top) Received levels during exercise 2. (Bottom) Calculated source level using Equations 4 and 5 during exercise 2.	62
Figure 52. ATLANTIC MERLIN. Source level calculated using Equations 4 and 5 during exercise 3.	62
Figure 53. Spectrogram calculated from ALTO2 recordings around the time when ATLANTIC MERLIN executed exercise 3.	63

Figure 54. SIEM SYMPHONY track referenced by ALTO 2 position as a black triangle around the time of the exercises.	63
Figure 55. SIEM SYMPHONY. (Top) Received levels during exercise 1 grouped by thruster level. (Bottom) Calculated source level using Equations 4 and 5 during exercise 1 grouped by thruster level.	64
Figure 56. SIEM SYMPHONY (Top) Received levels during exercise 2. (Bottom) Calculated source level using Equations 4 and 5 during exercise 2.	65
Figure 57. SIEM SYMPHONY calculated source level using Equations 4 and 5 during exercise 3.	65
Figure 58. Spectrogram calculated from ALTO2 recordings around the time when SIEM SYMPHONY executed exercise 3.	66
Figure 59. Correlation pairs plot for the ALTO2 recorder comparing wind speed and significant wave with median decidecade sound pressure level for the period when the drillship was at Ephesus well.	68
Figure 60. Decade band sound pressure levels from ALTO2. 0.8 % of the broadband sound pressure levels (10–16000 Hz) were above 120 dB re 1 $\mu$ Pa.	69
Figure 61. Comparison of the decidecade sound pressure level distributions before, during and after the drilling campaign at ALT02, 40 km from the drillship.	70
Figure 62. Mean source level as a function of frequency for each SV.	72
Figure 63. Mean Source Level as a function of frequency for each SV during exercise 3.	72
Figure A-1. Drillship source characterization mooring design with one Ultra Deep-housing Autonomous Multichannel Acoustic Recorder–Generation 4	A-2
Figure A-2. Photo of ALTO landers prior to deployment.	A-3
Figure A-3. Split view of a G.R.A.S. 42AC pistonphone calibrator with an M36 hydrophone.	A-3
Figure A-4. Major stages of the automated acoustic analysis process performed with JASCO's PAMlab software suite.	A-4
Figure A-5. Decidecade frequency bands (vertical lines) shown on (top) a linear frequency scale and (bottom) a logarithmic scale.	A-6
Figure A-6. Sound pressure spectral density levels and the corresponding decidecade band sound pressure levels of example ambient sound shown on a logarithmic frequency scale.	A-7
Figure A-7. Auditory weighting functions for functional marine mammal hearing groups used in this project as recommended by Southall et al. (2019).	A-9
Figure B-1. Flowchart of the automated click detector/classifier process.	B-2
Figure B-2. Flowchart of the click train automated detector/classifier process.	B-3
Figure B-3. Illustration of the contour detection process.	B-4
Figure B-4. Illustration of the search area used to connect spectrogram bins.	B-4
Figure B-5. Automated Data Selection for Validation (ADSV) process	B-8
Figure B-6. The total variation between the subset selected by Automated Data Selection for Validation (ADSV) for manual analysis and the full data set.	B-9
Figure B-7. Hydrophone geometry on the ALTO lander with table of the distances between hydrophones in mm.	B-11
Figure B-8. Root mean square (RMS) azimuthal bearing error for the MLE beamformer processing and orthogonal hydrophone array with a 50 cm spacing as a function of frequency.	B-12
Figure B-9. Minimum RMS Azimuth errors vs the array spacing (D) with SNR=10 dB for calls from six representative marine mammal calls using an orthogonal array.	B-12

Figure B-10. Directogram of a fishing vessel passing 650 m from an ALTO lander.	B-13
Figure B-11. Histograms of call counts by SNR before and after filtering on SNR.	B-14
Figure C-1. The $N \times 2$ -D and maximum-over-depth modelling approach used by MONM.	C-1
Figure C-2. Detection areas for fin whale song notes at ALTO2	C-5
Figure C-3. Detection areas for sei whale downsweeps at ALTO2	C-6
Figure C-4. Detection areas for dolphin clicks (left) and whistles (right) at ALTO2	C-7
Figure C-5. Detection areas for sperm whale clicks at ALTO2	C-8
Figure C-6. Detection areas northern bottlenose clicks at ALTO2	C-9
Figure D-1. Atlantic Kingfisher track referenced by ALTO 2 position as a black triangle around the time of the exercises.	D-1
Figure D-2. Atlantic Kingfisher. (Top) Received levels during exercise 1 grouped by thruster level. (Bottom) Calculated source level using Equations 4 and 5 during exercise 1 grouped by thruster level.	D-2
Figure D-3. Atlantic Kingfisher. (Top) Received levels during exercise 2. (Bottom) Calculated source level using Equations 4 and 5 during exercise 2.	D-2
Figure D-4. Atlantic Kingfisher calculated source level using Equations 4 and 5 during exercise 3.	D-3
Figure D-5. Maersk Mobiliser track referenced by ALTO 2 position as a black triangle around the time of the exercises.	D-3
Figure D-6. KJ Gardner track referenced by ALTO 2 position as a black triangle around the time of the exercises.	D-4
Figure D-7. KJ Gardner. (Top) Received levels during exercise 1 grouped by thruster level. (Bottom) Calculated source level using Equations 4 and 5 during exercise 1 grouped by thruster level.	D-5
Figure D-8. KJ Gardner. (Top) Received levels during exercise 2. (Bottom) Calculated source level using Equations 4 and 5 during exercise 2.	D-6
Figure D-9. KJ Gardner calculated source level using Equations 4 and 5 during exercise 3.	D-6
Figure D-10. Maersk Clipper track referenced by ALTO 2 position as a black triangle around the time of the exercises.	D-7
Figure D-11. Maersk Clipper. (Top) Received levels during exercise 1 grouped by thruster level. (Bottom) Calculated source level using Equations 4 and 5 during exercise 1 grouped by thruster level.	D-8
Figure D-12. Maersk Clipper. (Top) Received levels during exercise 2. (Bottom) Calculated source level using Equations 4 and 5 during exercise 2.	D-8
Figure D-13. Maersk Clipper calculated source level using Equations 4 and 5 during exercise 3.	D-9

## Tables

Table 1. Ephesus well times by depth provided by bp.	6
Table 2. Support Vessels Schedule.	7
Table 3. Western North Atlantic: List of cetacean and pinniped species known to occur off eastern Canada	14
Table 4. Acoustic signals used for identification or automated detection of the species that could potentially occur in the study area and supporting references.	15
Table 5. Operation period, location, and water depth of the Autonomous Multichannel Acoustic Recorders (AMARs) deployed for the Orphan Basin study.	19
Table 6. Parameters of the boat and vessel detector.	25

Table 7. Support vessels and the day they executed the required exercises at ALTO2.	34
Table 8. Automated detector performance	42
Table 9. Detection ranges for each detected species at 10, 50, and 90 % probabilities of detection as a function of in-band ambient sound levels (10, 50, and 90 % percentile) at station ALTO2 in the spring (April-June).	56
Table 10. Acoustic impairment effects of non-impulsive noise on marine mammals: SEL24h thresholds (Southall et al. 2019)	67
Table 11. Mean sound pressure level (10 – 256000 Hz) at ALTO2 during the phases of the acoustic monitoring operations.	70
Table 12. Median Source levels for each vessel for each exercise.	71
Table A-1. Decidecade-band frequencies (Hz).	A-7
Table A-2. Decade-band frequencies (Hz).	A-8
Table A-3. Parameters for the auditory weighting functions used in this project as recommended by Southall et al. (2019).	A-9
Table B-1. Discrete Fourier Transform (FFT) and detection window settings for all automated contour-based detectors used to detect tonal vocalizations of marine mammal species expected in the data.	B-5
Table B-2. A sample of automated detector classification definitions for the tonal vocalizations of cetacean species expected in the area.	B-6
Table B-3. A sample of vocalization sorter definitions for the tonal pulse train vocalizations of cetacean species expected in the area.	B-7
Table C-1. Geoacoustic profiles.	C-3
Table C-2. Marine mammal input parameters.	C-4

## Executive Summary

BP Canada Energy Group ULC (bp) conducted exploratory drilling activities in the Orphan Basin offshore Newfoundland and Labrador in April to July 2023. As part of the regulatory requirements, a marine sound monitoring program was undertaken to characterize and verify predictions of underwater sound levels associated with the drilling operations.

The monitoring program was designed to address conditions outlined in the Environmental Impact Statement (EIS) and subsequent Decision Statement issued under the Canadian Environmental Assessment Act, 2012. Specifically, the monitoring aimed to:

- Compare measured acoustic footprint distances from drilling-related sound sources to EIS predictions of 10–40 km. The key metric of interest is the distance to a broadband sound pressure level of 120 dB re 1  $\mu\text{Pa}^2$  which is the threshold associated with behavioural disturbance of marine mammals from continuous human sound sources like drillships (NOAA Fisheries 2019).
- Establish baseline sound levels at locations near the planned drilling area.
- Evaluate changes to the baseline acoustic conditions resulting from drilling activities.
- Assess the presence and acoustic occurrence of marine mammals before and during drilling operations.
- Measure the source levels of the drillship and the support vessels.

The program involved deployment of Autonomous Long-Term Observatories (ALTOs) at two locations approximately 1 km and 40 km from the planned Ephesus well. The ALTOs were positioned along the continental slope southwest of the well site, with the more distant recorder situated near the main vessel traffic route to St. John's, Newfoundland.

The ALTOs were deployed on 10 April 2023 and retrieved on 7 July 2023, spanning a period before, during, and after the Ephesus drilling operations conducted by the STENA ICEMAX drillship (07 May to 29 June 2023). This provided 26 days of data before drilling and 8 days after drilling to compare to the 54 day period when the STENA ICEMAX was on site.

The hydrophones on the ALTO nearest to the drillship became disconnected from the recorder at depth when the cable between them came under pressure; therefore, no useful data was available at that location. The ALTO at 40 km collected continuous acoustic data at sampling rates sufficient to detect vocalizations of all expected marine mammal species. The ALTO was equipped with four hydrophones, which allows to assess the direction arrival for sounds within a frequency band constrained by the distance between hydrophones. In this study, the only detected species whose calls occur within the appropriate band was sei whale.

The sound from the drilling operations were detected at 40 km throughout the program. Across the whole frequency band, the mean decidecade sound pressure levels increased by 0.8 dB and 6.7 dB when the drillship was present compared to the before and after periods, respectively. In the bands between 63 and 500 Hz the decidecade SPLs were 5-7 dB higher during drilling than before. The mean background levels before drilling differed by 5.9 dB compared to the levels after drilling, which was attributed to lower wind speeds after drilling than before. Gale and storm force winds occurred in May but did not occur in June. The levels were well below the threshold of 120 dB re 1  $\mu\text{Pa}^2$  from continuous sound for disturbance of marine mammals as described in the EIS. The sound levels were expected to fall below this threshold at 23–40 km and were rarely measured to be above 110 dB re 1  $\mu\text{Pa}^2$ . Only 0.8 % of the recording periods

exceeded the 120 dB re 1  $\mu$ Pa at ALTO2, and most of those recordings were associated with the support vessels being close to ALTO2 for measurements of their source levels.

Most mysticete whales decrease their vocalizations during the April – July period offshore of Newfoundland. This result was confirmed for the Ephesus drilling campaign in the Orphan Basin. Fin whales were detected on two occasions while sei whales were detected on 18 days. Directional analysis of the sei whale detections indicated that at most two individuals (or perhaps groups) were present at any one time. Small dolphins as well as pilot or killer whales were regularly present in the acoustic recordings, with their activity increasing in June. Sperm whales were detected intermittently, and dwarf/pygmy sperm whales or harbour porpoise were detected on three occasions. Northern Bottlenose whales were present daily from April to ~1 July. Marine mammal presence did not appear to be affected by the drillship 40 km away since there were no changes in call detection rates that correlated with the arrival and departure of the drillship.

The source levels of the support vessels while on dynamic positioning systems was higher than the source level employed during the EIS modelling. Nevertheless, the total sound field measured at 40 km was lower than the required threshold. For several of the vessels, their spectrum was also bimodal with peaks at 100 and 500 Hz rather than a single peak at 100 Hz. The source level of the SIEM SYMPHONY was particularly quiet compared to the other support vessels and most vessels assessed by JASCO.

# 1. Introduction

BP Canada Energy Group ULC (bp) conducted exploratory drilling activities in the Orphan Basin offshore Newfoundland and Labrador in 2023. As part of the regulatory requirements, a marine sound monitoring program was undertaken to characterize and verify predictions of underwater sound levels associated with the drilling operations.

The monitoring program was designed to address conditions outlined in the Environmental Impact Statement (EIS) and subsequent Decision Statement issued under the Canadian Environmental Assessment Act, 2012. Specifically, the monitoring aimed to:

- Compare measured acoustic footprint distances from drilling-related sound sources to EIS predictions of 10–40 km. The key metric of interest is the distance to a broadband sound pressure level of 120 dB re 1  $\mu\text{Pa}^2$  which is the threshold associated with behavioural disturbance of marine mammals from continuous human sound sources like drillships (NOAA Fisheries 2019).
- Establish baseline sound levels at locations near the planned drilling area.
- Assess the presence and acoustic occurrence of marine mammals before and during drilling operations.
- Evaluate changes to the baseline acoustic conditions resulting from drilling activities.
- Measure the source levels of the drillship and the support vessels.

The program involved deployment of Autonomous Long-Term Observatories (ALTOs) at two locations approximately 1 km and 40 km from the planned Ephesus well. The ALTOs were positioned along the continental slope southwest of the well site, with the more distant recorder situated near the main vessel traffic route to St. John's, Newfoundland.

The ALTOs were deployed on 10 Apr 2023 and retrieved on 7 July 2023, spanning a period before, during, and after the Ephesus drilling operations conducted by the STENA ICEMAX drillship (29 Apr to 29 June 2023). The ALTOs collected continuous acoustic data at sampling rates sufficient to detect vocalizations of all expected marine mammal species.

This report provides a detailed overview of the monitoring program methodology, equipment specifications, acoustic data analysis techniques, results for measured sound levels, marine mammal acoustic occurrence, and key findings in relation to the EIS predictions. The report aims to characterize the drilling operation's acoustic footprint and effects on the local soundscape and marine life.

The results will inform regulatory authorities and bp on the accuracy of impact predictions and help validate and improve future environmental assessments and mitigation strategies.

## 1.1. Project Overview

bp contracted with Stena Drilling Ltd. (Stena Drilling) to use the STENA ICEMAX (Figure 1) drillship to drill an exploratory well, the Ephesus well, on Exploration License EL 1168 (a consolidation of ELs 1145 and 1146) in the West Orphan Basin. The well is located ~395 km northeast of St. John's, NL, and will be drilled in a water depth of ~1340 m to evaluate the potential of oil-bearing formations. The location of the exploration well is displayed in Figure 2.

The Ephesus well site is also located in the Northeast Newfoundland Slope Other Effective Area Based Conservation Measure (OECM). The NE Newfoundland Slope OECM comprises an area of approximately 55,353 km<sup>2</sup> and contributes approximately 0.96% to Canada's marine conservation targets. The Northeast Newfoundland Slope OECM conservation objective is to protect corals and sponges and contribute to the long-term conservation of biodiversity.

A drillship is a self-propelled drilling vessel with large variable deck load capacity to allow for increased storage of equipment and materials to drill ultra-deep-water wells with depths similar to those encountered within the ELs, and in remote locations. Drillships use dynamic positioning technology (DP) to maintain position and rotate the ship over well centre to head the ship into prevailing weather, following shifts in wind or wave direction to minimize the pitch and roll motion. Drillships are different from typical offshore vessels, such as cargo vessels, by the presence of a drilling package and a moon pool. The moon pool is an opening in the bottom of the hull of the vessel, which allows direct access to the water, enabling drilling equipment on the vessel to connect to equipment on the seafloor to drill the well.

Drilling operations were supported via logistics arrangements for supply and servicing. Offshore supply vessels and helicopters were used for transportation and movement of materials and personnel between the drillship and land to ensure safe reliable drilling operations.

The STENA ICEMAX arrived in Bay Bulls, Newfoundland on 29 April 2023 and departed for the Ephesus well site 06 May 2023. Table 1 presents the Ephesus well times grouped by the depth of well, the spud date was 8 May in a water depth of 1362.3 m, the total vertical depth achieved was 5065 m, and the wellhead was cut approximately 1m below the mudline and removed on 29 June. The final rig sail and rig release were from 29 June to 1 Jul. A total of 62.63 days occurred from the rig mobilisation to the rig release with 55.51 days of activities recorded.



Figure 1. STENA ICEMAX.

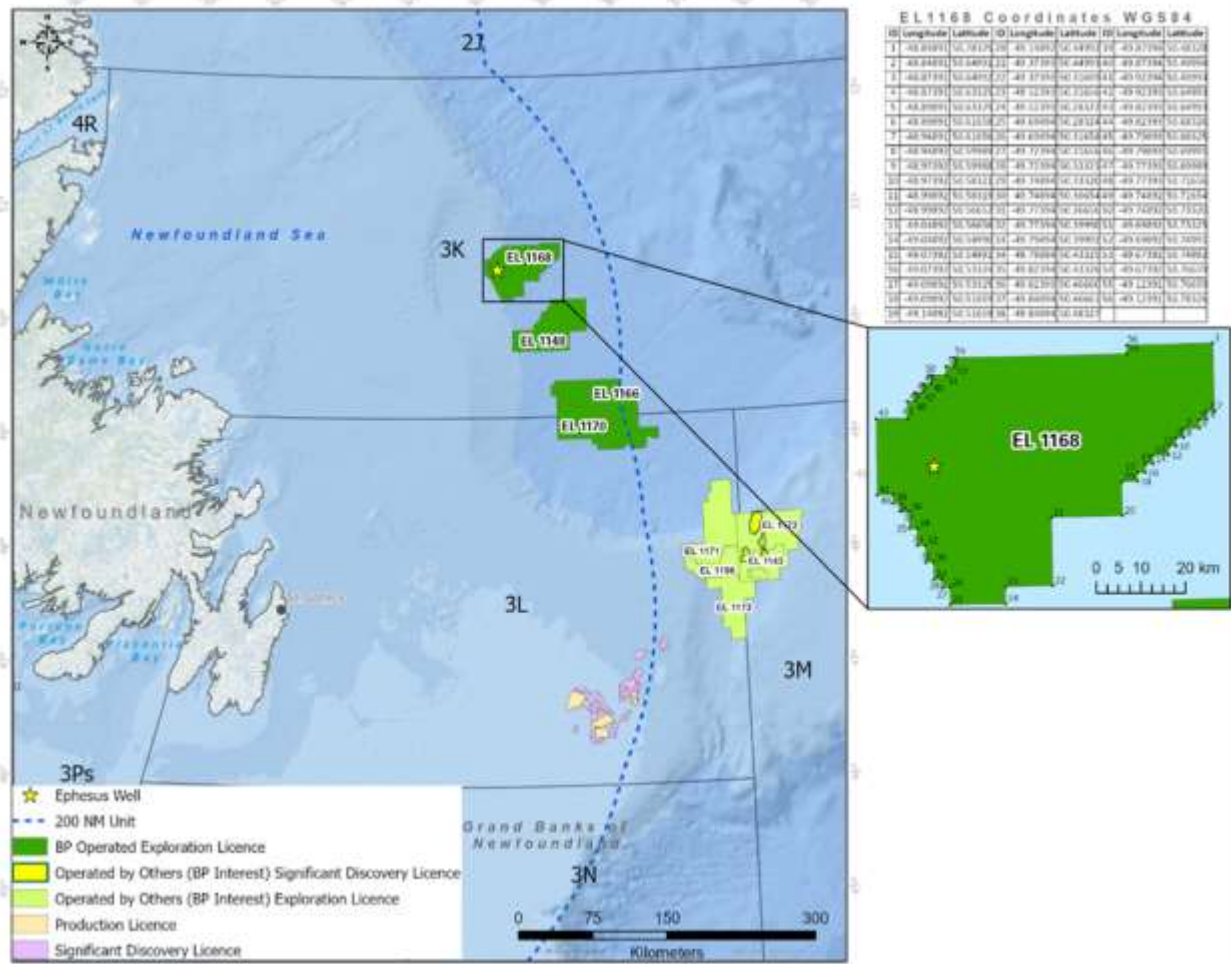


Figure 2. Overview of the project area in the West Orphan Basin. The two insets show the location of the exploration site EL 1168 and, within, the location of the Ephesus Well.

Table 1. Ephesus well times by depth provided by bp.

Depth (m)	From	To	Days
1362.3	29/04/2023 09:00	08/05/2023 00:00	8.63
1449	08/05/2023 00:00	09/05/2023 15:15	1.63
2205	09/05/2023 15:15	17/05/2023 18:00	8.11
2875	17/05/2023 18:00	25/05/2023 05:15	7.46
3210	25/05/2023 05:15	30/05/2023 06:15	5.05
4400	06/06/2023 06:15	09/06/2023 07:00	2.93
5064	09/06/2023 07:00	14/06/2023 15:30	5.35
5065	14/06/2023 15:30	01/07/2023 00:00	16.35
<b>Total days</b>			<b>55.51</b>

The STENA ICEMAX was serviced by the support vessels (SV): ATLANTIC MERLIN, KJ GARDNER, MAERSK CLIPPER, ATLANTIC KINGFISHER, SIEM SYMPHONY, and MAERSK MOBILISER (Figure 3). The ATLANTIC Merlin experienced mechanical difficulties before drilling commenced and was replaced by the

MAERSK Clipper and ATLANTIC Kingfisher until its return. The dates when each SV was on duty are presented in Table 2. The SVs were not in the field until 7 May, except for the MAERSK MOBILISER which deployed the ALTOs on 10 April and departed the field on 14 April. The location of the SVs was determined via the marine Automatic Identification System (AIS) data made available to JASCO by bp. Measuring the source level of the support vessels was an important component of this project and was performed at ALTO2 as the vessels passed by on their way to and from the rig.



Figure 3. Support vessels for the STENA ICEMAX from left to right and up to bottom: ATLANTIC MERLIN, KJ GARDNER, MAERSK CLIPPER, ATLANTIC KINGFISHER, SIEM SYMPHONY, and MAERSK MOBILISER. Images from marinetraffic.com. Accessed 22 Aug 2023.

Table 2. Support Vessels Schedule.

Support vessel	Dates
MAERSK MOBILISER	10/04/2023 to 29/06/2023
ATLANTIC MERLIN	24/04/2023 to 03/05/2023 17/06/2023 to 29/06/2023
SIEM SYMPHONY	26/04/2023 to 29/06/2023
KJ GARDNER	03/05/2023 to 29/06/2023
ATLANTIC KINGFISHER	26/05/2023 to 13/06/2023
MAERSK CLIPPER	06/05/2023 to 26/05/2023

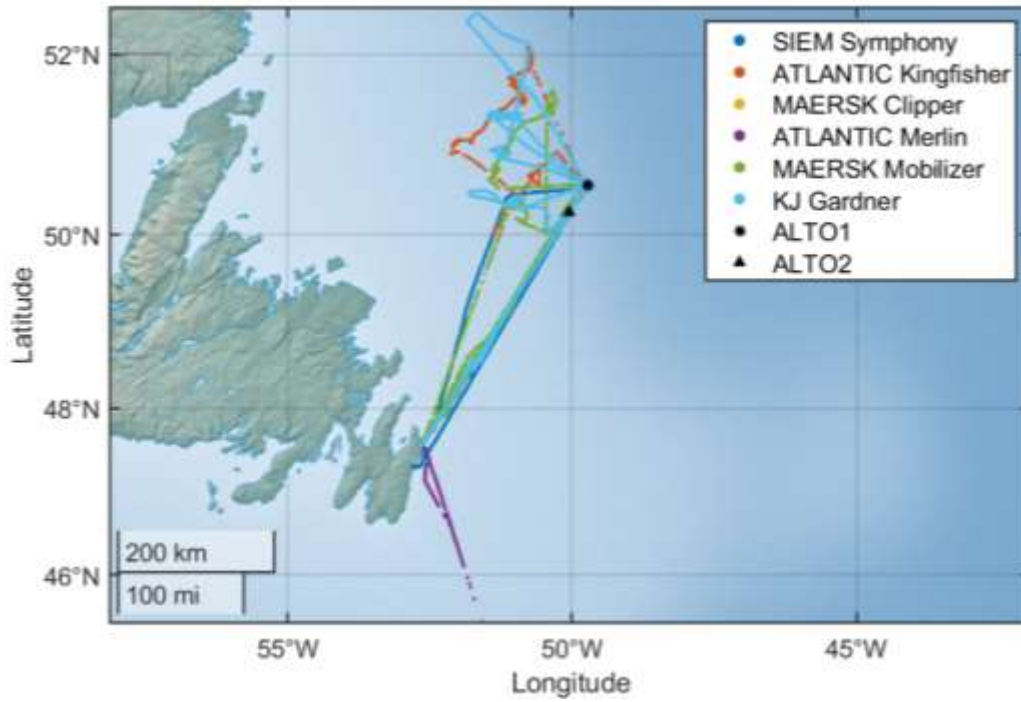


Figure 4. Tracks of the support vessels during the time of this study. ALTO1 was within 2 km of the well site.

## 1.2. Background

### 1.2.1. Ambient Ocean Soundscape

The acoustic environment of a location is known as its soundscape and is comprised of the cumulative contributions from abiotic (geophonic), biotic (biophonic), and human (anthrophonic) sound sources (Krause 2008). Ambient sound is defined as any sound that is present in the absence of human activity. It is also temporally and spatially specific (ISO 2017a). The typical frequencies and spectral levels of many of these activities are shown by the Wenz (1962) curves (Figure 5).

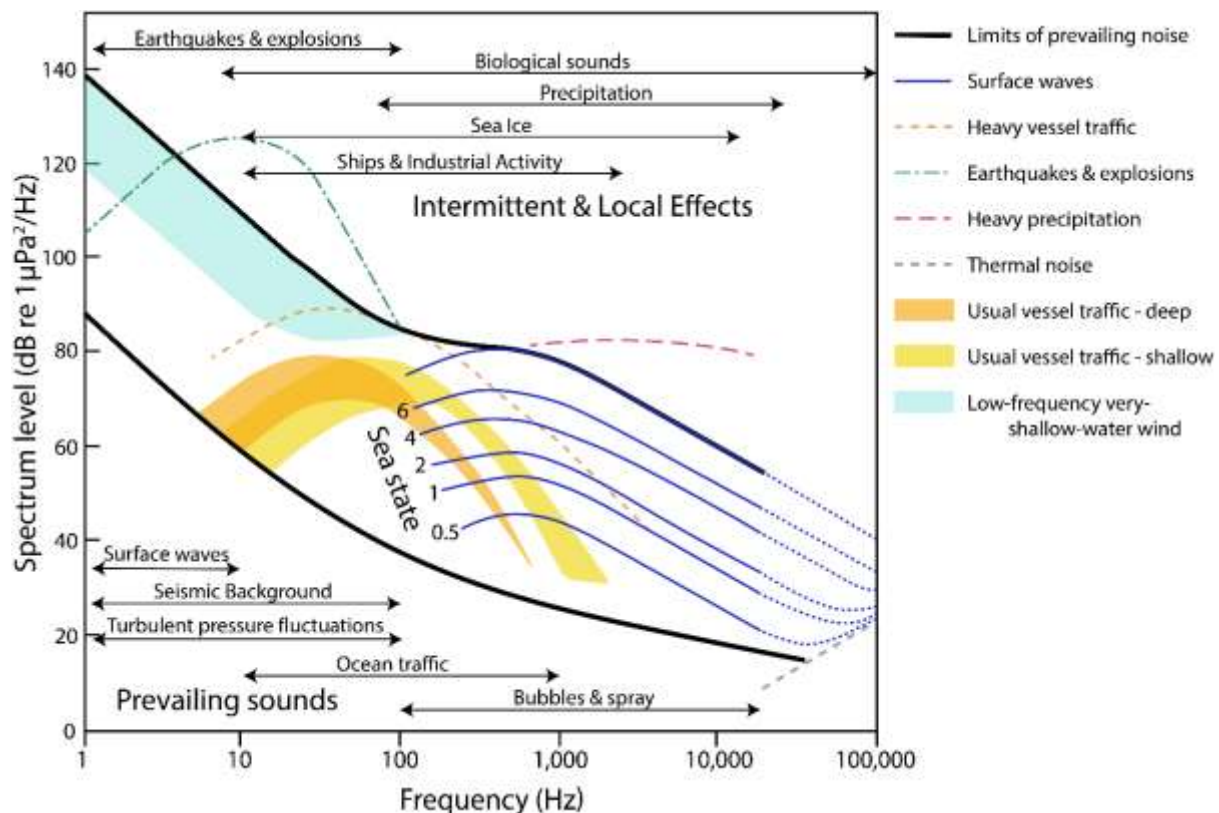


Figure 5. Wenz curves describing pressure spectral density levels of marine ambient sound from weather, wind, geologic activity, and commercial shipping (adapted from NRC 2003, based on Wenz 1962). The thick lines are the limits of prevailing ambient sound, which are included in some of the results plots to provide context.

In the marine environment, the geophonic elements of a soundscape can act as proxies for oceanographic conditions. Knudsen et al. (1948) and Wenz (1962) demonstrated that increased sea state and wind speed commonly correlate with higher sound intensities across frequencies from 500 Hz to 30 kHz due to breaking whitecaps, surface flow noise, wave generation, cavitation, and pressure change (Urlick 1983). Rainfall can elevate sound levels in the 1–15 kHz frequency range via sound from surface impacts and bubble entrainment (Heindsmann et al. 1955, Bom 1969, Scrimger et al. 1987).

In high latitude areas, ice can be a prominent feature of the soundscape. The soundscape contribution of sea ice is usually highest during formation and break-up. Under established sea ice, sound levels are usually

lower than in open water areas as the ice acts to attenuate or even eliminate the effects of wind and waves on the soundscape (Menze et al. 2017). The study area generally lies south of the southern edge of the pack ice off eastern Canada. Sea ice was not a factor driving soundscape patterns in this study since it took place between May and October during the ice-free season. Besides wind, waves, sea ice, currents, and seismic activity such as earth movement and subsea landslides can be loud, though short-duration, geophonic contributors. While geophonic and biophonic contributors comprise the natural soundscape, the total soundscape also includes anthropogenic (related to human activity) sounds.

Human sound sources are diverse and can have a large underwater acoustic footprint. The main sources are vessel noise, primarily caused by global shipping vessels, and seismic exploration for hydrocarbon deposits. Hydrocarbon drilling operations can influence soundscape over substantial areas and periods.

Measuring ambient sound and characterising the soundscape of an area is complicated by non-acoustic processes that often appear in acoustic recordings. One such issue is flow noise, caused by pressure eddies and vortices produced by water movement along the surfaces of hydrophone pressure transducers. This is similar to the buffeting sounds recorded by microphones in the wind. Flow noise is not part of a marine soundscape (Strasberg 1979, Urick 1983), but its intensity may indicate current strength (Willis and Dietz 1961). Current or wave action can also induce mooring noise when non-stationary components of a mooring create sound as they move or strum.

## 1.2.2. Anthropogenic Contributors to the Soundscape

Anthropogenic (human-generated) sound can be a by-product of vessel operations, such as engine sound radiating through vessel hulls and cavitating propulsion systems, or it can be a product of active acoustic data collection with seismic surveys, military sonar, and depth sounding as the main contributors. Marine construction projects can involve nearshore blasting to loosen sediment and pile driving that can produce high levels of impulsive-type noise. The contribution of anthropogenic sources to the ocean soundscape has increased from the 1950s to 2010, largely driven by greater maritime shipping traffic (Ross 1976, Andrew et al. 2011). Recent trends suggest that global sound levels are leveling off or potentially decreasing in some areas (Andrew et al. 2011, Miksis-Olds and Nichols 2016), even though other studies indicate that, in the absence of significant changes to the propulsion systems of ships, the contribution of vessel acoustic emissions has increased and will likely keep increasing (Kaplan and Solomon 2016, Jalkanen et al. 2022). Oil and gas seismic exploration programs, oil and gas production platforms and marine pile driving used to install offshore wind turbines and can elevate sound levels over radii of 10–1000 km (Bailey et al. 2010, Miksis-Olds and Nichols 2016, Delarue et al. 2018). The extent of seismic survey sounds has increased substantially following the expansion of oil and gas exploration into deep water, and seismic sounds can now be detected across ocean basins (Nieukirk et al. 2004). The offshore wind farm installations are accelerating around the globe as a source of clean and increasing low-cost energy.

The main anthropogenic contributors to underwater soundscape in the present study were SVs supporting drilling operations and other vessels transiting through the study area. There are several well-defined routes used by vessels transiting between St John's, NL, and the oil fields along the eastern edge of the Grand Banks, with tight track clusters identifying drilling platforms. These routes are supplemented by lower-density traffic associated with fishing vessels and transport vessels on transatlantic routes. In Figure 6, it can be seen that the exploration licence area EL 1168, shown as a red square, is close to a low-density fishing route in Figure 7. The relative contribution to the soundscape by these different vessel classes as measured by an acoustic recorder is driven by their proximity to the recorder and the duration of their presence in its vicinity.

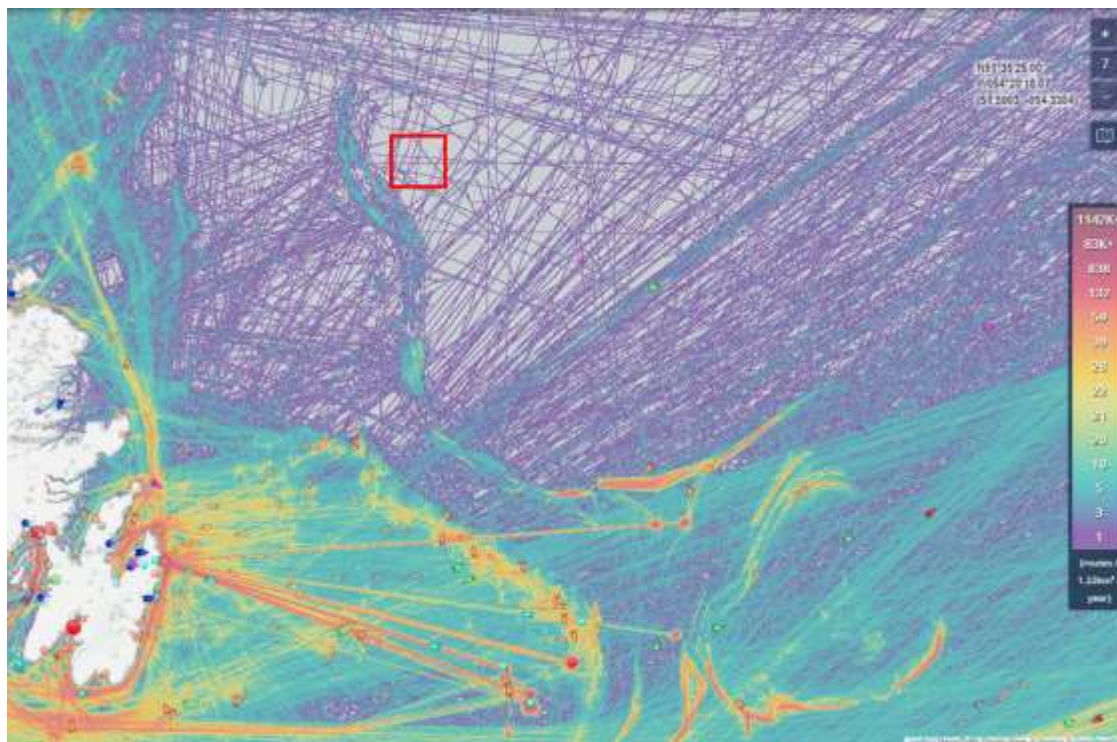


Figure 6. Vessel traffic east of Newfoundland in 2023 around the general location of the study area denoted by a red square. Source: marinetraffic.com; accessed 23 Aug 2023.

The STENA ICEMAX itself produced a range of sounds. Some sounds were expected to be constant, such as mechanical vibration and thruster cavitation from the DP system and other sounds expected to be limited in time, such as emissions from pumps and direct drilling sounds from the drill string and the drill bit. Ultra-short baseline (USBL) pingers, used to ensure the STENA ICEMAX remained within the safe operating radius over the well, were also persistent sound sources.

Finally, vessels involved in fishing activities also introduce underwater noise. Figure 7 shows the distribution of fishing effort east of Newfoundland during the recording period. The Ephesus well site was located in a designated marine refuge within which bottom contract fishing was prohibited thus fishing effort in the area was limited. However, fishing activity was expected to be sustained on the continental slope along the northern edge of the Grand Banks, north and west of the well site.

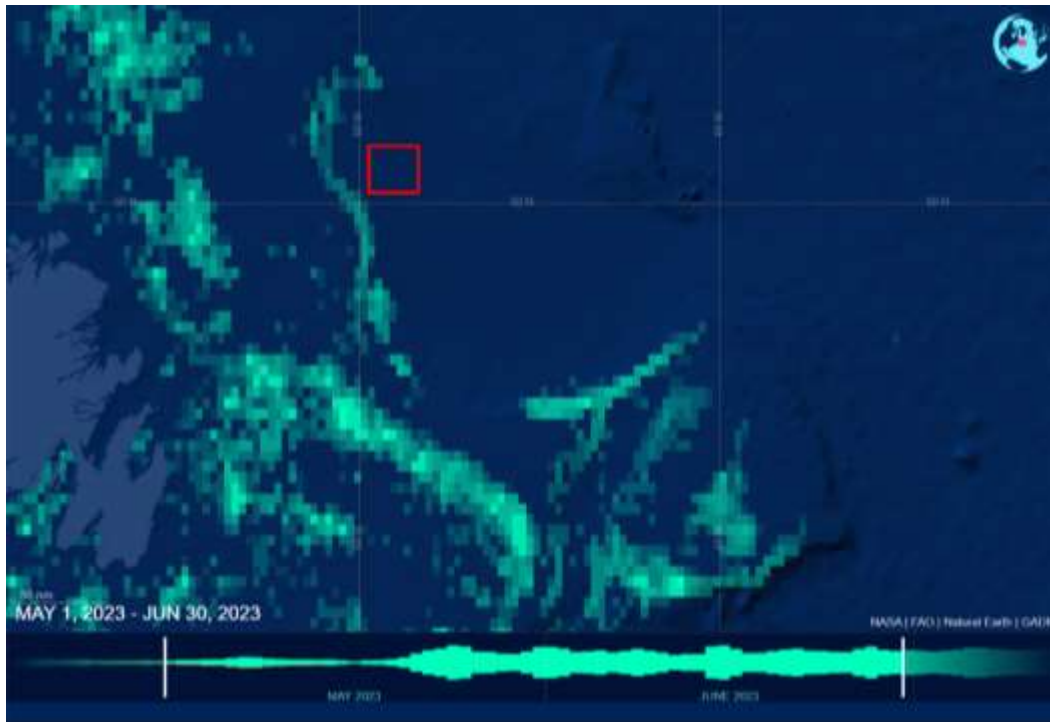


Figure 7. Fishing effort east of Newfoundland (1 May to 30 June) around the general location of the study area denoted by a red square (source: <https://globalfishingwatch.org/>; accessed 14 Sep 2023)

### 1.2.3. Soniferous Marine Life and Acoustic Monitoring

Biological sources of sound are diverse, and many marine taxa produce sounds. Animals that are known to produce acoustic signals include crustaceans, fish, and marine mammals. Biophonic signals include those generated for communicating, navigating, breeding, and foraging by sound-producing species (Clark 1990, Edds-Walton 1997, Tyack and Clark 2000). Many fish species produce sound during the breeding season or when engaged in agonistic behaviours (Amorim 2006). Several species of gadids (cod family), such as Northern cod (*Gadus morhua*) and haddock (*Melanogrammus aeglefinus*), form spawning aggregations that have been detected acoustically (Nordeide and Kjellsby 1999, Hawkins et al. 2002). The acoustic monitoring of fish is hindered by a limited understanding of their acoustic repertoire and behaviour. Irrespective of species identity, fish choruses can raise ambient sound levels and therefore influence local soundscapes (Erbe et al. 2015). Marine mammals are the main biological contributors to the underwater soundscape. For instance, fin whale song can raise noise levels in the 18–25 Hz band by at least 15 dB for extended durations (Simon et al. 2010, Delarue et al. 2018).

The biological focus of this study was marine mammals. Twenty-three cetacean and five pinniped species occur off eastern Canada (see Table 3). The presence of many of these species is well-documented based on two years of passive acoustic monitoring (PAM) (August 2015 to July 2017) throughout the eastern Canadian Exclusive Economic Zone (EEZ), including Orphan Basin (Stn 15 in Delarue et al. 2018, Delarue et al. 2022). Previous PAM in Orphan Basin confirmed the acoustic presence of northern bottlenose, Cuvier's beaked, Sowerby's beaked, long-finned pilot, sperm, blue, fin, and humpback whales as well as dolphins. North Atlantic right whales were rarely acoustically detected in the region from 2015 to 2017 (Stn 15 in Delarue et al. 2018, Delarue et al. 2022).

Knowledge of the acoustic signals of the marine mammals expected in the study area varies across species (see summary in Table 4). These sounds can be split into two broad categories: Tonal signals, including baleen whale moans and delphinid whistles, and echolocation clicks produced by all odontocetes. Although the signals of most species have been described to some extent, these descriptions are not always sufficient for reliable, systematic identification, let alone to design automated detectors to process large data sets. For instance, although the whistles of species in the subfamily *Delphinidae* (small dolphins) in the area have all been described to some extent, the overlap in their spectral characteristics complicates their identification by both analysts and automated detectors (Ding et al. 1995, Gannier et al. 2010). The echolocation clicks of all beaked whale species potentially present are well-described and can be reliably detected. In some cases, a general understanding of the spectral features of signals combined with knowledge of habitat preference and signal propagation allowed us to make inferences about the occurrence of a species. This may be appropriate to distinguish echolocation clicks from harbour porpoises and *Kogia* species. In most cases, baleen whale signals can be reliably identified to the species level, although seasonal variation in the types of vocalizations produced results in seasonal differences in our ability to detect these species acoustically. For example, the tonal signals produced by blue, fin, and sei whales tend to show lots of similarities in late spring and summer (Ou et al. 2015), but they are markedly different from September to April when acoustic displays become dominated by stereotypical songs with clear species signatures (Delarue et al. 2022). Because not all species vocalize regularly, and vocalization activity often depends on season, sex or age, passive acoustic monitoring effectiveness must be considered on a case-by-case basis.

Table 3. Western North Atlantic: List of cetacean and pinniped species known to occur off eastern Canada and their status according to Committee on the Status of Endangered Wildlife in Canada (COSEWIC) and Species at Risk Act (SARA).

Species	Scientific name	Status	
		COSEWIC	SARA
<b>Baleen whales</b>			
Minke whale	<i>Balaenoptera acutorostrata</i>	Not at risk	Not listed
Sei whale	<i>B. borealis</i>	Endangered	Not listed <sup>2</sup>
Blue whale	<i>B. musculus</i>	Endangered	Endangered
Fin whale	<i>B. physalus</i>	Special concern	Special concern
Humpback whale	<i>Megaptera novaeangliae</i>	Not at risk	Not listed
North Atlantic right whale	<i>Eubalaena glacialis</i>	Endangered	Endangered
<b>Toothed whales</b>			
Short-beaked common dolphin	<i>Delphinus delphis</i>	Not at risk	Not listed
Striped dolphin	<i>Stenella coeruleoalba</i>	Not at risk	Not listed
White-beaked dolphin	<i>Lagenorhynchus albirostris</i>	Not at risk	Not listed
White-sided dolphin	<i>L. acutus</i>	Not at risk	Not listed
Bottlenose dolphin	<i>Tursiops truncatus</i>	Not at risk	Not listed
Risso's dolphin	<i>Grampus griseus</i>	Not at risk	Not listed
Killer whale	<i>Orcinus orca</i>	Special concern	Not listed <sup>2</sup>
Atlantic spotted dolphin	<i>Stenella frontalis</i>	Not at Risk	Not listed
Long-finned pilot whale	<i>Globicephala melas</i>	Not at risk	Not listed
Harbour porpoise	<i>Phocoena phocoena</i>	Special concern	Not listed
Pygmy sperm whale	<i>Kogia breviceps</i>	Not at risk	Not listed
Dwarf sperm whale	<i>Kogia sima</i>	Not at risk	Not listed
Sperm whale	<i>Physeter macrocephalus</i>	Not at risk	Not listed
Cuvier's beaked whale	<i>Ziphius cavirostris</i>	Not at risk	Not listed
Sowerby's beaked whale	<i>Mesoplodon bidens</i>	Special concern	Special concern
Northern bottlenose whale (Davis Strait-Baffin Bay-Labrador Sea Population)	<i>Hyperoodon ampullatus</i>	Special Concern	Not Listed
Northern bottlenose whale (Scotian Shelf population)		Endangered	Endangered <sup>1</sup>
Gervais beaked whale	<i>M. europaeus</i>	Not assessed	Not listed
True's beaked whale	<i>M. mirus</i>	Not at risk	Not listed
<b>Pinnipeds</b>			
Grey seal	<i>Halichoerus grypus</i>	Not at risk	Not listed
Hooded seal	<i>Cystophora cristata</i>	Not at risk	Not listed
Bearded seal	<i>Erignathus barbatus</i>	Not assessed	Data deficient
Harp seal	<i>Phoca groenlandica</i>	Not at risk	Not assessed
Harbour seal	<i>P. vitulina</i>	Not at risk	Not listed
Ringed seal	<i>Pusa hispida</i>	Special Concern	Not listed

<sup>1</sup> Status of the Scotian shelf population

<sup>2</sup> Under consideration for addition.

Table 4. Acoustic signals used for identification or automated detection of the species that could potentially occur in the study area and supporting references.

Species	Identification signal	Example reference(s)
Minke whale	Pulse train	Risch et al. (2013)
Sei whale	Downsweep	Baumgartner et al. (2008)
Blue whale	A-B note, D-call, and Arch call	Mellinger and Clark (2003), Berchok et al. (2006)
Fin whale	20 Hz pulse, broadband downsweep, 130 Hz pulse	Watkins (1981), Watkins et al. (1987)
Humpback whale	Moans and grunts of songs and non-songs	Dunlop et al. (2008), Kowarski et al. (2018)
North Atlantic right whale	Upcall, gunshot, and moan	Parks et al. (2005), Parks and Tyack (2005)
Small dolphin <sup>1</sup>	Whistle and click	Steiner (1981), Rendell et al. (1999), Oswald et al. (2003)
Killer whale	Whistle and click	Ford (1989), Deecke et al. (2005)
Long-finned pilot whale	Whistle and click	Nemiroff and Whitehead (2009)
Harbour porpoise	Click	Au et al. (1999)
Pygmy sperm whale	Click	Marten (2000)
Sperm whale	Click	Møhl et al. (2000), Møhl et al. (2003)
Cuvier's beaked whale	Click	Zimmer et al. (2005)
Sowerby's beaked whale	Click	Cholewiak et al. (2013)
Northern bottlenose whale	Click	Hooker and Whitehead (2002), Wahlberg et al. (2011)
Gervais beaked whale	Click	Gillespie et al. (2009)
True's beaked whale	Click	DeAngelis et al. (2018)
Grey seal	Grunt and moan	Asselin et al. (1993)
Hooded seal	Miscellaneous sounds categorized as Class A and C	Ballard and Kovacs (1995)
Bearded seal	Trill	Cleator et al. (1989), Jones et al. (2014)
Harp seal	Miscellaneous sounds	Serrano (2001), Rossong and Terhune (2009)
Harbour seal	Roar	Van Parijs and Kovacs (2002)

<sup>1</sup>Small dolphin include all delphinid species from Table 3 other than killer and long-finned pilot whales.

## 1.2.4. Changes to Sound as it Travels in the Ocean

A key question in the study of underwater sound is how a sound changes in nature as it propagates from its source to a receiver some distance away. Understanding and modelling sound propagation in the ocean is a complex topic that is the subject of numerous textbooks. This section provides a descriptive overview of key sound propagation concepts to assist with interpreting the results presented in this report. These concepts are integral to interpreting how sounds emitted by a source are transformed into those received some distance away. The sounds are transformed by 1) geometric spreading; 2) reflection, scattering, and absorption at the seabed and sea surface; 3) refraction due to changes in sound speed with depth; and 4) absorption.

At one extreme, the echolocation clicks of porpoises at 130 kHz travel only 500 m before becoming inaudible. At the other extreme, sounds from fin whales (20 Hz) and low-frequency energy from seismic airguns (5–100 Hz) can be detected thousands of kilometers away under the right conditions (Nieukirk et al. 2012).

*Geometric spreading losses:* Sound levels from an omnidirectional point source in the water column are reduced with range, a process known as *geometric spreading loss*. As sound leaves the source, each spherical sound wave propagates outward and the sound energy is spread out over this ever-expanding

sphere, as depicted in purple in Figure 8. The farther you are from the source, the lower the sound level you will receive. The received sound pressure levels at a recorder located a distance  $R$  (in m) from the source are  $20\log_{10}R$  dB lower than the source level (SL) referenced to a standard range of 1 m. But the sound cannot spread uniformly in all directions forever. Once the waves interact with the sea surface and seabed, the spreading becomes cylindrical (as depicted in green in Figure 8) rather than spherical and is limited to the cylinder formed by the surface and seabed with a lower range-dependent decay of  $10\log_{10}R$  dB. Thus, the water depth is a key factor in predicting spreading losses and thus received sound levels. These spherical and cylindrical spreading factors provide limits for quick approximations of expected levels from a given source. In very shallow waters, sound rapidly attenuates if the water depth is less than a quarter of a wavelength (Urlick 1983).

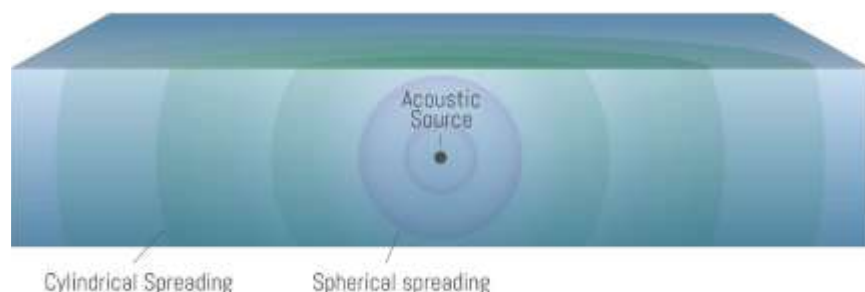


Figure 8. A depiction of the geometric spreading of sound as it propagates away from an acoustic source. Spherical spreading (purple) occurs at closer ranges, and, once the sound reaches the sea surface and seafloor, the spreading becomes cylindrical (green) at farther ranges.

*Absorption, reflection, and scattering at the sea surface and seabed:* If geometric spreading were the only factor governing sound attenuation in water, then at a given distance from a source, sound levels in shallow waters would almost always be higher than those in deep waters. In shallow water, however, the sound interacts more often with the seabed and sea surface than sound travelling in deep waters, and these interactions cause some of the sound to be reflected, absorbed, or scattered. The sea surface behaves approximately as a pressure release boundary, where incident sound is almost completely reflected with opposite phase. As a result, the sum of the incident and reflected sounds at the sea-surface is zero, i.e., there is no acoustic pressure at the surface. At the seabed, many types of interactions can occur depending on the composition of the bottom. Soft silt and clay bottoms absorb sound, sand and gravel bottoms tend to reflect sound like a partially reflective mirror, and some hard yet elastic bottoms, such as limestone, reflect some of the sound while absorbing some of the energy by converting the compressional waves to elastic shear waves that propagate through the seabed.

*Absorption by sea water:* As sound travels through the ocean, some of the energy is absorbed by molecular relaxation in the seawater, which turns that acoustic energy into heat. The amount of absorption that occurs is quantified by an attenuation coefficient, expressed in units of decibels per kilometre (dB/km). This absorption coefficient depends on the temperature, salinity, pH, and pressure of the water, as well as the sound frequency. In general, the absorption coefficient increases with the square of the frequency, so low frequencies are less affected. The absorption of acoustic wave energy has a noticeable effect ( $>0.05$  dB/km) at frequencies above 1 kHz. For example, at 10 kHz the absorption loss over 10 km distance can exceed 10 dB (as computed according to the formulae of François and Garrison (1982a, b)).

*Refraction due to sound speed changes:* As a rule of thumb, sound is 'lazy', it wants to travel at the slowest possible speed. When the sound speed changes with depth, which it almost always does, the sound refracts

toward the depth with the lowest sound speed, which can result in sound being trapped in a duct and travelling very long distances with minimal attenuation. Conversely, in conditions where the sound speed decreases with depth, sound is refracted towards the seabed and may not reach an intended receiver. The sound speed is a function of the temperature, salinity, and pressure (depth). Colder and fresher water has a lower sound speed and, conversely, warmer and saltier water has a higher sound speed. As the water depth increases the pressure increases the water density slightly, which increases the sound speed (Jensen et al. 2011). These effects combine with environmental forces such as solar heating, wind mixing, and currents to constantly affect the sound speed in the upper 500 m of the water column which has daily variations around typical seasonal means (Figure 9). The ability of a minimum in the sound speed profile to trap sound depends on the magnitude of the sound speed change at the minimum, the vertical height of the minimum and the sound's wavelength. Ducts must be several times larger than the wavelength for effective trapping of sound (Etter 1996). A corollary of this effect is that higher frequencies are refracted more readily by sound speed changes than lower frequencies that have longer wavelengths. It is also possible for the sound speed to change with horizontal location, which leads to three-dimensional refraction of sound, however, this is far less common than refraction due to sound speed changes with depth.

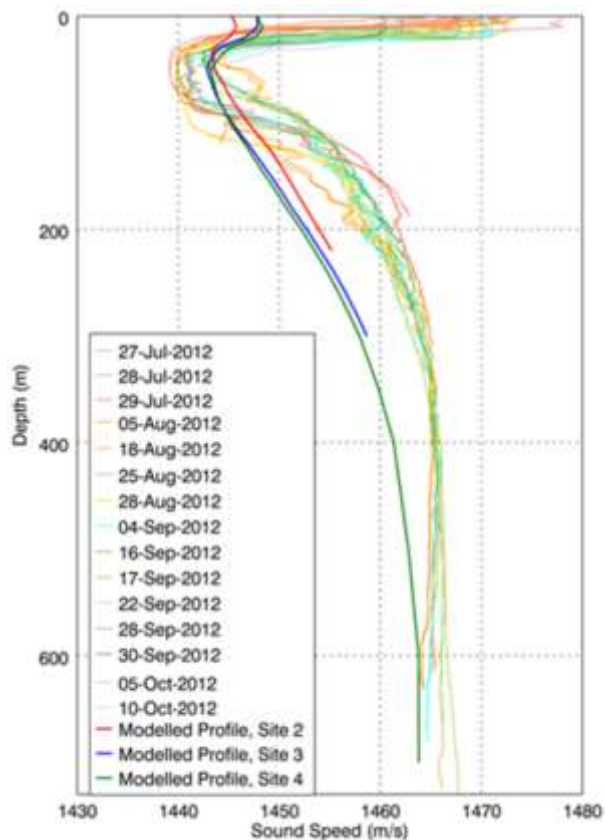


Figure 9. Example of seasonal sound speed profiles from (Teague et al. 1990) (Modelled Profiles) and actual sound speed profiles measured in situ in Baffin Bay.

## 2. Methods

### 2.1. Data Acquisition

#### 2.1.1. Deployment Locations

Underwater sound was intended to be recorded with two Autonomous Multichannel Acoustic Recorders–Generation 4 (AMAR; JASCO) in glass sphere housings. Each AMAR was fitted with four M36 omnidirectional hydrophones (GeoSpectrum Technologies Inc.;  $-165 \pm 3$  dB re 1 V/ $\mu$ Pa sensitivity). The AMAR hydrophones were protected by a hydrophone cage and encased in open-cell foam to minimize noise artifacts from water flowing over the hydrophone.

The AMARs were deployed at two locations indicated in Figure 10 as ALTO1 and ALTO2 and positioned 1 km and 40 km away from the STENA ICEMAX, respectively (see also Table 5). The AMARs recorded for 9 min out of 10 at 32 kHz, alternating with 1 min every 10 min at 512 kHz. Table 5 presents the exact coordinates, depths, duration of the deployment, and distance to the STENA ICEMAX.

Unfortunately, the AMAR (ALTO1) located 1 km from the well site did not collect any data due to equipment failure. All pre-deployment check were completed on deck and indicated the recorder was functioning properly. Data recording ceased when the equipment was at depth, presumably due to the electrical connection to the hydrophone being ‘pinched-off’ under pressure. During equipment recovery data recording resumed as the water pressure reduced. This type of equipment failure has never occurred before and the failed components replaced.

The lower frequency sampling rate of 32 kHz was higher than the 16 kHz stated in the Marine Sound Monitoring Plan. This change was made to during mobilization of the acoustic recorders because additional memory space was available. The change provided more data for evaluating the presence of delphinid whistles and had no other impacts on the monitoring objectives.

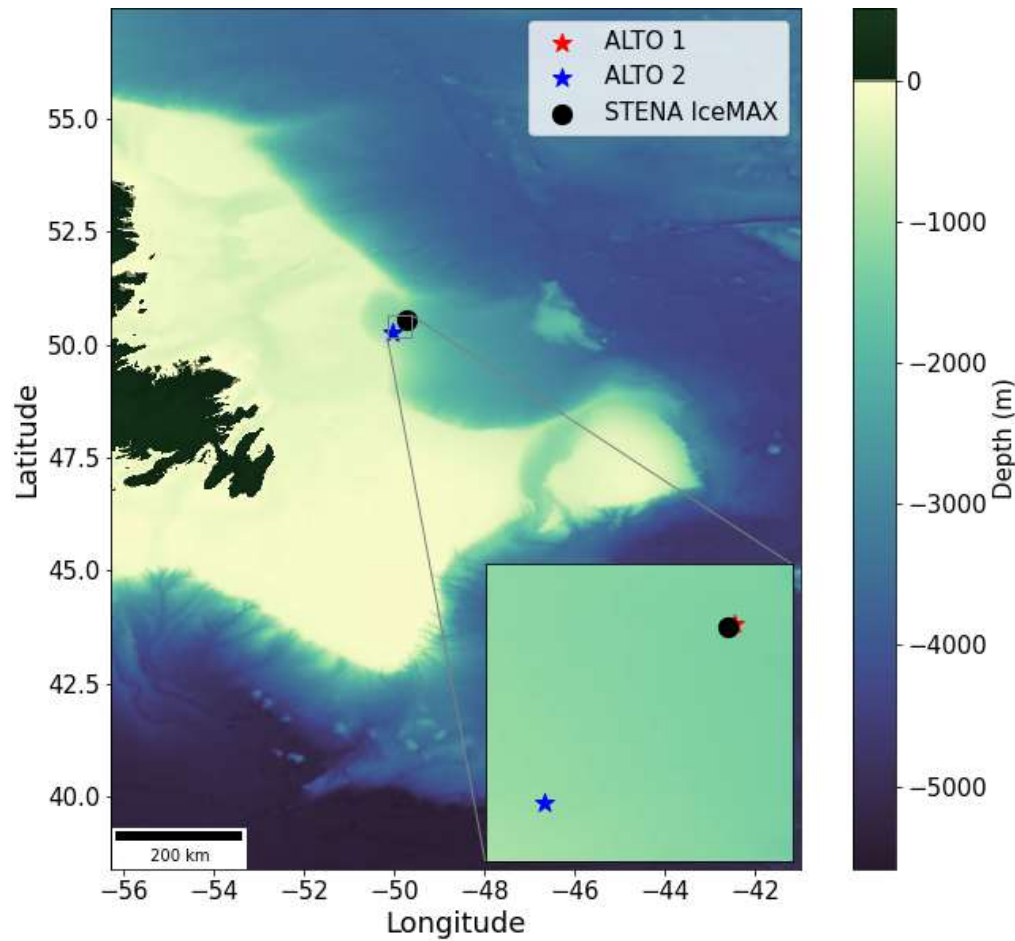


Figure 10. Study areas showing the recording locations ALTO 1 and ALTO 2 as red and blue stars, respectively, and the STENA ICEMAX as a black dot.

Table 5. Operation period, location, and water depth of the Autonomous Multichannel Acoustic Recorders (AMARs) deployed for the Orphan Basin study.

Station	Latitude (°N)	Longitude (°E)	Depth (m)	Start	End	Duration (days)	Distance to EPHEBUS (km)
ALTO 1	50.5611	-49.7320	1328	10 Apr 2023	07 Jul 2023	88	0.964
ALTO 2	50.2560	-50.0554	1308	10 Apr 2023	07 Jul 2023	88	40

## 2.1.2. Non-Acoustic Data

### 2.1.2.1. Meteorological Data

Meteorological and oceanographic data were compiled on the STENA ICEMAX in the form of daily reports generated by the onboard weather observer. Hourly wind speed and significant wave heights were extracted for comparisons to the sound from the STENA ICEMAX and ambient sound levels. Figure 11

shows the wind speed and significant wave height from 7 May to 1 July at ALTO1 corresponding to the period when the STENA ICEMAX was in field.

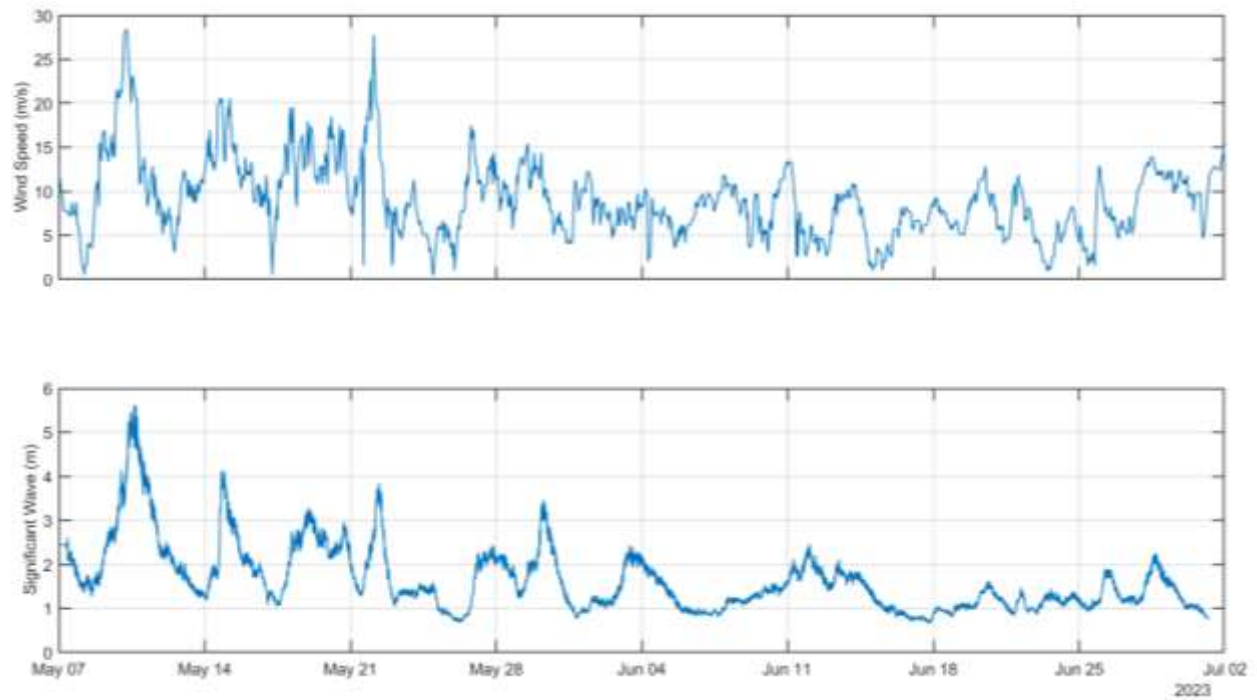


Figure 11. Wind speed and significant wave height data at ALTO1 station from 7 May to 1 July.

### 2.1.2.2. Sound Speed Profiles

Sound speed profiles near the ALTO1 and ALTO 2 stations were extracted from the Global Ice Ocean Prediction System (GIOPS) archive for 15 Apr, 15 May, 15 June, and 15 July 2023 (Environment and Climate Change Canada 2021). The sound speed profiles changed substantially near the surface as the seasons progressed from spring to summer; however, the deep-water conditions remained static throughout. The profile in April and May would cause the sound to refract upwards and reflect off the sea surface, enhancing low frequency propagation but impeding high frequency. The low-speed duct in the SSPs in June and July at 30 – 50 m support very efficient propagation of sounds above ~100 Hz at those depths. Transmission of sound to the recorders would be about the same in both cases.

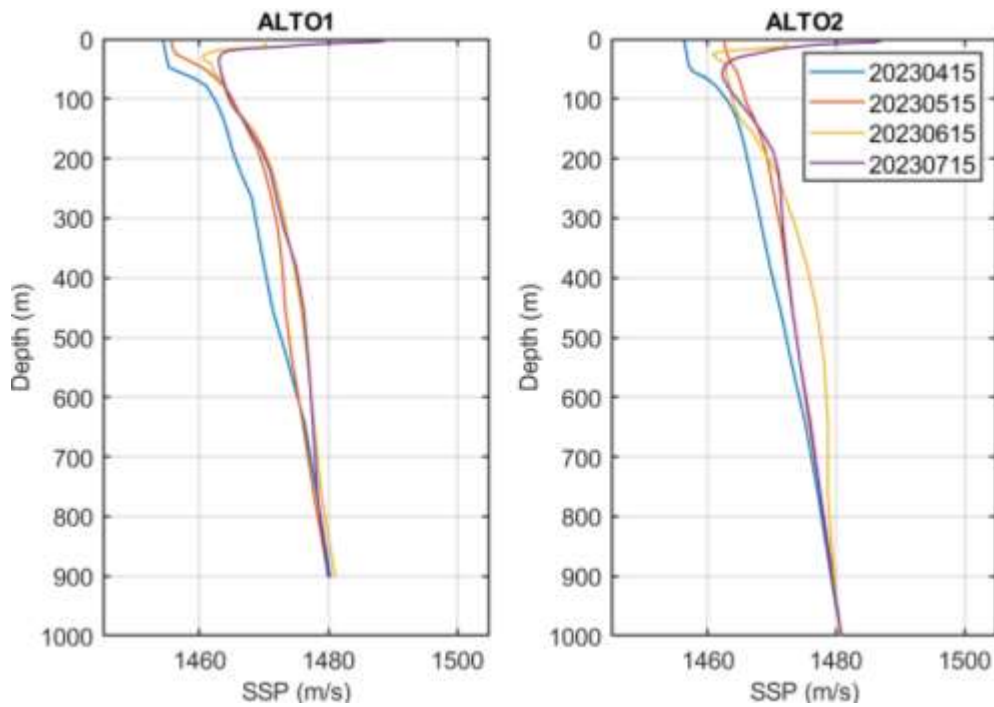


Figure 12. Sound speed profiles (SSPs) near the recording sites for 15 Apr, 15 May, 15 June, and 15 July 2023 as extracted from GIOPS archive.

## 2.2. Automated Data Analysis

The AMAR located at 40 km from the STENA ICEMAX collected approximately 3.9 TB of acoustic data. All acoustic data were processed with JASCO's PAMlab software suite, which processes acoustic data hundreds of times faster than real time. PAMlab performed automated analysis of total ocean noise and sounds from vessels, drilling activities, and marine mammal vocalizations. The following sections describe each type of analysis. Appendix A and A.1 provide further details of the processing algorithms.

### 2.2.1. Soundscape and Time Series Analysis

The recorded data were analyzed to quantitatively describe the area's underwater soundscape. The raw pressure waveform data were scaled according to the mean calibrated voltage sensitivity of the recorders and adjusted for the amplitude and frequency response of the hydrophone sensor. An end-to-end laboratory AMAR calibration was performed with a pistonphone type 42AC precision sound source (G.R.A.S. Sound & Vibration A/S) at 250 Hz and from about 4 Hz to 1000 kHz on all channels.

The first stage of the sound level analysis involved computing the peak (PK) and root-mean-square (rms) sound pressure level (SPL) for each minute of data. This reduced the data to a manageable size without compromising the value for characterising the soundscape (ISO 2017b, Ainslie et al. 2018, Martin et al. 2019). SPL analysis was performed by averaging 120 fast-Fourier transforms (FFTs) that each included 1 s of data with a 50 % overlap that use the Hann window to reduce spectral leakage. The 1-min average data were stored as power spectral densities (1 Hz resolution up to 435 Hz and millidecades frequency bands above 435 Hz) and summed over frequency to calculate decidecade band SPL. Decidecade band levels are very similar to 1/3-octave-band levels.

Martin et al. (2021) describes the millidecade band analysis approach. Millidecades are logarithmically spaced frequency bands but have a bandwidth equal to 1/1000th of a decade. Using millidecades instead of 1 Hz frequency bands reduced the size of the spectral data by a large factor without compromising the usefulness of the data.

Appendix A lists the decade-band frequencies. The decidecade analysis sums as many frequencies as contained in the recorded bandwidth in the power spectral density data to a manageable set of up to 45 bands that approximate the critical bandwidths of mammal hearing. Decade bands further summarize the sound levels into four frequency bands for manageability. Detailed descriptions of acoustic metrics and decidecade analysis can be found in Appendices A.1.1 and A.1.2.

The ambient sound level results are provided in spreadsheet format compiled by file and by minute as well as graphical outputs, as follows:

- **Band-level plots:** These strip charts show the averaged received sound pressure levels as a function of time within a given frequency band. We show the total sound levels (across the entire recorded bandwidth from 10–16,000 Hz) and the levels in the decade bands of 8.9–89.1 Hz (Decade A); 89.1–891.3 Hz (Decade B); 891.3–8,913 Hz (Decade C); and 8,913–16,000 Hz (Decade D), depending on the recording bandwidth. The 8.9–89.1 Hz band is generally associated with fin and blue whales, large shipping vessels, flow and mooring noise, and seismic survey impulses. Sounds within the 89.1–891.3 Hz band are generally associated with the physical environment such as wind and wave conditions but can also include both biological and anthropogenic sources such as minke and humpback whales, fish, smaller vessels, seismic surveys, and pile driving. Sounds above 1000 Hz include high-frequency components of humpback whale sounds, odontocete whistles and echolocation

signals, rain-generated sounds, and sounds from human sources at close range including pile driving, vessels, seismic surveys, and sonars.

- **Long-term Spectral Averages (LTSAs):** These colour plots show power spectral density levels as a function of time ( $x$ -axis) and frequency ( $y$ -axis). The frequency axis uses a logarithmic scale, which provides equal vertical space for each decade increase in frequency and allows the reader to equally see the contributions of low and high-frequency sound sources. The LTSAs are excellent summaries of the temporal and frequency variability in the data.
- **Decidecade box-and-whisker plots:** In these figures, the 'boxes' represent the middle 50 % of the range of sound pressure levels measured, so that the bottom of the box is the sound level 25th percentile ( $L_{25}$ ) of the recorded levels, the bar in the middle of the box is the median ( $L_{50}$ ), and the top of the box is the level that exceeded 75 % of the data ( $L_{75}$ ). The whiskers indicate the maximum and minimum range of the data.
- **Spectral density level percentiles:** The decidecade box-and-whisker plots are representations of the histogram of each band's sound pressure levels. The power spectral density data has too many frequency bins for a similar presentation. Instead, coloured lines are drawn to represent the  $L_{eq}$ ,  $L_5$ ,  $L_{25}$ ,  $L_{50}$ ,  $L_{75}$ , and  $L_{95}$  percentiles of the histograms. Shading is provided underneath these lines to provide an indication of the relative probability distribution. It is common to compare the power spectral densities to the results from Wenz (1962), which documented the variability of ambient spectral levels off the US Pacific coast as a function of frequency of measurements for a range of weather, vessel traffic, and geologic conditions. The Wenz levels are appropriate for approximate comparisons only since the data were collected in deep water before the known increase in low-frequency sound levels attributed to the increase in maritime shipping (Andrew et al. 2011).

In addition, daily frequency-weighted sound exposure levels (SEL) were calculated for all hearing frequency groups (see Appendix A.1.1 and A.2 for details).

A correlation analysis was also performed to assess the influence of wind speed on sound levels in selected decidecade bands. Wind speeds were acquired for each station from NOAA's ERDAPP database (NOAA 2023), which is based on the Navy Global Environmental Model (NAVEM) that provides 10-m wind speed at a 0.5 degree resolution.

## 2.2.2. Vessel Noise Detection

The boat and vessel detectors compare sound levels in established frequency range to criteria values. If the criterion is met, a 'shippingFlag' value of either 1 (boat/vessel is present) or 4 (boat/vessel is nearby) is set. The highest sound level within the minutes flagged as having a boat present is assigned as the closest point of approach (CPA). The criteria values are outlined in Table 6; criteria names are shown in italics in the description below. Previously, this detector detected vessels, so the following criteria were adjusted to detect boats, which are quieter and emit more sound at higher frequencies:

- The background SPL within the frequency range is calculated as a long-term average over the *Background window duration*.
- Each minute's SPL (within the frequency range) must be greater than the background value by the *Shipping to background threshold*.

- Each minute's SPL (within the frequency range) must exceed the total broadband SPL by the *Shipping to RMS Threshold*.
- Each minute's SPL must be greater than the *Minimum broadband SPL*.
- The average number of tonals detected over a *Minimum shipping duration* minute window must be greater than *Minimum number of shipping tonals*.
- The duration of the shipping detection must be greater than *Minimum shipping duration* and less than *Maximum shipping duration*.

If all criteria are met, the 'shippingFlag' is set to 1, indicating that a boat or vessel is present in that minute of data. We then assume that the anthropogenic shoulder before and after the shipping detection flag '1' values have energy from the vessel that did not meet the criteria and should not be considered as 'ambient'. This window is given a value of 4 for the shipping detection flag. This system of 1 and 4 attempts to distinguish between vessels/boats that are nearer and farther from the AMAR, i.e., for large vessels, the sequence is typically a series of flags of 4 (approach), then 1 (over/nearest), and then 4 (departure).

Vessel detections were defined by the following three criteria:

- SPL in the shipping band was at least 3 dB above the median.
- At least five shipping tonals (0.125 Hz bandwidth) were present.
- SPL in the shipping band was within 8 dB of the broadband SPL (Figure 13).

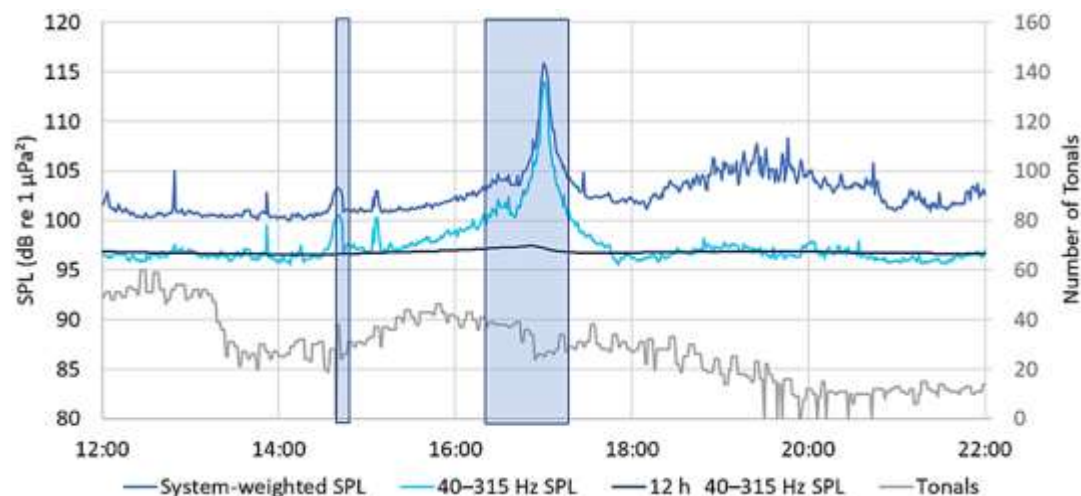


Figure 13. Example of broadband and 40–315 Hz band sound pressure level (SPL), as well as the number of tonals detected per minute as a vessel approached a recorder, stopped, and then departed. The shaded area is the period of shipping detection. Fewer tonals are detected at the ship's closest point of approach (CPA) at 17:00 because of masking by broadband cavitation noise and due to Doppler shift that affects the tone frequencies.

Table 6. Parameters of the boat and vessel detector.

Parameter	Unit	Vessel detector	Boat detector
$f_{\min}$ flag	Hz	40	315
$f_{\max}$ flag	Hz	315	2000
Minimum broadband SPL	dB	105	95
Minimum number of shipping tonals		3	0.49
Background window duration	min	720	720
Minimum shipping duration	min	5	3
Maximum shipping duration	min	360	60
Typical shipping passing duration	min	30	10
Shipping to background threshold	dB	3	3
Shipping to RMS threshold	dB	12	15
Anthropogenic shoulder	min	15	15

### 2.2.3. Marine Mammal Detection Overview

We used a combination of automated detector-classifiers (referred to as automated detectors) and manual review by experienced analysts to determine the presence of sounds produced by marine mammals in the acoustic data. First, a suite of automated detectors was applied to the full data set (see Appendices B.1 and B.2). Second, subsets (~0.8 %) of acoustic data for each sampling rate were selected for manual analysis of marine mammal acoustic occurrence. Each subset was selected based on automated detector results via our Automatic Data Selection for Validation (ADSV) algorithm (Kowarski et al. 2021) (see Appendix B.3). Third, manual analysis results were compared to automated detector results to determine automated detector performance (see Appendix B.4). Finally, hourly marine mammal occurrence plots that incorporated both manual and automated detections were created and automated detector performance metrics were provided (see Section 3.3) to give a reliable representation of marine mammal presence in the acoustic data. These marine mammal analysis steps are summarised here and described in detail in Appendix B. Where automated detector results were unreliable or did not add additional information to species occurrence, only the validated results from manual analysis are presented.

#### 2.2.3.1. Automated Click Detection

Odontocete clicks are high-frequency impulses ranging from 1 to over 150 kHz (Au et al. 1999, Møhl et al. 2000). We applied an automated click detector to the high-frequency data (audio bandwidth up to 256 kHz) to identify clicks from sperm whales, beaked whales, porpoises, and delphinids. This automated detector is based on zero-crossings in the acoustic time series. Zero-crossings are the rapid oscillations of a click's pressure waveform above and below the signal's normal level (e.g., see Figure B-1). Zero-crossing-based features of automatically detected events are then compared to templates of known clicks for classification (see Appendix B.1 for details).

### 2.2.3.2. Automated Tonal Signal Detection

Tonal signals are narrowband, often frequency-modulated, signals produced by many species across a range of taxa (e.g., baleen whale moans, delphinids whistles). They range predominantly between 15 Hz and 4 kHz (Berchok et al. 2006, Risch et al. 2007), thus automated detectors for these species were applied to the low-frequency data (audio bandwidth up to 16 kHz). In contrast, the automated detector for small dolphin tonal acoustic signals was applied to the high-frequency data, as these whistles can reach 20 kHz (Steiner 1981). The automated tonal signal detector identified continuous contours of elevated energy and classified them against a library of marine mammal signals (see Appendix B.2 for details).

### 2.2.3.3. Automated Detector Validation

JASCO's suite of automated detectors are developed, trained, and tested to be as reliable and broadly applicable as possible. However, the performance of marine mammal automated detectors varies across acoustic environments (e.g., Hodge et al. 2015, Širović et al. 2015, Erbs et al. 2017, Delarue et al. 2018). Therefore, automated detector results must always be supplemented by some level of manual review to evaluate automated detector performance. Here, we manually analysed a subset of acoustic files for the presence/absence of marine mammal acoustic signals via spectrogram review in JASCO's PAMlab software. A subset (0.8 %) of acoustic data was selected via ADSV for manual review (see Appendix B.3).

To determine the performance of the automated detectors per acoustic file, the automated and manual results (excluding files where an analyst indicated uncertainty in species occurrence) were fed into an algorithm that calculates precision ( $P$ ), recall ( $R$ ), and Matthew's Correlation Coefficient ( $MCC$ ) (see Appendix B.4 for formulas).  $P$  represents the proportion of files with detections that are true positives. A  $P$  value of 0.90 means that 90 % of the files with automated detections truly contain the targeted signal, but it does not indicate whether all files containing acoustic signals from the species were identified.  $R$  represents the proportion of files containing the signals of interest that were identified by the automated detector. An  $R$  value of 0.90 means that 90 % of files known to contain a target signal had automated detections, but it says nothing about how many files with automated detections were incorrect. An  $MCC$  is a combined measure of  $P$  and  $R$ , where an  $MCC$  of 1.00 indicates perfect performance: all known events were correctly automatically detected. The algorithm determines a per file automated detector threshold (the number of automated detections per file at and above which automated detections were considered valid) that maximizes the  $MCC$ .

For many species, more than one automated detector targeted their vocalisations. In these instances, the performance of all automated detectors was evaluated, and the highest performing detector (or combination of detectors) used to represent species/vocalisation-type occurrence in Section 3.3. Only automated detections associated with a  $P$  greater than or equal to 0.75 were considered. When  $P < 0.75$ , only the validated results were used to describe the acoustic occurrence of a species.

The occurrence of each species (both validated and automated, or validated only where appropriate) was plotted using JASCO's Ark software as time series showing presence/absence by hour over each day of the recording period and daily count of detection hours, where necessary. Automated detector performance metrics associated with results are included in Section 3.3 and should be considered when interpreting results.

#### 2.2.3.4. Absolute Minimum Number of Animals Present Analysis

The four hydrophones on the ALTO lander were processed to determine the direction of arrival of sounds. The analysis was performed using a maximum likelihood estimation (MLE) beamformer (Urazghildiiev and Hannay 2017). This beamformer estimates the sound level assuming the sounds are arriving from azimuthal directions separated by 10 degrees, and for each azimuth it evaluates 10 elevation angles, also separated by 10 degrees, for a total of 360 'look directions' or beams. The beam with the greatest received level is selected as the most likely direction of arrival. This process is applied to marine mammal detections in the frequency range of 10 – 750 Hz (see Section 2.2.3.2). It is applied to each frequency in the detection, and the bearing values are weighted by the energy in the frequency bin, so that the direction assigned to the call is the energy weighted direction.

The absolute minimum number (AMN) of marine mammals present can be determined by counting the number of directions that a species' calls arrive from over a short period of time; 10 min was employed here. The bearing errors from the beamformer are inversely proportional to the frequency and signal to noise ratios (SNR), i.e., the errors are greater at low frequency and low SNR (see Appendix B.5); therefore, low SNR calls are not considered for counting the minimum number of animals present. Once the low SNR calls are removed, the bearing accuracy for very low frequency fin and blue whale calls (~15–25 Hz) is on the order of 120 degrees, ~50 degrees for Sei whales and improving to 10 degrees for calls around 250 Hz from humpback whales or right whales. All calls within these bearing errors are assumed to be from the same animal, which establishes the AMN (i.e.,  $\pm 50$  degrees for Sei whales). The maximum number of animals detected in the 144 10-min windows per day is the daily AMN. This is a highly conservative estimation method since it does not allow for multiple animals to occur within the same bearing window. Validation of this assumption against visual monitoring or tagging studies would be helpful. Future versions of the ALTO landers will also include a wider spacing between hydrophones to reduce the bearing uncertainties at low frequency.

The resulting directional and AMN data are presented in a variety of formats. Figure 14 is an example summary presentation of the total daily detections, daily AMN, and bearing-time (BTI) results for a recording program that detected five types of mysticete calls. This figure may be used for a single species, or for all species detected in which case the species are colour-coded. In Figure 14 the BTI plot presents all detections as dots. The BTI can also be displayed as a density to investigate if there are preferred directions for a single species (Figure 15). The total number of calls as a function of bearing may be output as a polar plot (Figure 16).

Details of the beamforming and AMN analysis are provided in Appendix B.5.

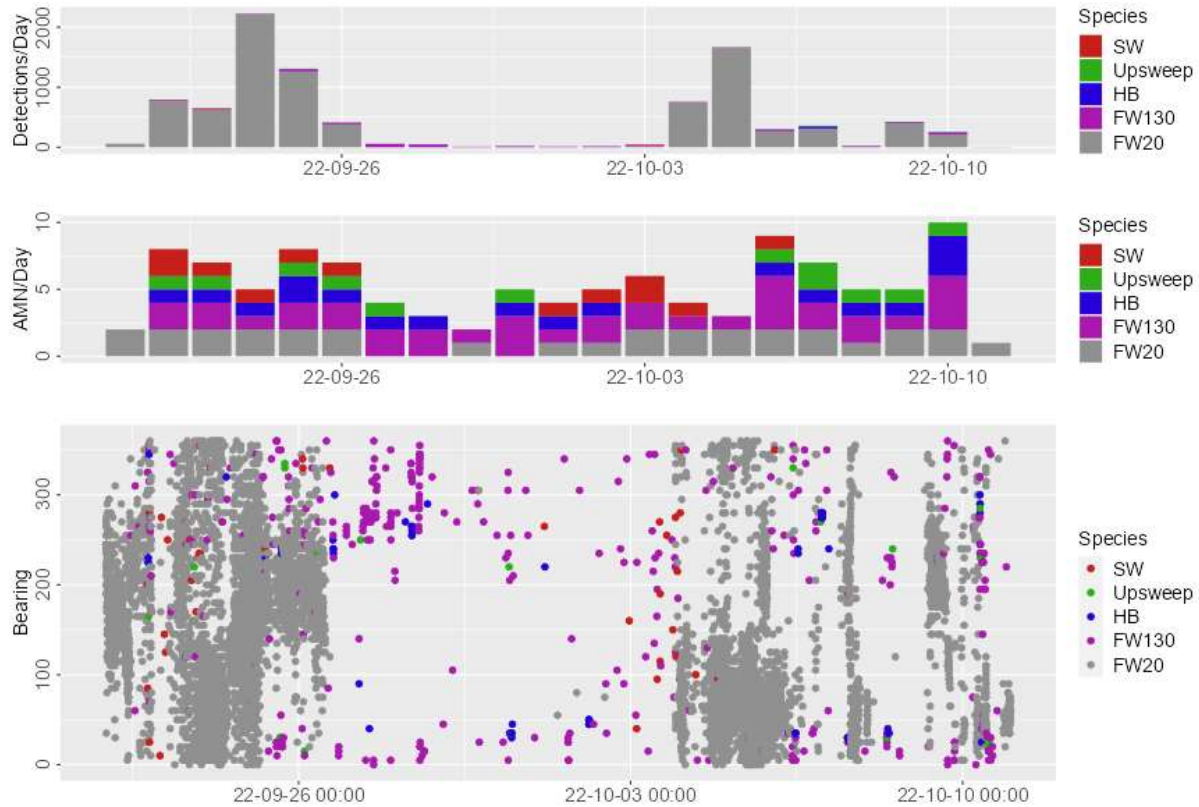


Figure 14. Example of a summary directional data presentation. (Top) Number of detections per day, coloured by species. (Middle) Absolute Minimum Number (AMN) of mammals detected per day, which is the maximum per day of the AMN per 10-min time block. (Bottom) Time-bearing presentation where the most common species is drawn behind the other species.

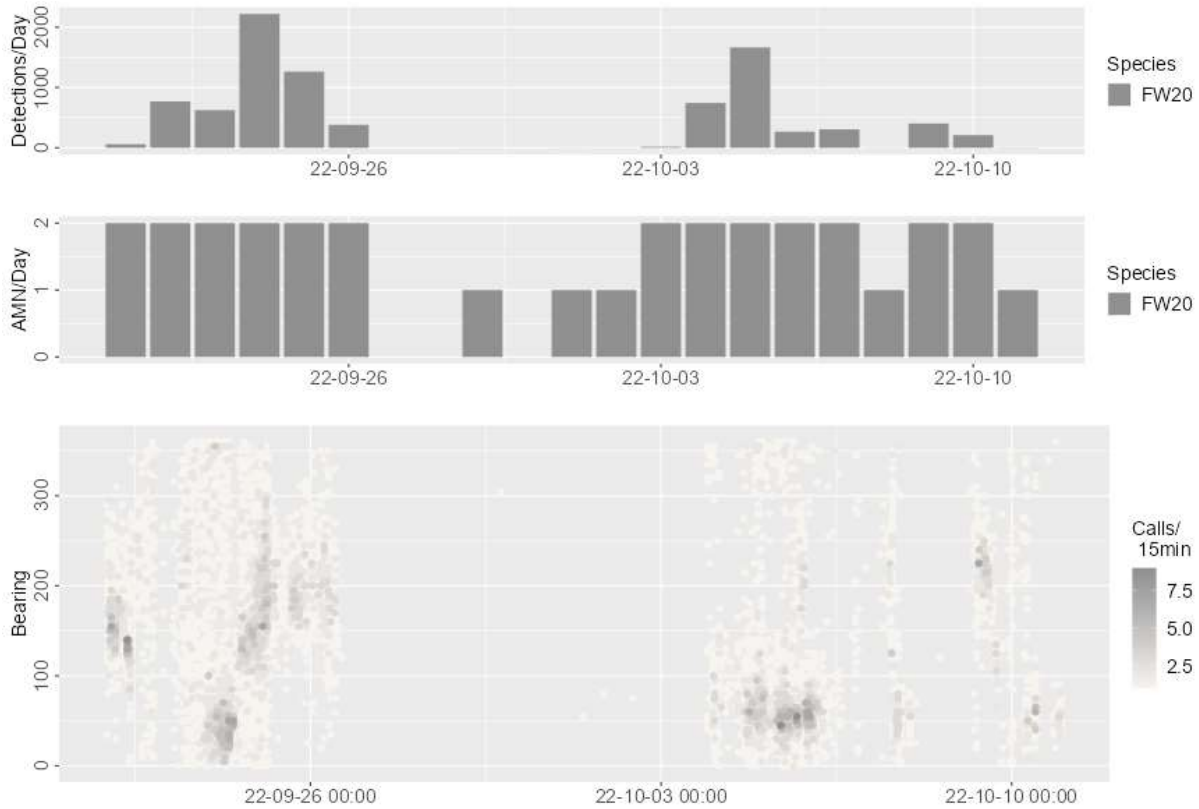


Figure 15. Data from Figure 14 where only the FW 20 Hz call detections have been selected and the BTI plot changed to a density plot.

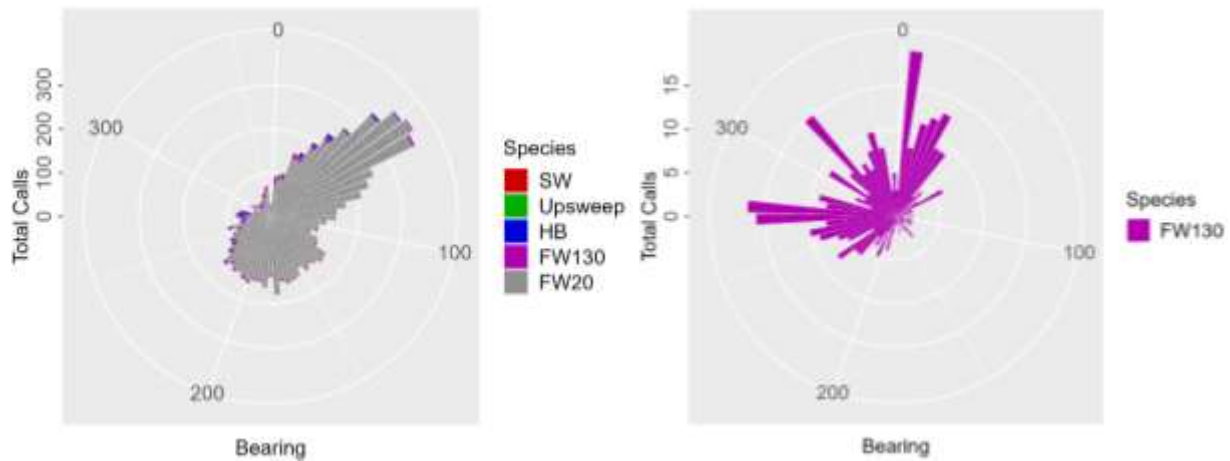


Figure 16. Example of a polar plot to show the distribution of directions of arrival for (left) all species and for a single species (fin whale 130 Hz pulses).

## 2.3. Detection Range Modelling

Detection Range Modelling (DRM) was conducted to estimate the detectability of vocalizations of all marine mammal species detected at each recorder. The detection range results offer an opportunity to assess the effects of drilling activities (primarily the presence of the drillship and support vessels) on the detection ranges of marine mammals, which influences the effectiveness of passive acoustic monitoring efforts and can also be seen as proxy for the communication space of each species.

The DRM considered the following data inputs to estimate species-specific detection distances:

- Ambient decedecade sound pressure level (SPL) percentiles measured at each station;
- Local bathymetry, geology, and sound speed profile (see Appendix C.2); and
- Published marine mammal vocalization source level and bandwidth characteristics, as well as vocalization depth (see Appendix C.3).

The detection range is defined as the range at which the expected sound level of a mammal vocalization is  $X$  dB above the expected background level, where  $X$  is the detection threshold of the relevant detector for a given species. Modelled signal-to-noise ratios (SNRs) were calculated at discrete locations within a three-dimensional (3-D) volume (easting, northing, and depth) to predict a detection range. The detection range, therefore, represents the maximum range at which a signal of a given source level can be identified by a detector in given background noise conditions. This underestimates the range to which vocalizations could be detected by experienced human analysts conducting a fine-scale analysis.

To compute the detection range, an estimate of the sound's propagation loss between the vocalizing animal and the recorder is required. To perform the propagation loss calculations in a computationally efficient manner, we applied the reciprocity principle, which states that an identical signal will be received between a source and receiver pair if their coordinates are inter-changed (Jensen et al. 2011). So rather than performing individual propagation loss calculations for a source at many locations (e.g., an animal) to the receiver to estimate SNR and detectability, the loss between source and receiver is computed by setting the source location for the propagation model to be the location of the seafloor recorder. The propagation loss from this position was then calculated to all locations within the ocean interior in a single execution of the model, thereby reducing the number of individual propagation loss computations that would be required otherwise.

Depending on the frequency characteristics of the marine mammal source level inputs, two potential sound propagation models were used to predict the loss between animal and recorder:

- JASCO's Marine Operations Noise Model (MONM; see Appendix C.1), a range-dependent parabolic equation model for frequencies up to 2 kHz, and/or
- The BELLHOP Gaussian beam acoustic ray-trace model for frequencies above 2 kHz.

The MONM and BELLHOP results were combined as required to produce results for the full frequency range for the species of interest. Appendix C contains additional information on the propagation models used for detection range estimation.

Propagation loss was calculated up to a maximum distance of 150 km at ALTO2 for baleen whale calls and sperm whale clicks. A horizontal separation of 50 m between receiver points along the modelled radials was used. For all other species (delphinids, beaked whales and harbour porpoise), propagation loss was calculated up to a maximum distance of 30 km with a horizontal separation of 20 m between receiver points. The propagation loss fields were modelled with a horizontal angular resolution of  $10^\circ$  for a total of 36 radial

planes. Receiver depths were chosen to span the entire water column over the modelled areas, with step sizes that increased with depth, from 2 m to a maximum of 100 m.

Ambient decedecade SPL percentile information was derived from acoustic measurements performed on the data recorded at each station. We used a geoacoustic profile defined using (Ainslie 2010) (see Appendix C.2). To evaluate the detection ranges, the received level,  $RL(r)$ , measured at the distance  $r$  from the source, is modelled as:

$$RL(r) = SL - PL(r), \quad (1)$$

where  $SL$  is the source level of the vocalization and  $PL(r)$  is the range-dependent propagation loss that is a non-random parameter computed with MONM or BELLHOP. The source level of each call type is defined as a Gaussian distribution with a specified mean and standard deviation (see Appendix C.3).

The detection of a given marine mammal vocalization is assumed to occur if the received level is greater than the local noise level in the frequency band of the vocalization ( $NL$ ), by a constant threshold  $c$ :

$$RL(r) \geq NL + c. \quad (2)$$

The threshold  $c$  must be chosen such that there is little chance of detecting a false alarm due to *ambient sound*, and such that the automated algorithms will have a 50 % chance of detecting a signal when present. Depending on the species of interest, JASCO's detectors use thresholds between 1 and 16 dB, which satisfy the constraints.

Equations 1 and 2 include two independent random variables,  $NL$  and  $SL$ . The distribution of the noise level is determined empirically from actual data recorded at the project site for the same time period that was used to select the sound speed profile. Thus,  $NL$  has discrete values, and the final probability of detecting a call as a function of range is:

$$P_d(r) = 1 - \sum_{NL_i} P(NL_i) CDF_{SL}(NL_i + c + PL(r)), \quad (3)$$

where  $CDF_{SL}(NL + c + PL(r))$  is the cumulative probability of the source level exceeding  $NL_i + c + PL(r)$ .

To further constrain the modelling so that the predicted detection ranges do not become unreasonably long, the maximum source level considered is the 90th percentile of the distribution, and the minimum noise level is the 10th percentile of the noise distribution. We then discretize the signal model into 0.5 dB bins ( $SL_j$ ) and compute  $P_d(r)$  for all combinations of  $NL_i$  and  $SL_j$ . We extract the 10th, 50th, and 90th percentiles of this distribution for generating plots and tables of detection performance.

## 2.4. Sound Source Characterization

In accordance with ISO 17208-2 (2019), the preferred method for measuring vessel source levels by averaging hydrophones at angles of 15, 30, and 45 degrees, located at a radial distance of at least 100 m or 1 ship length from the vessel track. Due to the deep-water measurement location, this approach was not feasible with the bottom mounted hydrophones moorings. Nevertheless, it is still possible to compute the source levels using the procedures in ISO 17208-2 using the correction provided in Annex B to the specification. For the purposes of this analysis, the vessels are treated as a point source enabling a direct computation of the source level ( $L_s$ ) using the method provided in ISO standard 17208-2 in which a correction,  $\Delta L$ , to the radiated noise level ( $L_{RN}$ ) is applied:

$$L_S = L_{RN} + \Delta L \quad (4)$$

$$L_{RN} = L_R + 20 \log_{10} R$$

$$\Delta L = -10 \log_{10} \left( \frac{1}{2} + \frac{1}{4k^2 d_s^2 \sin^2 \beta} \right) + L_\alpha \text{ dB} \quad (5)$$

where  $R$  is the slant distance from the source to the receiver,  $L_R$  is the sound pressure level at the receiver, the wavenumber  $k = \frac{2\pi f}{c}$ ,  $f$  is the frequency of interest,  $c$  the speed of sound in water,  $d$  is the source depth, for each support vessel (SV), and  $\beta$  is the depression angle of the recorder. The term  $L_\alpha$  was included in the computation to account for the absorption of sound by seawater in accordance with the equations of (François and Garrison 1982b).

The support vessel source levels were measured by requiring them to perform a series of exercises near ALTO2 station. The exercises are generally described as:

### Exercise 1

Single vessel on stationary dynamic positioning (DP). During this exercise, the support vessels maintained a total of 10 min of dynamic positioning 500 m away from ALTO2, described as hydrophone in Figure 17, for each of the three power levels with a 2 min idle period between them.

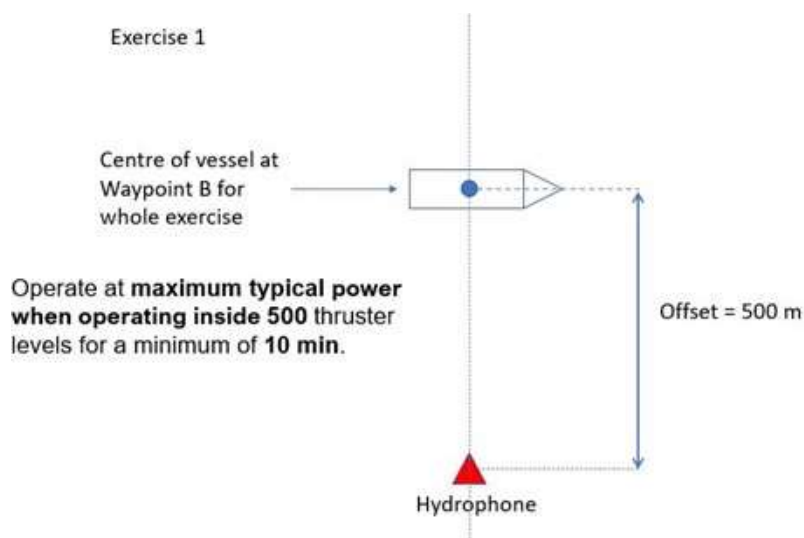


Figure 17. Exercise 1 diagram.

## Exercise 2

Single vessel moving away from the recorder with thrusters at maximum typical power. The SV was under operating power as determined by prevailing conditions with ALTO2 abeam at 500 m (Waypoint (WP) B)). The vessel then stepped away from ALTO2 at maximum typical thruster power when operating alongside in sea and winds approaching safe limits (see Figure 18). In maximum typical thruster power when operating inside 500 m in winds and seas approaching safe limits, the vessel stepped away in a perpendicular direction from ALTO2 with bow into the weather for 5 min (Figure 18).

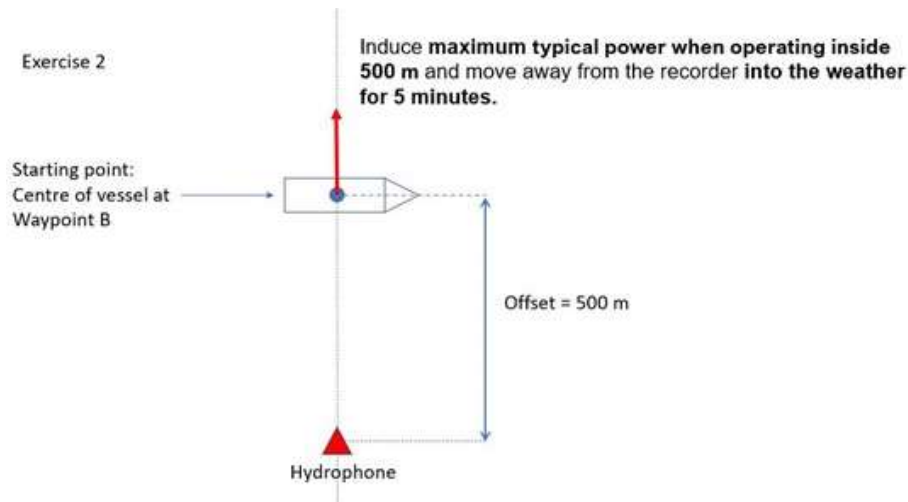


Figure 18. Exercise 2 diagram.

## Exercise 3

Single vessel transiting at normal speed. The vessel maintained a constant speed on a steady bearing, as dictated by weather conditions, on a straight track line between WP "A" and WP "C", or vice versa (see Figure 19). The key to this exercise was to maintain 500 m constant separation from the recorder when passing by WP B to achieve the CPA. Therefore, vessel heading was to be adjusted as required to ensure the straightest track possible is achieved, creating a track line between WP A and WP C.

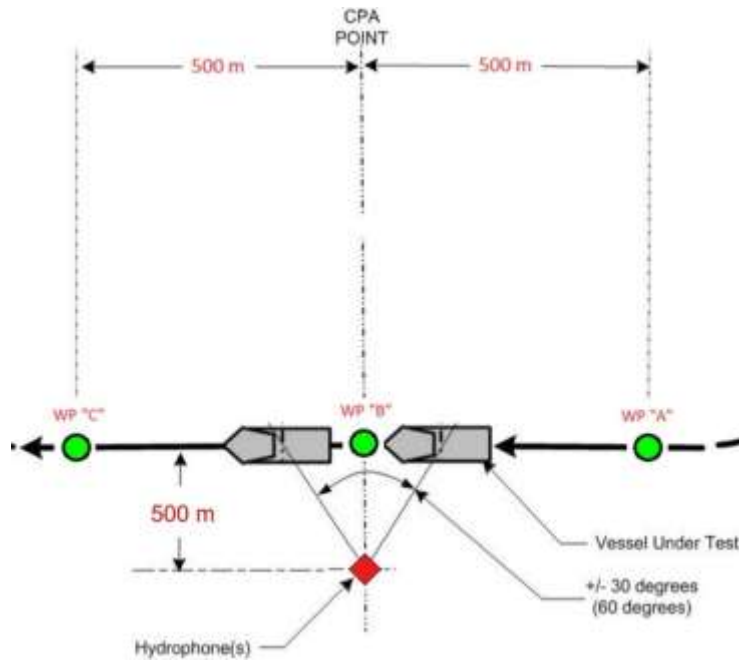


Figure 19. Exercise 3 diagram.

The days when each of the support vessels performed the exercises are shown in Table 7 and the source levels results are presented in Section 3.6.

Table 7. Support vessels and the day they executed the required exercises at ALTO2.

Support vessel	Exercise day at ALTO2 (2023)	Source depth (m)
MAERSK MOBILISER	14 Apr	7.7
ATLANTIC KINGFISHER	12 Jun	5.3
KJ GARDNER	16 Jun	6.4
SIEM SYMPHONY	15 Jun	6.0
ATLANTIC MERLIN	27 Jun	6.9
MAERSK CLIPPER	25 May	6.9

## 3. Results

### 3.1. Ambient Sound

The band-level plots, spectrograms (Long-term Spectral Averages), decidecade box-and-whisker plots, and spectral density level percentiles provide an overview of the sound variability in time and frequency presenting an overview of presence and level of contribution from different sources. Short-term events appear as vertical stripes on the spectrograms and spikes on the band level plots. Ambient sound results are presented for the low-frequency and high-frequency data independently.

#### 3.1.1. Low-Frequency Results

##### 3.1.1.1. ALTO 1

Unfortunately, a malfunction of the AMAR at ALTO1 station prevented the collection of any data. A preliminary investigation of the cause of the failure indicates that the AMAR extension cable had a defect that cut power to the AMAR when the cable was under pressure. Without the recordings from ALTO1, it is not possible to characterize the STENA ICEMAX source levels; however, the support vessel source levels were computed using the data from ALTO2.

##### 3.1.1.2. ALTO2

The results for the ALTO2 recordings sampled at 32 kHz are presented in Figure 20 and 21. In the bottom panel of Figure 20, it is possible to distinguish a horizontal line at 25 Hz during the period when the STENA ICEMAX was in the field from 8 May to 1 July. The vertical stripes on 14 Apr; 25 May; and 12, 15, 16, and 27 June, correspond to the days in which the support vessels executed the required exercises (see Section 3.6). The 25 Hz peak can also be identified in the lower panel of Figure 21 together with the some other tonal in the 30–100 Hz band, these peaks were produced by the STENA ICEMAX and the support vessels while on the field.

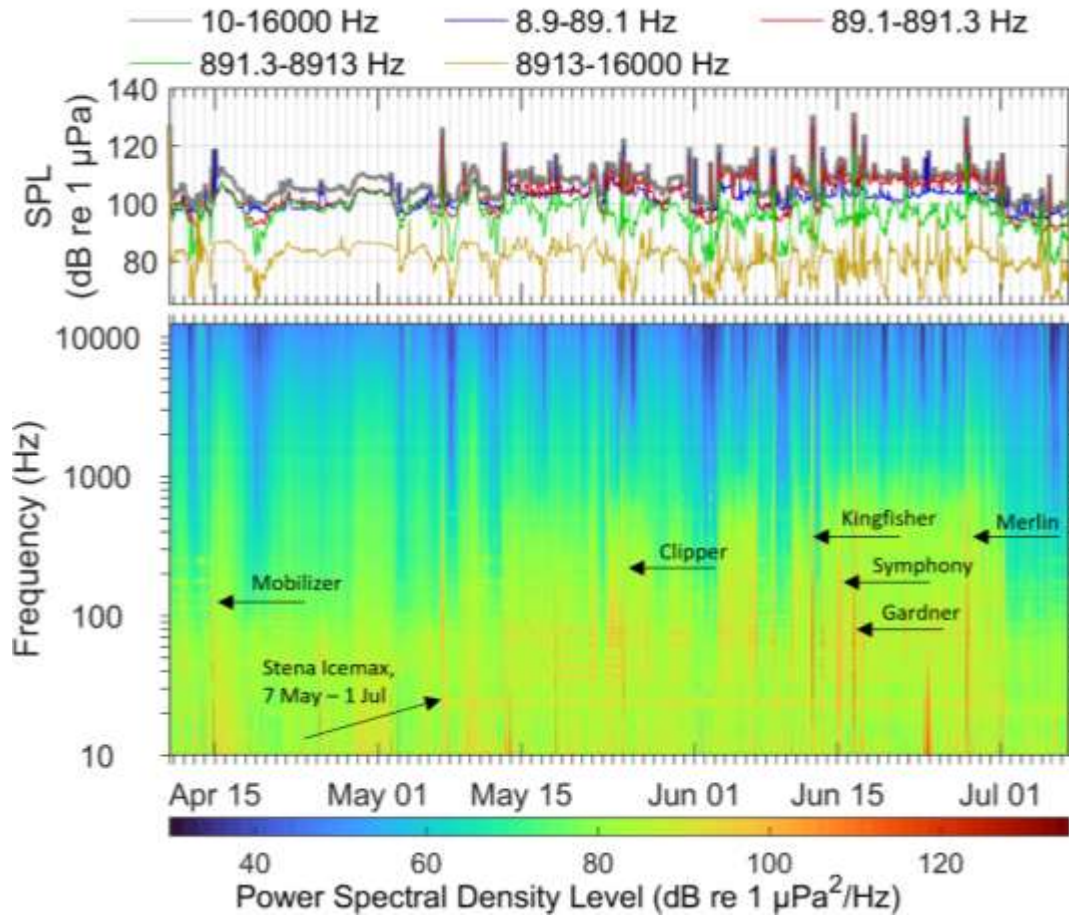


Figure 20. ALTO 2 Low-frequency results. (Top) In band sound pressure level for the duration of the deployment. (Bottom) Long term spectrogram of received sound for the duration of the deployment.

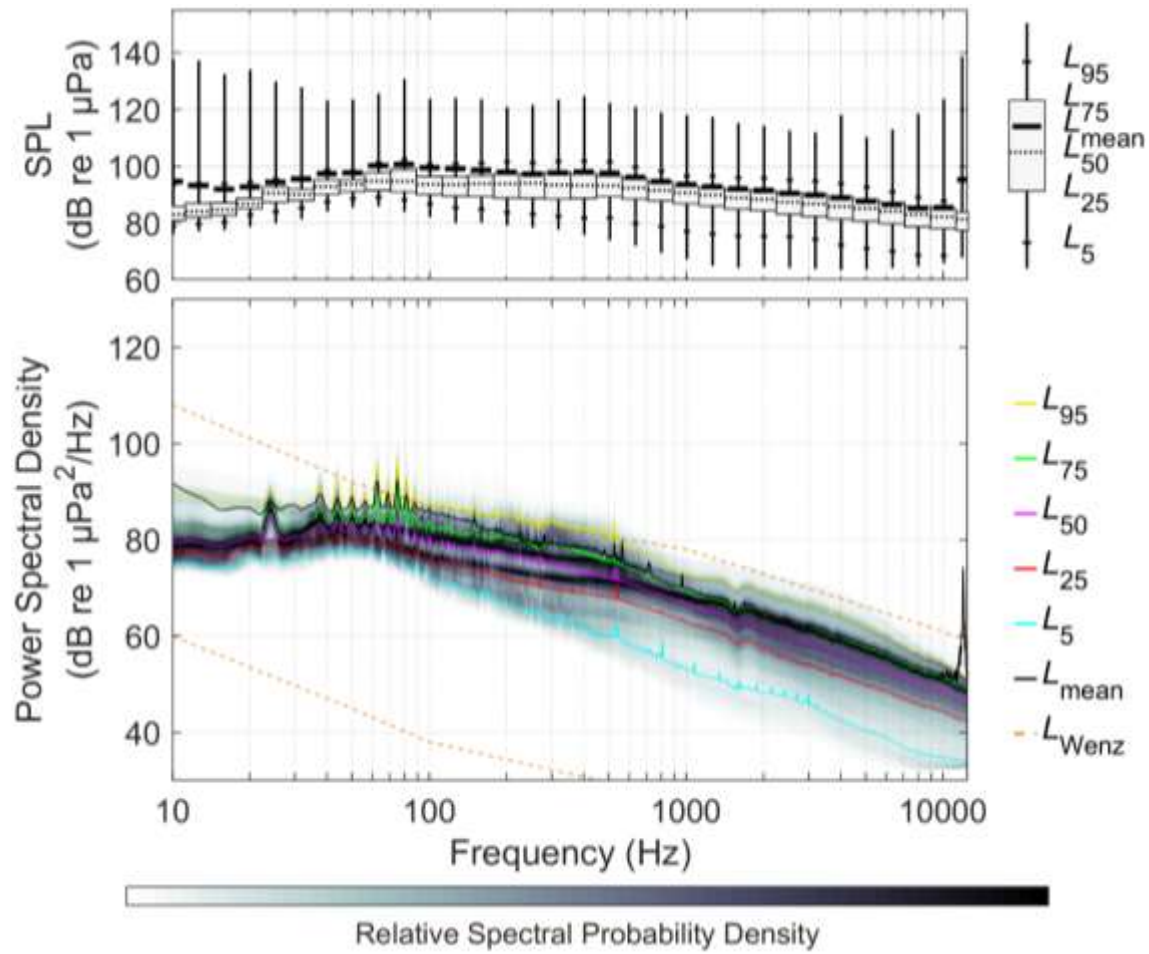


Figure 21. ALTO 2 Low Frequency. Distribution of received sound levels as a function of frequency. (Top) Decidecade boxplot showing the distribution of sound pressure level within a decidecade band. (Bottom) power spectral density percentile plot showing the distribution of received levels as a function of frequency.

### 3.1.2. High-Frequency Results

#### 3.1.2.1. ALTO 2

The results for the ALTO2 recordings sampled at 512 kHz are presented in Figures 22 and 24. The recorders were sampled at 512 kHz to document the sounds above 16 kHz, which are expected to include odontocete clicks and whistles, rain, and sounds from anthropogenic sources like echosounders.

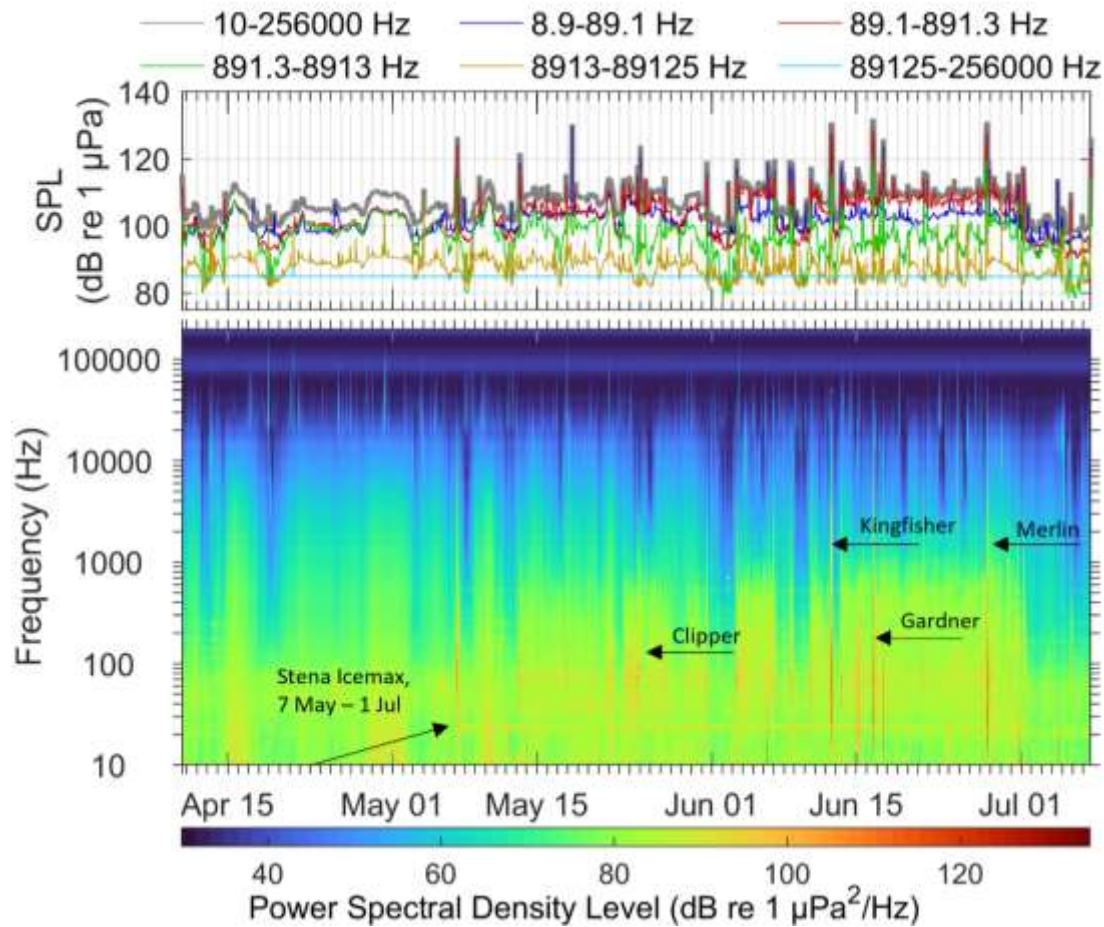


Figure 22. ALTO 2 high-frequency. (Top) In band sound pressure level for the duration of the deployment. (Bottom) Long term spectrogram of received sound for the duration of the deployment.

The broadband SPL is constantly under 120 dB re 1 $\mu$ Pa except for 7 May (drillship arriving to location), 13 May, 18 May, 25 May (Maersk Clipper exercise), 12 June (Atlantic Kingfisher exercise), 16 June (KJ Gardner exercise), 17 June, and 27 June (Atlantic Merlin exercise). For the 17 June peak (Figure 23), a closer inspection shows that the sound source to be a close pass by sperm whales.

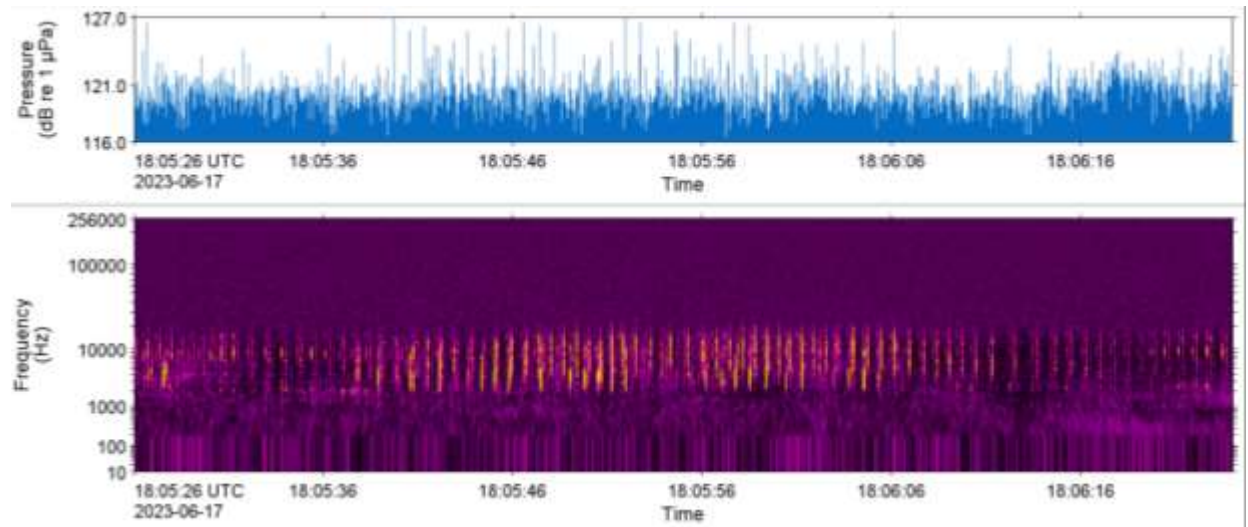


Figure 23. Spectrogram and pressure levels calculated from the recordings at ALTO2 around 18:00 on 17 June due to the presence of sperm whales.

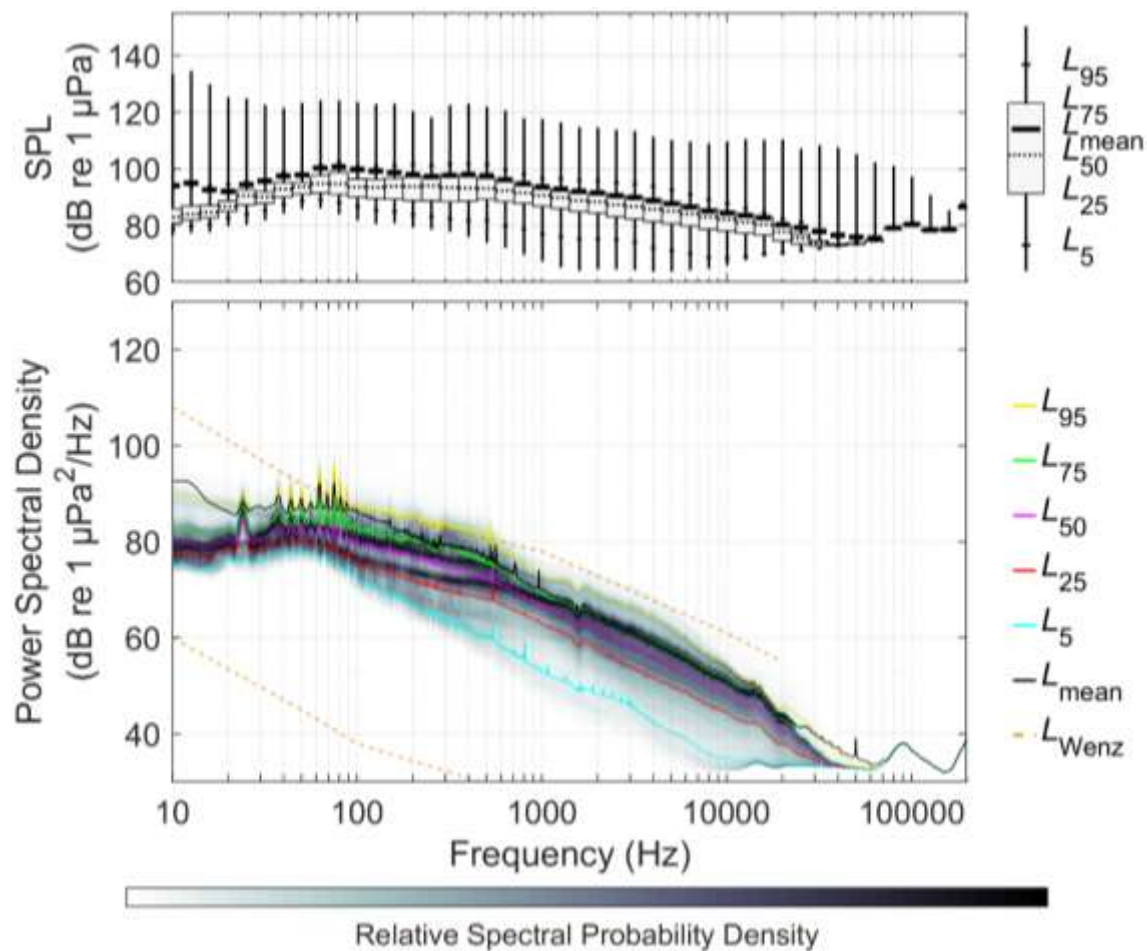


Figure 24. ALTO 2 High Frequency. Distribution of received sound levels as a function of frequency. (Top) Decidecade boxplot showing the distribution of sound pressure level within a decidecade band. (Bottom) power spectral density percentile plot showing the distribution of received levels as a function of frequency.

### 3.2. Sound Exposure Levels

The daily sound exposure levels (SEL) were computed from the high-frequency sampling rate data using the methods described in Martin et al. (2019). When weighted for the hearing ability of different marine mammal groups, daily SEL can serve as an indicator of possible hearing injury (see Appendix A.2). The auditory frequency weighted SEL for each of the marine mammal groups is shown in Figure 25 and discussed in Section 4.1.

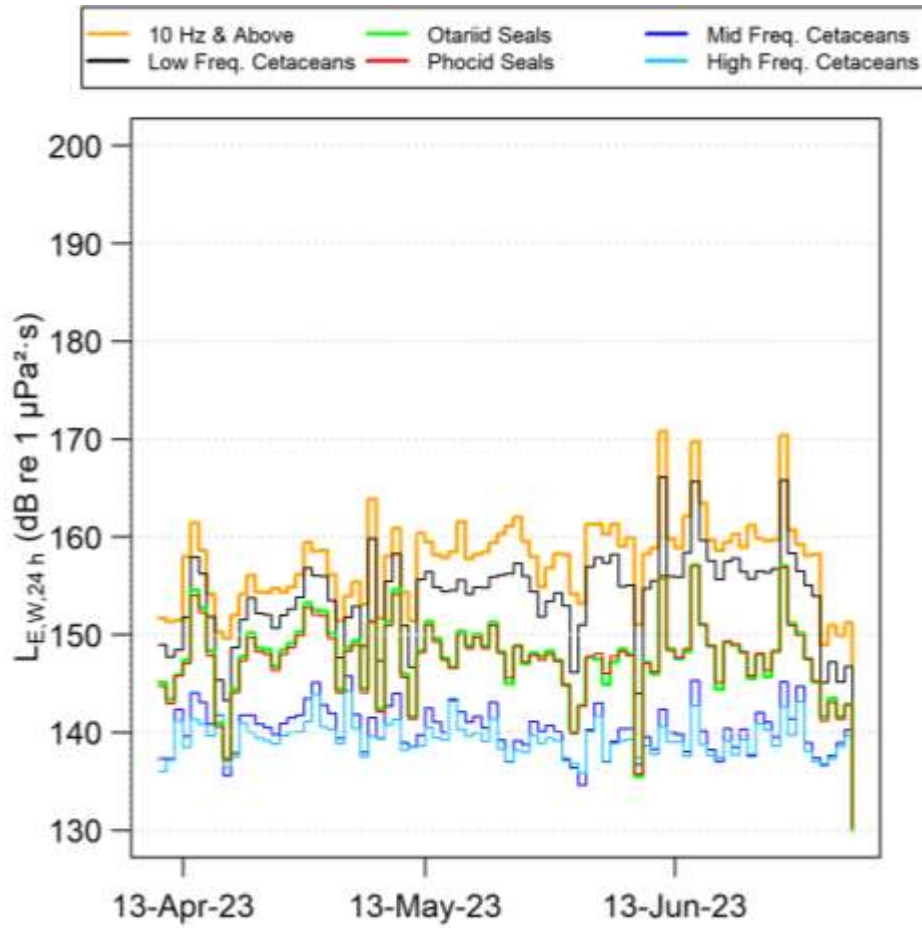


Figure 25. Daily auditory frequency weighted sound exposure levels at the ALTO2 station

### 3.3. Marine Mammals

The acoustic presence of marine mammals was identified automatically by JASCO’s detectors and validated via the manual review of 0.8 % of the low- and high-frequency data sets, which represents 200 sound files, or ~1.6 h worth of 1-min 512 kHz sound files and ~15 h worth of 9-min 32 kHz sound files. Detectors and analysts found acoustic signals of fin, sei, northern bottlenose, sperm, and pilot and/or killer whales as well as dolphins and harbour porpoise and/or pygmy sperm whales.

Table 8 provides the automated detector performance of the automated detector that performed best for each species or vocalization type per 9 min file for the low-frequency data and per 1 min file for the high-frequency data. Automated detector Precision was generally high, with 92 to 100 % of files with detections estimated to be correct for northern bottlenose, sperm, fin, and sei whales as well as the species producing narrow-band high frequency (NBHF) clicks (Table 8). For delphinid signals, click detections provide the highest Precision, with 81 % of files with detections correct, whereas whistle detectors were more often falsely triggered. The precision and recall for pilot or killer whale whistles were also good (0.78 and 0.73, respectively). Recall was high for northern bottlenose and fin whale detectors, with 89 to 100 % of files with detections captured by automated detectors. The per file occurrence of some other signals were underestimated with Recall values of 55 to 73 % (Table 8). NBHF click Recall was particularly low, only capturing one of three files with manual detections, therefore only manual detections are included for the species producing these clicks. No temporal or spatial restrictions on detections were required to improve their reliability.

Table 8. Automated detector performance including the threshold implemented (minimum number of automated detections per file for species to be considered present) and the post-threshold detector precision (*P*), recall (*R*) and MCC score. The unit of time over which the automated detector performance was calculated is provided where 9 min refers to the data sampled at 32 kHz and 1 min refers to the data sampled at 512 kHz. TP: true positive; FP: false positive; FN: false negative; TN: true negative.

Species/group (vocalization)	Automated detector	Per-file threshold	Final							Data
			<i>P</i>	<i>R</i>	<i>MCC</i>	<i>TP</i>	<i>FP</i>	<i>FN</i>	<i>TN</i>	
Dolphin (whistle)	WhistleHigh_Quiet20k	1	0.78	0.60	0.57	18	5	12	64	1 min files sampled at 512 kHz
Dolphin (click)	Dolphin:Click	12	0.81	0.68	0.58	26	6	12	44	
Northern bottlenose whale (click)	NBW:Click	9	0.93	0.89	0.87	25	2	3	59	
Sperm whale (click)	SpermWhale (Click Train)	2	1.00	0.55	0.70	11	0	9	76	
Fin whale (20 Hz pulses)	Atl_FW_21.2 detector	2	1.00	1.00	1.00	9	0	0	88	9 min files sampled at 32 kHz
Sei whale (downsweeps)	Sum of SeiWhale_HighThreshold and SeiWhale_LowThreshold	1	0.92	0.63	0.72	12	1	7	76	
Pilot/killer whale (whistles)	Sum of WhistleLow_Quiet and MFMoanHigh	2	0.78	0.73	0.59	29	8	11	47	
Narrow-band high frequency clicks	Porpoise: Click	2	1.00	0.33	0.57	1	0	2	95	

### 3.3.1. Mysticetes

#### 3.3.1.1. Fin Whales

Fin whale 20 Hz pulses and 130 Hz notes (Figure 26) (Watkins et al. 1987) were detected on 9 June and 2 July 2023 (Figure 27).

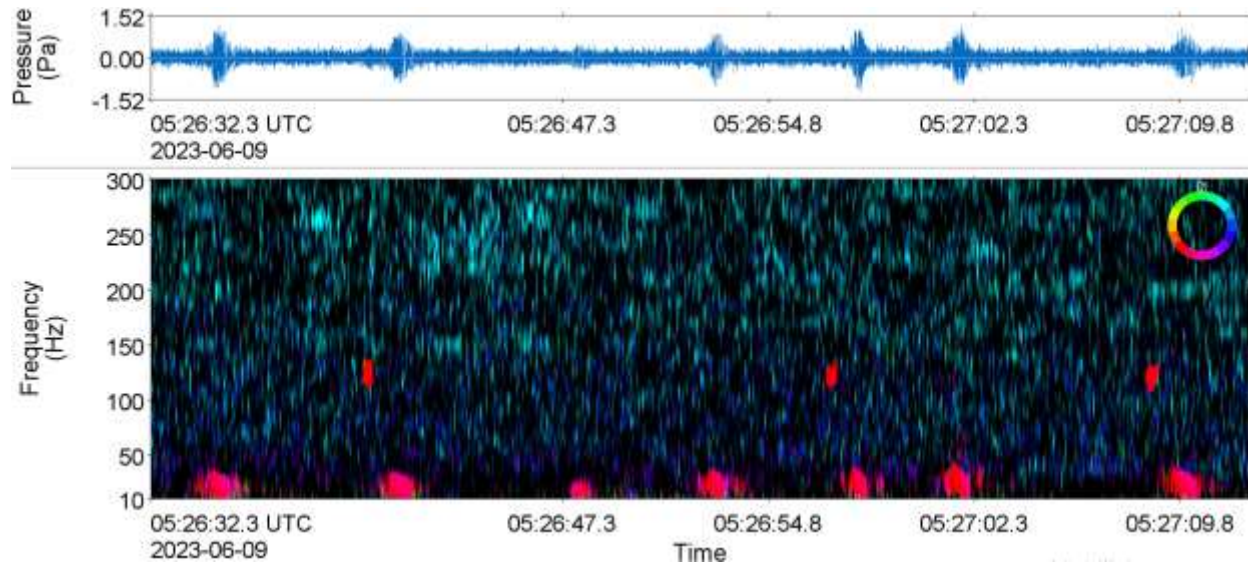


Figure 26. Fin whale: Waveform (top) and spectrogram (bottom) of 20 Hz pulses and 130 Hz notes recorded on 9 June 2023 where colour indicates bearing (2 Hz Discrete Fourier Transform (DFT) frequency step, 0.125 s DFT temporal observation window (TOW), 0.03125 s DFT time advance, and Hann window resulting in a 75 % overlap and DFT size (NDFT) of 32, normalized across time). The spectrogram is 40 s long.

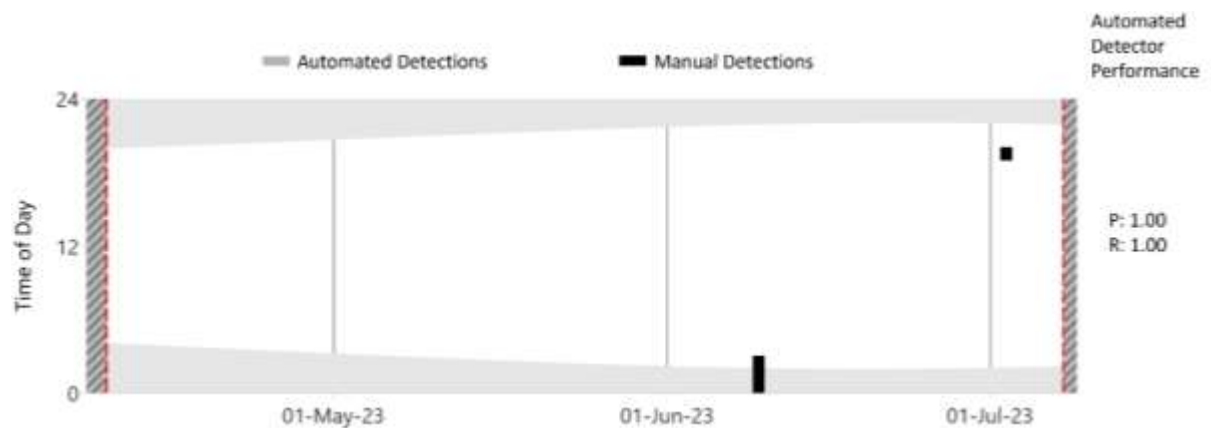


Figure 27. Fin whale occurrence: Daily and hourly occurrence of fin whale vocalizations recorded from 10 Apr to 7 July 2023 with automated detector performance metrics included along right side. The grey areas indicate hours of darkness from sunset to sunrise (Ocean Time Series Group 2009). Red dashed lines are the recorder deployment and retrieval dates. Automated detector results are for the Atl\_FW\_21.2 detector.

### 3.3.1.2. Sei Whales

Sei whale downsweeps (Baumgartner et al. 2008) (Figure 28) were detected throughout the recording duration, with an increase in detections seen in the summer months (June and July) (Figure 29).

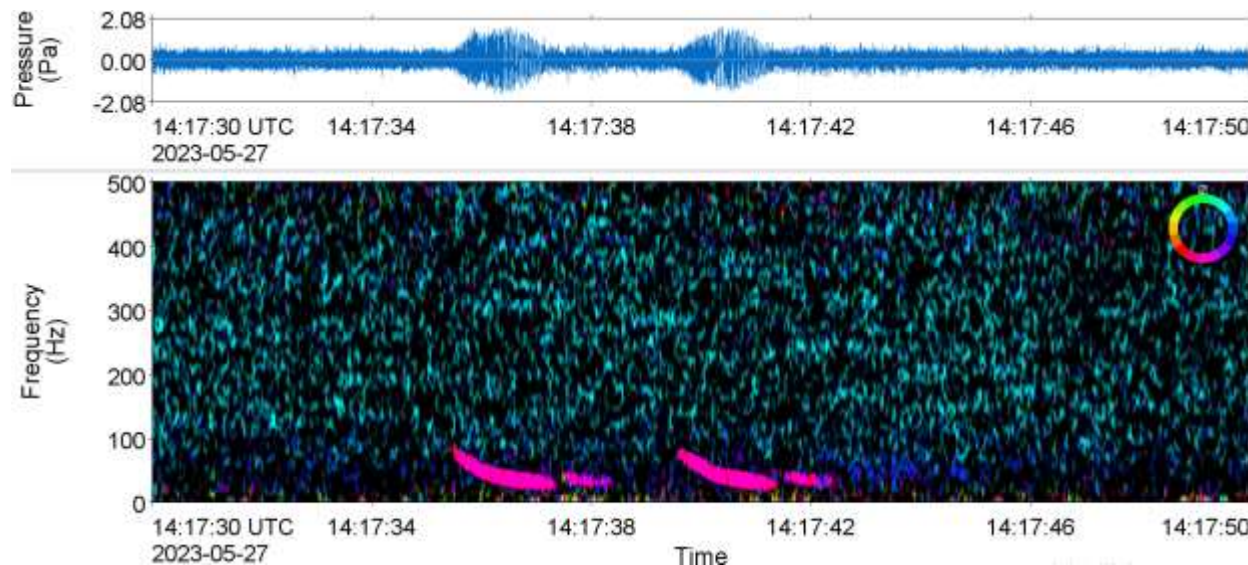


Figure 28. Sei whale: Waveform (top) and spectrogram (bottom) of sei whale downsweeps recorded on 27 May 2023 where colour indicates bearing (2 Hz discrete Fourier Transform (DFT) frequency step, 0.125 s DFT temporal observation window (TOW), 0.03125 s DFT time advance, and Hann window resulting in a 75 % overlap and DFT size (NDFT) of 32, normalized across time). The spectrogram is 20 s long.

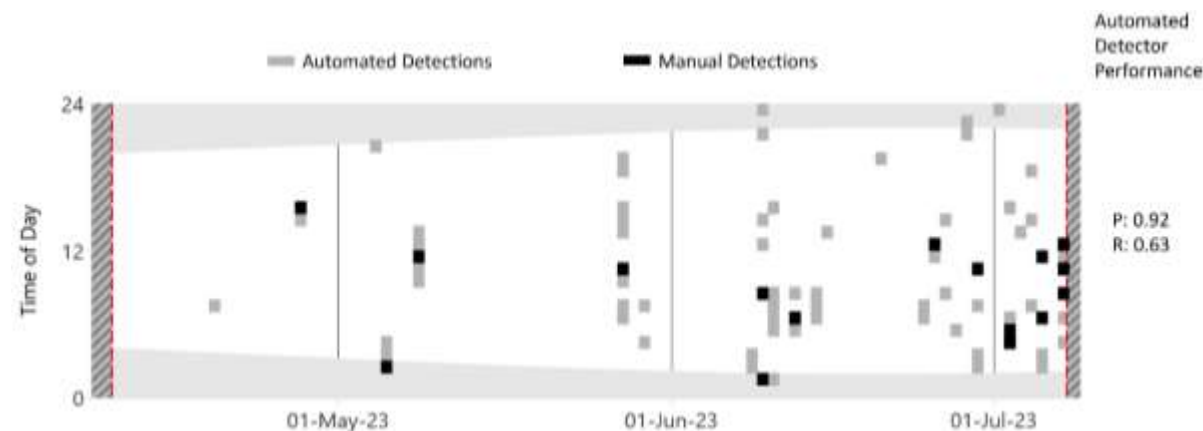


Figure 29. Sei whale occurrence: Daily and hourly occurrence of sei whale vocalizations recorded from 10 Apr to 7 July 2023 with automated detector performance metrics included along right side. The grey areas indicate hours of darkness from sunset to sunrise (Ocean Time Series Group 2009). Red dashed lines are the recorder deployment and retrieval dates. Automated detector results are for the sum of two detectors: Sei Whale High Threshold and Sei Whale Low Threshold.

## 3.3.2. Odontocetes

### 3.3.2.1. Delphinids

Unlike many odontocetes that only produce clicks, delphinids produce both impulsive (click) and tonal (whistle) sounds that show less species-level specificity (e.g., Steiner 1981) than other marine mammal signals and are therefore more difficult to distinguish acoustically.

Delphinid whistles with most energy of the fundamental frequency between 5 and 20 kHz were considered dolphins (Figure 30) while whistles below 5 kHz were assigned to killer/pilot whales (Figure 31). The overlap in spectral features of tonal signals from the different dolphin species expected in the study area and the expected (but unquantified) variability of these signals around the few described vocalization types prevented us from distinguishing small dolphin whistles by species. Dolphin whistles were detected throughout the recording period (Figure 32). Similarly, it was challenging for analysts to confidently distinguish between pilot and killer whale whistles, given their overlapping repertoires, but attempts were made. Most killer/pilot whale manual detections were suspected to be pilot whales, and these were detected throughout the recording period, with an increase in June (Figure 33).

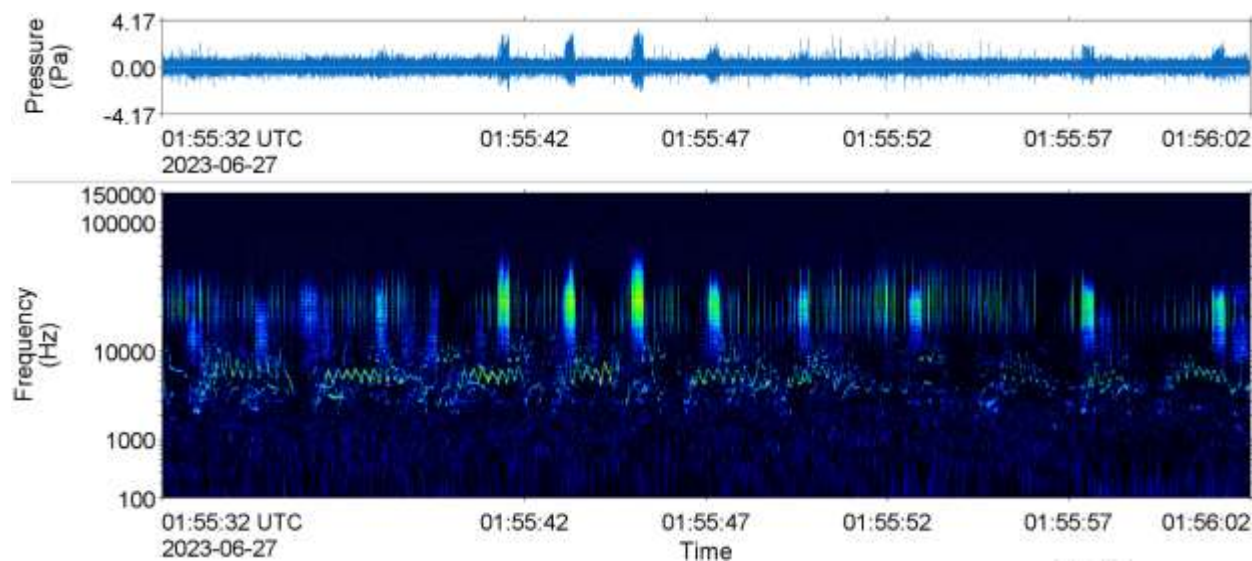


Figure 30. Dolphins: Waveform (top) and spectrogram (bottom) of dolphin (unknown species) whistles and clicks on 1 June 2023 (64 Hz discrete Fourier Transform (DFT) frequency step, 0.01 s DFT temporal observation window (TOW), 0.005 s DFT time advance, and Hann window resulting in a 75 % overlap and DFT size (NDFT) of 32, normalized across time, log scale). The spectrogram is 30 s long.

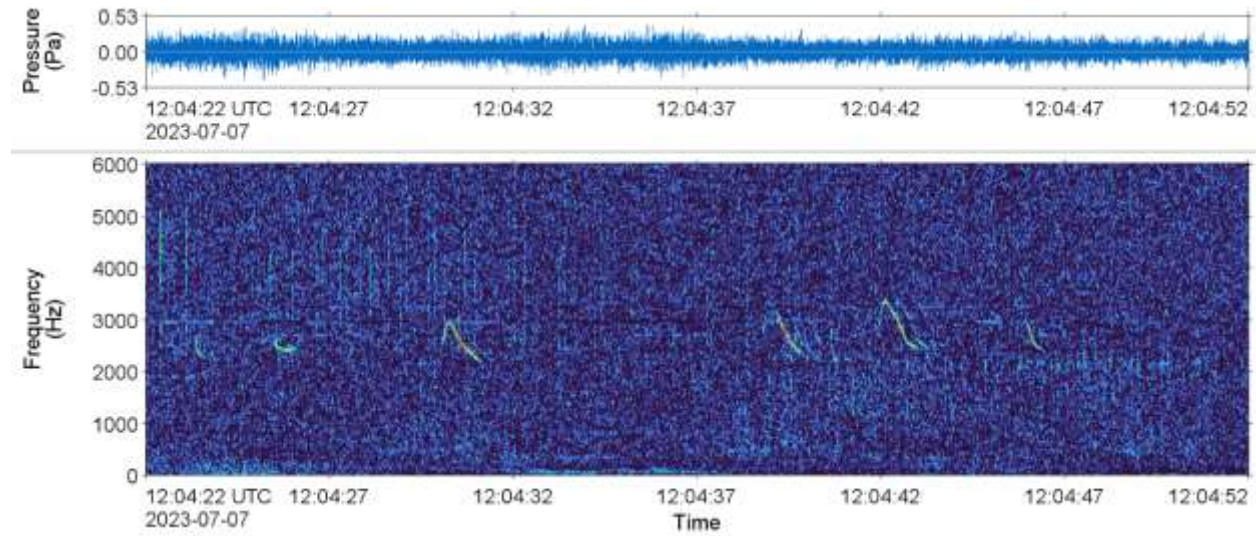


Figure 31. Pilot/killer whales: Waveform (top) and spectrogram (bottom) of whistles from either a pilot whale or killer whale on 7 July 2023 (64 Hz discrete Fourier Transform (DFT) frequency step, 0.01 s DFT temporal observation window (TOW), 0.005 s DFT time advance, and Hann window resulting in a 75 % overlap and DFT size (NDFT) of 32, normalized across time). The spectrogram is 30 s long.

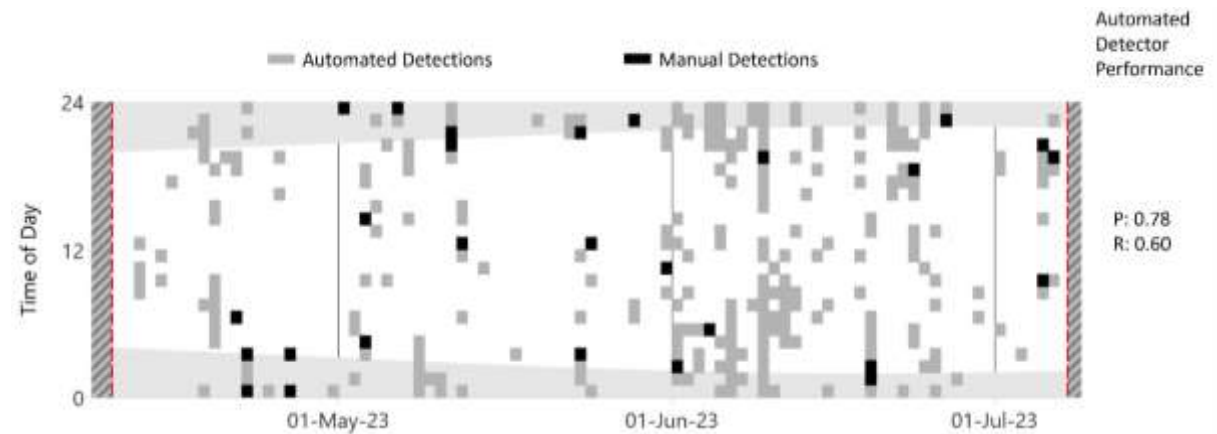


Figure 32. Dolphin whistle occurrence: Daily and hourly occurrence of dolphin whistles recorded from 10 Apr to 7 July 2023. The grey areas indicate hours of darkness from sunset to sunrise (Ocean Time Series Group 2009). Red dashed lines are the recorder deployment and retrieval dates. Hashed areas indicate when there was no acoustic data and red dashed lines indicate the start and end of recordings. Automated detector results are for the WhistleHigh\_Quiet20k detector.

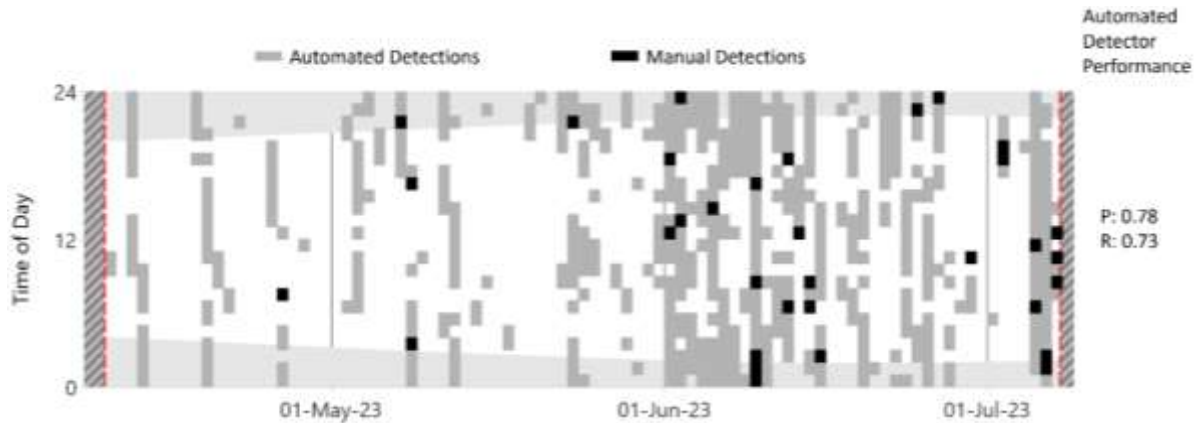


Figure 33. Killer/Pilot whales: daily and hourly occurrence of killer/pilot whale whistles recorded from 10 Apr to 7 July 2023. The grey areas indicate hours of darkness from sunset to sunrise (Ocean Time Series Group 2009). Red dashed lines are the recorder deployment and retrieval dates. Hashed areas indicate when there was no acoustic data and red dashed lines indicate the start and end of recordings. Automated detector results are for the sum of two detectors: Whistle Low Quiet and MF Moan High.

Delphinid clicks (Figures 30 and 34) were considered a single vocalization category that encompassed both small dolphin species and those of larger species, such as pilot and killer whales. These clicks occurred throughout the recording period (Figure 35).

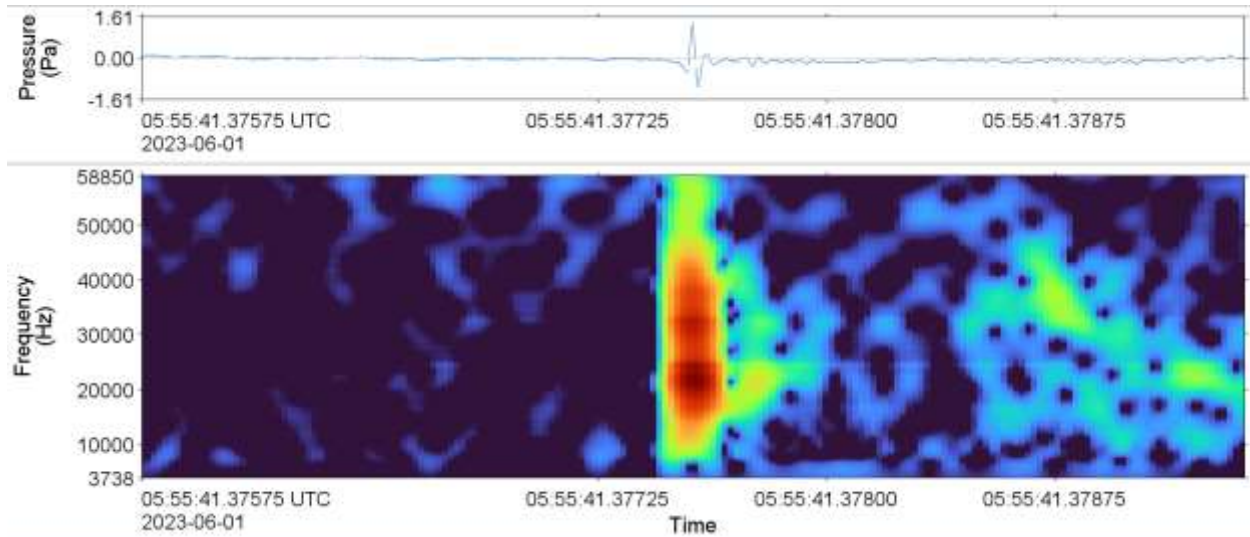


Figure 34. Delphinid click: Waveform (top) and spectrogram (bottom) of a delphinid click recorded on 1 June 2023 (512 Hz discrete Fourier Transform (DFT) frequency step, 0.26 ms DFT temporal observation window (TOW), 0.02 ms DFT time advance, and Hann window resulting in a 75 % overlap and DFT size (NDFT) of 32, normalized across time). The spectrogram length is 0.0036 s.

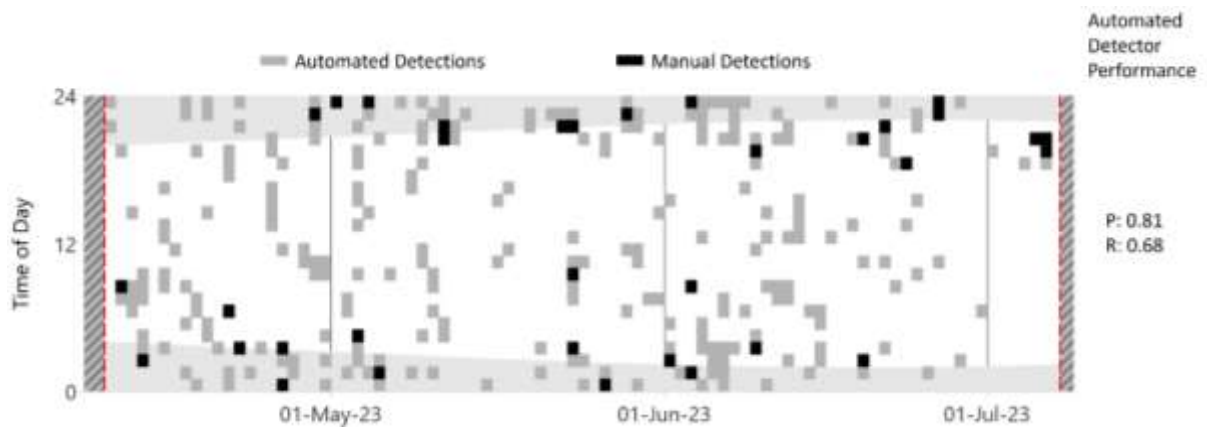


Figure 35. Dolphin click occurrence: Daily and hourly occurrence of dolphin clicks recorded from 10 Apr to 7 July 2023. The grey areas indicate hours of darkness from sunset to sunrise (Ocean Time Series Group 2009). Red dashed lines are the recorder deployment and retrieval dates. Hashed areas indicate when there was no acoustic data and red dashed lines indicate the start and end of recordings. Automated detector results are for the Dolphin:Click detector.

### 3.3.2.2. Narrow-band High Frequency Clicks

Narrow-band high frequency clicks (NBHF) (Figures 36 and 37) are produced by harbour porpoise and pygmy sperm whales (*Kogia breviceps*) in this region (Marten 2000, Madsen et al. 2005, Villadsgaard et al. 2007). NBHF clicks were acoustically detected in the study area infrequently (Figure 38), occurring on 11 May, 22 June, and 27 June 2023. While the automated detector had a perfect Precision, it was not triggered for two out of three manual detections, so only manual detections are shown in Figure 38.

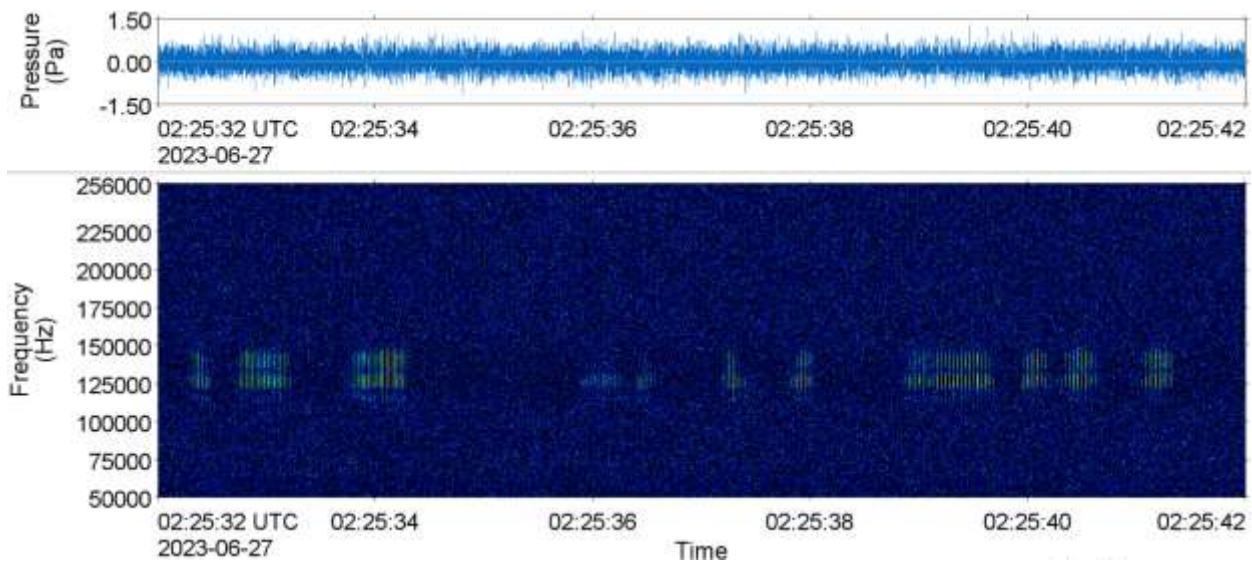


Figure 36. NBHF click train: Waveform (top) and spectrogram (bottom) of NBHF clicks recorded on 27 June 2023 (64 Hz discrete Fourier Transform (DFT) frequency step, 0.01 s DFT temporal observation window (TOW), 0.005 s DFT time advance, and Hann window resulting in a 75 % overlap and DFT size (NDFT) of 32, normalized across time). The spectrogram is 10 s long.

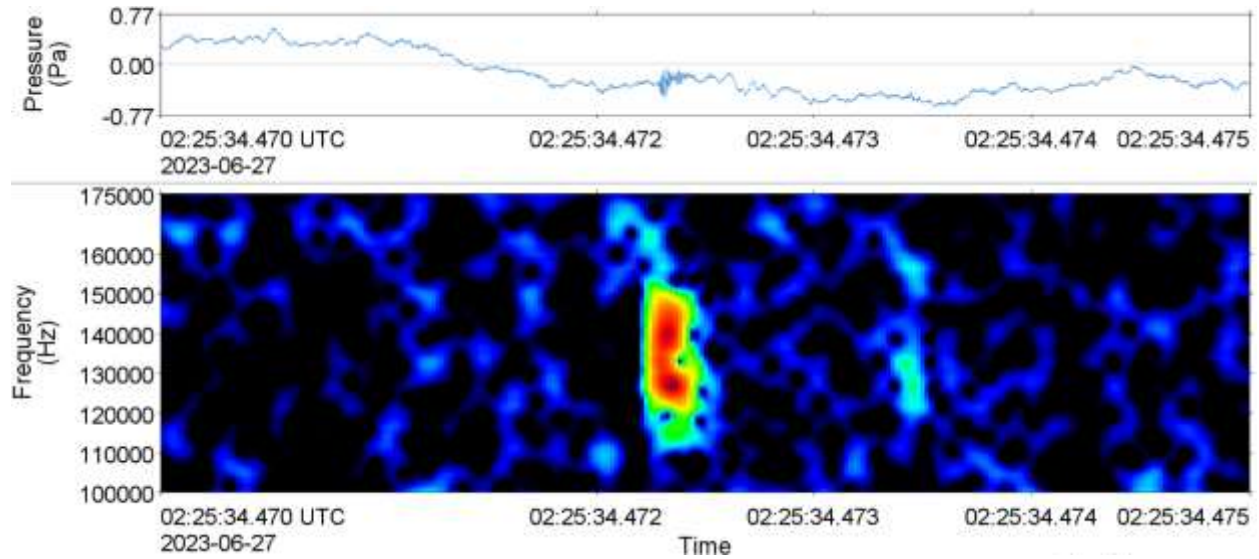


Figure 37. NBHF click: Waveform (top) and spectrogram (bottom) of a NBHF click recorded on 27 June 2023 (512 Hz discrete Fourier Transform (DFT) frequency step, 0.26 ms DFT temporal observation window (TOW), 0.02 ms DFT time advance, and Hann window resulting in a 75 % overlap and DFT size (NDFT) of 32, normalized across time). The spectrogram length is 0.005 s.

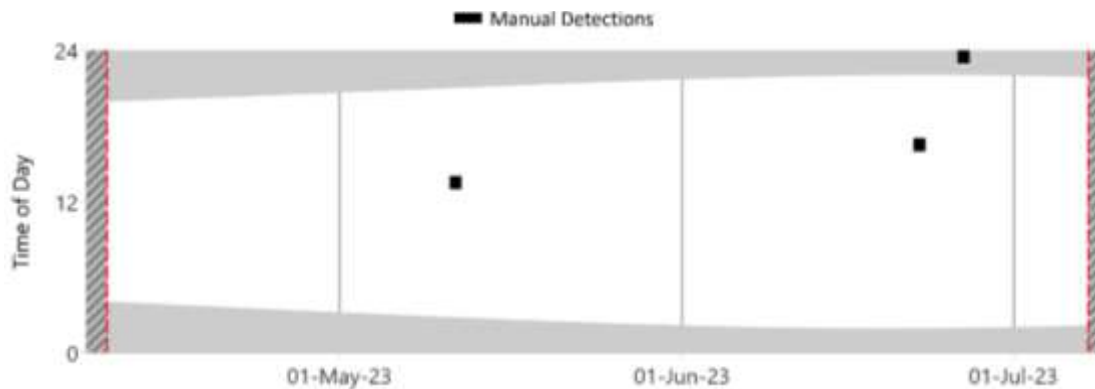


Figure 38. NBHF click occurrence: Daily and hourly occurrence of NBHF clicks recorded from 10 Apr to 7 July 2023. The grey areas indicate hours of darkness from sunset to sunrise (Ocean Time Series Group 2009). Red dashed lines are the recorder deployment and retrieval dates.

### 3.3.2.3. Sperm Whales

Sperm whale clicks (Figure 39) were detected sporadically throughout the recording period, with an increase in regularity of occurrence from mid-May to the end of the deployment (Figure 40).

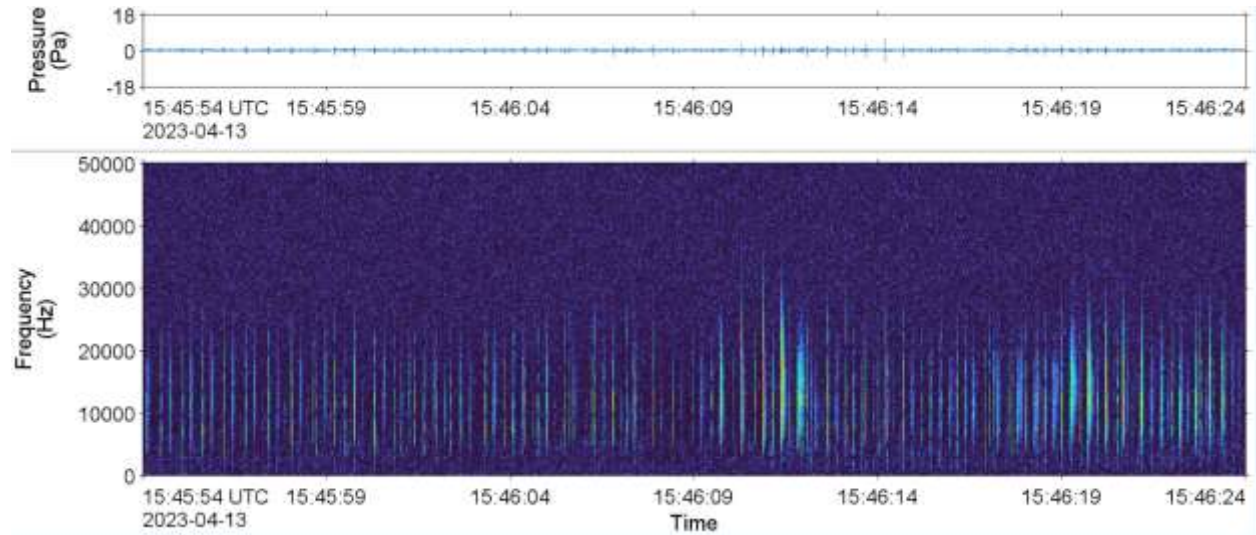


Figure 39. Sperm whale click train: Waveform (top) and spectrogram (bottom) of sperm whale clicks recorded on 13 Apr 2023 (64 Hz discrete Fourier Transform (DFT) frequency step, 0.01 s DFT temporal observation window (TOW), 0.005 s DFT time advance, and Hann window resulting in a 75 % overlap and DFT size (NDFT) of 32, normalized across time). The spectrogram is 30 s long.

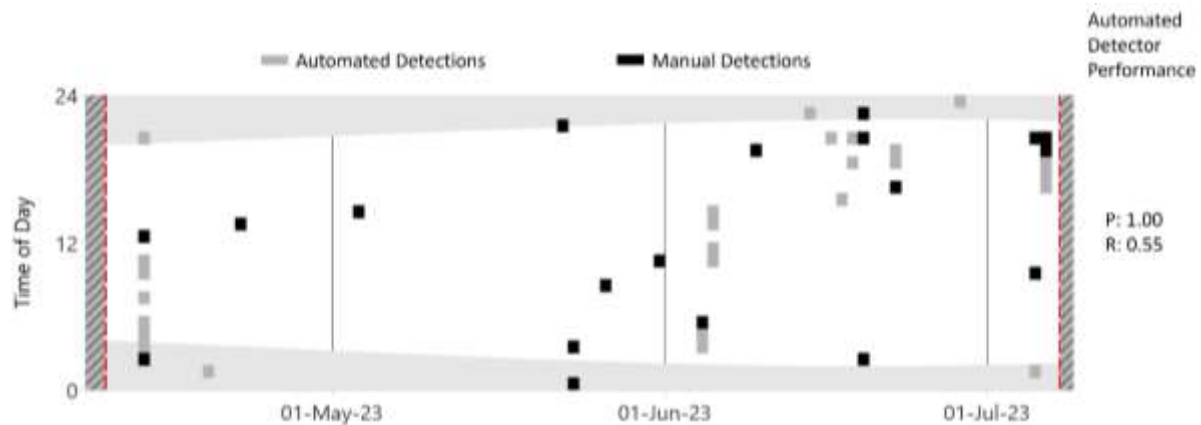


Figure 40. Sperm whale occurrence: Daily and hourly occurrence of sperm whale clicks recorded from 10 Apr to 7 July 2023 with automated detector performance metrics included along right side. The grey areas indicate hours of darkness from sunset to sunrise (Ocean Time Series Group 2009). Red dashed lines are the recorder deployment and retrieval dates. Automated detector results are for the Sperm Whale (Click Train) detector.

### 3.3.2.4. Northern Bottlenose Whales

Northern bottlenose whale clicks (Figures 41 and 42) were detected throughout the measurement (Figure 43).

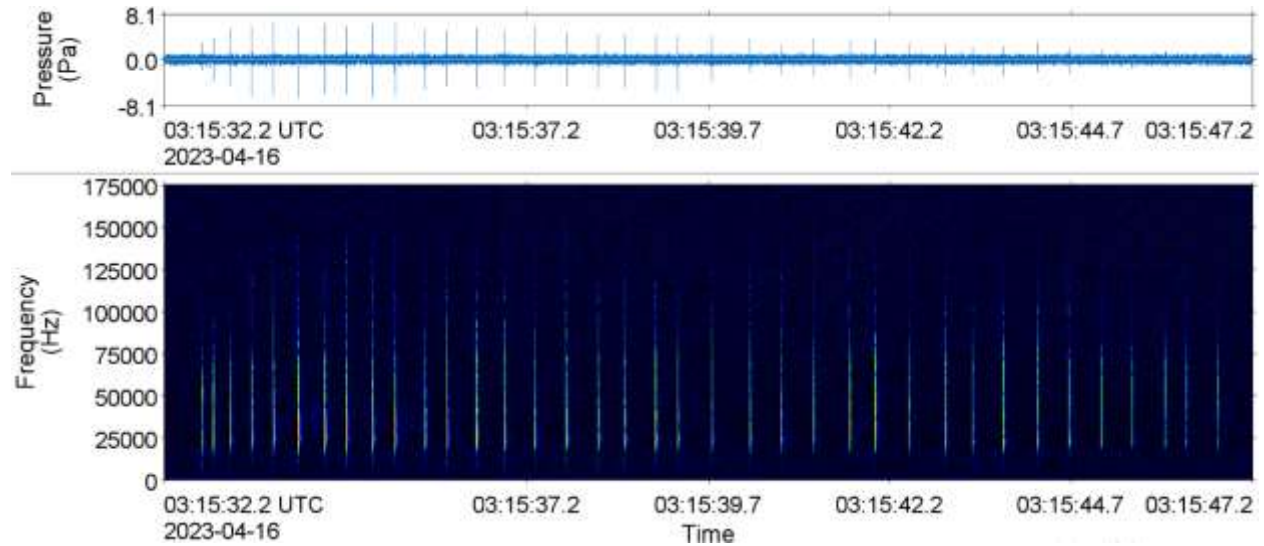


Figure 41. Northern bottlenose whale click train: Waveform (top) and spectrogram (bottom) of northern bottlenose whale clicks recorded on 16 Apr 2023 (64 Hz discrete Fourier Transform (DFT) frequency step, 0.01 s DFT temporal observation window (TOW), 0.005 s DFT time advance, and Hann window resulting in a 75 % overlap and DFT size (NDFT) of 32, normalized across time). The spectrogram is 15 s long.

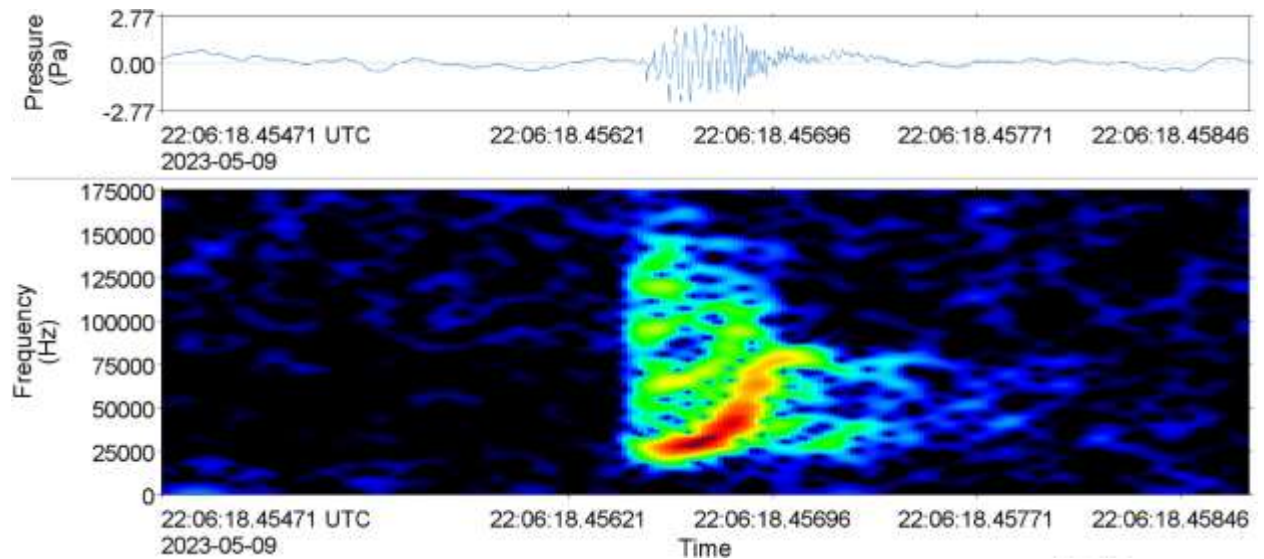


Figure 42. Northern bottlenose whale click: Waveform (top) and spectrogram (bottom) of a northern bottlenose whale click recorded on 9 May 2023 (512 Hz discrete Fourier Transform (DFT) frequency step, 0.26 ms DFT temporal observation window (TOW), 0.02 ms DFT time advance, and Hann window resulting in a 75 % overlap and DFT size (NDFT) of 32, normalized across time). The spectrogram length is 0.004 s.

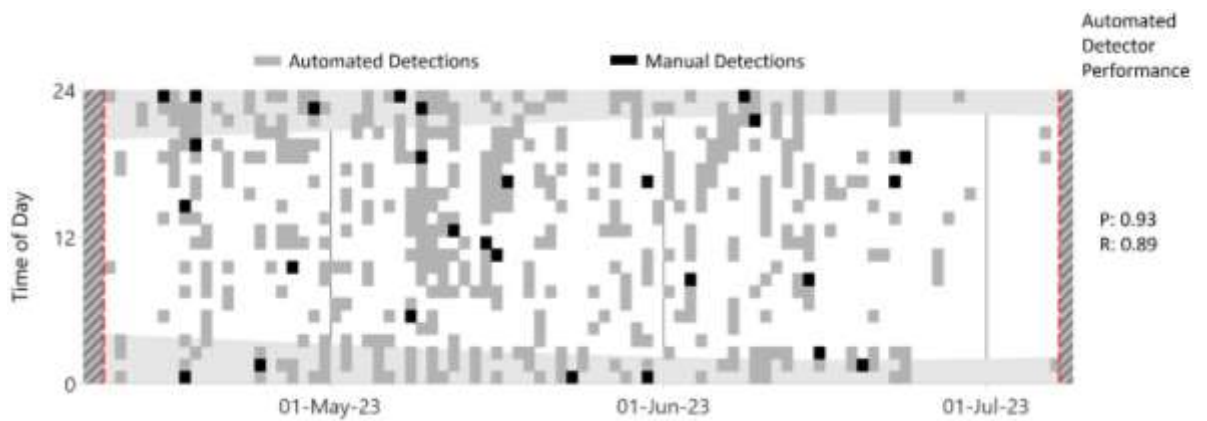


Figure 43. Northern bottlenose whale occurrence: Daily and hourly occurrence of northern bottlenose whale clicks recorded from 10 Apr to 7 July 2023 with automated detector performance metrics included along right side. The grey areas indicate hours of darkness from sunset to sunrise (Ocean Time Series Group 2009). Red dashed lines are the recorder deployment and retrieval dates. Automated detector results are for the NBW:Click detector.

### 3.4. Absolute Minimum Number of Animals Present

Sei whales were the only mysticetes with sufficient detections to perform the AMN analysis. Sei whales were detected on 16 days (Figure 44). Sei whales did not call very often: the maximum number of calls detected automatically per day was only 26. On two occasions two whales were detected at the same time (Figure 45). The predominant direction of detection was to the south, which is towards the shelf break (Figures 46 and 10).



Figure 44. AMN analysis of the Sei whale detections. (Top) Number of detections per day, coloured by species. (Middle) Absolute Minimum Number (AMN) of mammals detected per day, which is the maximum per day of the AMN per 10-min time block. (Bottom) Time-bearing presentation.

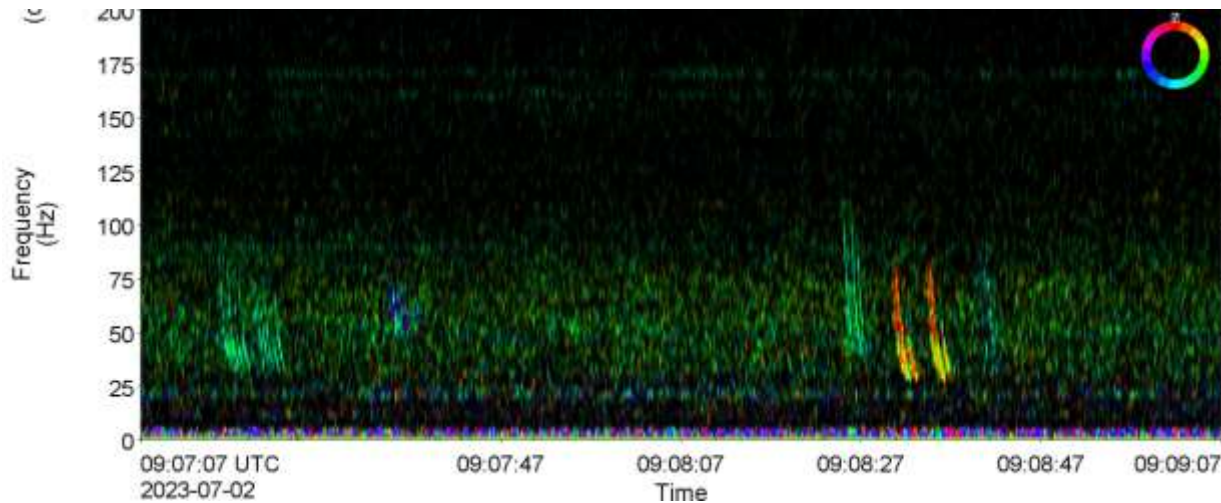


Figure 45. Example of sei whale calls arriving from at least two directions (green and red/orange) within the same 2-min, indicating that at least two whales were present on 2 July near ALTO 2. The calls shown in green have repeated patterns of arrivals in the calls which is likely due to a propagation phenomenon calls modal dispersion, which could be employed to determine the range to the animals.

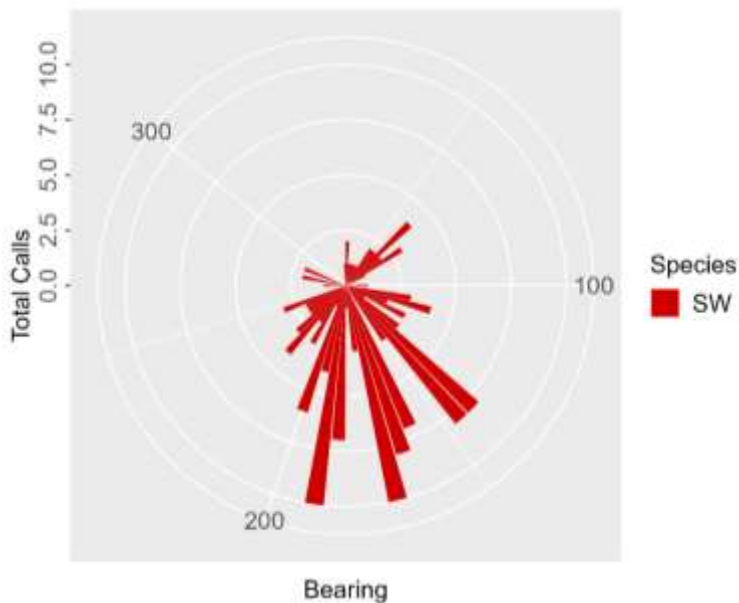


Figure 46. Polar plot of the directions of arrival to the sei whale detections.

### 3.5. Detection Range Modeling

Detection range modelling (DRM) was performed for all detected and potentially occurring species for which published source level information for the signals targeted by our analysis are available (see Appendix C.3). Detection ranges were modelled ALTO2 during the spring months (April to June) covering most of the recording period.

The DRM results are summarized in Table 9. This table compiles detection range (minimum to maximum range across all 36 modelled radials) for three noise percentiles (10th (N10), median/50th (N50) and 90th (N90) and three probabilities of detection (primarily influenced by the source level distribution). The results are also presented graphically in Appendix C.4 for the species actually detected during the study.

The main results can be summarized as follows:

- Blue and fin whale calls were the only species with long detection ranges. Detection ranges reached the limit of the modeling area (150 km) in quiet noise conditions and reached tens of km in most modeling scenarios.
- Detection ranges of sei whale calls were substantially shorter than those of fin and blue whales. Sei whale downsweeps were detectable up to 40 km in the best-case scenarios but more routinely around 5-10 km in average background noise conditions.
- The detection ranges of the other baleen whales (minke, humpback, and North Atlantic right whales) never exceeded 24 km and were generally less than 5 km.
- Sperm whale clicks had the longest detection ranges of all odontocetes, reaching 34.6 km at best but being most often around 5 km.
- Detection ranges of delphinid and ziphiid species were always less than 8 km and most often between 1 and 5 km.
- Harbour porpoise or Kogia clicks had short detection ranges, usually less than 1 km. The longer ranges associated with increasing diving depth suggest that the detections recorded in this study were likely produced by the Greenland ecotype of harbour porpoise (Olsen et al. 2022), known to dive down to 400 m and previously tracked near in the study area (Nielsen et al. 2018), or one of the Kogia species, presumably pygmy sperm whales. Note that there are no source level estimates for pygmy sperm whales; harbour porpoise estimates were used instead for comparison purposes.

Table 9. Detection ranges for each detected species at 10, 50, and 90 % probabilities of detection as a function of in-band ambient sound levels (10, 50, and 90 % percentile) at station ALTO2 in the spring (April-June).

Species	Noise percentile	Pd conditional		
		Pd=0.1	Pd=0.5	Pd=0.9
Delphinid whistles	NL10	8.0–8.1	4.9–4.9	2.8–2.8
	NL50	4.3–4.3	2.0–2.2	0.6–0.6
	NL90	2.9–3.0	1.1–1.2	0.0–0.0
Killer whale tonal calls	NL10	6.7–7.8	3.1–3.3	1.4–1.4
	NL50	2.5–2.7	1.0–1.0	0.0–0.0
	NL90	1.3–1.3	0.0–0.0	0.0–0.0
Pilot whale tonal calls	NL10	5.4–5.6	2.3–2.5	1.0–1.1
	NL50	2.0–2.0	0.6–0.7	0.0–0.0
	NL90	0.8–0.8	0.0–0.0	0.0–0.0
Northern bottlenose whale clicks	NL10	6.3–6.6	4.5–5.1	3.4–4.0
	NL50	4.5–5.0	3.4–4.0	2.3–2.7
	NL90	4.1–4.3	3.0–3.3	1.9–2.1
Cuvier beaked whale clicks	NL10	7.7–7.9	6.9–7.1	6.1–6.3
	NL50	6.5–6.9	5.9–6.1	5.3–5.4
	NL90	6.1–6.3	5.4–5.6	4.8–5.0
Delphinid clicks	NL10	6.0–6.1	4.2–4.2	2.5–2.6
	NL50	4.9–5.0	3.1–3.3	1.8–1.8
	NL90	4.5–4.5	2.8–2.8	1.6–1.6
Harbour porpoise clicks 186 dB	NL10	0.9 - 0.9	0.3 - 0.3	0.0 - 0.0
	NL50	0.9 - 0.9	0.3 - 0.3	0.0 - 0.0
	NL90	0.9 - 0.9	0.3 - 0.3	0.0 - 0.0
Harbour porpoise clicks 169 dB	NL10	0.0 - 0.0	0.0 - 0.0	0.0 - 0.0
	NL50	0.0 - 0.0	0.0 - 0.0	0.0 - 0.0
	NL90	0.0 - 0.0	0.0 - 0.0	0.0 - 0.0
Harbour porpoise clicks 178 dB Deep	NL10	0.7 - 0.7	0.6 - 0.6	0.3 - 0.3
	NL50	0.7 - 0.7	0.6 - 0.6	0.3 - 0.3
	NL90	0.7 - 0.7	0.6 - 0.6	0.3 - 0.3
Harbour porpoise clicks 178 dB Shallow	NL10	0.4 - 0.4	0.0 - 0.0	0.0 - 0.0
	NL50	0.4 - 0.4	0.0 - 0.0	0.0 - 0.0
	NL90	0.4 - 0.4	0.0 - 0.0	0.0 - 0.0
Kogia clicks	NL10	1.0 - 1.1	0.9 - 0.9	0.7 - 0.7
	NL50	1.0 - 1.1	0.9 - 0.9	0.7 - 0.7
	NL90	1.0 - 1.1	0.9 - 0.9	0.7 - 0.7
Fin whale	NL10	82.0–150.0	64.3–150.0	42.0–116.1
	NL50	71.5–150.0	52.7–127.7	38.3–81.9
	NL90	53.0–129.4	39.0–83.0	16.7–36.2
Blue whale	NL10	149.9–150.0	149.9–150.0	149.9–150.0
	NL50	149.9–150.0	149.9–150.0	149.9–150.0
	NL90	149.9–150.0	149.9–150.0	149.9–150.0
Sei whale	NL10	23.3–39.0	14.7–16.8	6.2–9.5
	NL50	15.4–18.5	6.4–10.3	4.4–4.8
	NL90	12.2–13.1	5.2–5.4	2.5–2.7
Minke whale	NL10	8.6–9.8	5.5–5.7	2.6–3.4
	NL50	4.5–5.0	2.1–2.8	0.9–1.4
	NL90	2.1–2.7	0.8–1.2	0.0–0.1
Humpback whale	NL10	12.5–14.8	5.4–5.8	1.5–1.8
	NL50	6.2–6.6	1.9–2.3	0.0–0.1

Species	Noise percentile	Pd conditional		
		Pd=0.1	Pd=0.5	Pd=0.9
Right whale 150 dB	NL90	3.2–3.5	0.8–0.9	0.0–0.0
	NL10	0.2–0.3	0.0–0.0	0.0–0.0
	NL50	0.0–0.0	0.0–0.0	0.0–0.0
	NL90	0.0–0.0	0.0–0.0	0.0–0.0
Right whale 172 dB	NL10	20.4–23.4	8.8–10.0	2.8–3.0
	NL50	12.0–13.2	4.9–5.6	1.0–1.1
	NL90	7.7–8.3	1.8–2.4	0.0–0.0
Right whale 165 dB	NL10	7.4–7.7	3.5–4.2	1.7–2.1
	NL50	3.0–3.3	1.3–1.8	0.1–0.2
	NL90	1.3–1.7	0.0–0.1	0.0–0.0
Sperm whale clicks	NL10	14.3–34.6	11.8–30.2	8.0–8.5
	NL50	7.3–7.9	4.4–5.1	2.9–4.9
	NL90	3.7–4.9	2.4–4.8	2.0–4.0

### 3.6. Support Vessels Source Levels

In principle, the support vessels' source levels were being calculated to improve the accuracy in the drillship source level calculation. Still, even if the STENA ICEMAX source level is not being calculated, it is important to characterize the sound signature from the support vessels and compare them to previous modelling/measurements. Figure 47 presents, the sound pressure levels calculated from the recordings at ALTO2 during the days of the exercises. While the estimated time to perform all three exercises is not longer than one hour, some of the SVs spent more than that near ALTO2. As an example, the acoustic signature from the ATLANTIC KINGFISHER, ATLANTIC MERLIN, and KJ GARDNER clearly indicates their time at ALTO2. The time spent by the MAERSK MOBILIZER is notably shorter than the others which was reflected in the acoustic data.

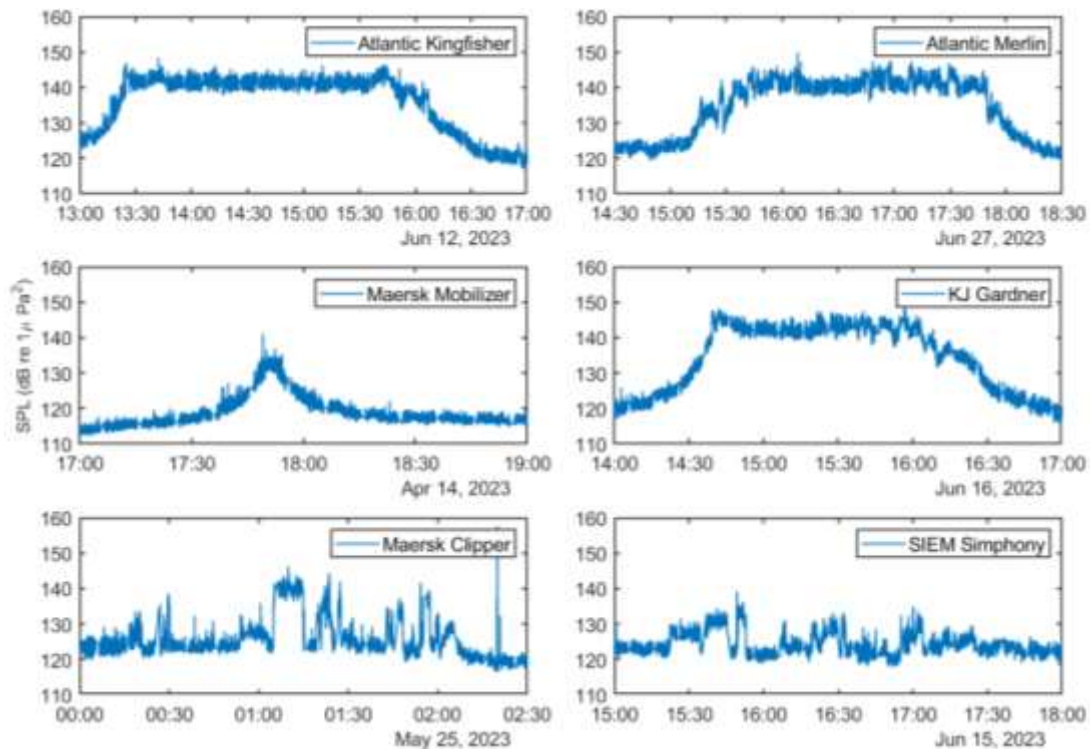


Figure 47. Recorded sound pressure levels around the time when the support vessels performed the exercises.

It is possible to zoom in into the exact times of each of the exercises as reported by the crew from the SVs. The case of the SIEM SYMPHONY (Figure 48) is a clear example of what was expected during the exercises: in exercise 1, there are three steps in the SPL of 10 min each corresponding to the three levels used in the thrusters; in exercise 2, it is expected for the SPL to decline as the SV gets away from ALTO2 for 5 min using full power on the thrusters; and in exercise 3, the SPL are expected to increase, reaching the maximum during CPA and then decline as the SV sails away.

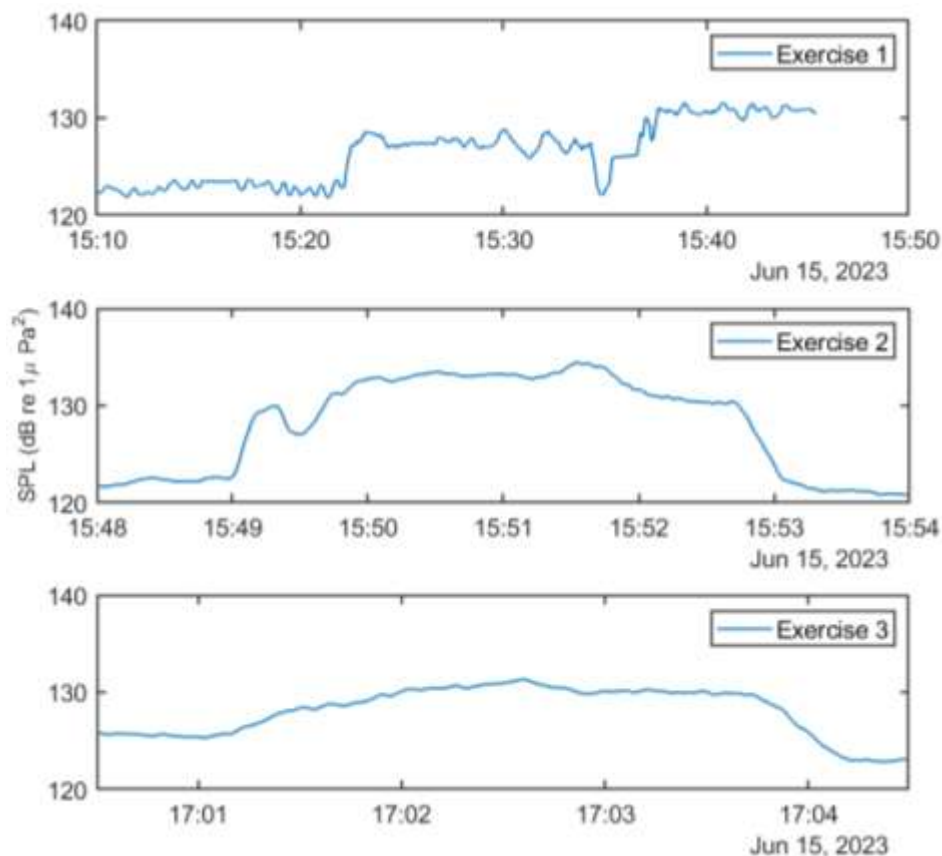


Figure 48. Sound pressure levels recorded around the approximate times of the exercises for support vessel SIEM Symphony.

To determine the position of the SV more accurately during the time of the exercises, the available AIS data was linearly interpolated to 1-sec intervals, then the source levels were calculated using Equations 4 and 5. In the following section, maps showing the locations of the vessels during the exercises, and plots of the received levels and the calculated source levels are presented for the ATLANTIC MERLIN and the SIEM SYMPHONY; the remainder are presented in Appendix D. The SIEM SYMPHONY was notable due to its significantly lower source levels which were attributed to its hybrid dual propulsion system. A discussion of the SV source levels is then presented in Section 4.2.3.

### 3.6.1. ALANTIC MERLIN

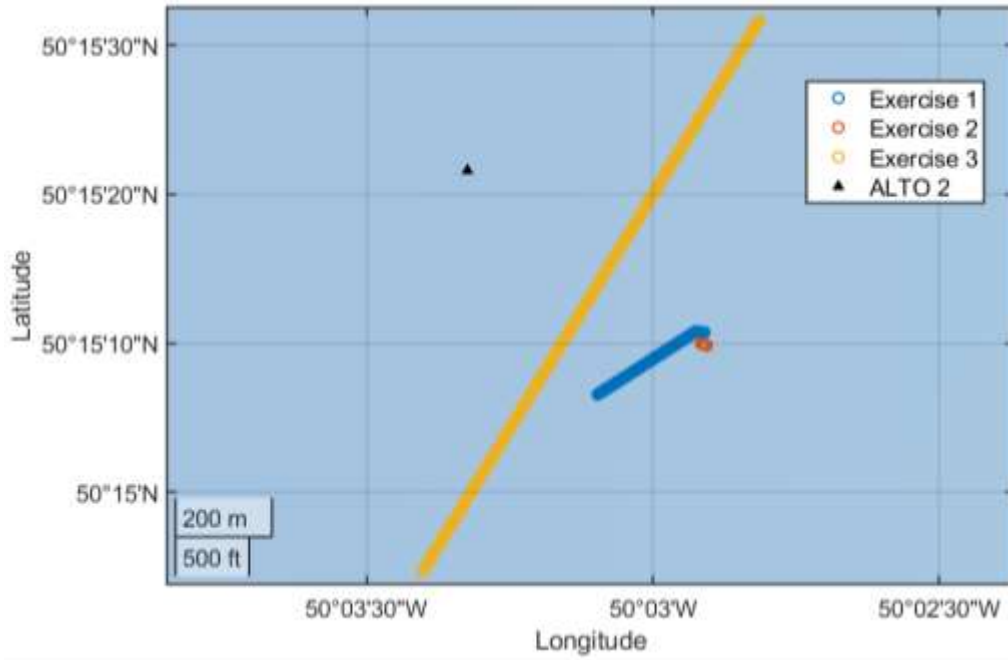


Figure 49. ATLANTIC MERLIN track referenced by ALTO 2 position as a black triangle around the time of the exercises.

3.6.1.1. Exercise 1

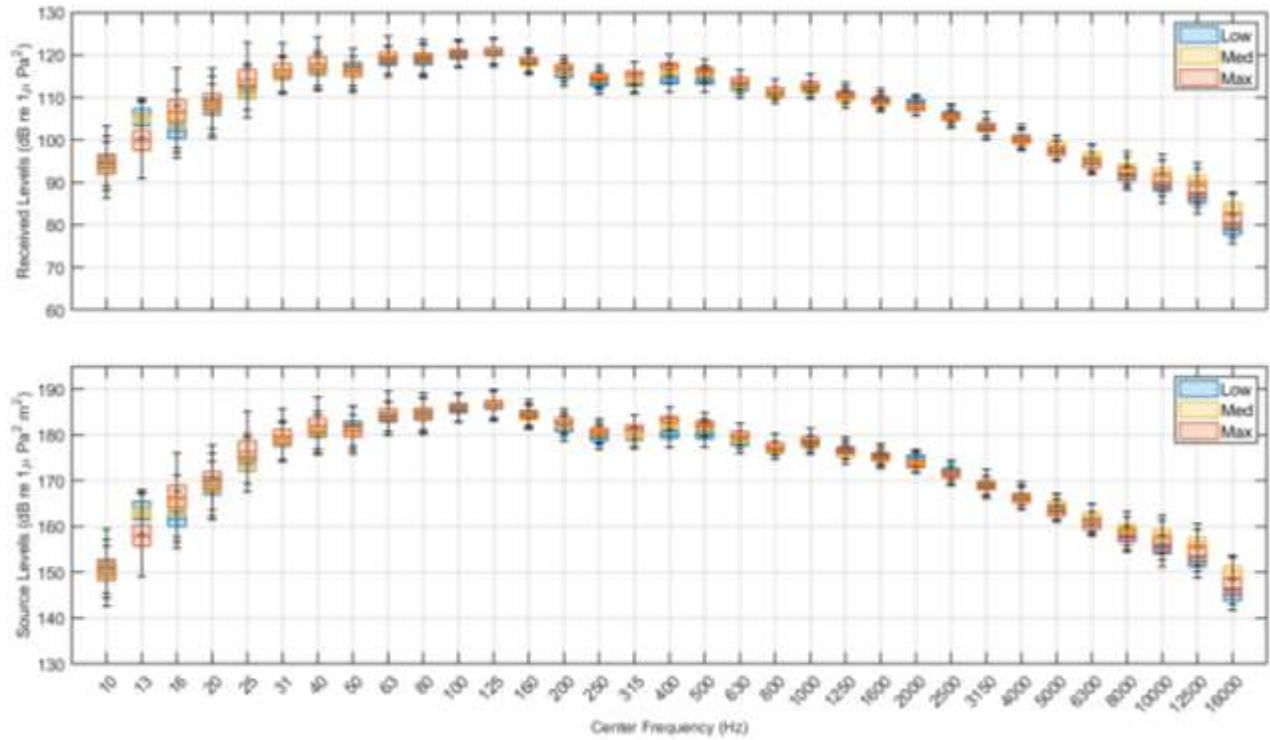


Figure 50. ATLANTIC MERLIN. (Top) Received levels during exercise 1 grouped by thruster level. (Bottom) Calculated source level using Equations 4 and 5 during exercise 1 grouped by thruster level.

### 3.6.1.2. Exercise 2

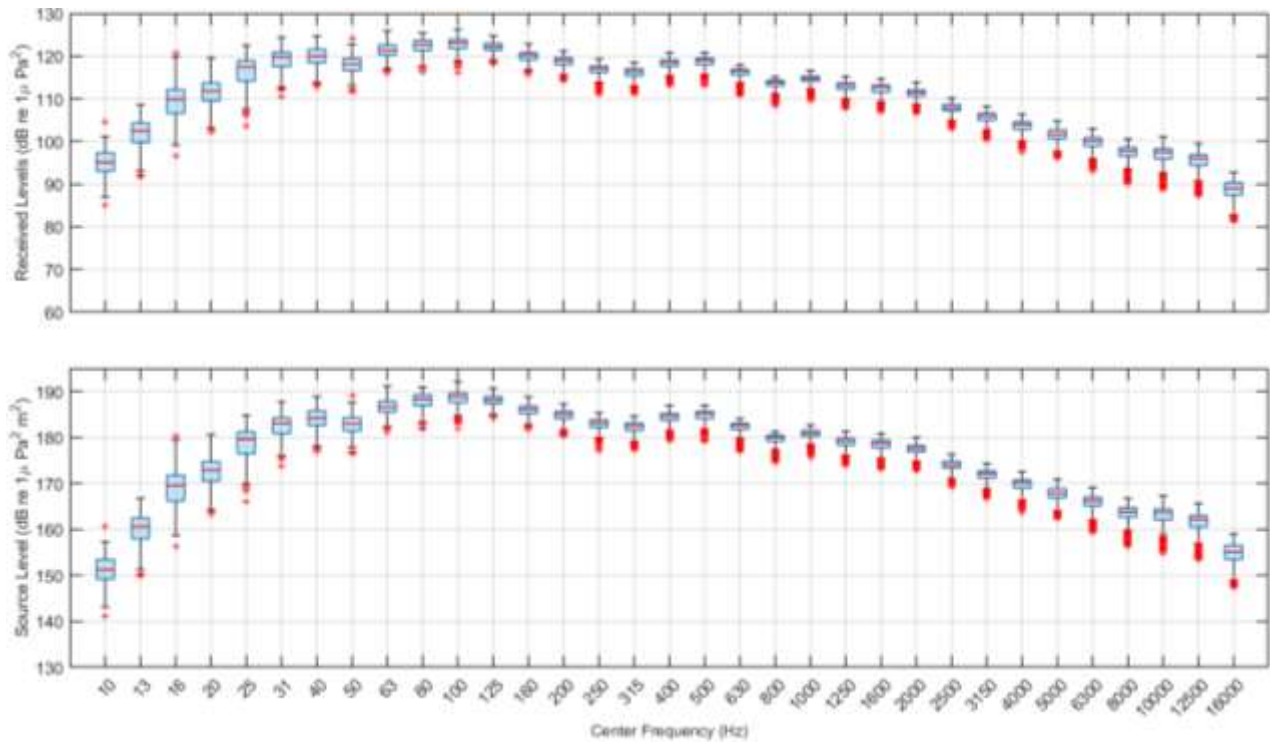


Figure 51. ATLANTIC MERLIN. (Top) Received levels during exercise 2. (Bottom) Calculated source level using Equations 4 and 5 during exercise 2.

### 3.6.1.3. Exercise 3

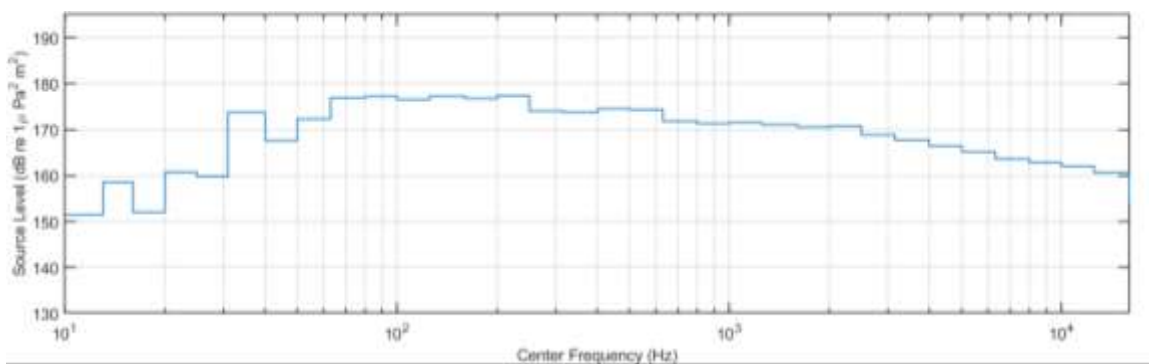


Figure 52. ATLANTIC MERLIN. Source level calculated using Equations 4 and 5 during exercise 3.

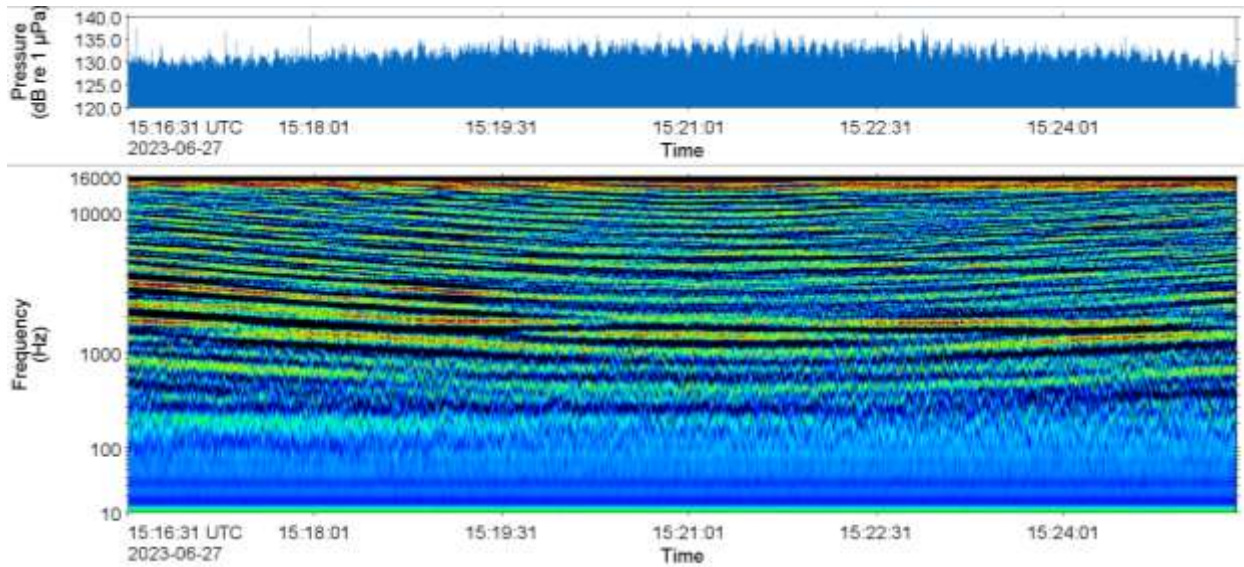


Figure 53. Spectrogram calculated from ALTO2 recordings around the time when ATLANTIC MERLIN executed exercise 3. The data shows the classic ‘bathtub’ or ‘U’ shaped spectrogram due the Lloyd’s mirror interference pattern. The vessel is at the closest point of approach at the bottom of the ‘U’.

### 3.6.2. SIEM SYMPHONY

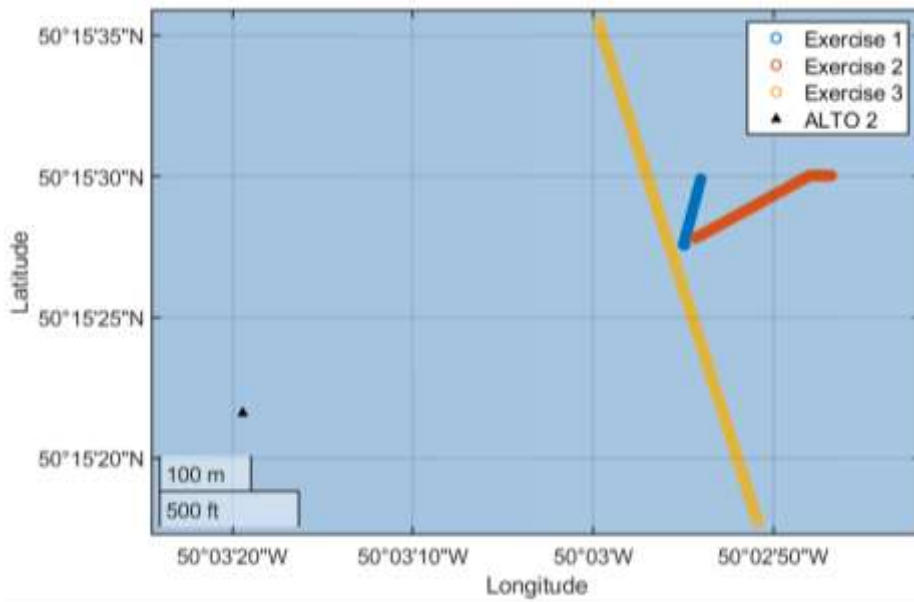


Figure 54. SIEM SYMPHONY track referenced by ALTO 2 position as a black triangle around the time of the exercises.

3.6.2.1. Exercise 1

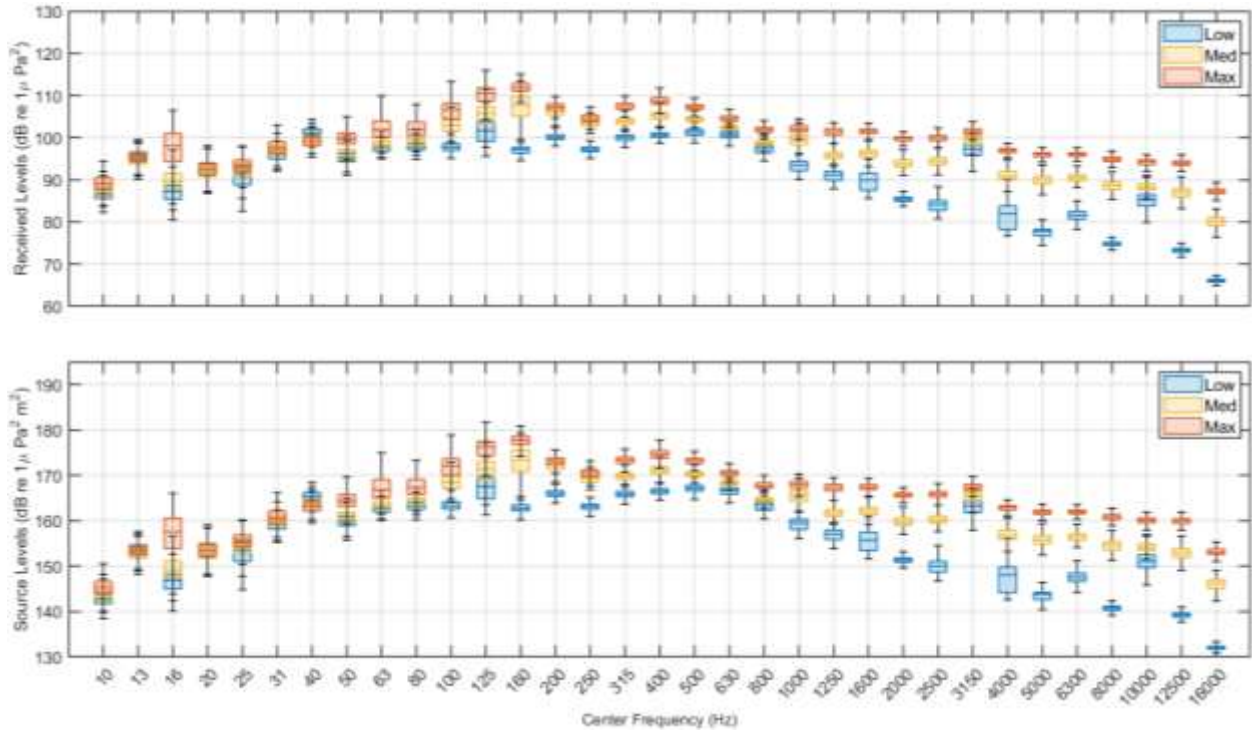


Figure 55. SIEM SYMPHONY. (Top) Received levels during exercise 1 grouped by thruster level. (Bottom) Calculated source level using Equations 4 and 5 during exercise 1 grouped by thruster level.

### 3.6.2.2. Exercise 2

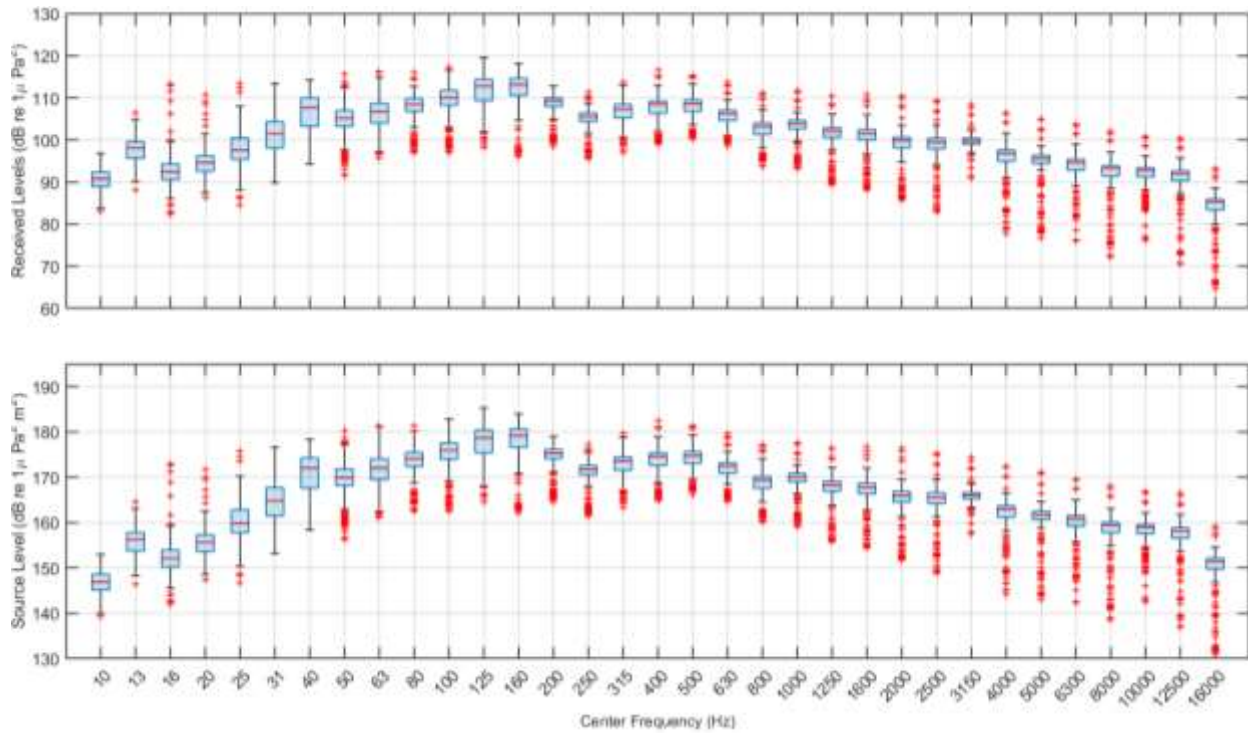


Figure 56. SIEM SYMPHONY (Top) Received levels during exercise 2. (Bottom) Calculated source level using Equations 4 and 5 during exercise 2.

### 3.6.2.3. Exercise 3

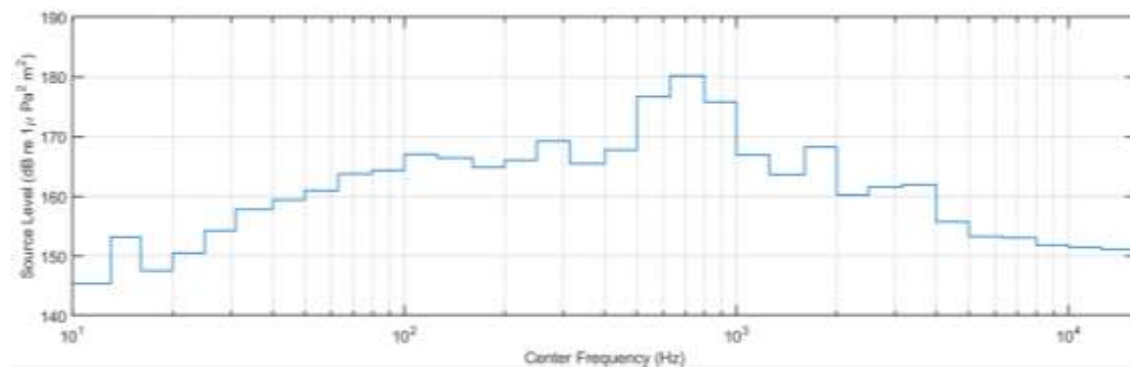


Figure 57. SIEM SYMPHONY calculated source level using Equations 4 and 5 during exercise 3.

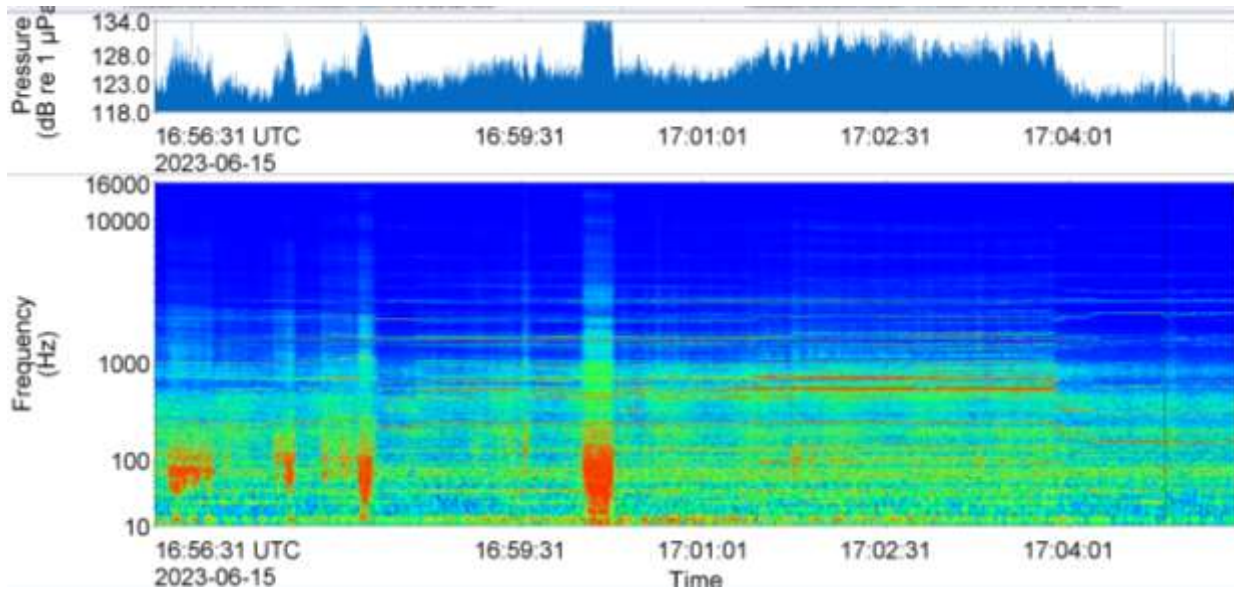


Figure 58. Spectrogram calculated from ALTO2 recordings around the time when SIEM SYMPHONY executed exercise 3. The bathtub pattern visible in Figure 53 is not present, likely due to the hybrid propulsion system on the SIEM SYMPHONY.

## 4. Discussion

### 4.1. Hearing Threshold Shifts

There are two categories of auditory threshold shifts (also termed Noise Induced Threshold Shift, NITS): Permanent Threshold Shift (PTS), a permanent physical injury to an animal's hearing system, and Temporary Threshold Shift (TTS), a temporary reduction in an animal's hearing sensitivity as the result of physiological and mechanical processes in the inner ear. There are no PTS studies on marine mammals, reflecting considerations for animal welfare and treatment. The onset level of PTS is conventionally assumed to be at 40 dB above TTS. While PTS undoubtedly constitutes an injury, TTS (as a temporary effect) was not considered in the same way. However, recent research clearly indicates that moderate levels (<12 dB) of TTS in terrestrial mammals produced an accelerated hearing loss (PTS) resulting from progressive neural degeneration with age (Kujawa and Liberman 2006, 2009, Maison et al. 2013, Kujawa and Liberman 2015). This relatively low level of TTS (12 dB) resulted in 22 % neuronal loss in the inner ear. Accumulated over multiple (low-level) TTS exposures this effect accumulates and leads to PTS. The most recent criteria for assessing possible effects of non-impulsive sound (such as vessel noise) on marine mammals are summarized in Table 10.

The threshold for daily SEL at which a very high-frequency mammal (VHF) (porpoises, dwarf/pygmy sperm whales) could experience temporary hearing threshold shifts (TTS) is 153 dB re 1  $\mu\text{Pa}^2\text{s}$ ; the thresholds are 178 and 179 dB re 1  $\mu\text{Pa}^2\text{s}$  for high-frequency (HF, delphinid) and low-frequency (LF, baleen whales) mammals respectively. The SEL at the ALTO2 recorder 40 km from the drillship shows that none of the mammal groups would have experienced TTS due to the noise generated by the support vessels (Figure 25). At ALTO2, three peaks of the daily SEL are noticeable for the broadband and LF mammals on 12, 16, and 27 June, corresponding to the day of the exercises for the Kingfisher, the Gardner, and the Merlin, respectively. The daily SEL in the absence of the support vessels during the exercises are typical for deep water temperate ocean environments (Martin et al. 2019).

Table 10. Acoustic impairment effects of non-impulsive noise on marine mammals: SEL<sub>24h</sub> thresholds (Southall et al. 2019)

Hearing group	Southall et al. (2019)	
	PTS onset thresholds (received level)	TTS onset thresholds (received level)
	Weighted SEL <sub>24h</sub> ( $L_{E,24h}$ ; dB re 1 $\mu\text{Pa}^2\text{s}$ )	Weighted SEL <sub>24h</sub> ( $L_{E,24h}$ ; dB re 1 $\mu\text{Pa}^2\text{s}$ )
LF cetaceans	199	179
HF cetaceans	198	178
VHF cetaceans	173	153

$L_E$  denotes cumulative sound exposure over a 24 h period and has a reference value of 1  $\mu\text{Pa}^2\text{s}$ .

## 4.2. Ambient Sound and Vessel Source Levels

### 4.2.1. Correlations of Ambient Sound with Wind and Wave Activity.

The wind speed and the significant wave height measured near ALTO1 were correlated with the decidecade sound pressure levels in the 100, 200, 315, 1000, and 3150 Hz bands recorded at ALTO2 (Figure 59). Apart from the expected positive correlations between the acoustical data, the most relevant correlations are between windspeed and the 1000 Hz (0.37) and 3150 Hz (0.68) decidecades; and between the significant wave height and the 1000 Hz (0.21) and 3150 Hz (0.49) decidecades. The correlation coefficient between the wind speed and the significant wave height is of 0.61.

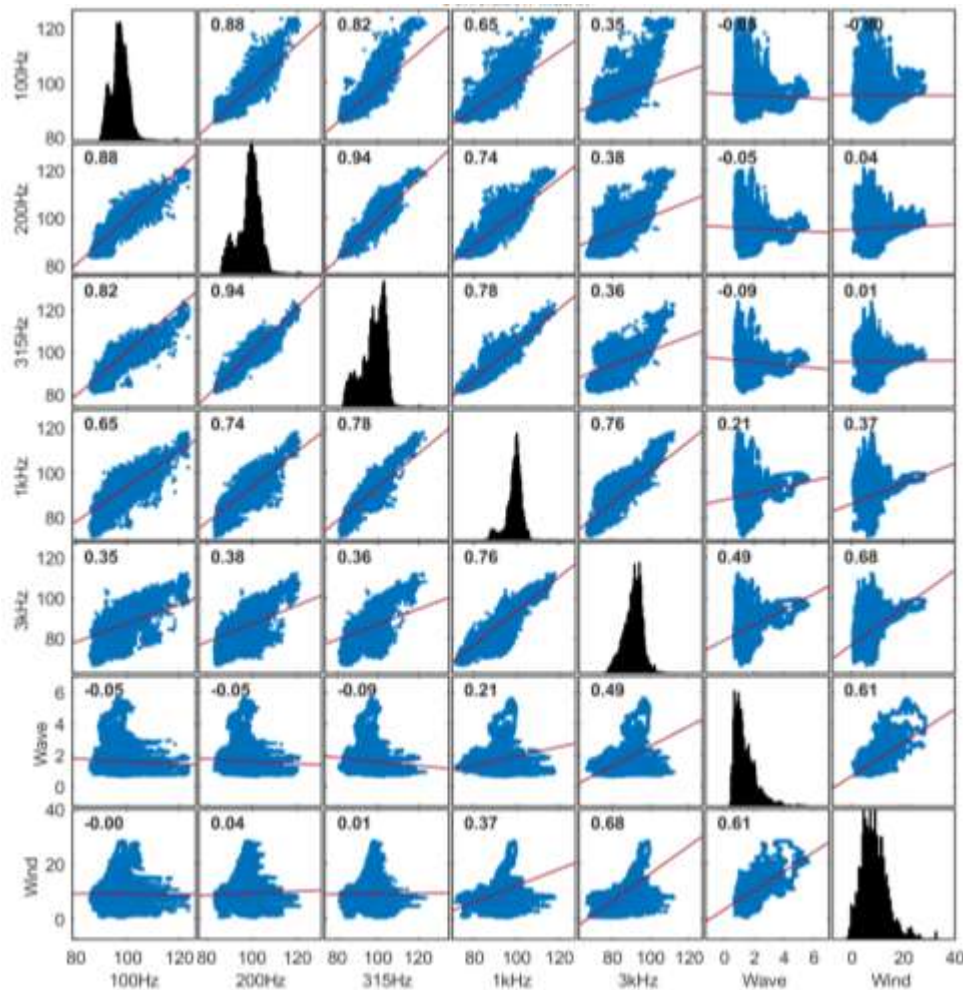


Figure 59. Correlation pairs plot for the ALTO2 recorder comparing wind speed and significant wave with median decidecade sound pressure level for the period when the drillship was at Ephesus well. The diagonal of the figure shows a histogram of the corresponding variable. The numbers at the corner of each individual panel show correspond to the correlation coefficient between variables. As an example, the lowest cell of the first column is the correlation between wind speed and the 100 Hz decidecade.

### 4.2.2. Ambient Sound and Exceedances of 120 dB re 1 $\mu$ Pa

The band-level plots, spectrograms (Long-term Spectral Averages; LTSA), decidecade box-and-whisker plots, and spectral density level percentiles presented in Section 3.1 provide an overview of the sound variability in time and frequency and permit an overall discussion of the soundscape during the time of this study near ALTO2. Both in the low and high frequency results, the presence of the STENA ICEMAX in the field was clearly observed. Additionally, horizontal lines of higher sound levels in the LTSA were associated with the times when the SV executed their exercises.

The EIS states that based on previous studies (Zykov 2016, Matthews et al. 2018), a 120 dB re 1  $\mu$ Pa threshold should be reached at 23-40 km from a drill rig using a  $R_{95\%}$  distance estimate. The decade band box-and-whisker plots confirm the EIS statement since ALTO2 is positioned 40 km from the STENA ICEMAX (Figure 60). A total of 0.8 % of the minutes of data recorded exceeded 120 dB re 1  $\mu$ Pa, most of which occurred during the support vessel exercises. Since the soundscape is the sum of many sources all around the recording site, it is not possible to determine the highest sound level that is attributable to the drilling operation.

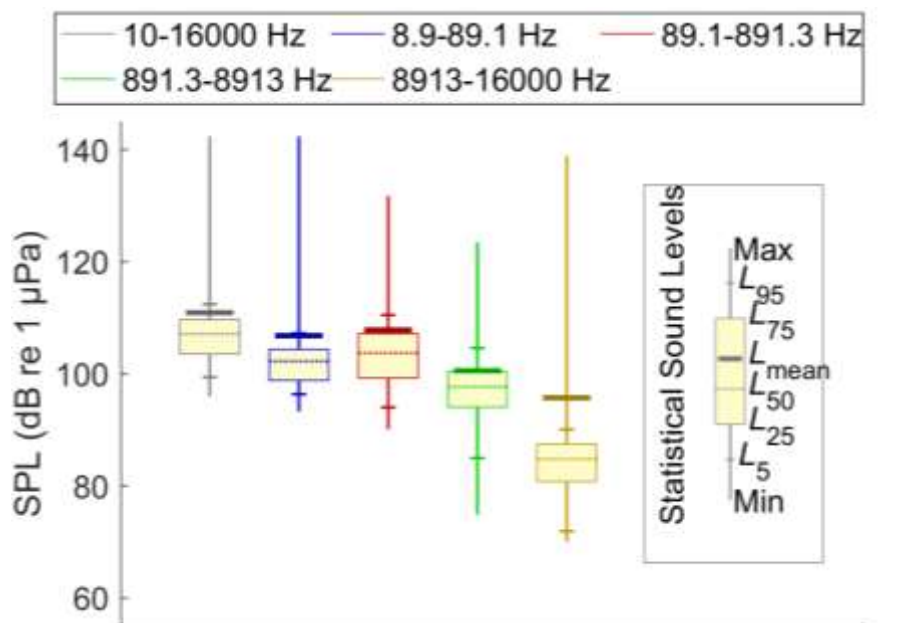


Figure 60. Decade band sound pressure levels from ALTO2. 0.8 % of the broadband sound pressure levels (10–16000 Hz) were above 120 dB re 1  $\mu$ Pa.

One of the objectives of the acoustic monitoring campaign was determining how the drillship affected the baseline soundscape. Figure 61 shows that the mean decidecade sound pressure levels increased by 0.8 and 6.7 dB during the drilling compared to before and after drilling, respectively; and that before and after differed by 5.9 dB. The sound levels at 63 to 500 Hz were 5-7 dB higher on average during drilling than before, however the levels above 1250 Hz were higher before than during drilling, resulting in an overall difference that was only 0.8 dB. The primary driver for decreases in decidecade band SPLs after drilling compared to before drilling were lower wind speeds. The mean sound pressure level and percentage of the minutes that exceeded 120 dB re 1  $\mu$ Pa<sup>2</sup> are provided in Table 11. There were no exceedances of 120 dB

re 1  $\mu\text{Pa}^2$  outside of the drilling program; 1.04% of the minutes recorded exceeded 120 dB re 1  $\mu\text{Pa}^2$  during the drilling.

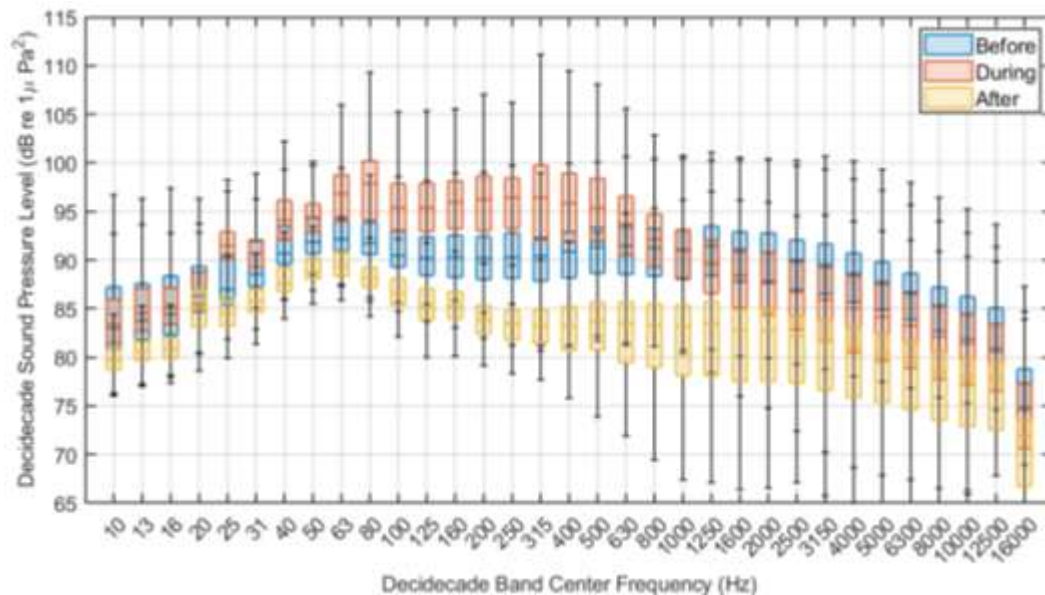


Figure 61. Comparison of the decidecade sound pressure level distributions before, during and after the drilling campaign at ALT02, 40 km from the drillship.

Table 11. Mean sound pressure level (10 – 256000 Hz) at ALTO2 during the phases of the acoustic monitoring operations.

Time Period	Mean Sound Pressure Level (10 – 256000 Hz, dB re 1 $\mu\text{Pa}^2$ )	Percent of 1 min samples > 120 dB re 1 $\mu\text{Pa}^2$
Before Arrival	105.5	0
During Drilling	111.6	1.04
After Departure	99.9	0

### 4.2.3. Support Vessel (SV) Source Levels

Three exercises were designed to provide uniformity and simulate real-time conditions when characterizing the SV source levels. Each vessel’s navigation officers reported the times and spatial coordinates at which the required exercises were executed, additionally, the provided AIS data allowed JASCO to interpolate to 1 s intervals the spatial position of the vessel, thus creating tracks of the vessels during the exercises. The following results were noted:

- For exercise 1, in which three levels of the thrusters were measured, the source levels of all SVs and all thrusters showed a similar behaviour as a function of frequency with the levels increasing up to 190 dB re 1  $\mu\text{Pa}^2 \text{ m}^2$  around the 100–200 Hz band and then decreasing to 140 dB re 1  $\mu\text{Pa}^2 \text{ m}^2$  for the higher frequencies. The ATLANTIC KINGFISHER, ATLANTIC MERLIN, and KJ GARDNER presented similar levels regardless of the thruster level, while the MAERSK CLIPPER\ and SIEM SYMPHONY had

higher levels with higher thruster levels, the difference between thruster levels being more substantial at higher frequencies.

- The MAERSK MOBILIZER did not execute the exercises properly and could not be included for the source level calculations. The tracks generated from AIS data during the times of the exercises, presented in Figure D-5, show that the MOBILIZER sailed past the ALTO2 station without following the indications for exercise 3. Additionally, the reports provided to JASCO indicate that during exercise 3, only one level of thrusters were used. While some calculation of the source levels could have been done, it wouldn't have been in-line with the rest of the SV and therefore would lack statistical value for comparison.
- For exercise 2, in which the SVs sailed away from the ALTO2 station, the source level behaviour as a function of frequency is similar to the results in exercise 1. The SIEM SYMPHONY had the lowest maximum source level of all the SVs with a median of 179 dB re 1  $\mu\text{Pa}^2 \text{m}^2$  at 160 Hz. The rest of the SV reached a maximum median of up to 190 dB re 1  $\mu\text{Pa}^2 \text{m}^2$ .
- For exercise 3, in which the sound profile of the SV sailing within a 60-degree angle, with ALTO2 as the vertex, was measured, the source levels were constantly lower compared to the previous exercises. Values in the 170 dB re 1  $\mu\text{Pa}^2 \text{m}^2$  were typical for all vessels in the 500–1000 Hz band, with MAERSK CLIPPER showing a maximum median value of 185 dB re 1  $\mu\text{Pa}^2 \text{m}^2$  at 100 Hz. Table 12 presents a summary of the calculated source levels in the form of the median value in the 10–16000 Hz broadband for each exercise and for each SV.

Additionally, the mean source level was calculated for each SV by grouping exercise 1 and 2 and then exercise 3, the results are presented in Figures 62 and 63. The ATLANTIC KINGFISHER, ATLANTIC MERLIN, and KJ GARDNER show a very similar behaviour with maxima around 100 Hz and values between 185 and 190 dB re 1  $\mu\text{Pa}^2 \text{m}^2$ . The MAERSK CLIPPER agrees well for lower and higher frequencies, however, in the 60 – 2000 Hz band the source levels are lower by up to 10 dB re 1  $\mu\text{Pa}^2 \text{m}^2$ . The SIEM SYMPHONY consistently shows the lowest source levels; during the time of the exercises, the received levels (Figure 47) from the SIEM SYMPHONY were lower than the rest of the SVs by up to 20 dB re 1  $\mu\text{Pa}^2$ . To further investigate, spectrograms were calculated for times when the transit exercise was being executed, exercise 3. The spectrogram corresponding to the ATLANTIC MERLIN transit is shown in Figure 53 with the typical U-shape or “bathtub” associated with Lloyd’s mirror interference pattern. For the SIEM SYMPHONY, Figure 58, the spectrogram does not show the bathtub shape.

Table 12. Median Source levels for each vessel for each exercise.

Support vessel	Exercise 1 Median SL (dB re 1 $\mu\text{Pa}^2 \text{m}^2$ )	Exercise 2 Median SL (dB re 1 $\mu\text{Pa}^2 \text{m}^2$ )	Exercise 3 Median SL (dB re 1 $\mu\text{Pa}^2 \text{m}^2$ )
Kingfisher	196.1	196.3	192.8
Gardner	198.7	199.3	192.1
Symphony	185.0	187.3	184.1
Merlin	195.4	198.2	187.5
Clipper	194.0	188.1	182.9

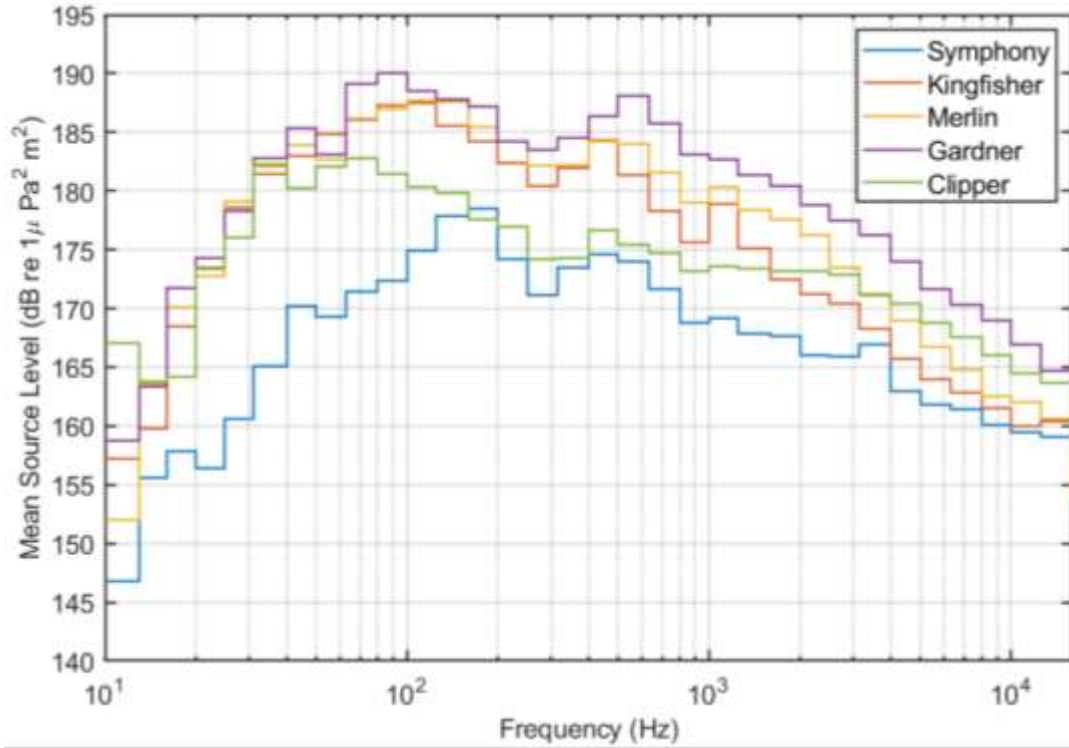


Figure 62. Mean source level as a function of frequency for each SV. The mean value was calculated considering exercise 1 and 2.

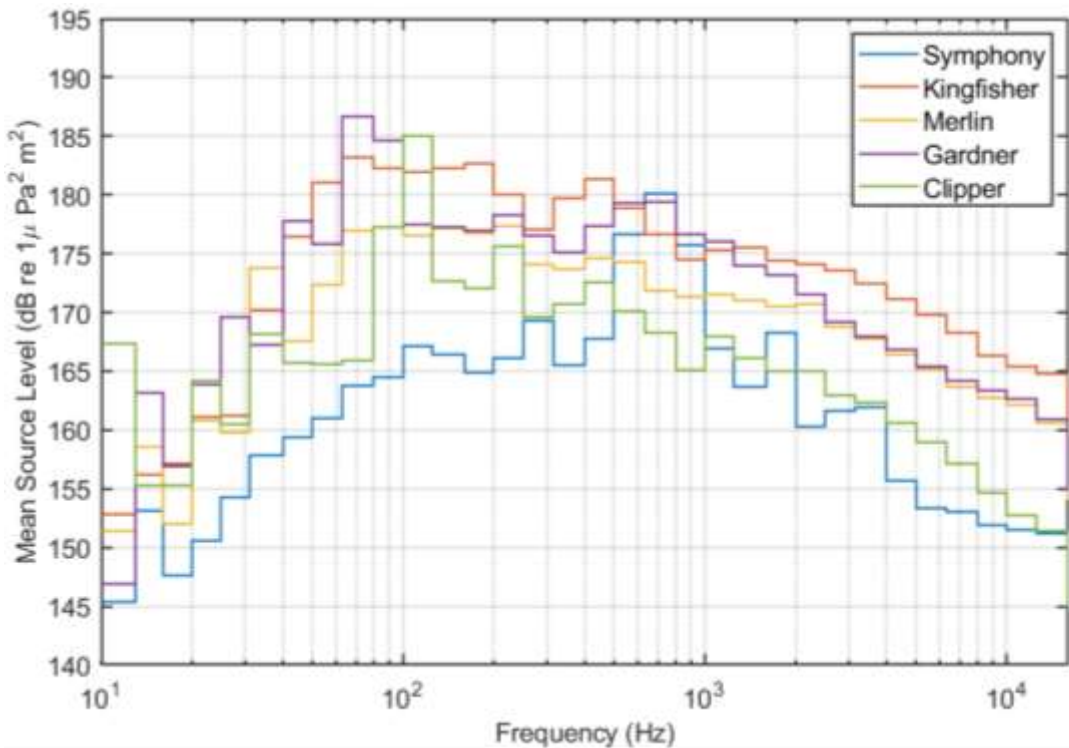


Figure 63. Mean Source Level as a function of frequency for each SV during exercise 3.

Overall, from Figures 62 and 63, the support vessel source levels are in line with the estimated value of 188.6 dB re 1  $\mu\text{Pa}^2 \text{ m}^2$  employed by Matthews et al. (2018) for the EIS predictions of the effects of the support vessels. This increases the confidence that the estimate of 196.7 dB re 1  $\mu\text{Pa}^2 \text{ m}^2$  that was employed as the source level of the drillship is likely also correct.

### 4.3. Marine Mammals

The marine mammal acoustic detection results presented in this report provide an index of acoustic occurrence for each species. Although they can be used to describe the relative abundance of a species across the study area, several factors influence the detectability of the targeted signals. Although acoustic detection does indicate presence, an absence of detections does not necessarily indicate absence of animals. An animal may be present but not detected if no individuals were vocalizing near the recorder, their signals were masked by environmental and/or anthropogenic noise sources, or a combination of these factors. Different sound propagation environments and different seasonal effects will impact the detection range of a given signal over time and, therefore, influence the number of detectable signals. Seasonal variations in vocalizing behaviour may falsely suggest changes in occurrence. Therefore, the acoustic occurrence of each species across stations is discussed in consideration of environmental, anthropogenic, and biological factors that influence the detectability of the targeted acoustic signals.

The mammal detectors (see Section 3.3) had high to very high precision scores (0.78 – 1.0), meaning that when a detector indicated presence, the mammals were almost always truly present. The lowest scores of 0.78 for dolphin whistles and pilot/killer whale whistles generally lowered by detecting the other species group rather than detecting a different type of sound (anthropogenic or natural). Recall scores were generally greater than 0.5, which is very good for the purposes of assessing daily presence of marine mammals. This means that over half of the files with calls were detected. When mammal calls occur, the calls per file generally increases as the animals enter the listening range of the recorder, reach a maximum, and then decrease again as they leave the area. This is especially true for the highly vocal odontocetes. Since the objective of the measurement program was documenting the temporal occurrence of marine mammal at an hourly – to – daily resolution, a high precision is more important than recall, that is, we can miss a significant proportion of the calls and still know that the animals were present. The levels of performance documented here support the assertion that the results accurately describe the presence of the marine mammals.

#### 4.3.1. Mysticetes

##### 4.3.1.1. Fin Whales

A cosmopolitan species found in all oceans from the tropics to polar regions both in coastal and pelagic areas, fin whales are common and widely distributed in the western North Atlantic (Edwards et al. 2015). For most populations, there does not appear to be clearly defined breeding areas and a continuum of migratory behavior has been described (Geijer et al. 2016). Previous PAM in Orphan Basin from 2015 to 2017 found fin whales to be acoustically common from mid July to mid April, but the species was acoustically rare to absent in May and June (Stn 15 in Delarue et al. 2018, Delarue et al. 2022). This trend was apparent in the present acoustic monitoring from 10 Apr to 7 July 2023, where the species was only acoustically detected on one day in June and one day in July. Seasonal decreases in acoustic activity can

be attributed to seasonal changes in song production rather than a reduction in animals present (Roy et al. 2018, Delarue et al. 2022). Indeed, the 20 Hz pulse was the primary signal used to detect fin whales, and the production of this signal changes seasonally (Watkins 1981, Delarue et al. 2009). In addition to the 20 Hz pulses, that make up the seasonal songs of fin whales, the species produces broadband downsweeps (Watkins 1981) year-round, albeit at much lower rates. These signals are more challenging to assign to the species as they overlap in characteristics with other baleen whales, including sei whales which were common in the present data set. Fin whale occurrence results should therefore be considered a minimum, as their some of their calls may not have been confirmed as fin whale's, or the species was present but not vocalizing due to their seasonal vocal behaviour.

#### 4.3.1.2. Sei Whales

North Atlantic sei whales seem to follow the general pattern of baleen whale migration where they forage in high latitudes in summer and migrate to lower latitude breeding grounds in winter (Prieto et al. 2014). Satellite tracking revealed migration routes from the Azores in spring to the Labrador Sea and Flemish Cap in summer (Prieto et al. 2014). In the Orphan Basin, previous PAM detected sei whale vocalizations from April to December, with inter-annual variations in detection peaks despite a trend towards higher detections between September and November (Stn 15 in Delarue et al. 2018, Macklin 2022). In the present data, sei whale detections were increasingly common through June and July 2023, before the acoustic equipment was retrieved 7 July. This trend may represent an influx of whales arriving at their summer feeding grounds from wintering areas. Detector precision was high (92%) but recall was moderate (63%) suggesting that the results presented here underestimate the acoustic occurrence of sei whales during the recording period.

### 4.3.2. Odontocetes

#### 4.3.2.1. Delphinids

We discuss delphinids in two categories or species groups, small dolphins (e.g., white-beaked dolphins), and the larger delphinids that include killer and pilot whales. Both species groups were acoustically present throughout the recording period, with detections becoming more regular in June.

##### 4.3.2.1.1. Dolphins

Many dolphin species can occur in the waters off Newfoundland, including white-beaked, Atlantic white-sided, and short-beaked common dolphins (Sergeant et al. 1970, Gowans and Whitehead 1995, Lawson and Gosselin 2011, Hayes et al. 2020).

White-beaked dolphins are generally abundant and have an extensive range throughout the North Atlantic to which they are restricted. In Newfoundland and Labrador, they were by far the most abundant cetacean in a 2016 survey (Lawson and Gosselin 2018). In summer, animals move north in summer into the Davis Strait following the movement of colder waters (Lien et al. 2001). White-beaked dolphins are frequently encountered in June on the Southeast Shoal of the Grand Banks, and they are the most common delphinid in summer on the Labrador shelf (Whitehead and Glass 1985, Alling and Whitehead 1987, Kingsley and Reeves 1998). This species is therefore expected to make up most dolphin acoustic detections in April to July 2023 in the Orphan Basin. Although

Atlantic white-sided dolphins are endemic to the North Atlantic. White-sided dolphins prefer cool water on the continental shelf (Selzer and Payne 1988). Based on sighting clusters and discontinuities in strandings and observations between three core areas, there may be three population units centred around the Gulf of Maine, Gulf of St. Lawrence, and Labrador Sea (Hayes et al. 2020). Relative to other areas off eastern Canada, white-sided dolphin abundance was much lower off Newfoundland and Labrador (Lawson and Gosselin 2018). The species was found to be substantially more common off southern Newfoundland than off eastern Newfoundland. Therefore, while white-sided dolphins may have contributed to a portion of the dolphin acoustic detections in Orphan Basin, they are not expected to occur in the area as regularly as white-beaked dolphins, particularly during the recording period (April-early July).

Short-beaked common dolphins are distributed worldwide in tropical and temperate seas. Sightings are usually concentrated over the continental shelf between the 100 and 2000 m isobaths. In the North Atlantic, they have been recorded in association with prominent bathymetric features and the Gulf Stream (Selzer and Payne 1988, Hamazaki 2002, Hayes et al. 2020). Short-beaked common dolphins exhibit seasonal movements. In summer and autumn, they tend to be found on Georges Bank, in the Gulf of Maine, and in Canadian waters on the Scotian Shelf and the Grand Banks. Compared to the Scotian Shelf and Gulf of St. Lawrence, the species is less abundant off Newfoundland (Gowans and Whitehead 1995, Hooker et al. 1997, Lawson and Gosselin 2009). Short-beaked common dolphins are therefore not expected to be as common in the Orphan Basin as other species and may only represent a subset of the dolphin acoustic detections.

While other dolphin species have been recorded in or near Orphan Basin (bottlenose dolphins, striped dolphins; Gomez et al. (2020)), their preference for relatively warm water makes it unlikely that they would have been present in the spring.

#### 4.3.2.1.2. Pilot/Killer Whales

In the North Atlantic, long-finned pilot whale range extends from North Carolina to Greenland, Iceland, and the Barents Sea and into the Mediterranean Sea. Long-finned pilot whales are a deep-diving species (Heide-Jørgensen et al. 2002) that typically occur in deep waters along the shelf slope but are also known to reside in coastal habitats (Kingsley and Reeves 1998). This species feeds on squid and fish, and there is a connection between the arrival of shortfin squid (*Illex illecebrosus*) and pilot whales in Newfoundland bays (Sergeant 1962, Mercer 1975). From 2015 to 2017, pilot whale vocalizations were detected in Orphan Basin, particularly in April to September (Stn 15 in Delarue et al. 2018), therefore, most, if not all whistle detections under 5 kHz in the present study are expected to be from pilot whales.

Most killer whale sightings off eastern Canada occur between June and September in coastal waters of Newfoundland and Labrador. However, cases of ice entrapment suggest that some killer whales may be present year round (Lawson et al. 2007). Sightings are relatively common on the southeastern and eastern shoals of the Grand Banks, and killer whales are seen at least occasionally in inshore waters of southeastern and southwestern Newfoundland (Lawson and Stevens 2013). Therefore, a portion of the detections, in the present study may have been of killer whale whistles.

#### 4.3.2.2. Narrow-band High Frequency Clicks

There is overlap in the click characteristics and distribution of harbour porpoises and pygmy sperm whales (Marten 2000, Madsen et al. 2005, Villadsgaard et al. 2007). It is therefore difficult to say with certainty which species was detected (once in May and twice in June 2023) in the Orphan Basin data. Although dwarf

sperm whales also produce NBHF clicks similar to those recorded here, their preference for warm and temperate waters presumably excludes them from the study area, particularly in springtime.

Pygmy sperm whales are found in deep waters in tropical to warm temperate zones of all oceans. They occur mainly in deeper slope waters along and seaward of the shelf edge, where they feed on mesopelagic squid (McAlpine et al. 1997). Pygmy sperm whales occasionally occur off eastern Canada (Baird et al. 1996, McAlpine et al. 1997, Lucas and Hooker 2000, Measures et al. 2004, Delarue et al. 2018, Hayes et al. 2020), but the Orphan Basin is presumably close to the northern edge of pygmy sperm whale's range.

While harbour porpoises were once considered a species that rarely occurs offshore, evidence from satellite tags, genetic data, and morphology indicate that the harbour porpoises found off West Greenland are a distinct ecotype unique among harbour porpoises of the rest of the North Atlantic (Nielsen et al. 2018, Louis et al. 2022, Olsen et al. 2022). In fall, as ice cover increases, harbour porpoises leave the Davis Strait and Labrador Sea and move to more southern offshore waters through winter and spring, before returning to Greenland in summer. It is animals from this ecotype that may occur in Orphan Basin. Indeed, harbour porpoises were sighted near the northern edge of Orphan Basin in August 2023 (personal communication Julien Delarue). The low detection rates may be related to the depth of the recorder in relation to the diving depth of the porpoises (up to 400 m) which results in typical detection ranges around 600 m.

#### 4.3.2.3. Sperm Whales

Sperm whales are the largest toothed whales and the largest toothed predator, with an extensive worldwide distribution. This species is usually found in deep, offshore waters where they forage at depth (Scott and Sadove 1997, Hayes et al. 2020). Mature males migrate on an unknown schedule between high-latitude feeding grounds and low-latitude breeding areas where they join groups of females and juveniles to breed. The range of female and juvenile groups is centred around tropical and subtropical waters, generally in areas where the sea surface temperature is greater than 15°C (Whitehead 2018).

Sperm whales routinely dive to depths over 1 km and are capable of remaining submerged for over one hour, but most dives probably last a half-hour or less (Drouot et al. 2004, Davis et al. 2007, Irvine et al. 2017). In Orphan Basin, previous PAM found the species to be acoustically present in most months of the year with detections most common from August to January (Stn 15 in Delarue et al. 2018). It is therefore unsurprising that sperm whales were acoustically present in Orphan Basin in April to July 2023. The low recall value (55%) suggests that acoustic occurrence is underestimated.

#### 4.3.2.4. Northern Bottlenose Whales

Northern bottlenose whales are endemic to the North Atlantic Ocean (Macleod et al. 2005). They occur primarily in cool and Subarctic waters. The two primary areas of occurrence in the western North Atlantic are along the eastern Scotian Shelf and the Davis Strait. As a result, the species is separated into two populations for management purposes: the Scotian Shelf population and the Davis Strait-Baffin Bay-Labrador Sea population. Northern bottlenose whales have also been recorded off southern and eastern Newfoundland (Lawson and Gosselin 2009, Feyrer et al. 2019) but the potential affiliation of these individuals between populations remains unresolved (Einfeldt et al. 2022). Acoustically detected almost daily in Orphan Basin from April to July 2023, the present work confirms the findings by Delarue et al. (2018) that Orphan Basin is an important habitat for northern bottlenose whale. The high precision and recall of the click detector indicate that the acoustic occurrence of this species is accurately characterized.

#### 4.4. Implications of the Failure of the Recorder at 1 km

The failure of the recorder at 1 km represents a 50% loss of the planned data, however, that did not translate to achieving only 50% of the project objectives. The primary objective that was not achieved was measurement of the drillship source level under improved geometries compared to previous measurements. The remaining key objectives were accomplished, most importantly, evaluating whether the 120 dB re 1  $\mu\text{Pa}^2$  threshold was exceeded at the 40 km distance (which it was not), and if there were detectable changes in marine mammal presence (which there were not).

Based on previous measurements we would expect that the sound exposure threshold for temporary hearing threshold shifts would be exceeded on many days for the baleen whales and very-high frequency marine mammals (porpoise and kogia species). The threshold for permanent threshold shift likely would have occurred on a few of the drilling days for the very-high frequency mammals. However, it is expected that none of the animals would remain close enough to the drillship for an entire day, and therefore the occurrence of hearing injuries would most likely not occur. It is expected that there would be a notable decrease in odontocete presence near the drillship that could not be explained by the changes in detection ranges alone (McPherson and Martin 2018).

## 5. Conclusion

The acoustic measurement plan was executed yielding ~26 days of data before the drillship arrived, 55 days of data with the drillship present, and 7 days of data after the drillship departure. The drillship was present 6 May – 1 July 2023. Only measurements at 40 km from the drillship were collected due to a failure of the hydrophone cable at 1 km when under pressure at the seabed. The key results by measurement objective were:

1. **Objective:** Compare measured acoustic footprint distances from drilling-related sound sources to EIS predictions of 10–40 km to a sound pressure levels 120 dB re 1  $\mu\text{Pa}^2$ .

**Result:** the mean broadband level at 40 km was 111.6 dB re 1  $\mu\text{Pa}^2$  during the drilling program, with 1.04% of the one-minute samples exceeding 120 dB re 1  $\mu\text{Pa}^2$ . There were no exceedances of 120 dB re 1  $\mu\text{Pa}^2$  threshold before or after the drillship presence. There were no exceedances of the thresholds for marine mammal hearing injury at 40 km from the drilling.

2. **Objective:** Establish baseline sound levels at locations near the planned drilling area and evaluate changes to the baseline acoustic conditions resulting from drilling activities

**Result:** The sound levels without the drilling program were quieter in July than April. The mean difference in SPL was 6.1 dB higher during drilling compared to before drilling. The mean SPL was 11.7 dB lower after drilling than during drilling when measured 40 km from the drillship. The frequency band affected by the drillship was ~30 – 3000 Hz. The difference between the before, during and after sound levels at the drill site was not assessed due to the failure of the hydrophone cable at ALTO1.

3. **Objective:** Assess the presence and acoustic occurrence of marine mammals before and during drilling operations.

**Result:** It is well known that mysticete whales decrease their vocalizations during the April – July period offshore of Newfoundland. This result was confirmed for the Ephesus drilling campaign in the Orphan Basin. Fin whales were detected on two occasions while sei whales were detected on 18 days. Directional analysis of the sei whale detections indicated that at most two individuals (or perhaps groups) were present at any one time. Small dolphins as well as pilot or killer whales were regularly present in the acoustic recordings, with their activity increasing in June. Sperm whales were detected intermittently, and dwarf/pygmy sperm whales or harbour porpoise were detected on three occasions. Northern Bottlenose whales were present daily from April to ~1 July. Marine mammal presence did not appear to be affected by the drillship 40 km away since there were no changes in call detection rates that correlated with the arrival and departure of the drillship. Changes in presence at the drill site could not be assessed due to the failure of the hydrophone cable. The high sound levels from the drilling would have masked most mammal detections.

4. **Objective:** Measure the source levels of the drillship and the support vessels.

**Result:** The source levels of the support vessels while on dynamic positioning systems was higher than the source level employed during the EIS modelling. Nevertheless, the total sound field measured at 40 km was lower than the required threshold. For several of the vessels, their spectrum was also bimodal with peaks at 100 and 500 Hz rather than a single peak at 100 Hz. The source level of the SIEM SYMPHONY was particularly quiet compared to the other support vessels and most vessels assessed by JASCO. The source level of the drillship was not determined due to the failure of the recorder at 1km.

## 6. Glossary of Acoustics Terms

Unless otherwise stated in an entry, these definitions are consistent with ISO 18405 (2017a).

### **1/3-octave**

One third of an [octave](#). *Note:* A 1/3-octave is approximately equal to one [decidecade](#) ( $1/3 \text{ oct} \approx 1.003 \text{ ddec}$ ).

### **1/3-octave-band**

[Frequency](#) band whose [bandwidth](#) is one [1/3-octave](#). *Note:* The [bandwidth](#) of a 1/3-octave-band increases with increasing centre frequency.

### **acoustic noise**

[Sound](#) that interferes with an acoustic process.

### **ambient sound**

[Sound](#) that would be present in the absence of a specified activity (ISO 18405:2017a). It is usually a composite of sound from many sources near and far, e.g., shipping vessels, seismic activity, precipitation, sea ice movement, wave action, and biological activity.

### **annotation**

Within a spectrogram, a labelled selection of a time interval and [frequency](#) range as created during [manual analysis](#).

### **audiogram**

A graph or table of [hearing threshold](#) as a function of [frequency](#) that describes the hearing sensitivity of an animal over its hearing range.

### **auditory frequency weighting**

The process of applying an [auditory frequency-weighting function](#). An example for marine mammals are the auditory frequency-weighting functions published by Southall et al. (2007).

### **auditory frequency-weighting function**

[Frequency-weighting function](#) describing a compensatory approach accounting for a species' (or [functional hearing group's](#)) [frequency](#)-specific hearing sensitivity.

### **automated detection**

The output of an [automated detector](#).

### **automated detector**

An algorithm that includes both the [automated detection](#) of a [sound](#) of interest (e.g., vessel noise, marine mammal call) based on how it stands out from the [background noise](#), and its automated classification based on similarities to templates in a library of reference signals.

### background noise

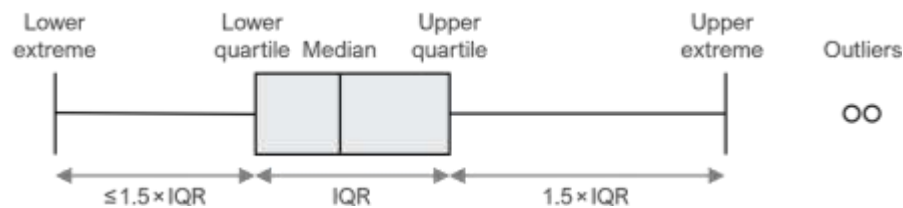
Combination of [ambient sound](#), acoustic self-noise, and, where applicable, sonar reverberation (ISO 18405:2017a) that is detected, measured, or recorded with a signal.

### bandwidth

A range within a continuous band of frequencies. Unit: hertz (Hz).

### box-and-whisker plot

A statistical data plot that illustrates the centre, spread, and overall range of data as a visual 5-number summary. The box is the interquartile range (IQR), which shows the middle 50 % of the data—from the lower quartile (25th percentile) to the upper quartile (75th percentiles). The line inside the box is the median (50th percentile). The whiskers show the lower and upper extremes excluding outliers, which are data points that fall more than  $1.5 \times \text{IQR}$  beyond the upper or lower quartiles.



### broadband level

The total [level](#) measured over a specified [frequency](#) range. If the frequency range is unspecified, the term refers to the entire measured frequency range.

### cavitation

A rapid formation and collapse of vapor cavities (i.e., bubbles or voids) in water, most often caused by a rapid change in pressure. Fast-spinning vessel propellers typically cause cavitation, which creates a lot of noise.

### cetacean

Member of the order Cetacea. Cetaceans are aquatic mammals and include whales, dolphins, and porpoises.

### compressional wave

A mechanical vibration wave in which the direction of particle motion is parallel to the direction of propagation. Also called a longitudinal wave. In seismology/geophysics, it's called a primary wave or P-wave. [Shear waves](#) in the seabed can be converted to compressional waves in water at the water-seabed interface.

### critical band

The auditory [bandwidth](#) within which [background noise](#) strongly contributes to [masking](#) of a single tone. Unit: hertz (Hz).

**decade**

Logarithmic **frequency** interval whose upper bound is ten times larger than its lower bound (ISO 80000-3:2006). For example, one decade up from 1000 Hz is 10,000 Hz, and one decade down is 100 Hz.

**decibel (dB)**

Unit of **level** used to express the ratio of one value of a power quantity to another on a logarithmic scale. Especially suited to quantify variables with a large dynamic range.

**decidecade**

One tenth of a **decade**. Approximately equal to one third of an octave (1 ddec  $\approx$  0.3322 oct), and for this reason sometimes referred to as a **1/3-octave**.

**decidecade band**

**Frequency** band whose **bandwidth** is one **decidecade**. *Note:* The bandwidth of a decidecade band increases with increasing centre frequency.

**delphinid**

Member of the family of oceanic dolphins (Delphinidae), composed of approximately 35 extant species, including dolphins, porpoises, and killer whales.

**duty cycle**

The percentage of time during which an intermittently activated acoustic monitoring system is recording **sound**. E.g., recording 30 min of every hour is a 50 % duty cycle.

**Fourier transform, Fourier synthesis**

A mathematical technique which, although it has varied applications, is referenced in a physical data acquisition context as a method used in the process of deriving a spectrum estimate from time-series data (or the reverse process, termed the inverse Fourier transform). A computationally efficient numerical algorithm for computing the Fourier transform is known as the fast Fourier transform (FFT).

**frequency**

The rate of oscillation of a periodic function measured in cycles per unit time. The reciprocal of the period. Unit: **hertz (Hz)**. Symbol: *f*. 1 Hz is equal to 1 cycle per second.

**frequency weighting**

The process of applying a **frequency-weighting function**.

**frequency-weighting function**

The squared magnitude of the **sound pressure** transfer function (ISO 18405:2017a). For **sound** of a given **frequency**, the frequency-weighting function is the ratio of output power to input power of a specified filter, sometimes expressed in decibels. Examples include the following:

- *Auditory frequency-weighting function:* compensatory frequency-weighting function accounting for a species' (or **functional hearing group**'s) frequency-specific hearing sensitivity.

- *System frequency-weighting function*: frequency-weighting function describing the sensitivity of an acoustic recording system, which typically consists of a [hydrophone](#), one or more amplifiers, and an analog-to-digital converter.

### **functional hearing group**

Category of animal species when classified according to their hearing sensitivity, hearing anatomy, and susceptibility to [sound](#). For marine mammals, initial groupings were proposed by Southall et al. (2007), and revised groupings are developed as new research/data becomes available. Revised groupings proposed by Southall et al. (2019) include low-frequency cetaceans, high-frequency cetaceans, very high-frequency cetaceans, phocid carnivores in water, other carnivores in water, and sirenians. See [auditory frequency-weighting functions](#), which are often applied to these groups. Example hearing groups for fish include species for which the swim bladder is involved in hearing, species for which the swim bladder is not involved in hearing, and species without a swim bladder (Popper et al. 2014).

### **geoacoustic**

Relating to the acoustic properties of the seabed.

### **hearing threshold**

For a given species or [functional hearing group](#), the [sound level](#) for a given [signal](#) that is barely audible (i.e., that would be barely audible for a given individual in the presence of specified [background noise](#) during a specific percentage of experimental trials).

### **hertz (Hz)**

Unit of [frequency](#) defined as one cycle per second. Often expressed in multiples such as kilohertz (1 kHz = 1000 Hz).

### **high-frequency (HF) cetaceans**

See [functional hearing group](#). *Note*: The mid- and high-frequency cetaceans groups proposed by Southall et al. (2007) were renamed high- and very-high-frequency cetaceans, respectively, by Southall et al. (2019).

### **hydrophone**

An underwater [sound pressure](#) transducer. A passive electronic device for recording or listening to underwater [sound](#).

### **impulsive sound**

Qualitative term meaning [sounds](#) that are typically transient, brief (less than 1 s), broadband, with rapid rise time and rapid decay. They can occur in repetition or as a single event. Sources of impulsive sound include, among others, explosives, seismic airguns, and impact pile drivers.

### **level**

A measure of a quantity expressed as the logarithm of the ratio of the quantity to a specified [reference value](#) of that quantity. For example, a value of [sound pressure level](#) with reference to 1  $\mu\text{Pa}^2$  can be written in the form  $x \text{ dB re } 1 \mu\text{Pa}^2$ .

**low-frequency (LF) cetaceans**

See [functional hearing group](#).

**manual analysis**

Human examination of acoustic data via visual review of spectrograms and/or aural inspection of data.

**manual detection**

The output of [manual analysis](#) as recorded in an [annotation](#).

**masking**

Obscuring of [sounds](#) of interest by other sounds at similar frequencies.

**median**

The 50th percentile of a statistical distribution.

**mid-frequency (MF) cetaceans**

See [functional hearing group](#). *Note:* The mid-frequency cetaceans group proposed by Southall et al. (2007) was renamed high-frequency cetaceans by Southall et al. (2019).

**mysticete**

Member of the Mysticeti, a suborder of [cetaceans](#). Also known as baleen whales, mysticetes have baleen plates (rather than teeth) that they use to filter food from water (or from sediment as for grey whales). This group includes rorquals (Balaenopteridae, such as blue, fin, humpback, and minke whales), right and bowhead whales (Balaenidae), and grey whales (*Eschrichtius robustus*).

**N percent exceedance level**

The [sound level](#) exceeded  $N$  % of the time during a specified time interval. See also [percentile level](#).

**non-impulsive sound**

[Sound](#) that is not an [impulsive sound](#). Not necessarily a continuous sound.

**octave**

The interval between a [sound](#) and another sound with double or half the [frequency](#). For example, one octave above 200 Hz is 400 Hz, and one octave below 200 Hz is 100 Hz.

**odontocete**

Member of Odontoceti, a suborder of [cetaceans](#). These whales, dolphins, and porpoises have teeth (rather than baleen plates). Their skulls are mostly asymmetric, an adaptation for their echolocation. This group includes sperm whales, killer whales, belugas, narwhals, dolphins, and porpoises.

**parabolic equation method**

A computationally efficient solution to the acoustic wave equation that is used to model propagation loss. The parabolic equation approximation omits effects of backscattered [sound](#) (which are negligible for most ocean-acoustic propagation problems), simplifying the computation of propagation loss.

**particle acceleration, particle displacement, particle motion, particle velocity**

See [sound particle acceleration](#), [sound particle displacement](#), [sound particle motion](#), [sound particle velocity](#).

**peak-to-peak sound pressure**

The difference between the maximum and minimum [sound pressure](#) over a specified [frequency](#) band and time window. Unit: pascal (Pa).

**percentile level**

The [sound level](#) not exceeded  $N$  % of the time during a specified time interval. The  $N$ th percentile level is equal to the  $(100-N)$  % exceedance level. See also [N percent exceedance level](#).

**permanent threshold shift (PTS)**

An irreversible loss of hearing sensitivity caused by excessive noise exposure. Considered auditory injury. Compare with [temporary threshold shift](#).

**pinniped**

Member of the superfamily Pinnipedia, which is composed of phocids (true seals or earless seals), otariids (eared seals or fur seals and sea lions), and walrus.

**point source**

A source that radiates [sound](#) as if from a single point.

**power spectral density**

Generic term, formally defined as power in a unit [frequency](#) band. Unit: watt per hertz (W/Hz). The term is sometimes loosely used to refer to the spectral density of other parameters such as squared [sound pressure](#). Ratio of energy spectral density,  $E_f$ , to time duration,  $\Delta t$ , in a specified temporal observation window. In equation form, the power spectral density  $P_f$  is given by  $P_f = E_f/\Delta t$ . Power spectral density can be expressed in terms of various field variables (e.g., [sound pressure](#), [sound particle displacement](#)).

**power spectral density level**

The [level](#) ( $L_{P_f}$ ) of the [power spectral density](#) ( $P_f$ ) in a stated [frequency](#) band and time window. Defined as:  $L_{P_f} = 10\log_{10}(P_f/P_{f0})$ . Unit: [decibel](#) (dB).

As with [power spectral density](#), power spectral density level can be expressed in terms of various field variables (e.g., [sound pressure](#), [sound particle displacement](#)). The [reference value](#) ( $P_{f0}$ ) for power spectral density level depends on the nature of the field variable.

**power spectral density source level**

A property of a sound source equal to the [power spectral density level](#) of the [sound pressure](#) measured in the far field plus the propagation loss from the acoustic centre of the source to the receiver position. Unit: [decibel](#) (dB). Reference value:  $1 \mu\text{Pa}^2 \text{m}^2/\text{Hz}$ .

**received level**

The [level](#) of a given field variable measured (or that would be measured) at a given location.

### reference value

Standard value of a quantity used for calculating underwater [sound level](#). The reference value depends on the quantity for which the level is being calculated:

Quantity	Reference value
Sound pressure	$p_0^2 = 1 \mu\text{Pa}^2$ or $p_0 = 1 \mu\text{Pa}$
Sound exposure	$E_0 = 1 \mu\text{Pa}^2 \text{ s}$
Sound particle displacement	$\delta_0^2 = 1 \text{ pm}^2$
Sound particle velocity	$u_0^2 = 1 \text{ nm}^2/\text{s}^2$
Sound particle acceleration	$a_0^2 = 1 \mu\text{m}^2/\text{s}^4$

### sensation level

Difference between the [sound pressure level](#) and [hearing threshold](#) at a specified [frequency](#). Unit: [decibel \(dB\)](#).

### shear wave

A mechanical vibration wave in which the direction of particle motion is perpendicular to the direction of propagation. Also called a secondary wave or S-wave. Shear waves propagate only in solid media, such as sediments or rock. Shear waves in the seabed can be converted to [compressional waves](#) in water at the water-seabed interface.

### sound

A time-varying disturbance in the pressure, stress, or material displacement of a medium propagated by local compression and expansion of the medium. In common meaning, a form of energy that propagates through media (e.g., water, air, ground) as pressure waves.

### sound exposure

Time integral of squared [sound pressure](#) over a stated time interval in a stated [frequency](#) band. The time interval can be a specified time duration (e.g., 24 h) or from start to end of a specified event (e.g., a pile strike, an airgun pulse, a construction operation). Unit: pascal squared second ( $\text{Pa}^2 \text{ s}$ ). Symbol:  $E$ .

### sound exposure level (SEL)

The [level](#) ( $L_E$ ) of the [sound exposure](#) ( $E$ ) in a stated [frequency](#) band and time window:  $L_E = 10\log_{10}(E/E_0)$  (ISO 18405:2017a). Unit: [decibel \(dB\)](#). [Reference value](#) ( $E_0$ ) for [sound](#) in water:  $1 \mu\text{Pa}^2 \text{ s}$ .

### sound field

Region containing [sound](#) waves.

### sound particle acceleration

The rate of change of [sound particle velocity](#). Unit: metre per second squared ( $\text{m}/\text{s}^2$ ). Symbol:  $a$ .

### sound particle motion

Movement caused by the action of [sound](#) of the smallest volume of a medium that represents its mean physical properties. Important for determining effects of underwater noise on fishes and invertebrates because their hearing organs sense particle motion rather than sound pressure.

### sound particle displacement

Displacement of a material element caused by the action of [sound](#), where a material element is the smallest element of the medium that represents the medium's mean density (ISO 18405:2017a). Unit: metre (m). Symbol:  $\delta$ .

### sound particle velocity

The velocity of a particle in a material moving back and forth in the direction of the pressure wave. Unit: metre per second (m/s). Symbol:  $u$ .

### sound pressure

The contribution to total pressure caused by the action of [sound](#) (ISO 18405:2017a). Unit: pascal (Pa). Symbol:  $p$ .

### sound pressure level (SPL), rms sound pressure level

The [level](#) ( $L_p$ ) of the time-mean-square [sound pressure](#) ( $p_{rms}^2$ ) in a stated [frequency](#) band and time window:  $L_p = 10\log_{10}(p_{rms}^2/p_0^2) = 20\log_{10}(p_{rms}/p_0)$ , where rms is the abbreviation for root-mean-square. Unit: [decibel \(dB\)](#). Reference value ( $p_0^2$ ) for [sound](#) in water:  $1 \mu\text{Pa}^2$ . SPL can also be expressed in terms of the root-mean-square (rms) with a [reference value](#) of  $p_0 = 1 \mu\text{Pa}$ . The two definitions are equivalent.

### sound speed profile

The speed of [sound](#) in the water column as a function of depth below the water surface.

### soundscape

The characterization of the [ambient sound](#) in terms of its spatial, temporal, and [frequency](#) attributes, and the types of sources contributing to the [sound](#) field (ISO 18405:2017a).

### source level (SL)

A property of a sound source equal to the sound pressure level measured in the far field plus the propagation loss from the acoustic centre of the source to the receiver position. Unit: [decibel \(dB\)](#). Reference value:  $1 \mu\text{Pa}^2 \text{m}^2$ .

### spectrogram

A visual representation of acoustic amplitude over time and frequency. A spectrogram's resolution in the time and frequency domains should generally be stated as it determines the information content of the representation.

### spectrum

Distribution of acoustic signal content over [frequency](#), where the signal's content is represented by its power, energy, mean-square [sound pressure](#), or [sound exposure](#).

### temporary threshold shift (TTS)

Reversible loss of hearing sensitivity caused by noise exposure. Compare with [permanent threshold shift](#).

**validated detection**

The output of an [automated detector](#) that has been subsequently validated by a human during [manual analysis](#).

**wavelength**

Distance over which a wave completes one cycle of oscillation. Unit: metre (m). Symbol:  $\lambda$ .

## 7. Acronyms

ADSV	Automatic Data Selection for Validation
AIS	Automatic Identification System
ALTO	Autonomous Long-Term Observatories
AMAR	AMAR
AMN	Absolute Minimum Number
ANSI	American National Standards Institute
ASA	Acoustical Society of America
BELLHOP	A beam tracing model for predicting acoustic pressure fields in the ocean
BTI	Bearing-time
BW	Blue Whale
COSEWIC	Committee on the Status of Endangered Wildlife in Canada
CPA	Closest Point of Approach
CTD	Conductivity-Temperature-Depth
DFT	Discrete Fourier Transform
DP	Dynamic Positioning
DRM	Detection Range Modelling
EEZ	Canadian Exclusive Economic Zone
EIS	Environmental Impact Statement
EL	Exploration License
ERDAPP	Easier Access to Scientific Data (NOAA)
FFT	Fast-Fourier Transforms
FP	False Positive
FW	Fin Whale
GIOPS	Global Ice Ocean Prediction System
GL	Glider
HBW	Humpback Whale
HF	High-frequency
HSE&C	Health, Safety, Environment and Carbon
HT	High Threshold
Hz	Hertz
IB	Instantaneous Bandwidth
ICI	Inter-click-interval
IM	Infrasound Moan
IQR	Interquartile range
ISO	International Organization for Standardization
LF	Low-frequency
LTSA	Long-term Spectral Averages

MCC	Matthew's Correlation Coefficient
MF	Mid-frequency
MLE	Maximum Likelihood Estimation
MONM	Marine Operations Noise Model
MOODS	US Navy's Master Oceanographic Observational Data Set
MW	Minke Whale
NARW	North Atlantic Right Whale
NAVEM	Navy Global Environmental Model
NBHF	Narrow-band High Frequency
NBW	Northern Bottlenose Whale
NDFT	Non-uniform Discrete Fourier Transform
NITS	Noise Induced Threshold Shift
NL	Newfoundland Labrador
NMFS	National Marine Fisheries Service
NOAA	Navy Global Environmental Model
NRC	National Research Council
OECA	Other Effective Area Based Conservation Measure
OMS	Operating Management System
PAM	Passive Acoustic Monitoring
PK	Peak
PL	Range-dependent Propagation Loss
PTS	Permanent Threshold Shift
RAM	Range-dependent Acoustic Model
RL	Received Level
RMS	Root-Mean-Square
SARA	Species at Risk Act
SD	Standard Deviation
SEL	Sound Exposure Levels
SL	Source Level
SNR	Signal-to-noise Ratio
SPL	Sound Pressure Level
SR	Seconds resolution
SV	Support Vessel
SW	Sei Whale
TB	Terabytes
TN	True Positive
TOW	Temporal Observation Window
TP	True Negatives
TTS	Temporary Hearing Threshold Shifts
US	United States

USBL	Ultra-short Baseline
VHF	Very High-frequency
WP	Waypoint

## 8. Literature Cited

- [ANSI] American National Standards Institute and [ASA] Acoustical Society of America. S1.1-2013. *American National Standard: Acoustical Terminology*. NY, USA. <https://webstore.ansi.org/Standards/ASA/ANSIASAS12013>.
- [ISO] International Organization for Standardization. 2006. *ISO 80000-3:2006 Quantities and units – Part 3: Space and time*. <https://www.iso.org/standard/31888.html>.
- [ISO] International Organization for Standardization. 2017a. *ISO 18405:2017. Underwater acoustics – Terminology*. Geneva. <https://www.iso.org/standard/62406.html>.
- [ISO] International Organization for Standardization. 2017b. *ISO 18406:2017(E). Underwater acoustics – Measurement of radiated underwater sound from percussive pile driving*. Geneva. <https://www.iso.org/obp/ui/#iso:std:iso:18406:ed-1:v1:en>.
- [ISO] International Organization for Standardization. 2019. *ISO 17208-2:2019. Underwater acoustics – Quantities and procedures for description and measurement of underwater sound from ships – Part 1: Requirements for precision measurements in deep water used for comparison purposes*. <https://www.iso.org/standard/62409.html>.
- [NMFS] National Marine Fisheries Service (US). 2018. *2018 Revision to: Technical Guidance for Assessing the Effects of Anthropogenic Sound on Marine Mammal Hearing (Version 2.0): Underwater Thresholds for Onset of Permanent and Temporary Threshold Shifts*. US Department of Commerce, NOAA. NOAA Technical Memorandum NMFS-OPR-59. 167 p. [https://media.fisheries.noaa.gov/dam-migration/tech\\_memo\\_acoustic\\_guidance\\_\(20\)\\_pdf\\_508.pdf](https://media.fisheries.noaa.gov/dam-migration/tech_memo_acoustic_guidance_(20)_pdf_508.pdf).
- [NOAA] National Oceanic and Atmospheric Administration (US). 2023. ERDAPP. Version 2.22. [https://coastwatch.pfeg.noaa.gov/erddap/griddap/erdNavgem05D10mWind\\_LonPM180.html](https://coastwatch.pfeg.noaa.gov/erddap/griddap/erdNavgem05D10mWind_LonPM180.html).
- [NRC] National Research Council (US). 2003. *Ocean Noise and Marine Mammals*. National Research Council (US), Ocean Studies Board, Committee on Potential Impacts of Ambient Noise in the Ocean on Marine Mammals. The National Academies Press, Washington, DC, USA. <https://doi.org/10.17226/10564>.
- Aerts, L.A.M., M. Blees, S.B. Blackwell, C.R. Greene, Jr., K.H. Kim, D.E. Hannay, and M.E. Austin. 2008. *Marine mammal monitoring and mitigation during BP Liberty OBC seismic survey in Foggy Island Bay, Beaufort Sea, July-August 2008: 90-day report*. Document Number P1011-1. Report by LGL Alaska Research Associates Inc., LGL Ltd., Greeneridge Sciences Inc., and JASCO Applied Sciences for BP Exploration Alaska. 199 p. [ftp://ftp.library.noaa.gov/noaa\\_documents.lib/NMFS/Auke%20Bay/AukeBayScans/Removable%20Disk/P1011-1.pdf](ftp://ftp.library.noaa.gov/noaa_documents.lib/NMFS/Auke%20Bay/AukeBayScans/Removable%20Disk/P1011-1.pdf).
- Ainslie, M.A. 2010. *Principles of Sonar Performance Modeling*. Praxis Books. Springer, Berlin. <https://doi.org/10.1007/978-3-540-87662-5>.
- Ainslie, M.A., J.L. Miksis-Olds, S.B. Martin, K.D. Heaney, C.A.F. de Jong, A.M. von Benda-Beckmann, and A.P. Lyons. 2018. *ADEON Underwater Soundscape and Modeling Metadata Standard*. Version 1.0. Technical report by JASCO Applied Sciences for ADEON Prime Contract No. M16PC00003. 35 p. <https://doi.org/10.6084/m9.figshare.6792359.v2>.
- Alling, A.K. and H. Whitehead. 1987. A Preliminary Study of the Status of White-beaked Dolphins, *Lagenorhynchus albirostris*, and Other Small Cetaceans off the Coast. *Canadian Field-Naturalist* 101(2): 131-135. <https://www.biodiversitylibrary.org/page/28089556>.
- Amorim, M.C.P. 2006. Diversity of sound production in fish. In Ladich, F., S.P. Collin, P. Moller, and B.G. Kapoor (eds.). *Communication in fishes*. Volume 1. Science Publishers. pp. 71-104.
- Andrew, R.K., B.M. Howe, and J.A. Mercer. 2011. Long-time trends in ship traffic noise for four sites off the North American West Coast. *Journal of the Acoustical Society of America* 129(2): 642-651. <https://doi.org/10.1121/1.3518770>.
- Asselin, S., M.O. Hammill, and C. Barrette. 1993. Underwater vocalizations of ice breeding grey seals. *Canadian Journal of Zoology* 71(11): 2211-2219. <https://doi.org/10.1139/z93-310>.

- Au, W.W.L., R.A. Kastelein, T. Rippe, and N.M. Schooneman. 1999. Transmission beam pattern and echolocation signals of a harbor porpoise (*Phocoena phocoena*). *Journal of the Acoustical Society of America* 106(6): 3699-3705. <https://doi.org/10.1121/1.428221>.
- Bailey, H., G. Clay, E.A. Coates, D. Lusseau, B. Senior, and P.M. Thompson. 2010. Using T-PODs to assess variations in the occurrence of coastal bottlenose dolphins and harbour porpoises. *Aquatic Conservation: Marine and Freshwater Ecosystems* 20(2): 150-158. <https://doi.org/10.1002/aqc.1060>.
- Baird, R.W., D. Nelson, J. Lein, and D.W. Nagorsen. 1996. Status of the pygmy sperm whale, *Kogia breviceps* in Canada. *Canadian Field-Naturalist* 110: 525-532. <https://www.biodiversitylibrary.org/page/34343431>.
- Ballard, K.A. and K.M. Kovacs. 1995. The acoustic repertoire of hooded seals (*Cystophora cristata*). *Canadian Journal of Zoology* 73(7): 1362-1374. <https://doi.org/10.1139/z95-159>.
- Baumgartner, M.F., S.M. Van Parijs, F.W. Wenzel, C.J. Tremblay, H.C. Esch, and A.M. Warde. 2008. Low frequency vocalizations attributed to sei whales (*Balaenoptera borealis*). *Journal of the Acoustical Society of America* 124(2): 1339-1349. <https://doi.org/10.1121/1.2945155>.
- Becker, J.J., D.T. Sandwell, W.H.F. Smith, J. Braud, B. Binder, J. Depner, D. Fabre, J. Factor, S. Ingalls, et al. 2009. Global Bathymetry and Elevation Data at 30 Arc Seconds Resolution: SRTM30\_PLUS. *Marine Geodesy* 32(4): 355-371. <https://doi.org/10.1080/01490410903297766>.
- Berchok, C.L., D.L. Bradley, and T.B. Gabrielson. 2006. St. Lawrence blue whale vocalizations revisited: Characterization of calls detected from 1998 to 2001. *Journal of the Acoustical Society of America* 120(4): 2340-2354. <https://doi.org/10.1121/1.2335676>.
- Bom, N. 1969. Effect of rain on underwater noise level. *Journal of the Acoustical Society of America* 45(1): 150-156. <https://doi.org/10.1121/1.1911351>.
- Carnes, M.R. 2009. *Description and Evaluation of GDEM-V 3.0*. US Naval Research Laboratory, Stennis Space Center, MS. NRL Memorandum Report 7330-09-9165. 21 p. <https://apps.dtic.mil/dtic/tr/fulltext/u2/a494306.pdf>.
- Cholewiak, D.M., S. Baumann-Pickering, and S.M. Van Parijs. 2013. Description of sounds associated with Sowerby's beaked whales (*Mesoplodon bidens*) in the western North Atlantic Ocean. *Journal of the Acoustical Society of America* 134(5): 3905-3912. <https://doi.org/10.1121/1.4823843>.
- Clark, C.W. 1990. Acoustic behaviour of mysticete whales. In Thomas, J.A. and R.A. Kastelein (eds.). *Sensory Abilities of Cetaceans*. Springer, Boston, MA. pp. 571-583. [https://doi.org/10.1007/978-1-4899-0858-2\\_40](https://doi.org/10.1007/978-1-4899-0858-2_40).
- Collins, M.D. 1993. A split-step Padé solution for the parabolic equation method. *Journal of the Acoustical Society of America* 93(4): 1736-1742. <https://doi.org/10.1121/1.406739>.
- Collins, M.D., R.J. Cederberg, D.B. King, and S. Chin-Bing. 1996. Comparison of algorithms for solving parabolic wave equations. *Journal of the Acoustical Society of America* 100(1): 178-182. <https://doi.org/10.1121/1.415921>.
- Coppens, A.B. 1981. Simple equations for the speed of sound in Neptunian waters. *Journal of the Acoustical Society of America* 69(3): 862-863. <https://doi.org/10.1121/1.382038>.
- Davis, R.W., N. Jaquet, D. Gendron, U. Markaida, G. Bazzino, and W. Gilly. 2007. Diving behavior of sperm whales in relation to behavior of a major prey species, the jumbo squid, in the Gulf of California, Mexico. *Marine Ecology Progress Series* 333: 291-302. <https://doi.org/10.3354/meps333291>.
- DeAngelis, A.I., J.E. Stanistreet, S. Baumann-Pickering, and D.M. Cholewiak. 2018. A description of echolocation clicks recorded in the presence of True's beaked whale (*Mesoplodon mirus*). *Journal of the Acoustical Society of America* 144(5): 2691-2700. <https://doi.org/10.1121/1.5067379>.
- Deecke, V.B., J.K.B. Ford, and P.J.B. Slater. 2005. The vocal behaviour of mammal-eating killer whales: Communicating with costly calls. *Animal Behaviour* 69(2): 395-405. <https://doi.org/10.1016/j.anbehav.2004.04.014>.
- Delarue, J.J.-Y., S.K. Todd, S.M. Van Parijs, and L. Di Iorio. 2009. Geographic variation in Northwest Atlantic fin whale (*Balaenoptera physalus*) song: Implications for stock structure assessment. *Journal of the Acoustical Society of America* 125(3): 1774-82. <https://doi.org/10.1121/1.3068454>.

- Delarue, J.J.-Y., K.A. Kowarski, E.E. Maxner, J.T. MacDonnell, and S.B. Martin. 2018. *Acoustic Monitoring Along Canada's East Coast: August 2015 to July 2017*. Document Number 01279, Environmental Studies Research Funds Report Number 215, Version 1.0. Technical report by JASCO Applied Sciences for Environmental Studies Research Fund, Dartmouth, NS, Canada. 120 pp + appendices.
- Delarue, J.J.-Y., H.B. Moors-Murphy, K.A. Kowarski, G.E. Davis, I.R. Urazghildiiev, and S.B. Martin. 2022. Acoustic occurrence of baleen whales, particularly blue, fin, and humpback whales, off eastern Canada, 2015–2017. *Endangered Species Research* 47: 265-289. <https://doi.org/10.3354/esr01176>.
- Ding, W., B. Würsig, and W. Evans. 1995. Comparisons of whistles among seven odontocete species. In Kastelein, R.A., J.A. Thomas, and P.E. Nachtigall (eds.). *Sensory Systems of Aquatic Mammals*. De Spil Publishers, The Netherlands. pp. 299-324.
- Drouot, V., A. Gannier, and J.C. Goold. 2004. Diving and Feeding Behaviour of Sperm Whales (*Physeter macrocephalus*) in the Northwestern Mediterranean Sea. *Aquatic Mammals* 30(3): 419-426. <https://doi.org/10.1578/AM.30.3.2004.419>.
- Dunlop, R.A., D.H. Cato, and M.J. Noad. 2008. Non-song acoustic communication in migrating humpback whales (*Megaptera novaeangliae*). *Marine Mammal Science* 24(3): 613-629. <https://doi.org/10.1111/j.1748-7692.2008.00208.x>.
- Edds-Walton, P.L. 1997. Acoustic communication signals of mysticetes whales. *Bioacoustics* 8(1-2): 47-60. <https://doi.org/10.1080/09524622.1997.9753353>.
- Edwards, E.F., C. Hall, T.J. Moore, C. Sheredy, and J.V. Redfern. 2015. Global distribution of fin whales *Balaenoptera physalus* in the post-whaling era (1980–2012). *Mammal Review* 45(4): 197-214.
- Einfeldt, A., L. Feyrer, I. Paterson, S. Ferguson, P. Miller, E. de Greef, and P. Bentzen. 2022. Characterization of population structure in northern bottlenose whales (*Hyperoodon ampullatus*) in the North Atlantic. *Canadian Technical Report of Fisheries and Aquatic Sciences* 3467.
- Environment and Climate Change Canada. 2021. Data and Products of the Global Ice-Ocean Prediction System (GIOPS). [https://eccc-msc.github.io/open-data/msc-data/nwp\\_giops/readme\\_giops\\_en/](https://eccc-msc.github.io/open-data/msc-data/nwp_giops/readme_giops_en/) (Accessed 31 Mar 2021).
- Erbe, C., A. Verma, R.D. McCauley, A. Gavrilov, and I. Parnum. 2015. The marine soundscape of the Perth Canyon. *Progress in Oceanography* 137: 38-51. <https://doi.org/10.1016/j.pocean.2015.05.015>.
- Erbs, F., S.H. Elwen, and T. Gridley. 2017. Automatic classification of whistles from coastal dolphins of the southern African subregion. *Journal of the Acoustical Society of America* 141(4): 2489-2500. <https://doi.org/10.1121/1.4978000>.
- Eskesen, I.G., M. Wahlberg, M. Simon, and O.N. Larsen. 2011. Comparison of echolocation clicks from geographically sympatric killer whales and long-finned pilot whales. *Journal of the Acoustical Society of America* 130(1): 9-12. <https://doi.org/10.1121/1.3583499>.
- Etter, P.C. 1996. *Underwater Acoustic Modeling - Principles, Techniques, and Applications*. Second edition. E & FN Spon, London, UK. 344 p.
- Feyrer, L.J., P. Bentzen, H. Whitehead, I.G. Paterson, and A. Einfeldt. 2019. Evolutionary impacts differ between two exploited populations of northern bottlenose whale (*Hyperoodon ampullatus*). *Ecology and Evolution* 9(23): 13567-13584. <https://doi.org/10.1002/ece3.5813>.
- Finneran, J.J. 2015. *Auditory weighting functions and TTS/PTS exposure functions for cetaceans and marine carnivores*. Technical report by SSC Pacific, San Diego, CA, USA.
- Finneran, J.J. 2016. *Auditory weighting functions and TTS/PTS exposure functions for marine mammals exposed to underwater noise*. Technical Report for Space and Naval Warfare Systems Center Pacific, San Diego, CA, USA. 49 p. <https://apps.dtic.mil/dtic/tr/fulltext/u2/1026445.pdf>.
- Ford, J.K.B. 1989. Acoustic behaviour of resident killer whales (*Orcinus orca*) off Vancouver Island, British Columbia. *Canadian Journal of Zoology* 67(3): 727-745. <https://doi.org/10.1139/z89-105>.
- François, R.E. and G.R. Garrison. 1982a. Sound absorption based on ocean measurements: Part I: Pure water and magnesium sulfate contributions. *Journal of the Acoustical Society of America* 72(3): 896-907. <https://doi.org/10.1121/1.388170>.

- François, R.E. and G.R. Garrison. 1982b. Sound absorption based on ocean measurements: Part II: Boric acid contribution and equation for total absorption. *Journal of the Acoustical Society of America* 72(6): 1879-1890. <https://doi.org/10.1121/1.388673>.
- Funk, D.W., D.E. Hannay, D.S. Ireland, R. Rodrigues, and W.R. Koski. 2008. *Marine mammal monitoring and mitigation during open water seismic exploration by Shell Offshore Inc. in the Chukchi and Beaufort Seas, July–November 2007: 90-day report*. LGL Report P969-1. Prepared by LGL Alaska Research Associates Inc., LGL Ltd., and JASCO Research Ltd. for Shell Offshore Inc., National Marine Fisheries Service (US), and US Fish and Wildlife Service. 218 p. [http://www-static.shell.com/static/usa/downloads/alaska/shell2007\\_90-d\\_final.pdf](http://www-static.shell.com/static/usa/downloads/alaska/shell2007_90-d_final.pdf).
- Gannier, A., S. Fuchs, P. Quèbre, and J.N. Oswald. 2010. Performance of a contour-based classification method for whistles of Mediterranean delphinids. *Applied Acoustics* 71(11): 1063-1069. <https://doi.org/10.1016/j.apacoust.2010.05.019>.
- Geijer, C.K., G. Notarbartolo di Sciara, and S. Panigada. 2016. Mysticete migration revisited: are Mediterranean fin whales an anomaly? *Mammal Review* 46(4): 284-296.
- Gillespie, D., C. Dunn, J. Gordon, D. Claridge, C.B. Embling, and I. Boyd. 2009. Field recordings of Gervais' beaked whales *Mesoplodon europaeus* from the Bahamas. *Journal of the Acoustical Society of America* 125(5): 3428-3433. <https://doi.org/10.1121/1.3110832>.
- Girola, E., M.J. Noad, R.A. Dunlop, and D.H. Cato. 2019. Source levels of humpback whales decrease with frequency suggesting an air-filled resonator is used in sound production. *The Journal of the Acoustical Society of America* 145(2): 869-880.
- Gomez, C., C.M. Konrad, A. Vanderlaan, H.B. Moors-Murphy, E. Marotte, J.W. Lawson, A.-L. Kouwenberg, C. Fuentes-Yaco, and A. Buren. 2020. *Identifying priority areas to enhance monitoring of cetaceans in the Northwest Atlantic Ocean*. Document Number 3370. Canadian Technical Report of Fisheries and Aquatic Sciences. 103 p. <https://waves-vagues.dfo-mpo.gc.ca/Library/40869155.pdf>.
- Gowans, S. and H. Whitehead. 1995. Distribution and habitat partitioning by small odontocetes in the Gully, a submarine canyon on the Scotian Shelf. *Canadian Journal of Zoology* 73(9): 1599-1608. <https://doi.org/10.1139/z95-190>.
- Hamazaki, T. 2002. Spatiotemporal prediction models of cetacean habitats in the mid-western North Atlantic Ocean (from Cape Hatteras, North Carolina, USA to Nova Scotia, Canada). *Marine Mammal Science* 18(4): 920-939. <https://doi.org/10.1111/j.1748-7692.2002.tb01082.x>.
- Hannay, D.E. and R. Racca. 2005. *Acoustic Model Validation*. Document Number 0000-S-90-04-T-7006-00-E, Revision 02, Version 1.3. Technical report by JASCO Research Ltd. for Sakhalin Energy Investment Company Ltd. 34 p.
- Hawkins, A.D., L. Casaretto, M. Picciulin, and K. Olsen. 2002. Locating Spawning Haddock by Means of Sound. *Bioacoustics* 12(2-3): 284-286. <https://doi.org/10.1080/09524622.2002.9753723>.
- Hayes, S.A., E. Josephson, K. Maze-Foley, and P.E. Rosel. 2020. *U.S. Atlantic and Gulf of Mexico Marine Mammal Stock Assessments - 2019*. US Department of Commerce. NOAA Technical Memorandum NMFS-NE-264, Woods Hole, MA, USA. 479 p. [https://media.fisheries.noaa.gov/dam-migration/2019\\_sars\\_atlantic\\_508.pdf](https://media.fisheries.noaa.gov/dam-migration/2019_sars_atlantic_508.pdf).
- Heide-Jørgensen, M.P., D. Bloch, E. Stefansson, B. Mikkelsen, L.H. Ofstad, and R. Dietz. 2002. Diving behaviour of long-finned pilot whales *Globicephala melas* around the Faroe Islands. *Wildlife Biology* 8(1): 307-313. <https://doi.org/10.2981/wlb.2002.020>.
- Heindsmann, T.E., R.H. Smith, and A.D. Arneson. 1955. Effect of rain upon underwater noise levels [Letter to the editor]. *Journal of the Acoustical Society of America* 27(2): 378-379. <https://doi.org/10.1121/1.1907897>.
- Hodge, K.B., C.A. Muirhead, J.L. Morano, C.W. Clark, and A.N. Rice. 2015. North Atlantic right whale occurrence near wind energy areas along the mid-Atlantic US coast: Implications for management. *Endangered Species Research* 28(3): 225-234. <https://doi.org/10.3354/esr00683>.
- Holt, M.M., D.P. Noren, and C.K. Emmons. 2011. Effects of noise levels and call types on the source levels of killer whale calls. *Journal of the Acoustical Society of America* 130(5): 3100-3106. <https://doi.org/10.1121/1.3641446>.

- Hooker, S.K., R.W. Baird, and M.A. Showell. 1997. *Cetacean strandings and bycatches in Nova Scotia, eastern Canada, 1991-1996*. Document Number SC/49/O5. Unpublished report for the International Whaling Commission, Cambridge, UK. 11 p.
- Hooker, S.K. and H. Whitehead. 2002. Click characteristics of northern bottlenose whales (*Hyperoodon ampullatus*). *Marine Mammal Science* 18(1): 69-80. <https://doi.org/10.1111/j.1748-7692.2002.tb01019.x>.
- Ireland, D.S., R. Rodrigues, D.W. Funk, W.R. Koski, and D.E. Hannay. 2009. *Marine mammal monitoring and mitigation during open water seismic exploration by Shell Offshore Inc. in the Chukchi and Beaufort Seas, July–October 2008: 90-Day Report*. Document Number P1049-1. 277 p.
- Irvine, L., D.M. Palacios, J. Urbán, and B. Mate. 2017. Sperm whale dive behavior characteristics derived from intermediate-duration archival tag data. *Ecology and Evolution* 7(19): 7822-7837. <https://doi.org/10.1002/ece3.3322>.
- Jalkanen, J.-P., L. Johansson, M.H. Andersson, E. Majamäki, and P. Sigray. 2022. Underwater noise emissions from ships during 2014–2020. *Environmental Pollution* 311: 119766.
- Jensen, F.B., W.A. Kuperman, M.B. Porter, and H. Schmidt. 2011. *Computational Ocean Acoustics*. 2nd edition. AIP Series in Modern Acoustics and Signal Processing. AIP Press - Springer, New York. 794 p. <https://doi.org/10.1007/978-1-4419-8678-8>.
- Kaplan, M.B. and S. Solomon. 2016. A coming boom in commercial shipping? The potential for rapid growth of noise from commercial ships by 2030. *Marine Policy* 73: 119-121. <https://doi.org/10.1016/j.marpol.2016.07.024>.
- Kingsley, M.C.S. and R.R. Reeves. 1998. Aerial surveys of cetaceans in the Gulf of St. Lawrence in 1995 and 1996. *Canadian Journal of Zoology* 76(8): 1529-1550. <https://doi.org/10.1139/z98-054>.
- Knudsen, V.O., R.S. Alford, and J.W. Emling. 1948. Underwater ambient noise. *Journal of Marine Research* 7: 410-429.
- Kowarski, K.A., C. Evers, H. Moors-Murphy, S.B. Martin, and S.L. Denes. 2018. Singing through winter nights: Seasonal and diel occurrence of humpback whale (*Megaptera novaeangliae*) calls in and around the Gully MPA, offshore eastern Canada. *Marine Mammal Science* 34(1): 169-189. <https://doi.org/10.1111/mms.12447>.
- Kowarski, K.A., J.J.-Y. Delarue, B.J. Gaudet, and S.B. Martin. 2021. Automatic data selection for validation: A method to determine cetacean occurrence in large acoustic data sets. *JASA Express Letters* 1: 051201. <https://doi.org/10.1121/10.0004851>.
- Krause, B. 2008. Anatomy of the Soundscape: Evolving Perspectives. *Journal of the Audio Engineering Society* 56(1/2): 73-80. <http://www.aes.org/e-lib/browse.cfm?elib=14377>.
- Kyhn, L.A., J. Tougaard, K. Beedholm, F.H. Jensen, E. Ashe, R. Williams, and P.T. Madsen. 2013. Clicking in a killer whale habitat: Narrow-band, high-frequency biosonar clicks of harbour porpoise (*Phocoena phocoena*) and Dall's porpoise (*Phocoenoides dalli*). *PLOS ONE* 8(5): e63763. <https://doi.org/10.1371/journal.pone.0063763>.
- Lawson, J.W., T.S. Stevens, and D. Snow. 2007. *Killer whales of Atlantic Canada, with particular reference to the Newfoundland and Labrador Region*. Fisheries and Oceans Canada, Canadian Science Advisory Secretariat, Research Document 2007/062. <https://waves.vagues.dfo-mpo.gc.ca/Library/333996.pdf>.
- Lawson, J.W. and J.-F. Gosselin. 2009. *Distribution and preliminary abundance estimates for cetaceans seen during Canada's Marine Megafauna Survey-A component of the 2007 TNASS*. Document Number 2009/031. DFO Canadian Science Advisory Secretariat Research Document. © Her Majesty the Queen in Right of Canada. 28 p. <http://www.dfo-mpo.gc.ca/csas/>
- Lawson, J.W. and J.-F. Gosselin. 2011. *Fully-corrected cetacean abundance estimates from the Canadian TNASS survey*. Department of Fisheries and Oceans. Working Paper 10. National Marine Mammal Peer Review Meeting, Ottawa, ON Canada.
- Lawson, J.W. and T.S. Stevens. 2013. Historic and seasonal distribution patterns and abundance of killer whales (*Orcinus orca*) in the northwest Atlantic. *Journal of the Marine Biological Association of the United Kingdom* 94(6): 1253-1265. <https://doi.org/10.1017/S0025315413001409>.
- Lawson, J.W. and J.-F. Gosselin. 2018. *Estimates of cetacean abundance from the 2016 NAISS aerial surveys of eastern Canadian waters, with a comparison to estimates from the 2007 TNASS*. Document Number NAMMCO SC/25/AE/09. Report for the NAMMCO Secretariat. 40 p.

- Lien, J., D. Nelson, and D.J. Hai. 2001. Status of the white-beaked dolphin, *Lagenorhynchus albirostris*, in Canada. *Canadian Field-Naturalist* 115(1): 118-126.
- Louis, M., J. Routledge, M.P. Heide-Jørgensen, P. Szpak, and E.D. Lorenzen. 2022. Sex and size matter: foraging ecology of offshore harbour porpoises in waters around Greenland. *Marine Biology* 169(11): 140.
- Lucas, Z.N. and S.K. Hooker. 2000. Cetacean strandings on Sable Island, Nova Scotia, 1970-1998. *Canadian Field-Naturalist* 114(1): 45-61. <https://www.biodiversitylibrary.org/page/34236541>.
- Macklin, G. 2022. *Spatiotemporal Patterns in Acoustic Presence of Sei Whales (Balaenoptera borealis) in Atlantic Canada*.
- Macleod, C.D., W.F. Perrin, R. Pitman, J.P. Barlow, L. Ballance, A. D'Amico, T. Gerrodette, G. Joyce, K.D. Mullin, et al. 2005. Known and inferred distributions of beaked whale species (Cetacea: Ziphiidae). *Journal of Cetacean Research and Management* 7(3): 271-286.
- Madsen, P.T., M. Johnson, N. Aguilar de Soto, W.M.X. Zimmer, and P.L. Tyack. 2005. Biosonar performance of foraging beaked whales (*Mesoplodon densirostris*). *Journal of Experimental Biology* 208(2): 181-194. <https://doi.org/10.1242/jeb.01327>.
- Malinka, C.E., P. Tønnesen, C.A. Dunn, D.E. Claridge, T. Gridley, S.H. Elwen, and P.T. Madsen. 2021. Echolocation click parameters and biosonar behaviour of the dwarf sperm whale (*Kogia sima*). *Journal of Experimental Biology* 224(6). <https://doi.org/10.1242/jeb.240689>.
- Marten, K. 2000. Ultrasonic analysis of pygmy sperm whale (*Kogia breviceps*) and Hubb's beaked whale (*Mesoplodon carlhubbsi*) clicks. *Aquatic Mammals* 26(1): 45-48. [https://www.aquaticmammalsjournal.org/share/AquaticMammalsIssueArchives/2000/AquaticMammals\\_26-01/26-01\\_Marten.pdf](https://www.aquaticmammalsjournal.org/share/AquaticMammalsIssueArchives/2000/AquaticMammals_26-01/26-01_Marten.pdf).
- Martin, S.B., K. Bröker, M.-N.R. Matthews, J.T. MacDonnell, and L. Bailey. 2015. Comparison of measured and modeled air-gun array sound levels in Baffin Bay, West Greenland. *OceanNoise 2015*. 11-15 May 2015, Barcelona, Spain.
- Martin, S.B., C. Morris, K. Bröker, and C. O'Neill. 2019. Sound exposure level as a metric for analyzing and managing underwater soundscapes. *Journal of the Acoustical Society of America* 146(1): 135-149. <https://doi.org/10.1121/1.5113578>.
- Mathias, D., A.M. Thode, J. Straley, and R.D. Andrews. 2013. Acoustic tracking of sperm whales in the Gulf of Alaska using a two-element vertical array and tags. *Journal of the Acoustical Society of America* 134(3): 2446-2461. <https://doi.org/10.1121/1.4816565>.
- Matthews, M.-N.R., T.J. Deveau, C.J. Whitt, and S.B. Martin. 2018. *Underwater Sound Assessment for Newfoundland Orphan Basin Exploration Drilling Program*. Document Number 01592, Version 4.0. Technical report by JASCO Applied Sciences for Stantec.
- McAlpine, D.F., L.D. Murison, and E.P. Hoberg. 1997. New records for the pygmy sperm whale, *Kogia breviceps* (Physeteridae) from Atlantic Canada with notes on diet and parasites. *Marine Mammal Science* 13(4): 701-704. <https://doi.org/10.1111/j.1748-7692.1997.tb00093.x>.
- McDonald, M.A., J. Calambokidis, A.M. Teranishi, and J.A. Hildebrand. 2001. The acoustic calls of blue whales off California with gender data. *Journal of the Acoustical Society of America* 109(4): 1728-1735. <https://doi.org/10.1121/1.1353593>.
- McPherson, C.R. and S.B. Martin. 2018. *Characterisation of Polarcus 2380 in<sup>3</sup> Airgun Array*. Document Number 001599, Version 1.0. Technical report by JASCO Applied Sciences for Polarcus Asia Pacific Pte Ltd.
- Measures, L., B. Roberge, and R. Sears. 2004. Stranding of a pygmy sperm whale, *Kogia breviceps*, in the northern Gulf of St. Lawrence, Canada. *Canadian Field-Naturalist* 118(4): 495-498. <https://doi.org/10.22621/cfn.v118i4.52>.
- Mellinger, D.K. and C.W. Clark. 2003. Blue whale (*Balaenoptera musculus*) sounds from the North Atlantic. *Journal of the Acoustical Society of America* 114(2): 1108-1119. <https://doi.org/10.1121/1.1593066>.
- Menze, S., D.P. Zitterbart, I. van Opzeeland, and O. Boebel. 2017. The influence of sea ice, wind speed and marine mammals on Southern Ocean ambient sound. *Royal Society Open Science* 4(1): 160370.
- Mercer, M.C. 1975. Modified Leslie-DeLury Population Models of the Long-Finned Pilot Whale (*Globicephala melaena*) and Annual Production of the Short-Finned Squid (*Illex illecebrosus*)

- Based upon their Interaction at Newfoundland. *Journal of the Fisheries Research Board of Canada* 32(7): 1145-1154. <https://doi.org/10.1139/f75-135>.
- Miksis-Olds, J.L. and S.M. Nichols. 2016. Is low frequency ocean sound increasing globally? *Journal of the Acoustical Society of America* 139(1): 501-511. <https://doi.org/10.1121/1.4938237>.
- Miksis-Olds, J.L., D.V. Harris, and K.D. Heaney. 2019. Comparison of estimated 20-Hz pulse fin whale source levels from the tropical Pacific and Eastern North Atlantic Oceans to other recorded populations. *The Journal of the Acoustical Society of America* 146(4): 2373-2384.
- Miller, P.J.O. 2006. Diversity in sound pressure levels and estimated active space of resident killer whale vocalizations. *Journal of Comparative Physiology A* 192: 449-459. <https://doi.org/10.1007/s00359-005-0085-2>.
- Møhl, B., M. Wahlberg, P.T. Madsen, L.A. Miller, and A. Surlykke. 2000. Sperm whale clicks: Directionality and source level revisited. *Journal of the Acoustical Society of America* 107(1): 638-648. <https://doi.org/10.1121/1.428329>.
- Møhl, B., M. Wahlberg, P.T. Madsen, A. Heerfordt, and A. Lund. 2003. The monopulsed nature of sperm whale clicks. *Journal of the Acoustical Society of America* 114(2): 1143-1154. <https://doi.org/10.1121/1.1586258>.
- Nedwell, J.R. and A.W. Turnpenny. 1998. The use of a generic frequency weighting scale in estimating environmental effect. *Workshop on Seismics and Marine Mammals*. 23–25 Jun 1998, London, UK.
- Nedwell, J.R., A.W. Turnpenny, J. Lovell, S.J. Parvin, R. Workman, J.A.L. Spinks, and D. Howell. 2007. A validation of the  $dB_{ht}$  as a measure of the behavioural and auditory effects of underwater noise. Document Number 534R1231 Report by Subacoustech Ltd. for Chevron Ltd, TotalFinaElf Exploration UK PLC, Department of Business, Enterprise and Regulatory Reform, Shell UK Exploration and Production Ltd, The Industry Technology Facilitator, Joint Nature Conservation Committee, and The UK Ministry of Defence. 74 p. <https://tethys.pnnl.gov/sites/default/files/publications/Nedwell-et-al-2007.pdf>.
- Nemiroff, L. and H. Whitehead. 2009. Structural characteristics of pulsed calls of long-finned pilot whales *Globicephala melas*. *Bioacoustics* 19(1-2): 67-92. <https://doi.org/10.1080/09524622.2009.9753615>.
- Nielsen, N.H., J. Teilmann, S. Sveegaard, R.G. Hansen, M.-H.S. Sinding, R. Dietz, and M.P. Heide-Jørgensen. 2018. Oceanic movements, site fidelity and deep diving in harbour porpoises from Greenland show limited similarities to animals from the North Sea. *Marine Ecology Progress Series* 597: 259-272. <https://doi.org/10.3354/meps12588>.
- Nieukirk, S.L., K.M. Stafford, D.K. Mellinger, R.P. Dziak, and C.G. Fox. 2004. Low-frequency whale and seismic airgun sounds recorded in the mid-Atlantic Ocean. *Journal of the Acoustical Society of America* 115(4): 1832-1843. <https://doi.org/10.1121/1.1675816>.
- Nieukirk, S.L., D.K. Mellinger, S.E. Moore, K. Klinck, R.P. Dziak, and J. Goslin. 2012. Sounds from airguns and fin whales recorded in the mid-Atlantic Ocean, 1999–2009. *Journal of the Acoustical Society of America* 131(2): 1102-1112. <https://doi.org/10.1121/1.3672648>.
- NOAA Fisheries. 2019. *Marine Mammal Acoustic Thresholds* (webpage). [https://archive.fisheries.noaa.gov/wcr/protected\\_species/marine\\_mammals/threshold\\_guidance.html](https://archive.fisheries.noaa.gov/wcr/protected_species/marine_mammals/threshold_guidance.html).
- Nordeide, J.T. and E. Kjellsby. 1999. Sound from spawning cod at their spawning grounds. *ICES Journal of Marine Science* 56(3): 326-332. <https://doi.org/10.1006/jmsc.1999.0473>.
- O'Neill, C., D. Leary, and A. McCrodan. 2010. Sound Source Verification. (Chapter 3) In Blees, M.K., K.G. Hartin, D.S. Ireland, and D.E. Hannay (eds.). *Marine mammal monitoring and mitigation during open water seismic exploration by Statoil USA E&P Inc. in the Chukchi Sea, August-October 2010: 90-day report*. LGL Report P1119. Prepared by LGL Alaska Research Associates Inc., LGL Ltd., and JASCO Applied Sciences Ltd. for Statoil USA E&P Inc., National Marine Fisheries Service (US), and US Fish and Wildlife Service. pp. 1-34.
- Ocean Time Series Group. 2009. *MATLAB Numerical Scientific and Technical Computing*. Scripps Institution of Oceanography, University of California San Diego. <http://mooring.ucsd.edu/software>.
- Olsen, M.T., N.H. Nielsen, V. Biard, J. Teilmann, M.C. Ngô, G. Víkingsson, T. Gunnlaugsson, G. Stenson, J. Lawson, et al. 2022. Genetic and behavioural data confirm the existence of a distinct harbour

- porpoise ecotype in West Greenland. *Ecological Genetics and Genomics* 22: 100108. <https://doi.org/10.1016/j.egg.2021.100108>.
- Oswald, J.N., J.P. Barlow, and T.F. Norris. 2003. Acoustic identification of nine delphinid species in the eastern tropical Pacific Ocean. *Marine Mammal Science* 19(1): 20-37. <https://doi.org/10.1111/j.1748-7692.2003.tb01090.x>.
- Ou, H., W.W.L. Au, S.M. Van Parijs, E.M. Oleson, and S. Rankin. 2015. Discrimination of frequency-modulated baleen whale downsweep calls with overlapping frequencies. *Journal of the Acoustical Society of America* 137(6): 3024-3032. <https://doi.org/10.1121/1.4919304>.
- Parks, S.E., P.K. Hamilton, S.D. Kraus, and P.L. Tyack. 2005. The gunshot sound produced by male North Atlantic right whales (*Eubalaena glacialis*) and its potential function in reproductive advertisement. *Marine Mammal Science* 21(3): 458-475. <https://doi.org/10.1111/j.1748-7692.2005.tb01244.x>.
- Parks, S.E. and P.L. Tyack. 2005. Sound production by North Atlantic right whales (*Eubalaena glacialis*) in surface active groups. *Journal of the Acoustical Society of America* 117(5): 3297-3306. <https://doi.org/10.1121/1.1882946>.
- Popper, A.N., A.D. Hawkins, R.R. Fay, D.A. Mann, S. Bartol, T.J. Carlson, S. Coombs, W.T. Ellison, R.L. Gentry, et al. 2014. *Sound Exposure Guidelines for Fishes and Sea Turtles: A Technical Report prepared by ANSI-Accredited Standards Committee S3/SC1 and registered with ANSI. ASA S3/SC1.4 TR-2014*. SpringerBriefs in Oceanography. ASA Press and Springer. <https://doi.org/10.1007/978-3-319-06659-2>.
- Porter, M.B. and Y.C. Liu. 1994. Finite-element ray tracing. In: Lee, D. and M.H. Schultz (eds.). *International Conference on Theoretical and Computational Acoustics*. Volume 2. World Scientific Publishing Co. pp. 947-956.
- Prieto, R., M.A. Silva, G.T. Waring, and J.M.A. Gonçalves. 2014. Sei whale movements and behaviour in the North Atlantic inferred from satellite telemetry. *Endangered Species Research* 26(2): 103-113. <https://doi.org/10.3354/esr00630>.
- Racca, R., A.N. Rutenko, K. Bröker, and M.E. Austin. 2012a. A line in the water - design and enactment of a closed loop, model based sound level boundary estimation strategy for mitigation of behavioural impacts from a seismic survey. *11th European Conference on Underwater Acoustics*. Volume 34(3), Edinburgh, UK.
- Racca, R., A.N. Rutenko, K. Bröker, and G. Gailey. 2012b. Model based sound level estimation and in-field adjustment for real-time mitigation of behavioural impacts from a seismic survey and post-event evaluation of sound exposure for individual whales. In: McMinn, T. (ed.). *Acoustics 2012*. Fremantle, Australia. [http://www.acoustics.asn.au/conference\\_proceedings/AAS2012/papers/p92.pdf](http://www.acoustics.asn.au/conference_proceedings/AAS2012/papers/p92.pdf).
- Rendell, L.E., J.N. Matthews, A. Gill, J.C.D. Gordon, and D.W. MacDonald. 1999. Quantitative analysis of tonal calls from five odontocete species, examining interspecific and intraspecific variation. *Journal of Zoology* 249(4): 403-410. <https://doi.org/10.1111/j.1469-7998.1999.tb01209.x>.
- Risch, D., C.W. Clark, P.J. Corkeron, A. Elepfandt, K.M. Kovacs, C. Lydersen, I. Stirling, and S.M. Van Parijs. 2007. Vocalizations of male bearded seals, *Erignathus barbatus*: Classification and geographical variation. *Animal Behaviour* 73(5): 747-762. <https://doi.org/10.1016/j.anbehav.2006.06.012>.
- Risch, D., C.W. Clark, P.J. Dugan, M. Popescu, U. Siebert, and S.M. Van Parijs. 2013. Minke whale acoustic behavior and multi-year seasonal and diel vocalization patterns in Massachusetts Bay, USA. *Marine Ecology Progress Series* 489: 279-295. <https://doi.org/10.3354/meps10426>.
- Risch, D., U. Siebert, and S.M. Van Parijs. 2014. Individual calling behaviour and movements of North Atlantic minke whales (*Balaenoptera acutorostrata*). *Behaviour* 151(9): 1335-1360. <https://doi.org/10.1163/1568539X-00003187>.
- Romagosa, M., O. Boisseau, A.-C. Cucknell, A. Moscrop, and R. McLanaghan. 2015. Source level estimates for sei whale (*Balaenoptera borealis*) vocalizations off the Azores. *Journal of the Acoustical Society of America* 138(4): 2367-2372. <https://doi.org/10.1121/10.0000931>.
- Ross, D. 1976. *Mechanics of Underwater Noise*. Pergamon Press, NY, USA.

- Scott, T.M. and S.S. Sadove. 1997. Sperm whale, *Physeter macrocephalus*, sightings in the shallow shelf waters off Long Island, New York. *Marine Mammal Science* 13(2): 317-321. <https://doi.org/10.1111/j.1748-7692.1997.tb00636.x>.
- Scrimger, J.A., D.J. Evans, G.A. McBean, D.M. Farmer, and B.R. Kerman. 1987. Underwater noise due to rain, hail, and snow. *Journal of the Acoustical Society of America* 81(1): 79-86. <https://doi.org/10.1121/1.394936>.
- Selzer, L.A. and P.M. Payne. 1988. The distribution of white-sided (*Lagenorhynchus acutus*) and common dolphins (*Delphinus delphis*) vs. environmental features of the continental shelf of the northeastern United States. *Marine Mammal Science* 4(2): 141-153. <https://doi.org/10.1111/j.1748-7692.1988.tb00194.x>.
- Sergeant, D.E. 1962. The biology of the pilot or pothead whale *Globicephala melaena* (Traill) in Newfoundland waters. *Bulletin of the Fisheries Research Board of Canada* 132: 84. <https://waves-vagues.dfo-mpo.gc.ca/Library/10012.pdf>.
- Sergeant, D.E., A.W. Mansfield, and B. Beck. 1970. Inshore Records of Cetacea for Eastern Canada, 1949–68. *Journal of the Fisheries Research Board of Canada* 27(11): 1903-1915. <https://doi.org/10.1139/f70-216>.
- Simon, M., K.M. Stafford, K. Beedholm, C.M. Lee, and P.T. Madsen. 2010. Singing behavior of fin whales in the Davis Strait with implications for mating, migration and foraging. *Journal of the Acoustical Society of America* 128(5): 3200-3210. <https://doi.org/10.1121/1.3495946>.
- Širović, A., A. Rice, E. Chou, J.A. Hildebrand, S.M. Wiggins, and M.A. Roch. 2015. Seven years of blue and fin whale call abundance in the Southern California Bight. *Endangered Species Research* 28(1): 61-76. <https://doi.org/10.3354/esr00676>.
- Smith, W.H.F. and D.T. Sandwell. 1997. Global sea floor topography from satellite altimetry and ship depth soundings. *Science* 277(5334): 1956-1962. <https://doi.org/10.1126/science.277.5334.1956>.
- Southall, B.L., A.E. Bowles, W.T. Ellison, J.J. Finneran, R.L. Gentry, C.R. Greene, Jr., D. Kastak, D.R. Ketten, J.H. Miller, et al. 2007. Marine Mammal Noise Exposure Criteria: Initial Scientific Recommendations. *Aquatic Mammals* 33(4): 411-521. <https://doi.org/10.1578/AM.33.4.2007.411>.
- Southall, B.L., J.J. Finneran, C.J. Reichmuth, P.E. Nachtigall, D.R. Ketten, A.E. Bowles, W.T. Ellison, D.P. Nowacek, and P.L. Tyack. 2019. Marine Mammal Noise Exposure Criteria: Updated Scientific Recommendations for Residual Hearing Effects. *Aquatic Mammals* 45(2): 125-232. <https://doi.org/10.1578/AM.45.2.2019.125>.
- Steiner, W.W. 1981. Species-specific differences in pure tonal whistle vocalizations of five western North Atlantic dolphin species. *Behavioral Ecology and Sociobiology* 9(4): 241-246. <https://doi.org/10.1007/BF00299878>.
- Strasberg, M. 1979. Nonacoustic noise interference in measurements of infrasonic ambient noise. *Journal of the Acoustical Society of America* 66(5): 1487-1493. <https://doi.org/10.1121/1.383543>.
- Teague, W.J., M.J. Carron, and P.J. Hogan. 1990. A comparison between the Generalized Digital Environmental Model and Levitus climatologies. *Journal of Geophysical Research* 95(C5): 7167-7183. <https://doi.org/10.1029/JC095iC05p07167>.
- Thode, A.M., G.L. D'Spain, and W.A. Kuperman. 2000. Matched-field processing, geoacoustic inversion, and source signature recovery of blue whale vocalizations. *Journal of the Acoustical Society of America* 107(3): 1286-1300. <https://doi.org/10.1121/1.428417>.
- Tyack, P.L. and C.W. Clark. 2000. Communication and Acoustic Behavior of Dolphins and Whales. (Chapter 4) In Au, W.W.L., R.R. Fay, and A.N. Popper (eds.). *Hearing by Whales and Dolphins*. Springer, New York. pp. 156-224. [https://doi.org/10.1007/978-1-4612-1150-1\\_4](https://doi.org/10.1007/978-1-4612-1150-1_4).
- Urazghildiiev, I.R. and D.E. Hannay. 2017. Maximum likelihood estimators and Cramér–Rao bound for estimating azimuth and elevation angles using compact arrays. *Journal of the Acoustical Society of America* 141(4): 2548-2555. <https://doi.org/10.1121/1.4979792>.
- Urick, R.J. 1983. *Principles of Underwater Sound*. 3rd edition. McGraw-Hill, New York, London. 423 p.
- Van Parijs, S.M. and K.M. Kovacs. 2002. In-air and underwater vocalizations of eastern Canadian harbour seals, *Phoca vitulina*. *Canadian Journal of Zoology* 80(7): 1173-1179. <https://doi.org/10.1139/z02-088>.

- Villadsgaard, A., M. Wahlberg, and J. Tougaard. 2007. Echolocation signals of wild harbour porpoises, *Phocoena phocoena*. *Journal of Experimental Biology* 210: 56-64. <https://doi.org/10.1242/jeb.02618>.
- Wahlberg, M., K. Beedholm, A. Heerfordt, and B. Møhl. 2011. Characteristics of biosonar signals from the northern bottlenose whale, *Hyperoodon ampullatus*. *Journal of the Acoustical Society of America* 130(5): 3077-3084. <https://doi.org/10.1121/1.3641434>.
- Wang, D., W. Huang, H. Garcia, and P. Ratilal. 2016. Vocalization Source Level Distributions and Pulse Compression Gains of Diverse Baleen Whale Species in the Gulf of Maine. *Remote Sensing* 8(11): 881. <https://doi.org/10.3390/rs8110881>.
- Warner, G.A., C. Erbe, and D.E. Hannay. 2010. Underwater Sound Measurements. (Chapter 3) In Reiser, C.M., D. Funk, R. Rodrigues, and D.E. Hannay (eds.). *Marine Mammal Monitoring and Mitigation during Open Water Shallow Hazards and Site Clearance Surveys by Shell Offshore Inc. in the Alaskan Chukchi Sea, July-October 2009: 90-Day Report*. LGL Report P1112-1. Report by LGL Alaska Research Associates Inc. and JASCO Applied Sciences for Shell Offshore Inc., National Marine Fisheries Service (US), and Fish and Wildlife Service (US). pp. 1-54.
- Watkins, W.A. 1981. Activities and underwater sounds of fin whales. *Scientific Reports of the Whales Research Institute* 33: 83-117. <https://www.icrwhale.org/pdf/SC03383-117.pdf>.
- Watkins, W.A., P.L. Tyack, K.E. Moore, and J.E. Bird. 1987. The 20-Hz signals of finback whales (*Balaenoptera physalus*). *Journal of the Acoustical Society of America* 82(6): 1901-1912. <https://doi.org/10.1121/1.395685>.
- Weirathmueller, M.J., W.S.D. Wilcock, and D.C. Soule. 2013. Source levels of fin whale 20 Hz pulses measured in the Northeast Pacific Ocean. *Journal of the Acoustical Society of America* 133(2): 741-749. <https://doi.org/10.1121/1.4773277>.
- Wenz, G.M. 1962. Acoustic Ambient Noise in the Ocean: Spectra and Sources. *Journal of the Acoustical Society of America* 34(12): 1936-1956. <https://doi.org/10.1121/1.1909155>.
- Whitehead, H. and C. Glass. 1985. Orcas (killer whales) attack humpback whales. *Journal of Mammalogy* 66(1): 183-185. <https://doi.org/10.2307/1380982>.
- Whitehead, H. 2018. Sperm Whale: *Physeter macrocephalus*. In Würsig, B., J.G.M. Thewissen, and K.M. Kovacs (eds.). *Encyclopedia of Marine Mammals*. 3rd edition. Academic Press. pp. 919-925. <https://doi.org/10.1016/B978-0-12-804327-1.00242-9>.
- Willis, J. and F.T. Dietz. 1961. Effect of Tidal Currents on 25 cps Shallow Water Ambient Noise Measurements. *Journal of the Acoustical Society of America* 33(11): 1659-1659. <https://doi.org/10.1121/1.1936636>.
- Zhang, Z.Y. and C.T. Tindle. 1995. Improved equivalent fluid approximations for a low shear speed ocean bottom. *Journal of the Acoustical Society of America* 98(6): 3391-3396. <https://doi.org/10.1121/1.413789>.
- Zimmer, W.M.X., M.P. Johnson, P.T. Madsen, and P.L. Tyack. 2005. Echolocation clicks of free-ranging Cuvier's beaked whales (*Ziphius cavirostris*). *Journal of the Acoustical Society of America* 117(6): 3919-3927. <https://doi.org/10.1121/1.1910225>.
- Zykov, M.M. 2016. *Modelling Underwater Sound Associated with Scotian Basin Exploration Drilling Project: Acoustic Modelling Report*. Document Number 01112, Version 2.0. Technical report by JASCO Applied Sciences for Stantec Consulting Ltd. <https://www.ceaa.gc.ca/050/documents/p80109/116305E.pdf>.

## Appendix A. Underwater Acoustic Recorders

Two Autonomous Multichannel Acoustic Recorders–Generation 4 (AMAR; JASCO) in glass spheres housings were deployed to record the drilling sound fields. Each AMAR was fitted with M36 omnidirectional hydrophones (GeoSpectrum Technologies Inc.;  $-165 \pm 3$  dB re 1 V/ $\mu$ Pa sensitivity). The AMAR hydrophones were protected by a hydrophone cage and encased in open-cell foam to minimize noise artifacts from water flowing over the hydrophone. All AMARs recorded continuously on a duty cycle, alternating between 60 s at 512 kHz, and 9 min at 32 kHz. Recordings at 1 km from the drill site contained no usable data due to a failure in the hydrophone cabling when it was under pressure.

Figure A-2 shows a photo of the Autonomous Long-Term Observatory (ALTO) landers developed by JASCO to provide a platform for directional passive acoustics recordings. The landers are also able to carry various oceanographic sensors such as conductivity-temperature-dissolved (CTD) loggers, VEMCO fish tag loggers, and active echosounders. The landers sit directly on the ocean bottom and integrate a pair of acoustic releases as well as an iridium beacon to ensure the landers are retrieved.

## Mooring Diagram 182 Free-Fall Mooring Frame

Rev 1.0

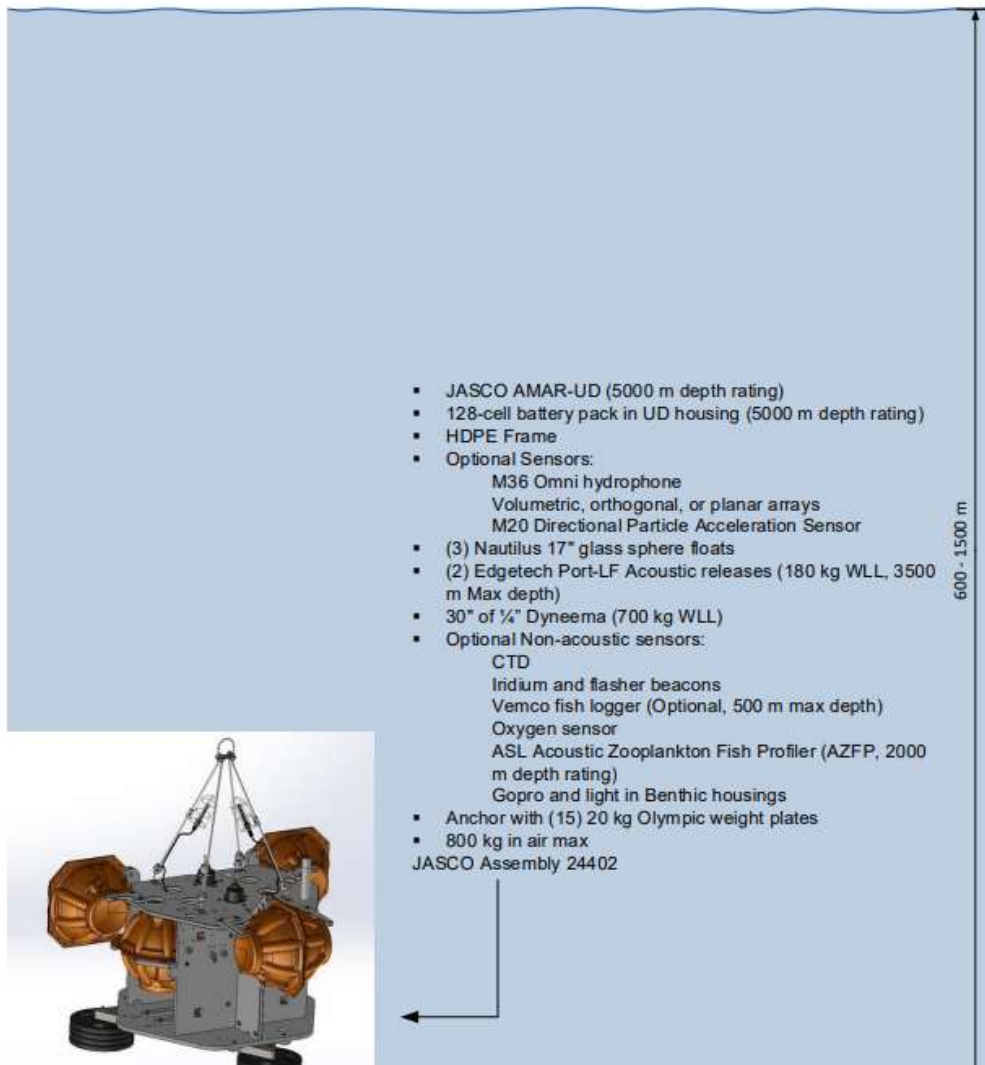


Figure A-1. Drillship source characterization mooring design with one Ultra Deep-housing Autonomous Multichannel Acoustic Recorder–Generation 4 (AMAR G4). This configuration was used 1 km from the drillship.



Figure A-2. Photo of ALTO landers prior to deployment. Each lander has an orthogonal array of four omnidirectional hydrophones spaced 50 cm apart (the hydrophones are inside the yellow flow shields). By using beamforming analysis methods, the direction of arrival of sounds can be determined from the four hydrophones. This configuration was used at ALTO1 and ALTO2 stations.

Each AMAR was calibrated before shipment to the field site and upon retrieval with a pistonphone type 42AC precision sound source (G.R.A.S. Sound & Vibration A/S; Figure A-3). The pistonphone calibrator produces a constant tone at 250 Hz at a fixed distance from the hydrophone sensor in an airtight space of known volume. The recorded level of the reference tone on the AMAR yields the system gain for the AMAR and hydrophone. To determine absolute sound pressure levels, this gain was applied during data analysis. Typical calibration variance using this method is less than 0.7 dB absolute pressure.



Figure A-3. Split view of a G.R.A.S. 42AC pistonphone calibrator with an M36 hydrophone.

## A.1. Acoustic Data Analysis

The sampled data were processed for ambient sound analysis, vessel noise detection, and detection of all marine mammal vocalizations with JASCO's PAMlab acoustic analysis software suite. The major processing stages are outlined in Figure A-4. The results are calculated in terms of various acoustics metrics, defined in Appendix A.1.1, and in various frequency bands, defined in Appendix A.1.2.

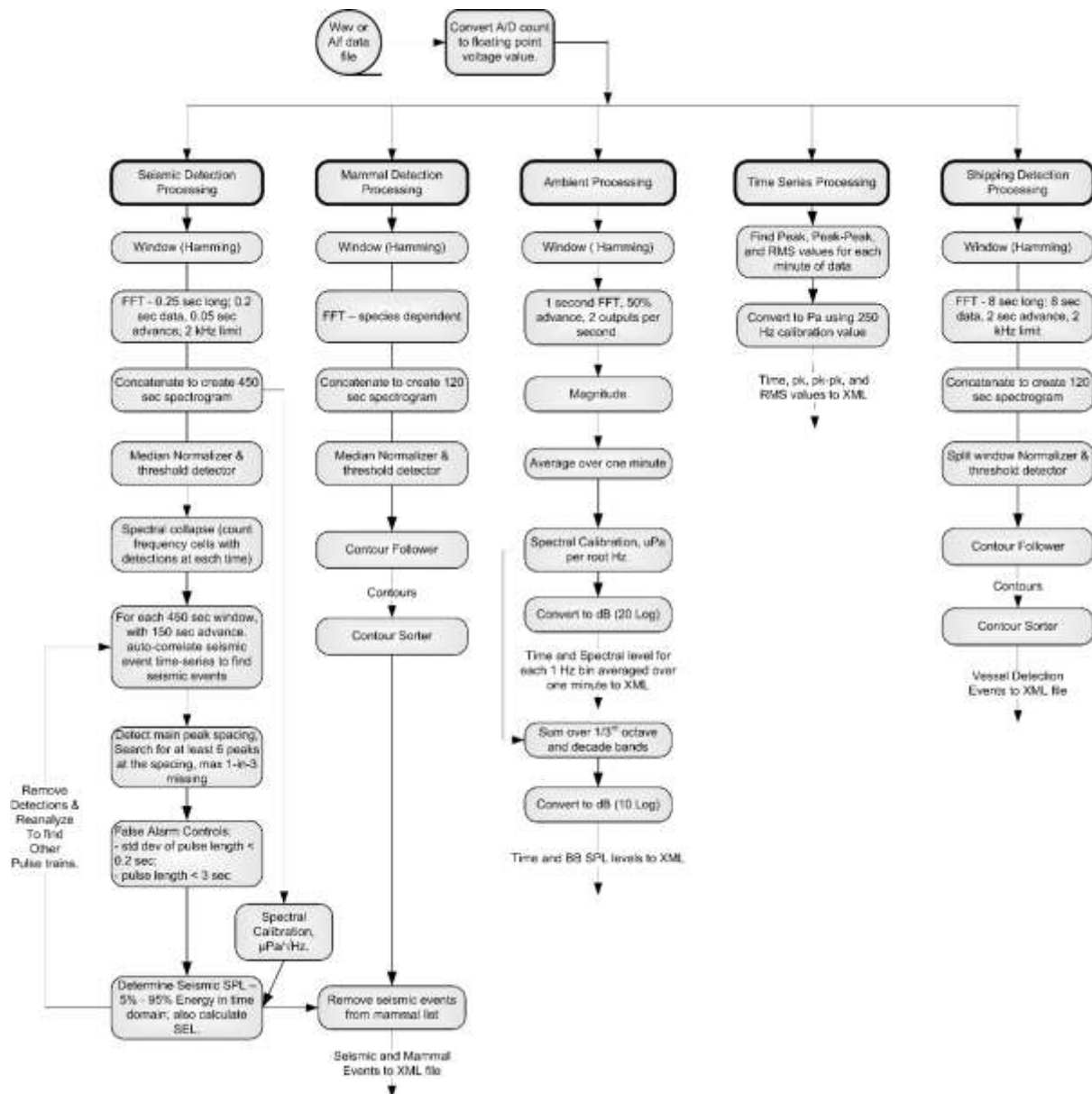


Figure A-4. Major stages of the automated acoustic analysis process performed with JASCO's PAMlab software suite.

### A.1.1. Acoustic Metrics

Underwater sound pressure amplitude is quantified in decibels (dB) relative to a fixed reference pressure of  $p_0 = 1 \mu\text{Pa}$ . Because the perceived loudness of sound, especially pulsed sound such as from seismic airguns, pile driving, and sonar, is not generally proportional to the instantaneous acoustic pressure, several sound level metrics are commonly used to evaluate sound and its effects on marine life. Here we provide specific definitions of relevant metrics used in the accompanying report. Where possible, we follow International Organization for Standardization definitions and symbols for sound metrics (e.g., ISO 18405:2017a, ANSI S1.1-2013).

The zero-to-peak sound pressure, or peak sound pressure (PK or  $L_{pk}$ ; dB re  $1 \mu\text{Pa}$ ), is the decibel level of the maximum instantaneous sound pressure in a stated frequency band attained by an acoustic pressure signal,  $p(t)$ :

$$L_{pk} = 10 \log_{10} \frac{p_{pk}^2}{p_0^2} = 20 \log_{10} \frac{p_{pk}}{p_0} = 20 \log_{10} \frac{\max|p(t)|}{p_0} \quad (\text{A-1})$$

PK is often included as a criterion for assessing whether a sound is potentially injurious; however, because it does not account for the duration of an acoustic event, it is generally a poor indicator of perceived loudness.

The sound pressure level (SPL or  $L_p$ ; dB re  $1 \mu\text{Pa}$ ) is the root-mean-square (rms) pressure level in a stated frequency band over a specified time window ( $T$ ; s):

$$L_p = 10 \log_{10} \frac{p_{rms}^2}{p_0^2} = 10 \log_{10} \left( \frac{1}{T} \int_T p^2(t) dt / p_0^2 \right) \quad (\text{A-2})$$

It is important to note that SPL always refers to an rms pressure level (i.e., a quadratic mean over a time interval) and therefore not instantaneous pressure at a fixed point in time. The SPL can also be defined as the *mean-square* pressure level, given in decibels relative to a reference value of  $1 \mu\text{Pa}^2$  (i.e., in dB re  $1 \mu\text{Pa}^2$ ). The two definitions of SPL are numerically equivalent, differing only in reference value.

### A.1.2. Decidecade Band Analysis

The distribution of a sound's power with frequency is described by the sound's spectrum. The sound spectrum can be split into a series of adjacent frequency bands. Splitting a spectrum into 1 Hz wide bands, called passbands, yields the power spectral density of the sound. These values directly compare to the Wenz curves, which represent typical deep ocean sound levels (see Figure 5) (Wenz 1962). This splitting of the spectrum into passbands of a constant width of 1 Hz, however, does not represent how animals perceive sound.

Animals perceive exponential increases in frequency rather than linear increases, so analyzing a sound spectrum with passbands that increase exponentially in size better approximates real-world scenarios. In underwater acoustics, a spectrum is commonly split into decidecade bands, which are one tenth of a decade wide. A decidecade is sometimes referred to as a "1/3-octave" because one tenth of a decade is

approximately equal to one third of an octave. Each decade represents a factor of 10 in sound frequency. Each octave represents a factor of 2 in sound frequency. The centre frequency of the  $i$ th decade band,  $f_c(i)$ , is defined as:

$$f_c(i) = 10^{\frac{i}{10}} \text{ kHz} \tag{A-3}$$

and the low ( $f_{lo}$ ) and high ( $f_{hi}$ ) frequency limits of the  $i$ th decade band are defined as:

$$f_{lo,i} = 10^{\frac{-1}{20}} f_c(i) \text{ and } f_{hi,i} = 10^{\frac{1}{20}} f_c(i) \tag{A-4}$$

The decade bands become wider with increasing frequency, and on a logarithmic scale the bands appear equally spaced (Figure A-5).

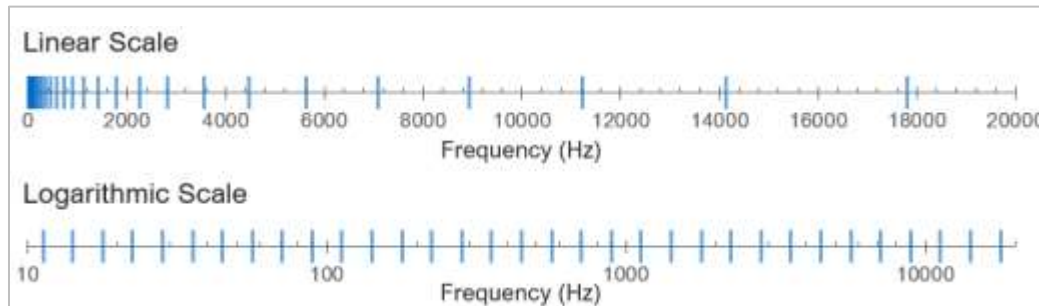


Figure A-5. Decidecade frequency bands (vertical lines) shown on (top) a linear frequency scale and (bottom) a logarithmic scale. On the logarithmic scale, the bands are equally spaced.

The sound pressure level in the  $i$ th band ( $L_{p,i}$ ) is computed from the spectrum  $S(f)$  between  $f_{lo,i}$  and  $f_{hi,i}$ :

$$L_{p,i} = 10 \log_{10} \int_{f_{lo,i}}^{f_{hi,i}} S(f) df \text{ dB} \tag{A-5}$$

Summing the sound pressure level of all the bands yields the broadband sound pressure level:

$$\text{Broadband SPL} = 10 \log_{10} \sum_i 10^{\frac{L_{p,i}}{10}} \text{ dB} \tag{A-6}$$

Figure A-6 shows an example of how the decade band sound pressure levels compare to the sound pressure spectral density levels of an ambient sound signal. Because the decade bands are wider than 1 Hz, the decade band SPL is higher than the spectral levels at higher frequencies. Decade band analysis can be applied to continuous and impulsive sound sources. For impulsive sources, the decade band SEL is typically reported.

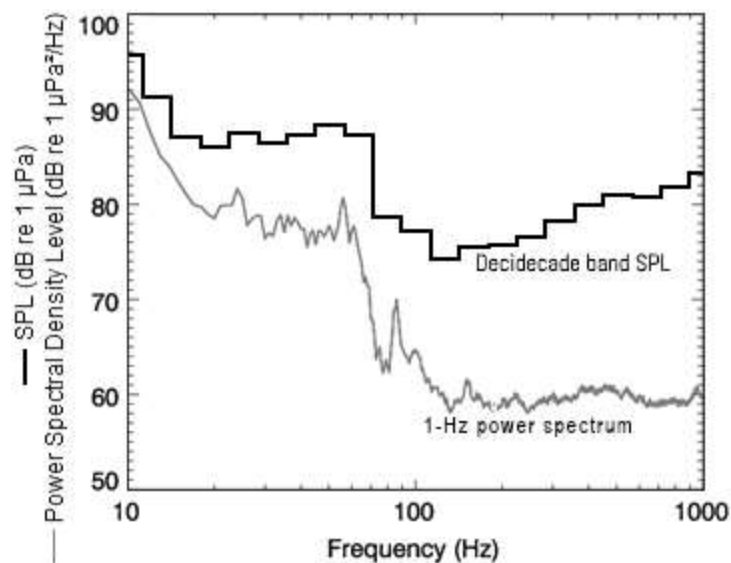


Figure A-6. Sound pressure spectral density levels and the corresponding decidecade band sound pressure levels of example ambient sound shown on a logarithmic frequency scale. Because the decidecade bands are wider with increasing frequency, the decidecade band SPL is higher than the power spectrum, which is based on bands with a constant width of 1 Hz.

Table A-1. Decidecade-band frequencies (Hz).

Band	Lower frequency	Nominal centre frequency	Upper frequency	Band	Lower frequency	Nominal centre frequency	Upper frequency
10	8.9	10.0	11.2	31	1122	1259	1413
11	11.2	12.6	14.1	32	1413	1585	1778
12	14.1	15.8	17.8	33	1778	1995	2239
13	17.8	20.0	22.4	34	2239	2512	2818
14	22.4	25.1	28.2	35	2818	3162	3548
15	28.2	31.6	35.5	36	3548	3981	4467
16	35.5	39.8	44.7	37	4467	5012	5623
17	44.7	50.1	56.2	38	5623	6310	7079
18	56.2	63.1	70.8	39	7079	7943	8913
19	70.8	79.4	89.1	40	8913	10000	11220
20	89.1	100.0	112.2	41	11220	12589	14125
21	112	126	141	42	14260	16000	17952
22	141	158	178	43	17825	20000	22440
23	178	200	224	44	22281	25000	28050
24	224	251	282	45	28074	31500	35344
25	282	316	355	46	35650	40000	44881
26	355	398	447	47	44563	50000	56101
27	447	501	562	48	56149	63000	70687
28	562	631	708	49	71300	80000	89761
29	708	794	891	50	89125	100000	112202
30	891	1000	1122	51	111406	125000	NA- above Nyquist

Table A-2. Decade-band frequencies (Hz).

Decade band	Lower frequency	Nominal centre frequency	Upper frequency
A	8.9	50	89.1
B	89.1	500	891
C	891	5,000	8913
D	8913	50,000	89125

## A.2. Auditory Frequency Weighting Functions

### A.2.1. Marine Mammal Frequency Weighting

The potential for noise to affect animals depends on how well the animals can hear it. Noises are less likely to disturb or injure an animal if they are at frequencies that the animal cannot hear well. An exception occurs when the sound pressure is so high that it can physically injure an animal by non-auditory means (i.e., barotrauma). For sound levels below such extremes, the importance of sound components at particular frequencies can be scaled by frequency weighting relevant to an animal's sensitivity to those frequencies (Nedwell and Turnpenny 1998, Nedwell et al. 2007).

### A.2.2. Marine Mammal Frequency Weighting Functions

In 2015, a US Navy technical report by Finneran (2015) recommended new auditory weighting functions. The overall shape of the auditory weighting functions is similar to human A-weighting functions, which follows the sensitivity of the human ear at low sound levels. The new frequency-weighting function is expressed as:

$$G(f) = K + 10 \log_{10} \left[ \left( \frac{(f/f_{lo})^{2a}}{[1 + (f/f_{lo})^2]^a [1 + (f/f_{hi})^2]^b} \right) \right] \quad (A-7)$$

Finneran (2015) proposed five functional hearing groups for marine mammals in water: low-, mid- and high-frequency cetaceans (LF, MF, and HF cetaceans, respectively), phocid pinnipeds, and otariid pinnipeds. The parameters for these frequency-weighting functions were further modified the following year (Finneran 2016) and were adopted in NOAA's technical guidance that assesses acoustic impacts on marine mammals (NMFS 2018), and in the latest guidance by Southall (2019). The updates did not affect the content related to either the definitions of frequency-weighting functions or the threshold values. Table A-3 lists the frequency-weighting parameters for each hearing group. Figure A-7 shows the resulting frequency-weighting curves.

Table A-3. Parameters for the auditory weighting functions used in this project as recommended by Southall et al. (2019).

Hearing group	a	b	$f_{lo}$ (Hz)	$f_{hi}$ (kHz)	$K$ (dB)
Low-frequency cetaceans (baleen whales)	1.0	2	200	19,000	0.13
High-frequency cetaceans (dolphins, plus toothed, beaked, and bottlenose whales)	1.6	2	8,800	110,000	1.20
Very-high-frequency cetaceans (true porpoises, <i>Kogia</i> , river dolphins, cephalorhynchid, <i>Lagenorhynchus cruciger</i> and <i>L. australis</i> )	1.8	2	12,000	140,000	1.36
Phocid seals in water	1.0	2	1,900	30,000	0.75
Otariid seals in water	2.0	2	940	25,000	0.64

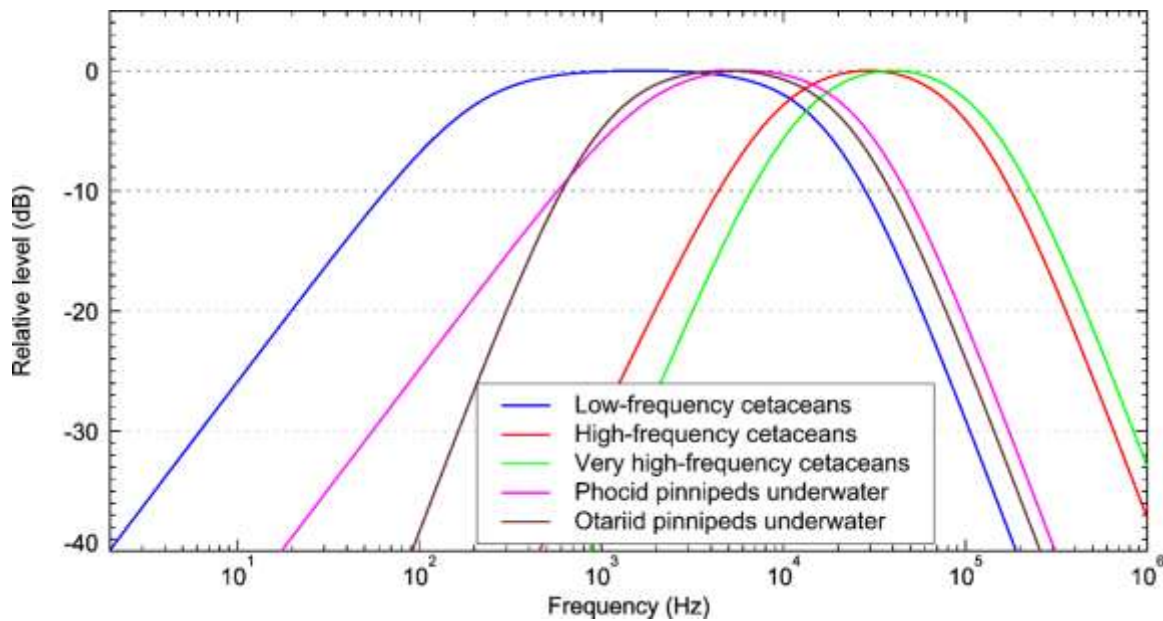


Figure A-7. Auditory weighting functions for functional marine mammal hearing groups used in this project as recommended by Southall et al. (2019).

## Appendix B. Marine Mammal Detection Methodology

### B.1. Automated Click Detector for Odontocetes

Figure B-1 shows how we apply an automated click detector/classifier to the data to detect clicks from odontocetes. This detector/classifier is based on the zero-crossings in the acoustic time series. Zero-crossings are the rapid oscillations of a click's pressure waveform above and below the signal's normal level. Clicks are detected by the following steps:

1. The raw data are high-pass filtered to remove all energy below 5 kHz. This removes most energy from sources other than odontocetes (such as shrimp, vessels, wind, and cetacean tonal calls) yet allows the energy from all marine mammal click types to pass.
2. The filtered samples are summed to create a 0.334 ms rms time series. Most marine mammal clicks have a 0.1–1 ms duration.
3. Possible click events are identified with a split-window normalizer that divides the 'test' bin of the time series by the mean of the 6 'window' bins on either side of the test bin, leaving a 'notch' that is 1-bin wide.
4. A Teager-Kaiser energy detector identifies possible click events.
5. The high-pass filtered data are searched to find the maximum peak signal within 1 ms of the detected peak.
6. The high-pass filtered data are searched backwards and forwards to find the time span when the local data maxima are within 9 dB of the maximum peak. The algorithm allows for two zero-crossings to occur where the local peak is not within 9 dB of the maximum before stopping the search. This defines the time window of the detected click.
7. The classification parameters are extracted. The number of zero crossings within the click, the median time separation between zero crossings, and the slope of the change in time separation between zero-crossings are computed. The slope parameter helps identify beaked whale clicks, because beaked whales can be identified by the increase in frequency (upsweep) of their clicks.
8. The Mahalanobis distance between the extracted classification parameters and the templates of known click types is computed. The covariance matrices for the known click types (computed from thousands of manually identified clicks for each species) are stored in an external file. Each click is classified as a type with the minimum Mahalanobis distance, unless none of them are less than the specified distance threshold.

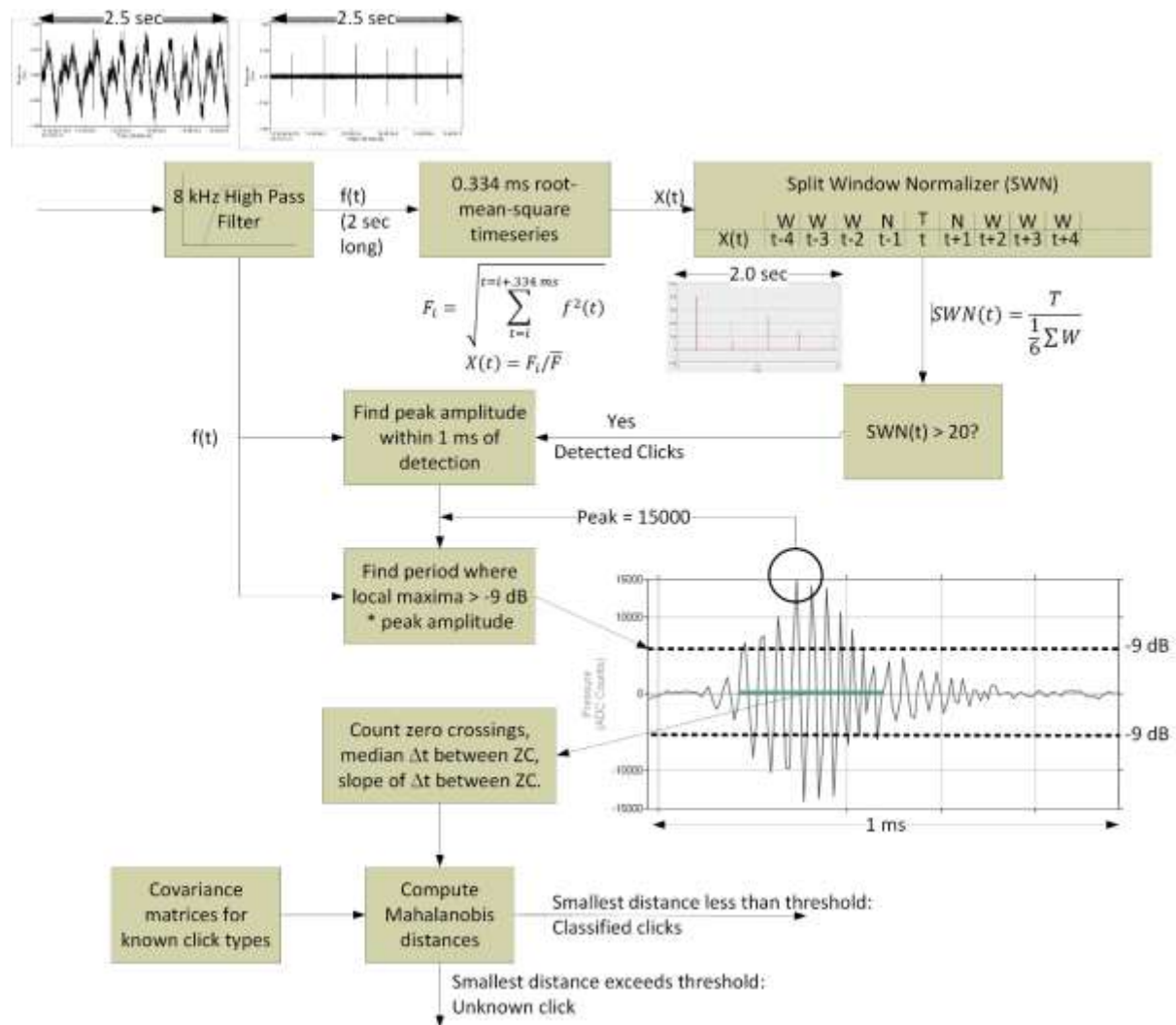


Figure B-1. Flowchart of the automated click detector/classifier process.

Odontocete clicks occur in groups called click trains. Each species has a characteristic inter-click-interval (ICI) and number of clicks per train. The automated click detector includes a second stage that associates individual clicks into trains (Figure B-2). The click train associator algorithm performs the following steps:

1. Queue clicks for  $N$  seconds, where  $N$  is twice the maximum number of clicks per train times the maximum ICI.
2. Search for all clicks within the window that have Mahalanobis distances less than 5 for a species of interest (this finds 80 % of all clicks for the species as defined by the template).
3. Create a candidate click train if:
  - a. The number of clicks is greater or equal to the minimum number of clicks in a train;
  - b. The maximum time between any two clicks is less than 2.5 times the maximum ICI, and
  - c. The smallest Mahalanobis distance for all clicks in the candidate train is less than 4.1.

4. Create a new 'time series' with a value of 1 at the time of arrival for each click and zero everywhere else (using a 'time series' with a bin duration of 0.5 ms)
5. Apply a Hann window to the time series, and then compute the cepstrum.
6. A click train is classified if a peak in the cepstrum with an amplitude greater than five times the standard deviation of the cepstrum occurs at a quefrequency between the minimum maximum ICI.
7. For each click related to the previous Ncepstrum, create a new time series and compute ICI. If there is a good match, then extend the click train.
8. Output a species click train detection if the click features, total clicks, and mean ICI match the species.

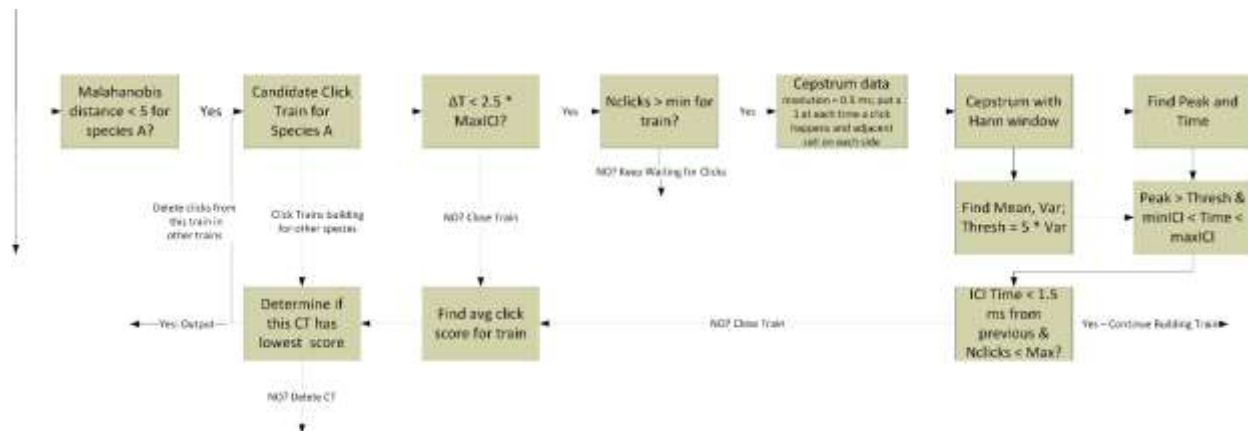


Figure B-2. Flowchart of the click train automated detector/classifier process.

## B.2. Automated Tonal Signal Detection

Marine mammal tonal acoustic signals are automatically detected using a contour detection and following algorithm that is depicted in (Figure B-3). The algorithm has the following steps:

1. Create spectrograms of the appropriate resolution for each mammal vocalization type that were normalized by the median value in each frequency bin for each detection window (Table B-1).
2. Join adjacent bins and create contours via a contour-following algorithm (Figure B-4).
3. Apply a sorting algorithm to determine if the contours match the definition of a marine mammal vocalization (Table B-2).

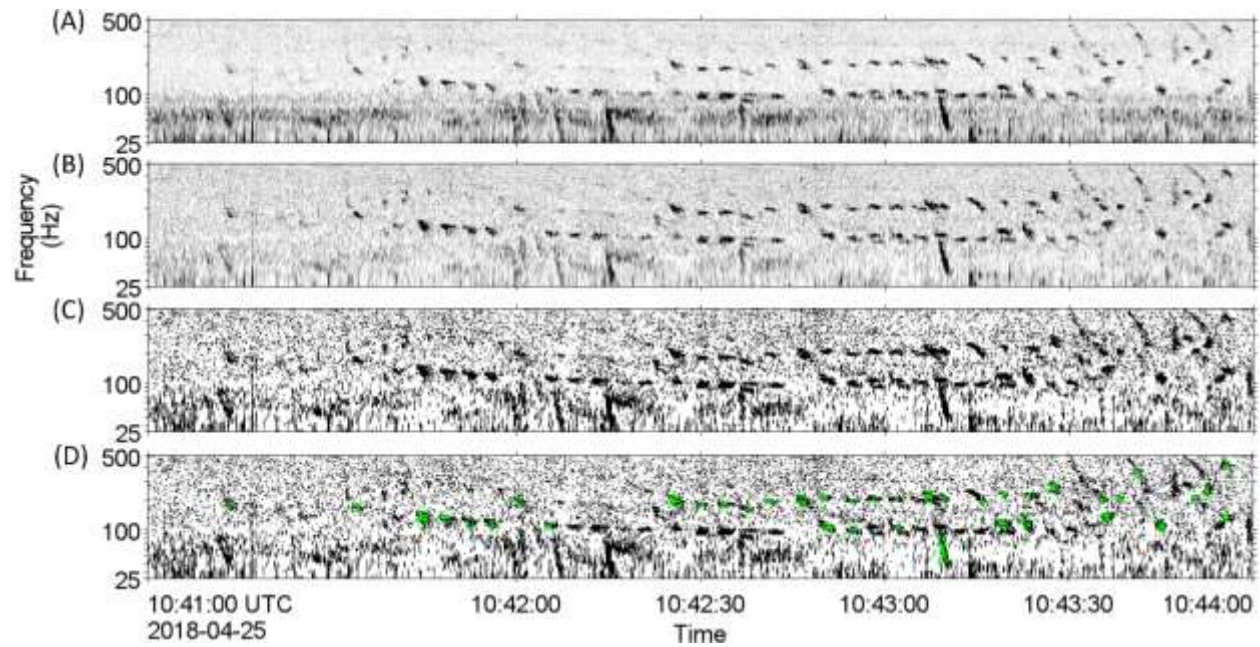


Figure B-3. Illustration of the contour detection process. (A) A spectrogram is generated at the frequency and time resolutions appropriate for the tonal calls of interest. (B) A median normalizer is applied at each frequency. (C) The data is turned into a binary representation by setting all normalized values less than the threshold to 0 and all values greater than the threshold to 1. (D) The regions that are '1' in the binary spectrogram are connected to create contours, which are then sorted to detect signals of interest, shown here as green overlays.

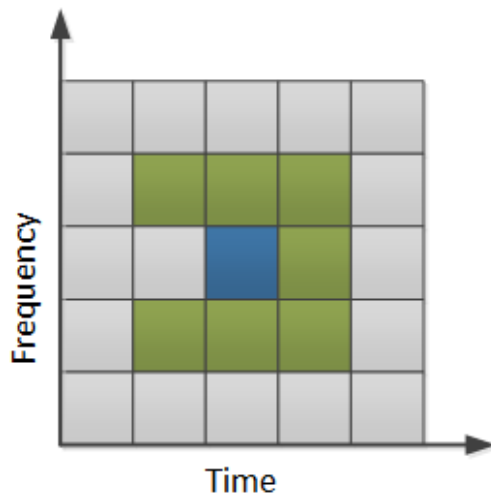


Figure B-4. Illustration of the search area used to connect spectrogram bins. The blue square represents a bin of the binary spectrogram equalling 1 and the green squares represent the potential bins it could be connected to. The algorithm advances from left to right, so grey cells left of the test cell need not be checked.

The tonal signal detector is expanded into a pulse train detector through the following steps:

1. Detect and classify contours as described in [Steps 1 and 2](#) above.
2. A sorting algorithm determines if any series of contours can be assembled into trains that match a pulse train template (Table B-2).

Table B-1. Discrete Fourier Transform (FFT) and detection window settings for all automated contour-based detectors used to detect tonal vocalizations of marine mammal species expected in the data. Values are based on JASCO's experience and empirical evaluation of various data sets.

Species targeted	Automated detector	Signal targeted	Discrete Fourier transform			Detection window (s)	Detection threshold
			Frequency step (Hz)	Temporal observation window (s)	Time advance (s)		
Blue whale	Atl_BlueWhale_IM	A-B tonal song note at 17 Hz	0.125	2	0.5	40	4
	Atl_BlueWhale_IM_HT		0.125	2	0.5	40	6
	Atl_BlueWhale_IM2		0.125	2	0.5	120	4
	Atl_BlueWhale_IM2_HT		0.125	2	0.5	120	6
	Atl_BlueWhale_GL_IM		0.125	2	0.5	40	4
	NPac_BlueWhale_D	D call	2	0.25	0.05	10	2
NPac_BlueWhale_D_HT	2		0.25	0.05	10	4	
Fin whale	Atl_FinWhale_21	20 Hz pulse	1	0.2	0.05	5	1.7
	Atl_FinWhale_21_HT		1	0.2	0.05	5	3.7
	Atl_FinWhale_21.2		1	0.2	0.05	5	4
	Atl_FinWhale_21.2_HT		1	0.2	0.05	5	6
	NPac_FinWhale_21HSNR		1	0.2	0.05	5	5
	NPac_FinWhale_21LSNR		1	0.2	0.05	5	1.7
	Atl_FinWhale_130		2	0.2	0.05	5	3
Right whale	N_RightWhale_Up1	Upcall	4	0.128	0.032	8	2.5
	N_RightWhale_Up2		4	0.128	0.032	8	3
	N_RightWhale_Up3		7	0.17	0.025	10	3
Sei whale	SeiWhale	Downsweeps	3.25	0.2	0.035	5	3.5
	SeiWhale_LowThreshold		3.25	0.2	0.035	5	2.5
	SeiWhale_MidThreshold		3.25	0.2	0.035	5	5
	SeiWhale_HighThreshold		3.25	0.2	0.035	5	5.5
Minke whale	MinkePulseTrain	Pulse train	8	0.1	0.025	40	3.5
Humpback, killer whale	MFMoanHigh	Moan	8	0.125	0.05	5	3
	MFMoanHigh_HT		8	0.125	0.05	5	5
Humpback whale	MFMoanLow	Moan	4	0.2	0.05	5	3
	MFMoanLow_HT		4	0.2	0.05	5	5
Right, minke whale	ShortLow	Moan, pulse	7	0.17	0.025	10	3
Blue, right, sei whale	LFMoan	Moan	2	0.25	0.05	10	3
Fin whale	VLFMoan	Moan	2	0.2	0.05	15	4

Small dolphins	WhistleHigh_Suppress20k	Whistle with energy between 4–20 kHz	64	0.015	0.005	10	1.5
	WhistleHigh_Quiet20k		64	0.015	0.005	10	1.5
	WhistleHigh_Loud20k		64	0.015	0.005	10	4.5
Pilot, killer whale	WhistleLow_Suppress	Whistle with energy between 1–10 kHz	8	0.125	0.05	10	1.5
	WhistleLow_Quiet		8	0.125	0.05	10	1.5
	WhistleLow_Loud		8	0.125	0.05	10	4.5
Harbour seal	HarbourSeal_1	Roar	8	0.128	0.032	30	3
	HarbourSeal_2		20	0.06	0.03	35	2.2

Table B-2. A sample of automated detector classification definitions for the tonal vocalizations of cetacean species expected in the area. Automated detectors are capable of triggering on species and signals beyond those targeted.

Species targeted	Automated detector	Frequency (Hz)	Duration (s)	Bandwidth (Hz)	Other parameters
Blue whale	Atl_BlueWhale_IM	14–22	8.00–30.00	1–5	-500 to 0 Hz/s min. SR; <18 Hz $f_{min}$ ; 16.5–18 Hz $f$ of peak intensity
	Atl_BlueWhale_IM_HT	14–22	8.00–30.00	1–5	-500 to 0 Hz/s min. SR; <18 Hz $f_{min}$ ; 16.5–18 Hz $f$ of peak intensity
	Atl_BlueWhale_IM2	15–22	8.00–30.00	1–5	<18 Hz $f_{min}$
	Atl_BlueWhale_IM2_HT	15–22	8.00–30.00	1–5	<18 Hz $f_{min}$
	Atl_BlueWhale_GL_IM	14–22	8.00–30.00	1–5	-500 to 0 Hz/s min. SR; <18 Hz $f_{min}$ ; 16.5–17.5 Hz $f$ of peak intensity
	NPac_BlueWhale_D	20–100	2.00–10.00	>15	Max. IB: <30 Hz; SR: -15 to -5 Hz/s
	NPac_BlueWhale_D_HT	20–100	2.00–10.00	>15	Max. IB: <30 Hz; SR: -15 to -5 Hz/s
Fin whale	Atl_FinWhale_21	10–40	0.40–3.00	>6	-100 to 0 Hz/s SR; <17 Hz $f_{min}$ ; 20–22 Hz $f$ of peak intensity
	Atl_FinWhale_21_HT	10–40	0.40–3.00	>6	-100 to 0 Hz/s SR; <17 Hz $f_{min}$ ; 20–22 Hz $f$ of peak intensity
	Atl_FinWhale_21.2	8–40	0.30–3.00	>6	-100 to 0 Hz/s SR; <17 Hz $f_{min}$
	Atl_FinWhale_21.2_HT	8–40	0.30–3.00	>6	-100 to 0 Hz/s SR; <17 Hz $f_{min}$
	NPac_FinWhale_21HSNR	3–50	0.40–3.00	>6	-100 to 0 Hz/s SR; <17 Hz $f_{min}$ ; 20–23.5 Hz $f$ of peak intensity; <30 Hz max IB
	NPac_FinWhale_21LSNR	3–50	0.40–3.00	>6	-100 to 0 Hz/s SR; <17 Hz $f_{min}$ ; 20–23.5 Hz $f$ of peak intensity; <20 Hz max IB
	Atl_FinWhale_130	110–150	0.30–1.50	>6	<125 Hz $f_{min}$
Right whale	N_RightWhale_Up1	65–260	0.60–1.20	70–195	<75 Hz $f_{min}$ ; 30 to 290 Hz/s SR
	N_RightWhale_Up2	65–260	0.50–1.20	-	30 to 290 Hz/s SR
	N_RightWhale_Up3	30–400	0.50–10.00	>25	10 to 500 Hz/s SR

Sei whale	SeiWhale	20-150	0.50-1.70	19-120	-100 to -6 Hz/s SR; 70 Hz max. IB;
	SeiWhale_LowThreshold	20-100	1.00-1.70	30-80	-80 to -12 Hz/s SR; 100 Hz max. IB; <50 Hz $f$ of peak intensity
	SeiWhale_MidThreshold	20-80	1.00-1.70	30-80	-80 to -12 Hz/s SR; 100 Hz max. IB
	SeiWhale_HighThreshold	20-150	0.50-1.70	19-120	-100 to -6 Hz/s SR; 70 Hz max. IB
Humpback whale, killer whale	MFMoanHigh	500-2500	0.50-5.00	>150	<1500 Hz $f_{min}$ ; 300 Hz max. IB
	MFMoanHigh_HT	500-2500	0.50-5.00	>150	<1500 Hz $f_{min}$ ; 300 Hz max. IB
Humpback whale	MFMoanLow	100-700	0.50-5.00	>50	<450 Hz $f_{min}$ ; 200 Hz max. IB
	MFMoanLow_HT	100-700	0.50-5.00	>50	<450 Hz $f_{min}$ ; 200 Hz max. IB
Right, minke whale	ShortLow	30-400	0.08-0.60	>25	None
Blue, right, sei whale	LFMoan	40-250	0.50-10.00	>15	50 Hz max. IB
Fin whale	VLFMoan	10-100	0.30-10.00	>10	<40 Hz $f_{min}$
Small dolphins	WhistleHigh_Suppress20k	4000-20,000	0.30-5.00	>700	2000 Hz max. IB; Suppress detections for high SPL (>125 dB) between 5-1000 Hz
	WhistleHigh_Quiet20k	4000-20,000	0.30-5.00	>700	2000 Hz max. IB
	WhistleHigh_Loud20k	4000-20,000	0.30-5.00	>700	2000 Hz max. IB
Pilot, killer whale	WhistleLow_Suppress	1000-10,000	0.80-5.00	>300	<5000 Hz $f_{min}$ ; 1000 Hz max. IB
	WhistleLow_Quiet	1000-10,000	0.80-5.00	>300	<5000 Hz $f_{min}$ ; 1000 Hz max. IB
	WhistleLow_Loud	1000-10,000	0.80-5.00	>300	<5000 Hz $f_{min}$ ; 1000 Hz max. IB
Harbour seal	HarbourSeal_1	70-1200	0.75-2.00	250-1000	<150 Hz $f_{min}$
	HarbourSeal_2	75-1200	0.50-2.00	100-1000	<150 Hz $f_{min}$

f = frequency, IB = instantaneous bandwidth, SR = sweep rate

Table B-3. A sample of vocalization sorter definitions for the tonal pulse train vocalizations of cetacean species expected in the area.

Automated detector	Target species	Frequency (Hz)	Pulse duration (s)	Inter-pulse interval (s)	Train duration (s)	Train length (# pulses)
MinkePulseTrain	Minke whale	50 to 500	0.025 to 0.3	0.25 to 2	10 to 100	20 to 40

### B.3. Automatic Data Selection for Validation (ADSV)

To standardise the file selection process for the selection of data for manual analysis, we applied our Automated Data Selection for Validation (ADSV) algorithm. Kowarski et al. (2021) details the ADSV algorithm, and Figure B-5 shows a schematic of the process. ADSV computes the distribution of three descriptors that describe the automated detections in the full data set: Diversity (number of automated detectors triggered per file), Counts (number of automated detections per file for each automated detector), and Temporal Distribution (spread of detections for each automated detector across the recording period). The algorithm removes files from the temporary data set that have the least impact on the distribution of the three descriptors in the full data set. Files are removed until a predetermined data set size ( $N$ ) is reached, at which point the temporary data set becomes the subset to be manually reviewed.

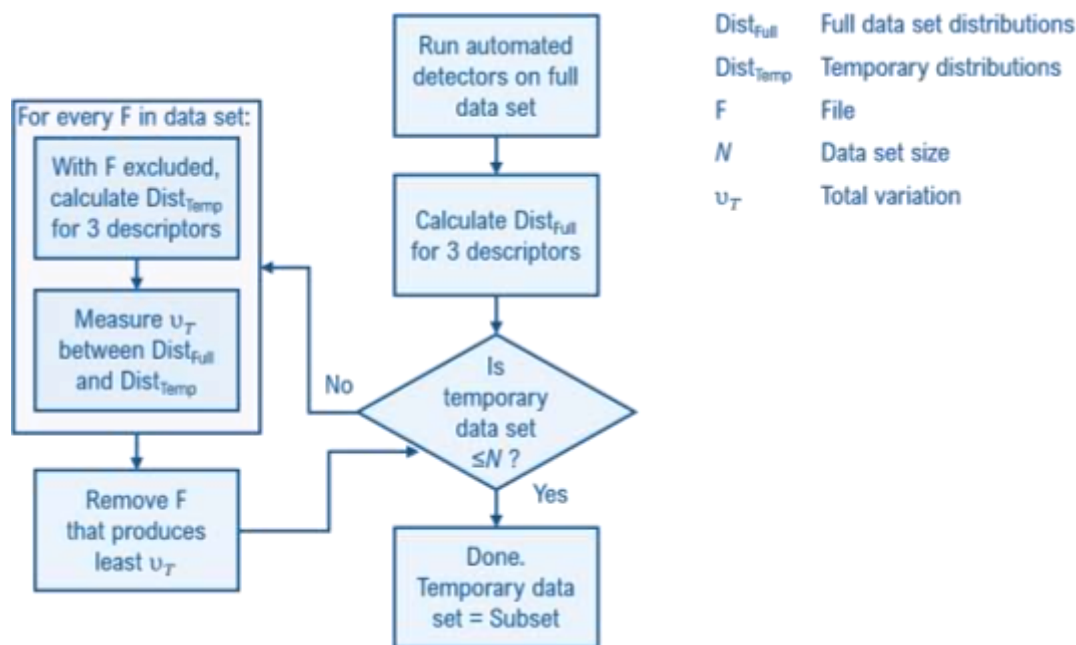


Figure B-5. Automated Data Selection for Validation (ADSV) process based on Figure 1 in Kowarski et al. (2021).

For the present work, an  $N$  of 0.8 % was selected, largely due to limited scope for marine mammal analysis in this project. It is important to note that with such limited manual review, very rare species may have been missed or their occurrence underestimated. The ADSV algorithm is designed to build a subset with as little variation from the full data set as possible. Figure B-6 shows the variation between subsets and dataset as a function of subset size. Here at 0.8 % of the full data set, the variation has neared a plateau close to its minimum and analyzing a subset greater than 0.8 % would only reduce the variation slightly. This provides evidence that sufficient data were analyzed to assess species occurrence, although a slightly larger subset size would have been ideal. The main effect of insufficiently large subsets is that they do not generate enough manually validated detections to assess the performance of some detectors, particularly those that are relatively rarely triggered, and that acoustic occurrence may be underestimated. Additionally, a small subset may not adequately capture the full range of acoustic environments in the full data set such that the resulting automated detector performance metrics may deviate slightly from those obtained using a larger subset.

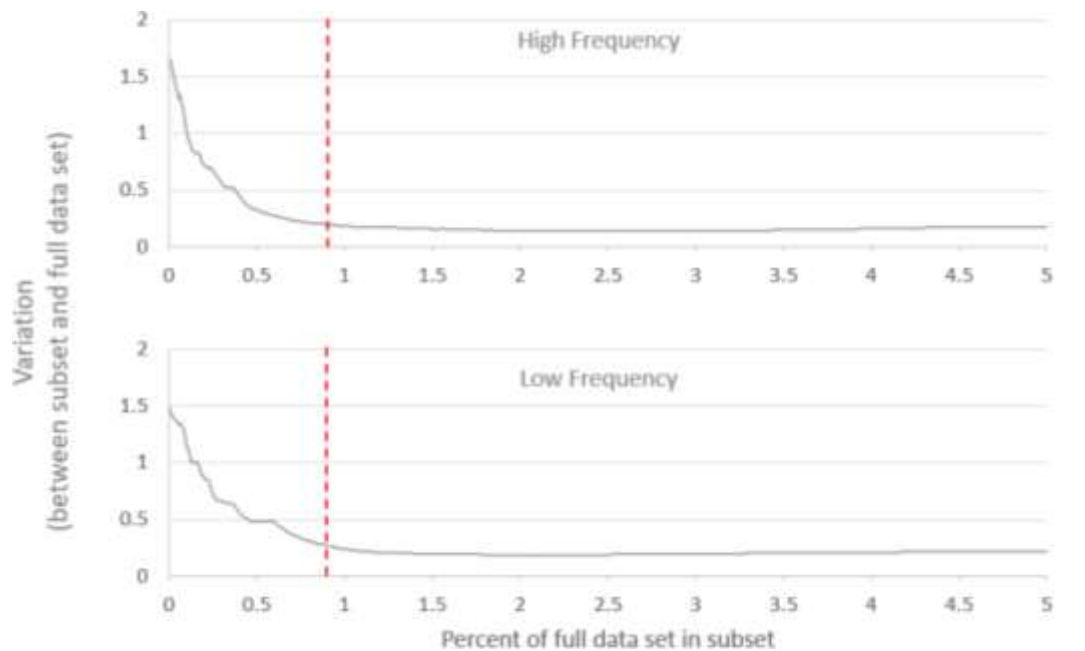


Figure B-6. The total variation between the subset selected by Automated Data Selection for Validation (ADSV) for manual analysis and the full data set. Total variation combines the three automated detector result descriptors used in ADSV: Counts, Diversity, and Temporal Distribution. ADSV subsets were created for the high-frequency (512 kHz sampling rate; top) and low-frequency (32 kHz, bottom) data. The red dashed line indicates the size of the subset selected by ADSV for the present analysis.

## B.4. Automated Detector Performance Calculation and Optimization

All files selected for manual validation were reviewed by one of two experienced analysts using JASCO's PAMlab software to determine the presence or absence of every species, regardless of whether a species was automatically detected in the sound file. Although the automated detectors classify specific signals, we validated the presence/absence of species at the file level, not the detection level. Acoustic signals were only assigned to a species if the analyst was confident in their assessment. When unsure, analysts would consult one another, peer reviewed literature, and other experts in the field. If certainty could not be reached, the file of concern would be classified as possibly containing the species in question or containing an unknown acoustic signal. Next, the validated results were compared to the automated detector results in three phases to refine the results and ensure they accurately represent the occurrence of each species in the study area.

In Phase 1, the human validated versus automated detector results were plotted as time series and critically reviewed to determine when and where automated detections should be excluded. Questionable detections that overlap with the detection period of other species were scrutinized. By restricting detections spatially and/or temporally where appropriate, we can maximize the reliability of the results. No temporal restrictions were necessary for our automated detector results.

In Phase 2, the performance of the automated detectors was calculated and optimized for each species using a threshold, defined as the number of automated detections per file at and above which detections of species were considered valid.

To determine the performance of each automated detector and any necessary thresholds, the automated and validated results (excluding files where an analyst indicated uncertainty in species occurrence) were fed to a maximum likelihood estimation algorithm that maximizes the probability of detection and minimizes the number of false alarms using the Matthews Correlation Coefficient (MCC):

$$MCC = \frac{TP \cdot TN - FP \cdot FN}{\sqrt{(TP + FP)(TP + FN)(TN + FP)(TN + FN)}}$$

$$P = \frac{TP}{TP + FP}; \quad R = \frac{TP}{TP + FN}$$

where *TP* (true positive) is the number of files in the subset with both manual and automated detections, *FP* (false positive) is the number of files in the subset with automated detections but no manual detections, *FN* (false negatives) is the number of files in the subset with manual detections but no automated detections, and *TN* (true negatives) is the number of files in the subset with neither automated or manual detections. Automated detector performance was calculated for each species and station.

In Phase 3, detections were further restricted to include only those where *P* was greater than or equal to 0.75. When *P* was less than 0.75, only validated results were used to describe the acoustic occurrence of a species. The occurrence of each species was plotted using JASCO's Ark software as time series showing presence/absence by hour over each day.

## B.5. Beamforming and Absolute Minimum Number Analysis

This appendix describes how the ALTO lander data were analyzed to determine the direction of arrival of sounds.

### B.5.1. Hydrophone Locations

The hydrophones were arranged in an orthogonal array, with a spacing of approximately 50 cm between them. The relative locations of the hydrophones must be known exactly as part of the beamforming process described in Appendix B.5.2. The distances between hydrophones are measured on deployment and retrieval and kept in the deployment log file (Figure B-7). These values are used in an optimization script to then determine the positions of hydrophones A, B and D relative to C; this process generally corrects the positions by several mm. The final hydrophone positions are stored in the 'ChannelAssociations.xml' file that is associated with the data.

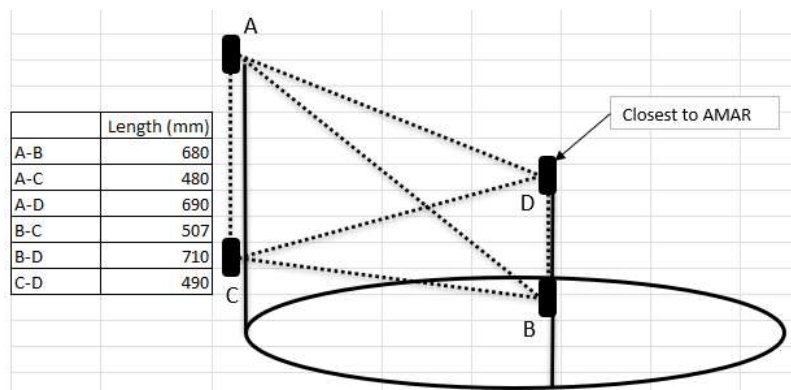


Figure B-7. Hydrophone geometry on the ALTO lander with table of the distances between hydrophones in mm.

### B.5.2. Maximum Likelihood Estimation Beamformer

The analysis was performed using a maximum likelihood estimation (MLE) beamformer (Urazghildiiev and Hannay 2017). This beamformer estimates the sound level assuming the sounds are arriving from azimuthal directions separated by 10 degrees, and for each azimuth it evaluates 10 elevation angles, also separated by 10 degrees, for a total of 360 ‘look directions’ or beams. For each beam, the time delay of arrival between hydrophones are computed assuming that plane wave arrives from that direction. The time delay is converted to a phase change as a function of frequency, and the beams are then formed using fast Fourier transforms (FFT). The duration of the FFT is selected based on the type of analysis being performed (i.e. for a particular type of mammal call, or for vessel detection). The beam with the greatest received level per frequency is selected as the most likely direction of arrival. In cases where a detection spans many frequencies, it is applied to each, and the bearing values are weighted by the energy in the frequency bin, so that the direction assigned to the call is the energy weighted direction.

The ability of the MLE beamformer to determine the direction of arrival depends on the time delay between hydrophones. When the delay is greater than the time required for one half of a wavelength to travel between the hydrophones, the results become ambiguous, which sets an upper limit on the frequencies that may be analyzed. For a 50 cm spaced array, this value is 750 Hz. If the delay, which equates to a phase change, is not long enough, then there is not information to determine the direction of arrival, which sets a lower limit on the frequencies that can be analyzed as a function of the spacing between the hydrophones. This is manifested by an increase in the bearing estimation error that increases as the frequency decreases. It also depends on the signal-to-noise ratio (SNR) between the signal of interest and the background (Figure B-8). The error can be reduced by increasing the spacing between hydrophones, however, that also lowers the maximum usable frequency (Figure B-9).

For the analysis performed using this data, we assume the minimum bearing error is assumed to be 10 degrees.

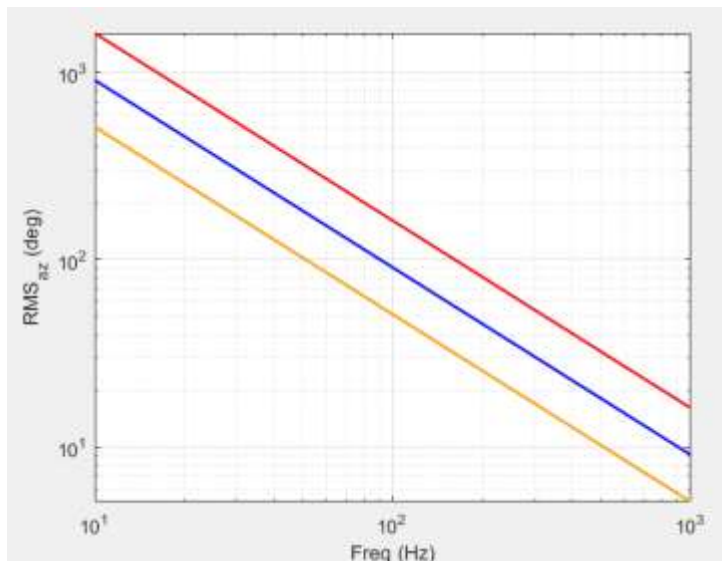


Figure B-8. Root mean square (RMS) azimuthal bearing error for the MLE beamformer processing and orthogonal hydrophone array with a 50 cm spacing as a function of frequency. The error is shown for SNRs of 5 dB (red), 10 dB (blue) and 15 dB (orange).

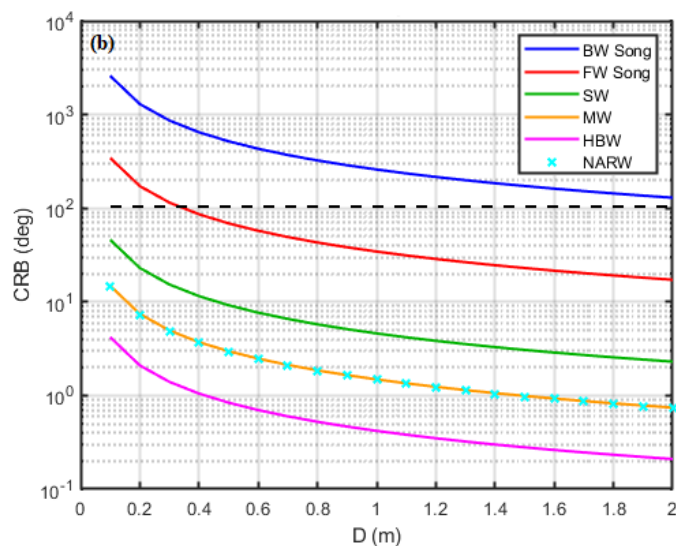


Figure B-9. Minimum RMS Azimuth errors vs the array spacing (D) with SNR=10 dB for calls from six representative marine mammal calls using an orthogonal array. Species acronyms: BW – blue whale (~17 Hz), FW – fin whale (~21 Hz), SW – Sei whale (~40 Hz), MW – minke whale (125 Hz), HBW – humpback whale (400 Hz) and NARW – north Atlantic right whale (~125 Hz).

### B.5.3. Orienting the ALTO Lander

The beamformer provides bearing relative to it's 'x-axis' (C-B). To orient these values to north, the rotation of the lander on the seabed must be determined. This is achieved by computing the direction of arrival for a sound arriving from known location, typically the deployment vessel. The rotation needed to align the

outputs from the beamformer with the known direction is stored in the Channel-Associations.xml file and then used for all future data analysis (Figure B-10).

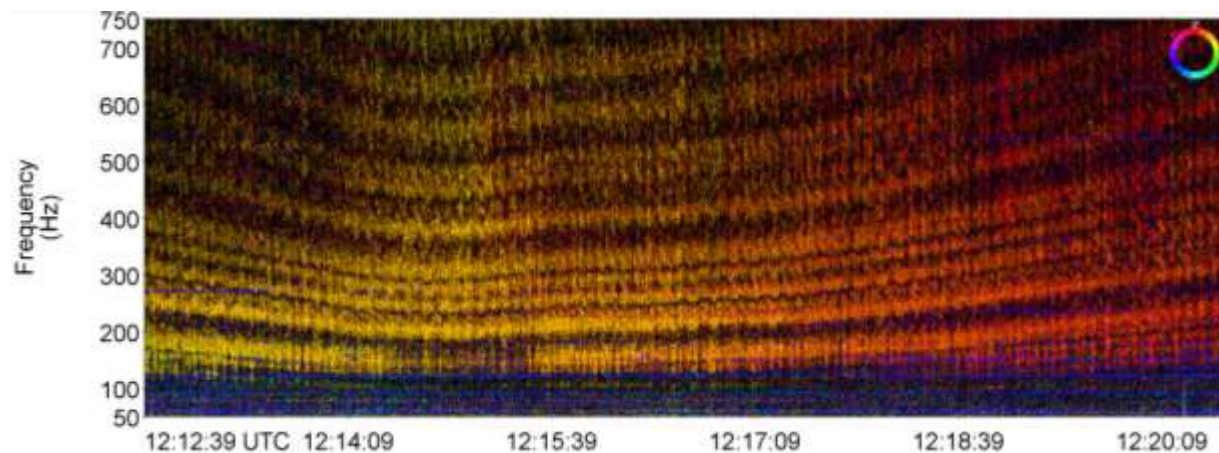


Figure B-10. Directogram of a fishing vessel passing 650 m from an ALTO lander. At 12:12 the vessel was at 060 degrees, moving to 000 degrees at 12:20. In this data presentation, the colour represents the direction of arrival, as shown by the colour wheel at the top right of the figure. A rotation of 95 degrees was needed to yield the correct results compared to the data without correction. There is a second source to the south-west (blue) that is also present in the sample.

#### B.5.4. Determining the Absolute Minimum Number of Animals Present

The MLE beamformer is applied to each marine mammal detection below 750 Hz which generates a data table of the time, duration, minimum and maximum frequencies, SPL, bearing, SNR and the energy weighted mean frequency of the data in the detection. These data are analyzed to find the absolute minimum number (AMN) of animals present. The analysis steps are:

1. Remove species where the manual analysis indicated that the detectors did not have a precision greater than 0.75. This is set as a parameter in the species definition file.
2. Filtering out low SNR data. As discussed in Appendix B.5.2, the bearing errors increase as the frequency and SNR decrease. Therefore, the first stage of analysis is to remove data where the SNR is deemed to be too low:
  - a. For detections with a mean weighted frequency below 22 Hz, detections with an SNR below 9 dB are discarded.
  - b. For detections with a mean weighted frequency between 22 and 30 Hz, detections with an SNR below 8 dB are discarded.
  - c. For detections with a mean weighted frequency between 30 and 40 Hz, detections with an SNR below 7 dB are discarded.
  - d. For detections with a mean weighted frequency between 40 and 100 Hz, detections with an SNR below 6 dB are discarded.
  - e. For detections above 100 Hz, detections with an SNR below 5 dB are discarded.

Examples of the distributions of calls by SNR before and after filtering are shown in Figure B-11.

3. The data are then grouped in 10-min windows. It is assumed that an individual will not move outside of one bearing sector over this time period. This assumption may be false if the animal is very close to the hydrophone array.
4. Round the bearings to the nearest 5-degrees. This resolution is one half of the minimum bearing error (10 degrees, see Appendix B.5.2).
5. For each 10-min block, find the number of calls per species. If this is less than the number of calls required to have a sufficient precision, per the manual analysis, the calls are removed. The number of calls per 5-degree bearing bin is stored to be available for plotting as call densities.
6. For each 10-min block, compute the AMN for each species:
  - a. Find the mean of the weighted frequencies; use this value to compute the bearing error as  $2500 / \text{mean\_weighted\_frequency}$  (see Figure B-8; this is  $\frac{1}{2}$  the error at 10 dB).
  - b. Select the highest SNR call in the 10-min window, then find all calls that are within the bearing error of that call. These are associated with the first animal.
  - c. Repeat the associations for all calls not associated with other calls until the number of unique calling directions is determined. This is the AMN for the 10-min block.
  - d. Find the maximum AMN per day and per hour for each species for use in the data presentations. These values are also stored for external review and analysis.

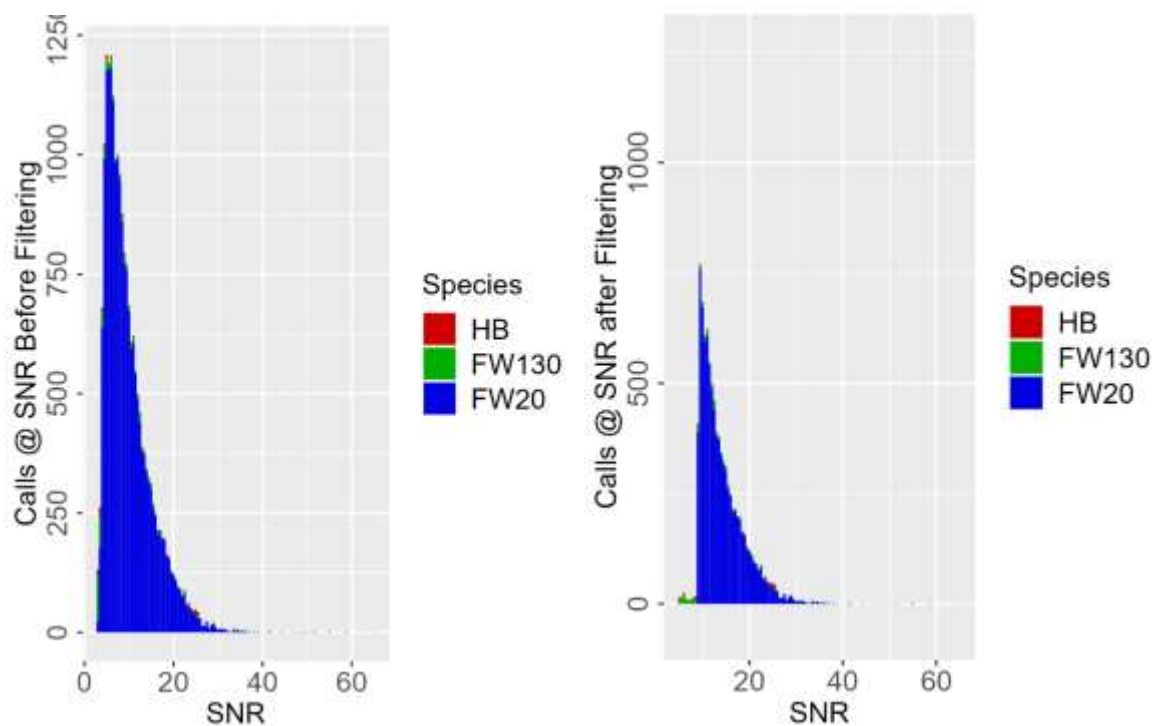


Figure B-11. Histograms of call counts by SNR before and after filtering on SNR.

## Appendix C. Detection Range Modelling Methods and Input Data

### C.1. Propagation Loss Modelling with MONM

Underwater sound propagation (i.e., transmission loss) at frequencies of 10 Hz to 2 kHz was predicted with JASCO's Marine Operations Noise Model (MONM). MONM computes received per-pulse SEL at a specified source depth.

For frequencies up to 2 kHz, MONM computes acoustic propagation via a wide-angle parabolic equation solution to the acoustic wave equation (Collins 1993) based on a version of the US Naval Research Laboratory's Range-dependent Acoustic Model (RAM), which has been modified to account for a solid seabed (Zhang and Tindle 1995). The parabolic equation method has been extensively benchmarked and is widely employed in the underwater acoustics community (Collins et al. 1996). For frequencies above 2 kHz, propagation losses were computed via the BELLHOP Gaussian beam acoustic ray-trace model (Porter and Liu 1994).

MONM accounts for the additional reflection loss at the seabed, which results from partial conversion of incident compressional waves to shear waves at the seabed and sub-bottom interfaces, and it includes wave attenuations in all layers. MONM incorporates the following site-specific environmental properties: a bathymetric grid of the modelled area, underwater sound speed as a function of depth, and a geoacoustic profile based on the overall stratified composition of the seafloor. The environmental input data used are described in Appendix C.2.

MONM computes acoustic fields in three dimensions by modelling transmission loss within two-dimensional (2-D) vertical planes aligned along radials covering a 360° swath from the source, an approach commonly referred to as  $N \times 2$ -D. These vertical radial planes are separated by an angular step size of  $\Delta\theta$ , yielding  $N = 360^\circ/\Delta\theta$  number of planes (Figure C-1).

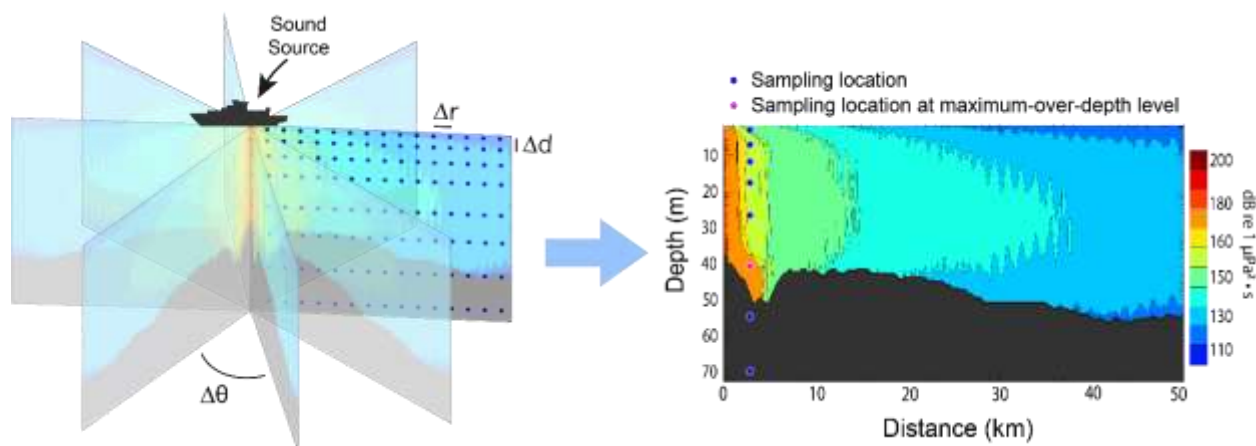


Figure C-1. The  $N \times 2$ -D and maximum-over-depth modelling approach used by MONM.

MONM treats frequency dependence by computing acoustic transmission loss at the centre frequencies of decidecade bands. Sufficiently many decidecade frequency-bands for the source characteristics are modelled to include most of the acoustic energy emitted by the source. At each centre frequency, the transmission loss is modelled within each of the  $N$  vertical planes as a function of depth and range from the source. The decidecade received per-pulse SEL are computed by subtracting the band transmission loss values from the directional source level in that frequency band. Composite broadband received per-pulse SEL are then computed by summing the received decidecade levels.

The frequency-dependent transmission loss computed by MONM can be corrected to account for the acoustic energy attenuated by molecular absorption in seawater. The volumetric sound absorption is quantified by an attenuation coefficient, expressed in units of decibels per kilometre (dB/km). The absorption coefficient depends on the temperature, salinity, and pressure of the water as well as the sound frequency. In general, the absorption coefficient increases with the square of the frequency. The absorption of acoustic wave energy has a noticeable effect ( $>0.05$  dB/km) at frequencies above 1 kHz. For example, at 10 kHz the absorption loss over 10 km distance can exceed 10 dB. The attenuation coefficient for seawater can be computed according to the formulae of François and Garrison (1982a, 1982b), which consider the contributions of pure seawater, magnesium sulfate, and boric acid. The formula applies to all oceanic conditions and frequencies from 200 Hz to 1 MHz. For this project, absorption coefficients were computed and applied for all modelled frequencies.

MONM's predictions have been validated against experimental data from several underwater acoustic measurement programs conducted by JASCO (Hannay and Racca 2005, Aerts et al. 2008, Funk et al. 2008, Ireland et al. 2009, O'Neill et al. 2010, Warner et al. 2010, Racca et al. 2012a, Racca et al. 2012b, Martin et al. 2015).

## C.2. Environmental Input Data

Water depths throughout the modelled area were extracted from the SRTM15+ grid (Smith and Sandwell 1997, Becker et al. 2009).

The sound speed profiles for the modelled site were derived from temperature and salinity profiles from the U.S. Naval Oceanographic Office's Generalized Digital Environmental Model V 3.0 (GDEM; Teague et al. 1990, Carnes 2009). GDEM provides an ocean climatology of temperature and salinity for the world's oceans on a latitude-longitude grid with  $0.25^\circ$  resolution, with a temporal resolution of one month, based on global historical observations from the US Navy's Master Oceanographic Observational Data Set (MOODS). The climatology profiles include 78 fixed depth points to a maximum depth of 6800 m (where the ocean is that deep). The GDEM temperature-salinity profiles were converted to sound speed profiles according to Coppens (1981).

The geoacoustic properties of the modelled areas (Table C-1) were derived from Ainslie (2010).

Table C-1. Geoacoustic profiles.

Depth below seafloor (m)	Density (g/cm <sup>3</sup> )	P-wave velocity (m/s)	P-wave attenuation (dB/λ)	S-wave velocity (m/s)	S-wave attenuation (dB/λ)
0	1.35	1462.53	0.08	100	3.65
5	1.36	1469.03	0.08		
10	1.37	1475.49	0.08		
10	1.39	1475.49	0.08		
25	1.41	1494.67	0.09		
40	1.41	1513.5	0.1		
40	1.41	1513.5	0.1		
70	1.45	1550.26	0.11		
100	1.48	1585.77	0.13		

### C.3. Marine Mammal Call Input Parameters

The marine mammal call parameters used as inputs to the detection range modelling are summarized in Table C-2. The maximum extent of the modelled area was set at 150 km for blue, fin, and sei whales calls and 30 km for all other species.

Table C-2. Marine mammal input parameters. The detection threshold refers to the threshold of the relevant detectors. SD = standard deviation.

Call type	Decidecade Band (Hz)	Source level (dB)		Source depth (m)	Detection threshold	Reference
		Mean	SD			
Blue whale A-B calls	16	182	3	10–30	4	Thode et al. (2000), McDonald et al. (2001)
Fin whale 20-Hz calls	20, 25	185	5	5–25	2.7	Weirathmueller et al. (2013), Wang et al. (2016), Miksis-Olds et al. (2019)
Sei whale downsweeps	32–80	176.5	4	5–25	4	Romagosa et al. (2015)
Humpback whale moans	50–500	171.5	5.7	10–30	3	Girola et al. (2019)
Minke whale pulse trains	50–200	170	3	5–25	3.5	Risch et al. (2014)
Right whale upcalls	80–200	165	3.5	5–25	3	Parks and Tyack (2005)
Sperm whale clicks	2000–16000	186	3	50–1000	16	Mathias et al. (2013)
Delphinid whistles	8000–125000	158	6	1–50	1.5	
Killer whale tonal calls	800–1200	154	5	1–50	1.5	Miller (2006), Holt et al. (2011)
Pilot whale tonal calls	2000–4000	154	5	1–50	1.5	Same as killer whale
Northern bottlenose whale clicks	25000	186	5	50–1000	16	(Wahlberg et al. 2011)
Delphinid clicks	31500	188	8	10–100	16	Used Pilot whales as representative species; Eskesen et al. (2011)
Harbour porpoise clicks high	125000	186	8	1–50	16	Villadsgaard et al. (2007), Kyhn et al. (2013)
Harbour porpoise clicks low	125000	169	8	1–50	16	Villadsgaard et al. (2007), Kyhn et al. (2013)
Harbour porpoise clicks median shallow	125000	178	5	1–50	16	Villadsgaard et al. (2007), Kyhn et al. (2013)
Harbour porpoise clicks median deep	125000	178	5	1–400	16	Villadsgaard et al. (2007), Kyhn et al. (2013); Nielsen et al. (2018)
Pygmy sperm whale	125000	178	5	100–1000	16	Derived from Malinka et al. (2021)

### C.4. Results

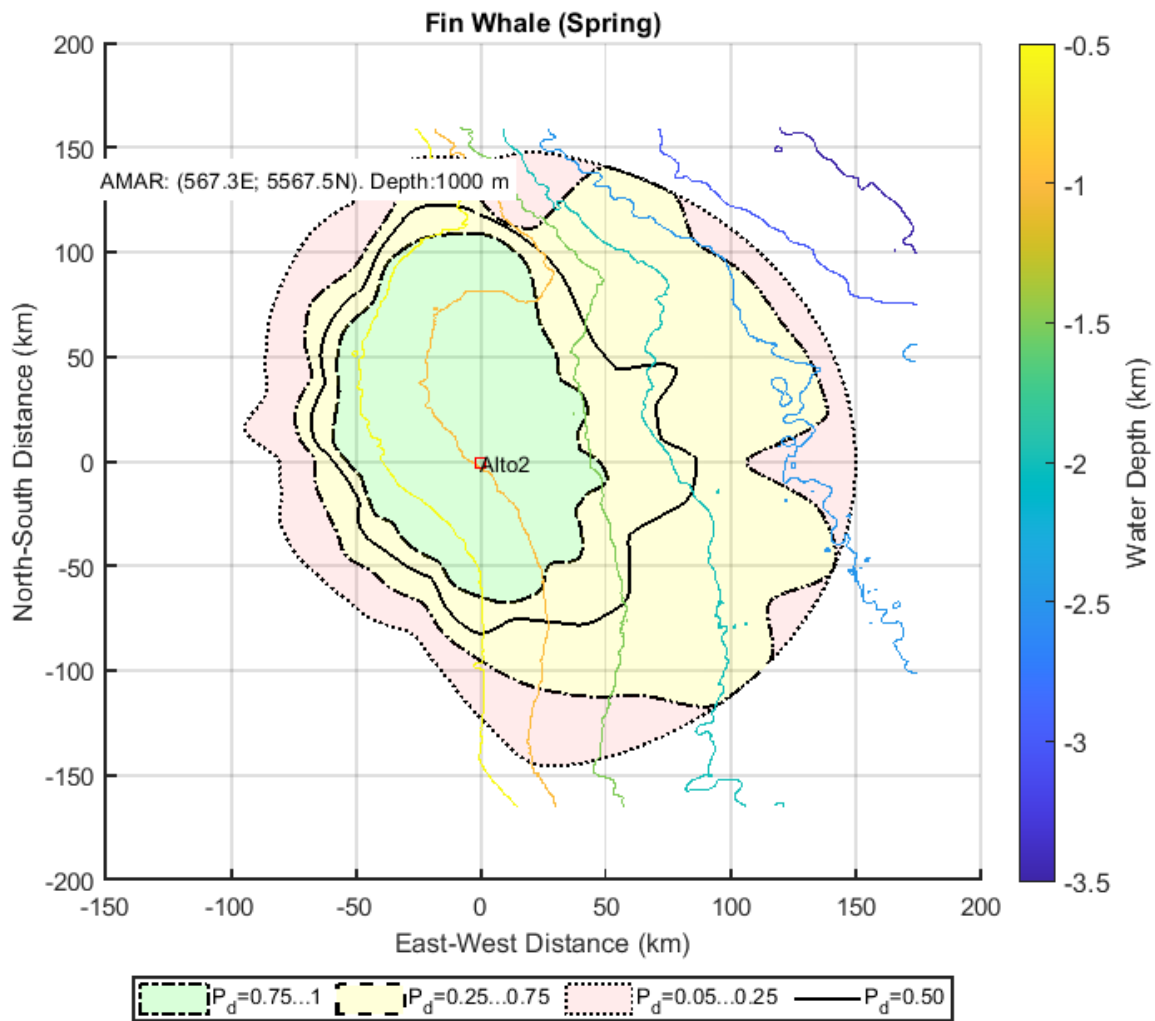


Figure C-2. Detection areas for fin whale song notes at ALTO2 associated with various probabilities of detection under the range of noise conditions recorded in spring. The solid black line shows the range for a 50 % probability of detection.

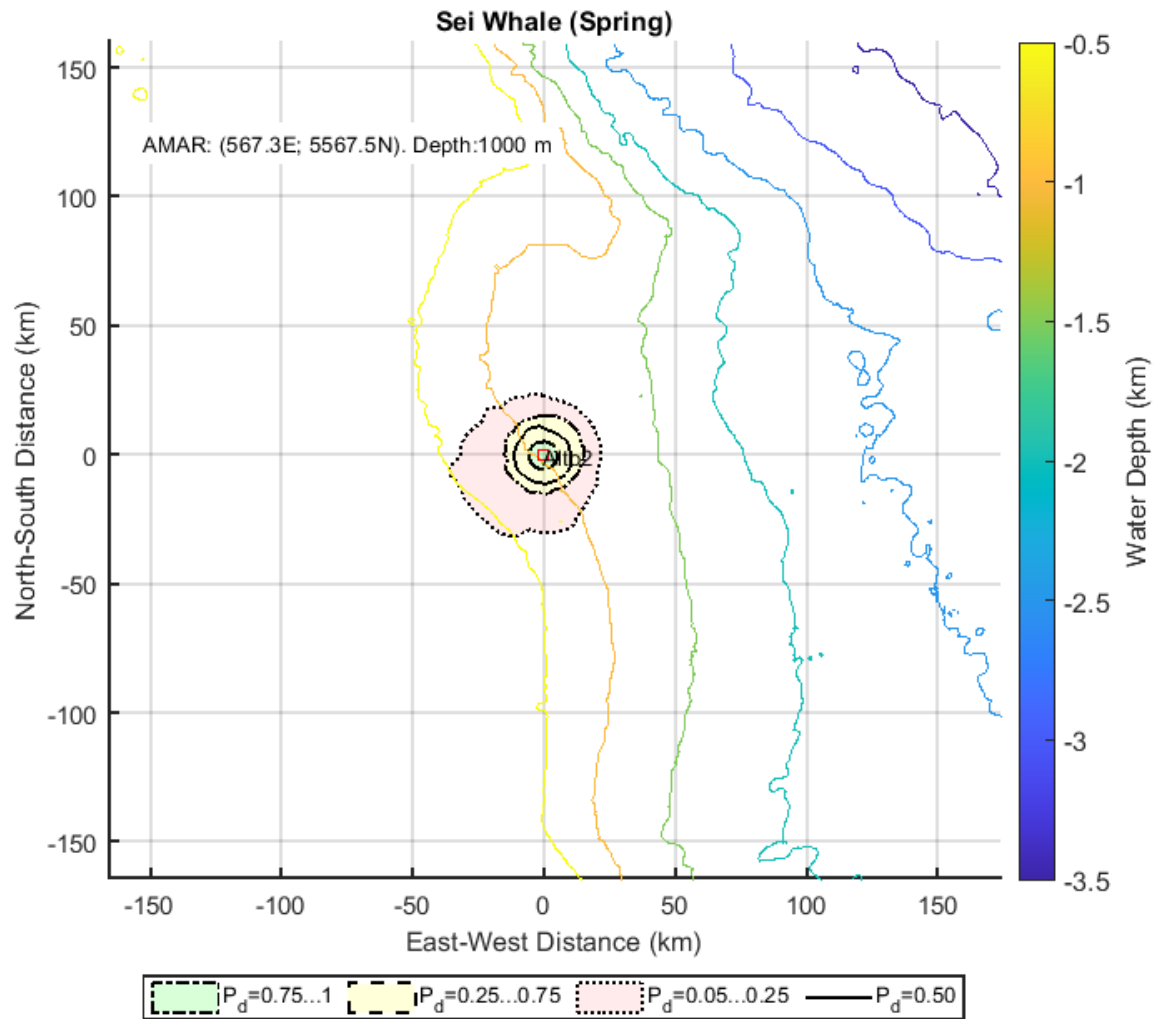


Figure C-3. Detection areas for sei whale downsweeps at ALTO2 associated with various probabilities of detection under the range of noise conditions recorded in spring. The solid black line shows the range for a 50 % probability of detection.

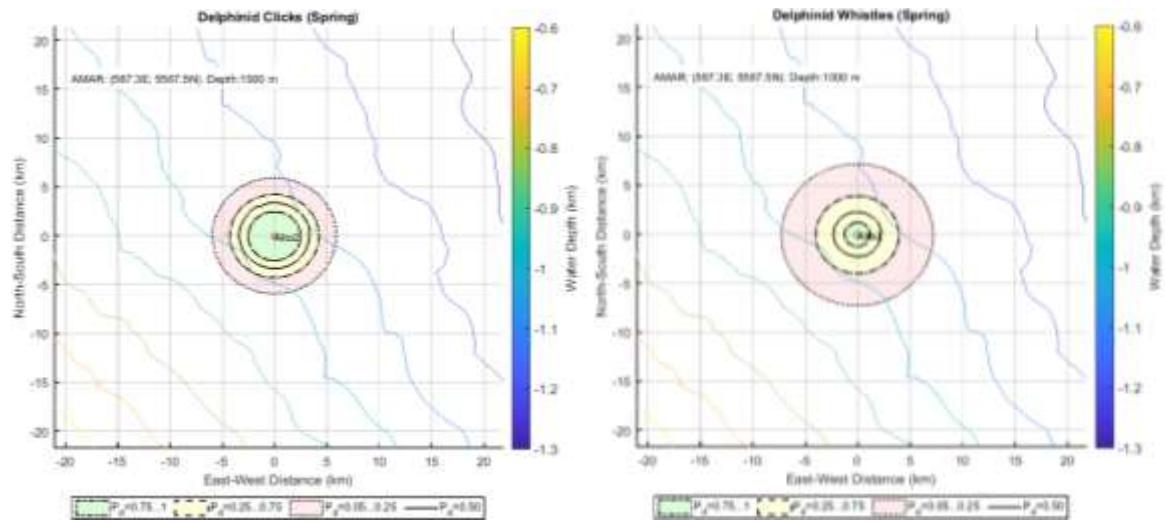


Figure C-4. Detection areas for dolphin clicks (left) and whistles (right) at ALTO2 associated with various probabilities of detection under the range of noise conditions recorded in spring. The solid black line shows the range for a 50 % probability of detection.

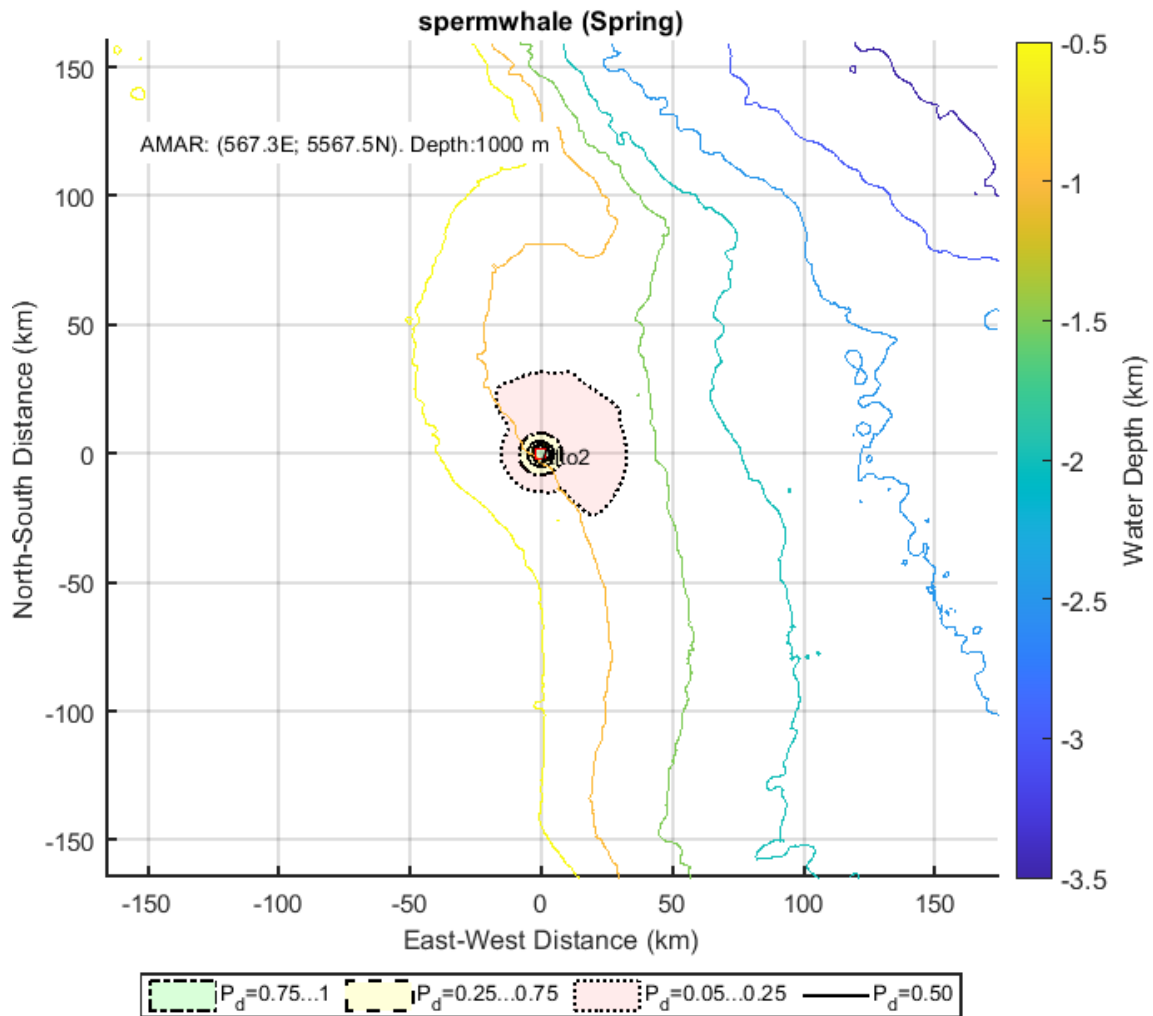


Figure C-5. Detection areas for sperm whale clicks at ALTO2 associated with various probabilities of detection under the range of noise conditions recorded in spring. The solid black line shows the range for a 50 % probability of detection.

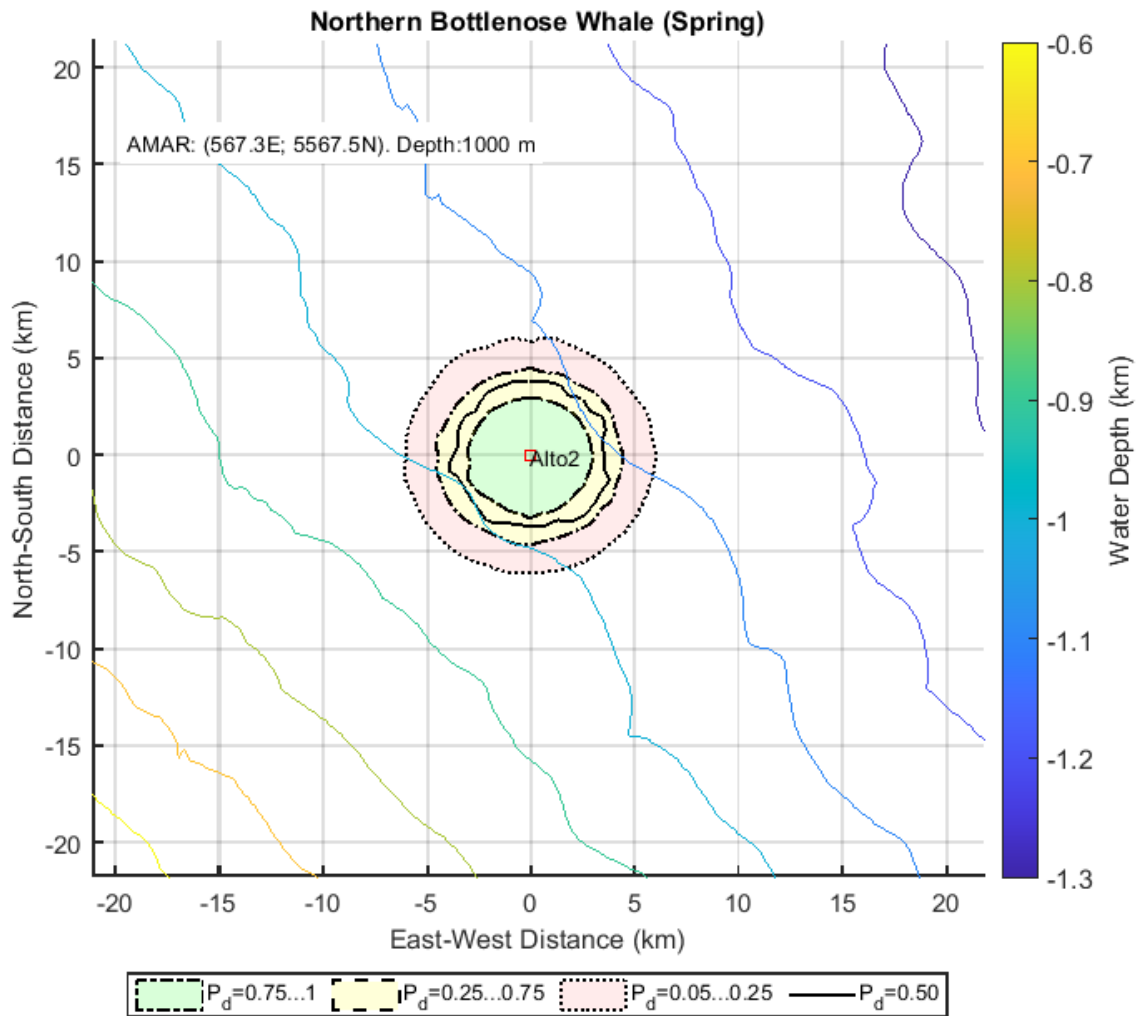


Figure C-6. Detection areas northern bottlenose clicks at ALTO2 associated with various probabilities of detection under the range of noise conditions recorded in spring. The solid black line shows the range for a 50 % probability of detection.

## Appendix D. Vessel Source Level Results

### D.1. Atlantic Kingfisher

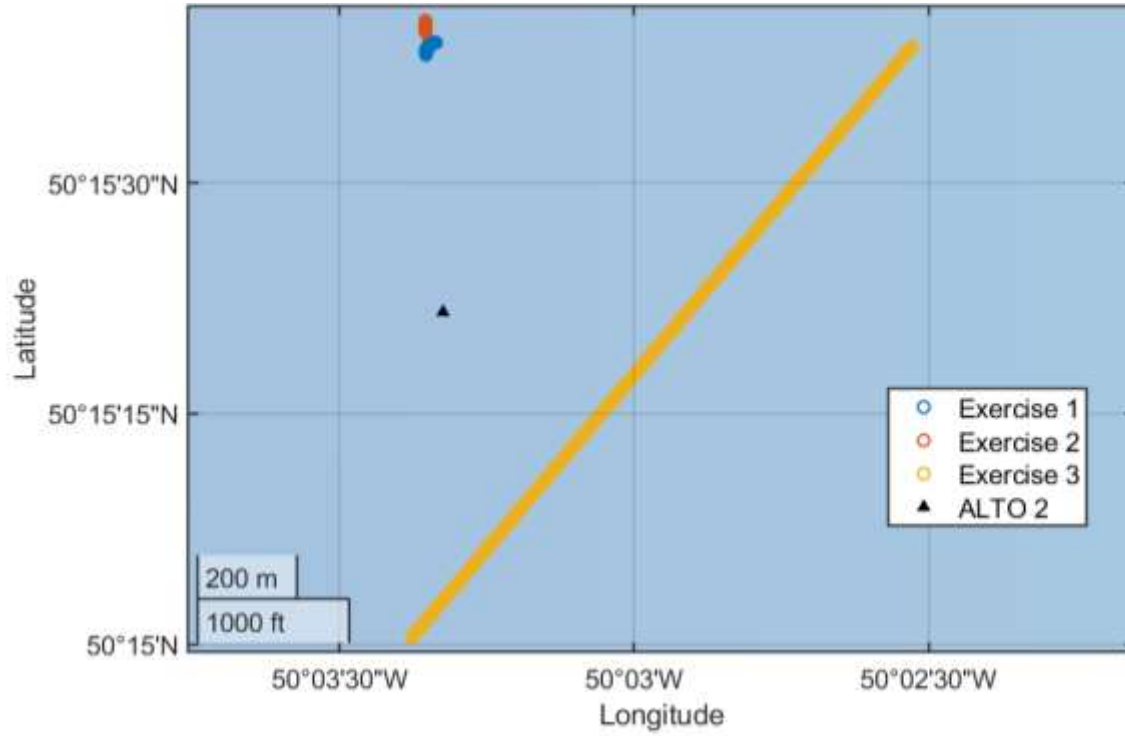


Figure D-1. Atlantic Kingfisher track referenced by ALTO 2 position as a black triangle around the time of the exercises.

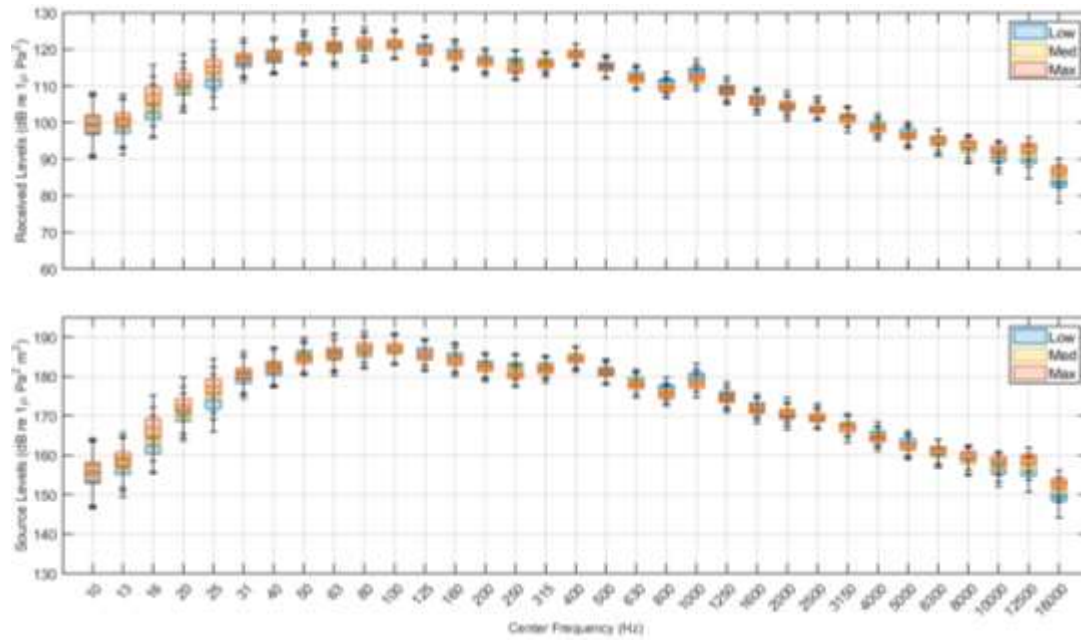


Figure D-2. Atlantic Kingfisher. (Top) Received levels during exercise 1 grouped by thruster level. (Bottom) Calculated source level using Equations 4 and 5 during exercise 1 grouped by thruster level.

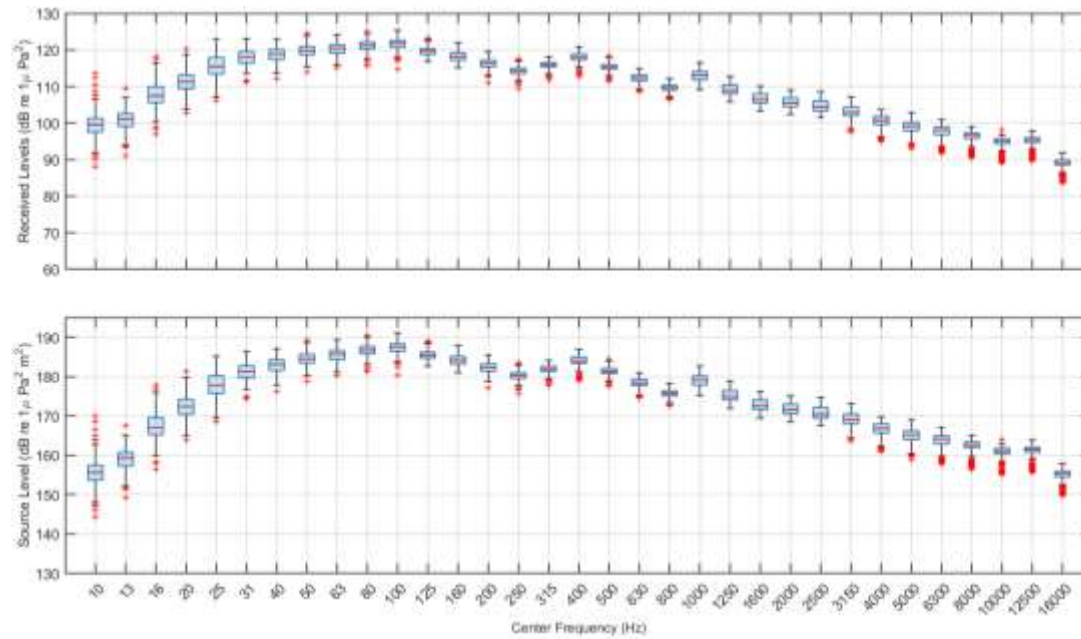


Figure D-3. Atlantic Kingfisher. (Top) Received levels during exercise 2. (Bottom) Calculated source level using Equations 4 and 5 during exercise 2.

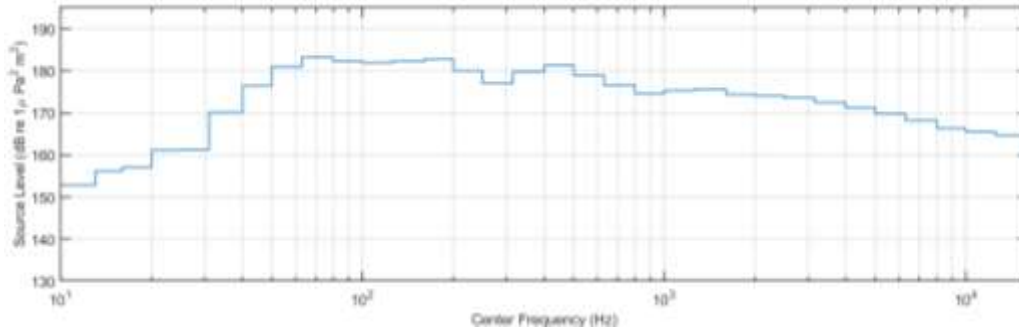


Figure D-4. Atlantic Kingfisher calculated source level using Equations 4 and 5 during exercise 3.

## D.2. Maersk Mobiliser

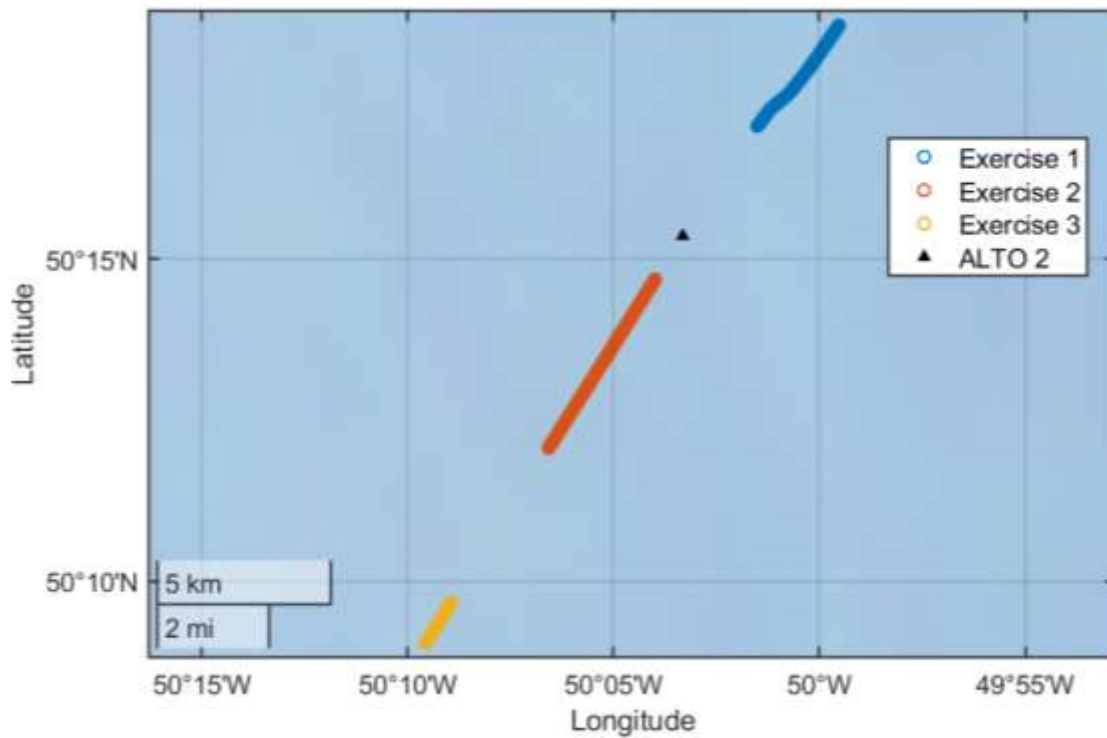


Figure D-5. Maersk Mobiliser track referenced by ALTO 2 position as a black triangle around the time of the exercises.

As can be seen in Figure D-5, and also inferred from Figure 47, the MAERSK MOBILIZER did not correctly execute the monitoring plan and hence the data can not be analyzed and presented for comparison to the other support vessels.

### D.3. KJ Gardner

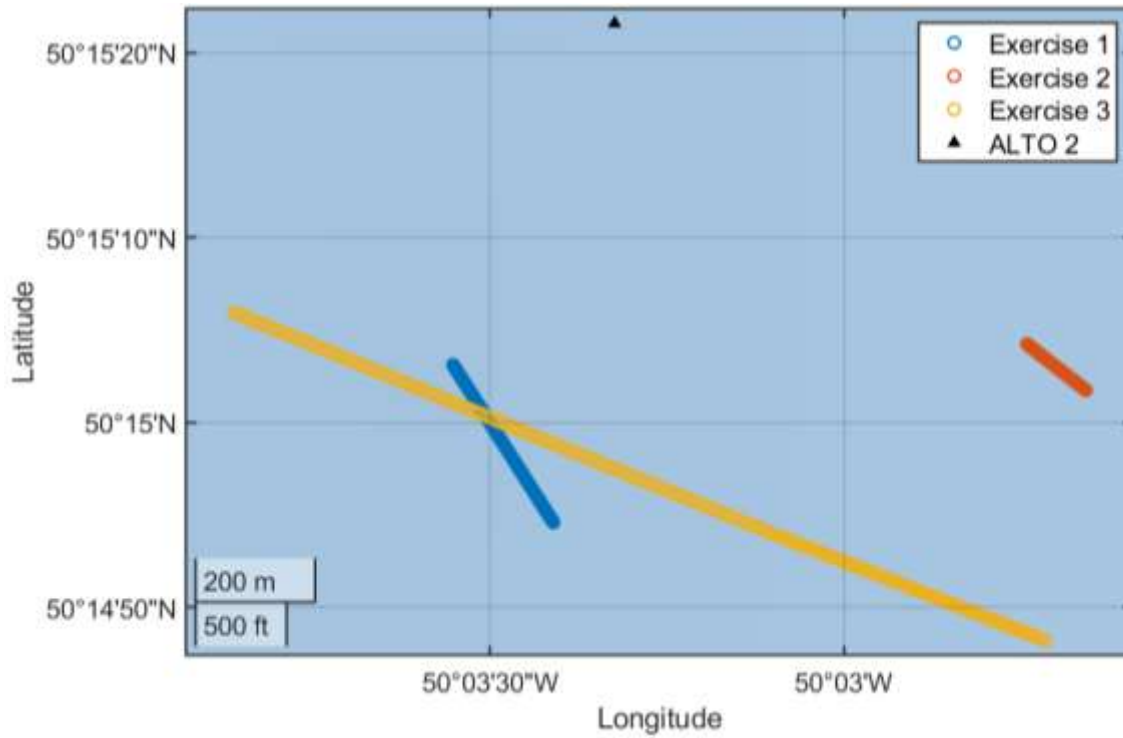


Figure D-6. KJ Gardner track referenced by ALTO 2 position as a black triangle around the time of the exercises.

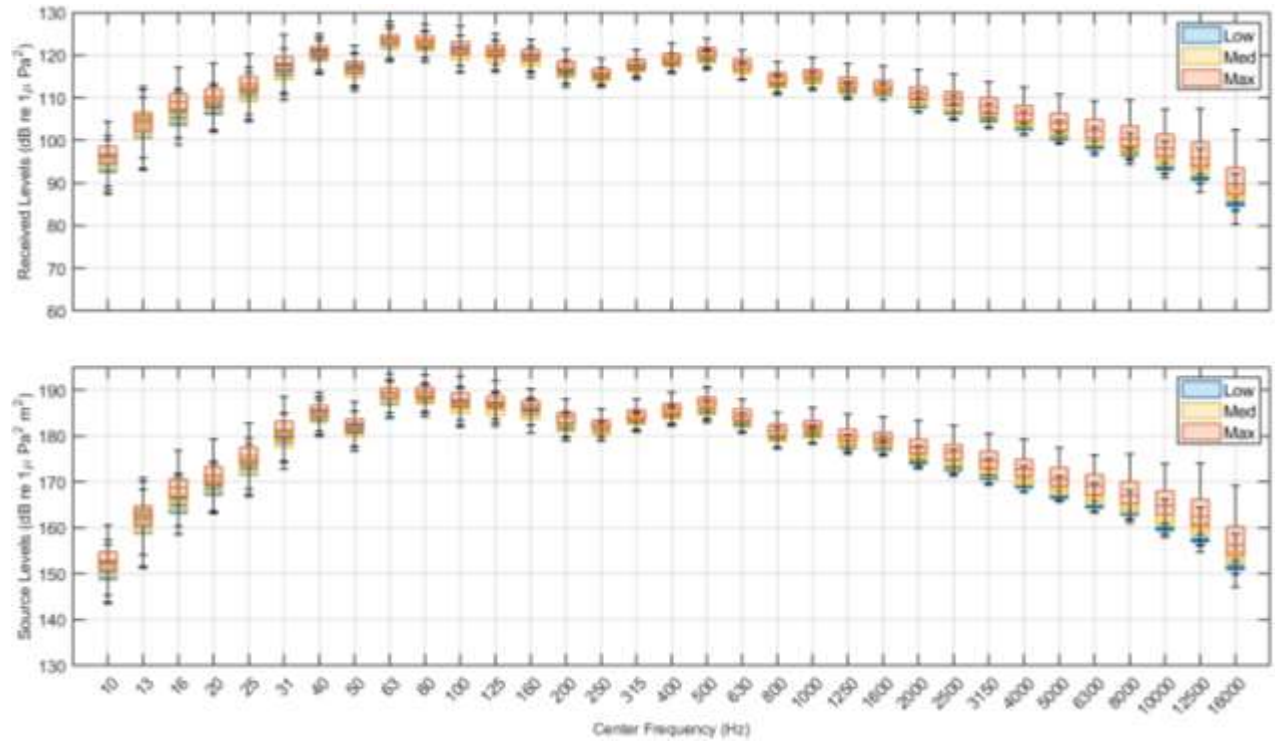


Figure D-7. KJ Gardner. (Top) Received levels during exercise 1 grouped by thruster level. (Bottom) Calculated source level using Equations 4 and 5 during exercise 1 grouped by thruster level.

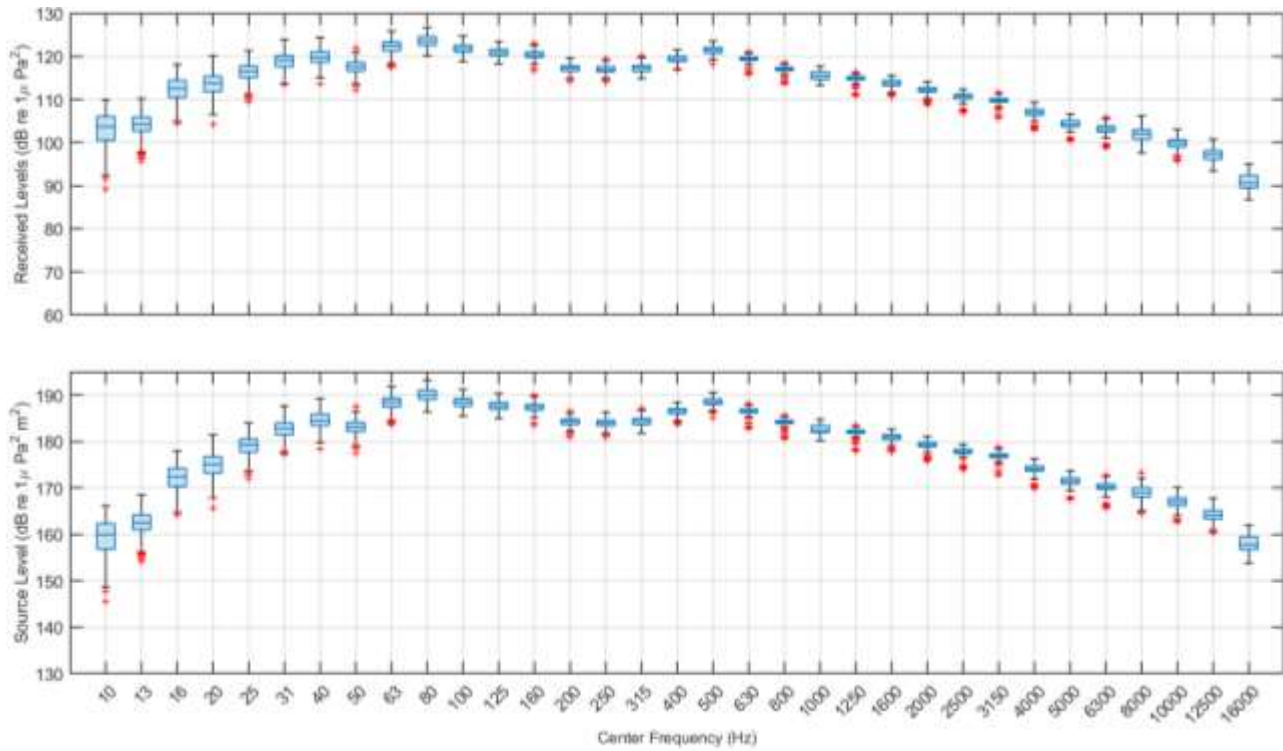


Figure D-8. KJ Gardner. (Top) Received levels during exercise 2. (Bottom) Calculated source level using Equations 4 and 5 during exercise 2.

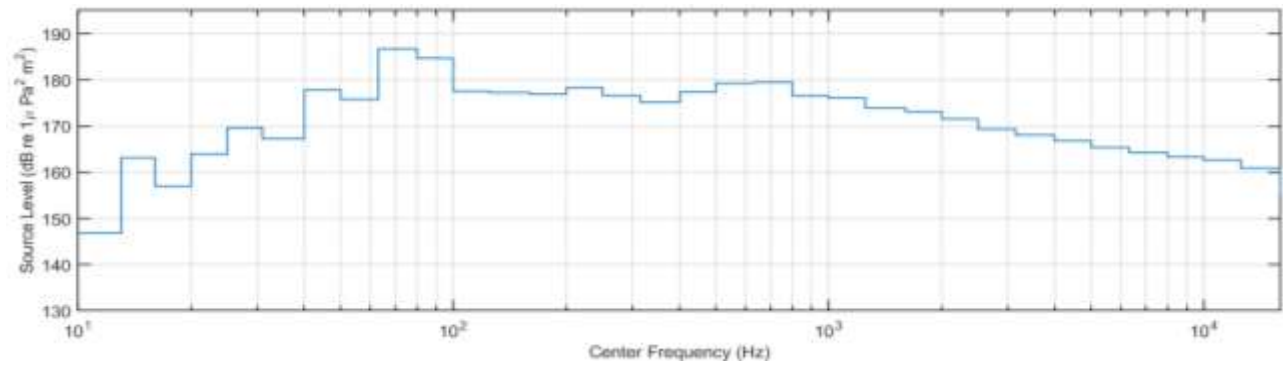


Figure D-9. KJ Gardner calculated source level using Equations 4 and 5 during exercise 3.

### D.4. Maersk Clipper

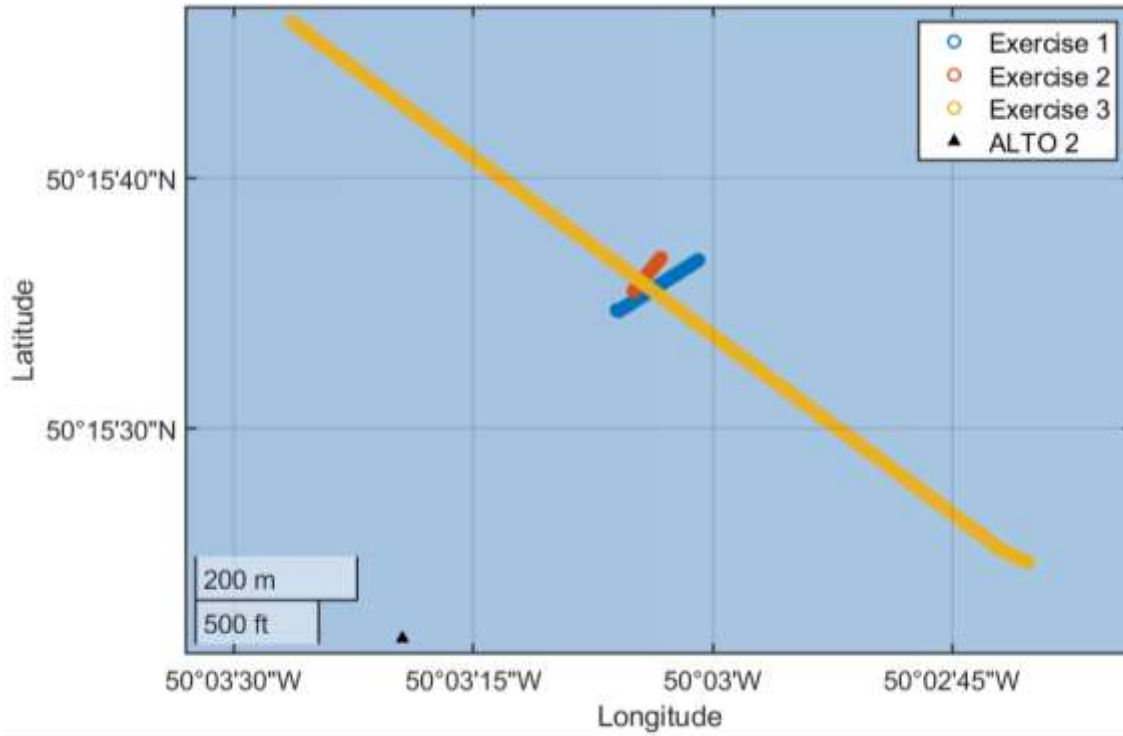


Figure D-10. Maersk Clipper track referenced by ALTO 2 position as a black triangle around the time of the exercises.

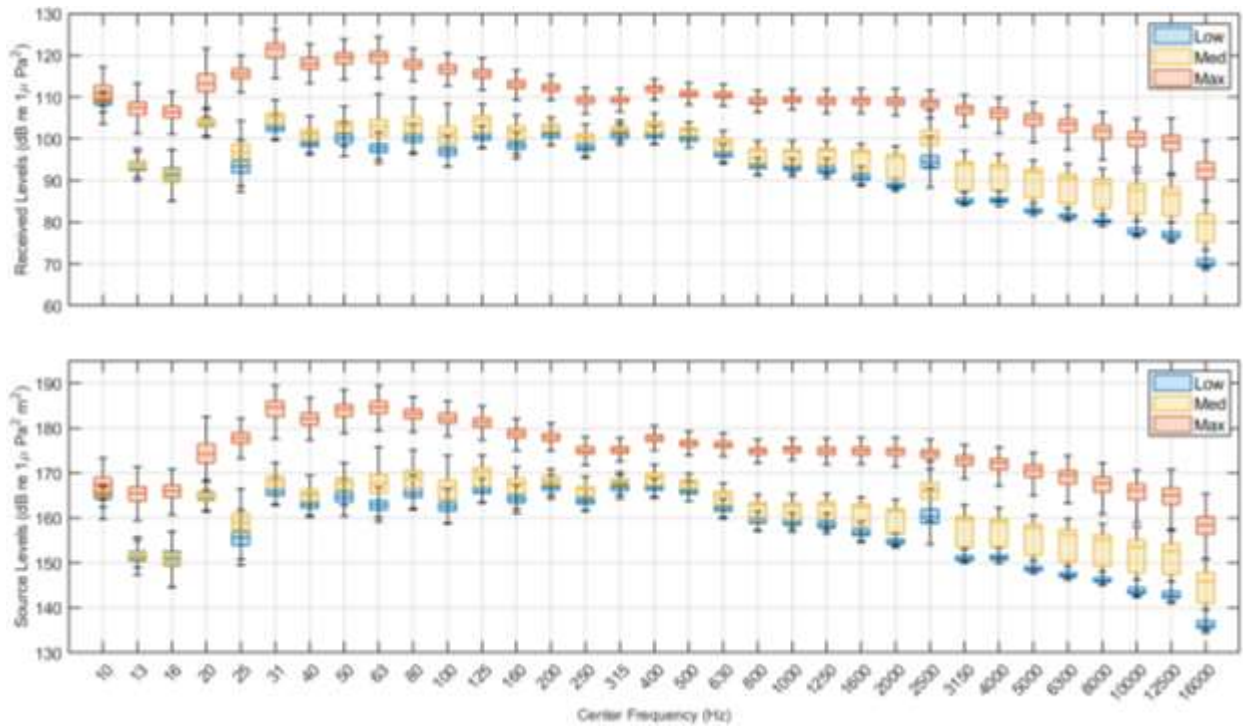


Figure D-11. Maersk Clipper. (Top) Received levels during exercise 1 grouped by thruster level. (Bottom) Calculated source level using Equations 4 and 5 during exercise 1 grouped by thruster level.

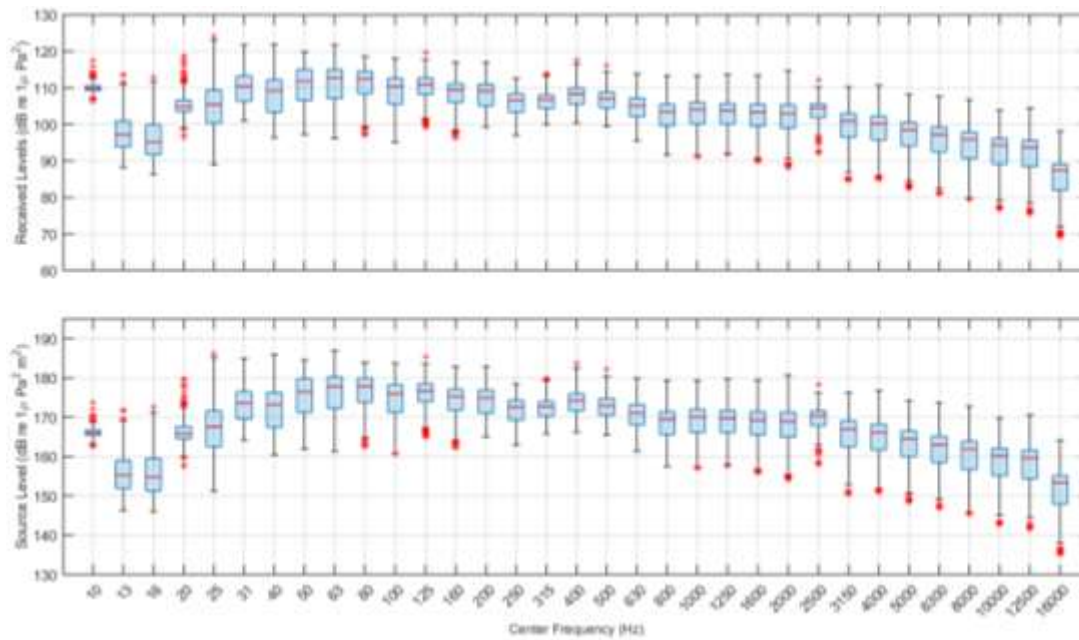


Figure D-12. Maersk Clipper. (Top) Received levels during exercise 2. (Bottom) Calculated source level using Equations 4 and 5 during exercise 2.

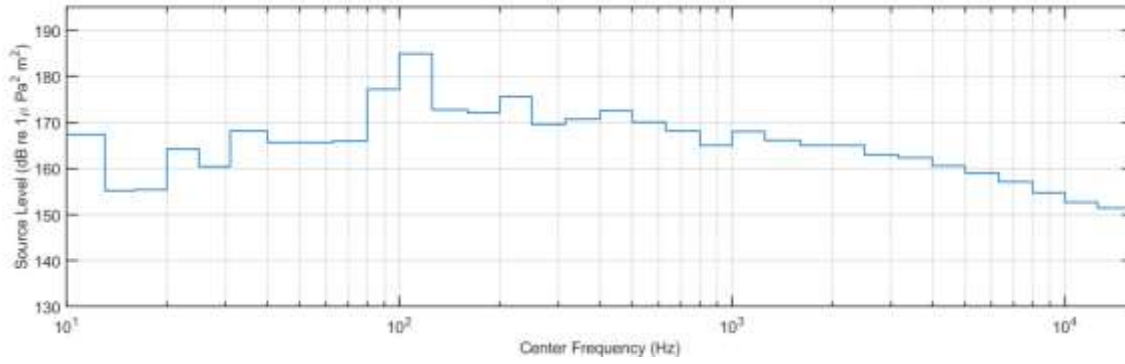


Figure D-13. Maersk Clipper calculated source level using Equations 4 and 5 during exercise 3.